Lesions and cellular tropism of natural Rift Valley fever virus infection in sheep

by

LIEZA ODENDAAL

Submitted in partial fulfilment of the requirements for the degree

Philosophiae Doctor

in the Department of Veterinary Tropical Diseases, Faculty of Veterinary Science, University of Pretoria

Date submitted: November 2019

DECLARATION

I, **Lieza Odendaal,** declare that the thesis, which I hereby submit for the degree, *Philosophiae Doctor* at the University of Pretoria is my own independent work and that neither the whole work nor part of it has been, is being, or shall be submitted for another degree at this or another university, institution for tertiary education or professional examination body.

I, **Lieza Odendaal**, further declare that for the research described in this work, the applicable research ethics approval has been obtained. I declare that I have observed the ethical standards required in terms of the University of Pretoria's Code of ethics for researchers and the Policy guidelines for responsible research.

_____

Lieza Odendaal

_____

Date

ACKNOWLEDGEMENTS

I wish to express my sincere thanks and appreciation for the following people:

My supervisors, Professor Estelle Venter and Assistant Professor Sally Davis for their continued encouragement and support throughout this project. They both cared a great deal about the work and provided excellent guidance, thereby giving me the opportunity to grow as a scientist. I am very grateful for this and hope to emulate their example in future.

My co-authors and friends, Dr Sarah Clift and Professor Geoffrey Fosgate for assisting with the design the project.

To my supervisors and co-authors for patiently proof reading and editing multiple versions of manuscripts and making excellent suggestions for improvements.

The staff of the histopathology laboratory of the Department of Paraclinical Sciences, Section of Pathology, especially Rephima Phaswane, Naomi Timmerman, Peter Mokonoto and Marie Smit for their assistance, knowledge, input and support.

Colleagues at the National Department of Agriculture, Fisheries and Forestry, Directorate of Veterinary Services for providing access to original diagnostic data and colleagues at IDEXX laboratories (South Africa) for providing specimens.

The Agricultural Sector Education Training Authority for providing funding for the project.

My sister, Antoinette Odendaal, for her patience and expertise in compiling all the photo panels for this thesis and the submitted papers on weekends and sometimes in the evenings on weekdays when revisions were urgent.

Mal Hoover for providing additional support with the photo panels and teaching us about the exceedingly useful dropper tool.

My mother, Marie Odendaal, for her constant encouragement, love and support.

The rest of my family and friends for always being there and for your love and encouragement.

SUMMARY

Lesions and cellular tropism of natural Rift Valley fever virus infection in sheep

by

Lieza Odendaal

Promoter: **Prof Estelle H Venter**
Professor Emeritus: University of Pretoria
Professor of Veterinary Education
College of Public Health, Medical and Veterinary Sciences
James Cook University, Townsville
Australia

Co-promoter: **Dr A Sally Davis**
Assistant Professor: Experimental Pathology
Department of Diagnostic Medicine/Pathobiology
College of Veterinary Medicine
Kansas State University, Manhattan, Kansas
United States of America

For the degree: Philosophiae Doctor

Rift Valley fever (RVF) is a viral haemorrhagic disease caused by a segmented single stranded RNA virus of the *Bunyavirales* order, *Phenuiviridae* family. The virus causes severe disease in both humans and animals and epidemics have been reported in most countries in Africa and the Arabian Peninsula. The virus is primarily transmitted by mosquitoes, mainly of the genera *Aedes* and *Culex*. Characteristically RVF virus (RVFV) causes abortion storms in sheep during which approximately 10 to 20% of adult ewes die. In the summers of 2010-2011, South Africa had an extensive outbreak of RVF affecting livestock and humans. The diagnosis of RVF was confirmed using real-time reverse transcription quantitative polymerase chain reaction (RT-qPCR), and in selected cases also by immunohistochemistry (IHC). Sheep necropsied during the outbreak were examined by histopathology and IHC.

The first chapter is a review of research conducted regarding RVF infection in sheep, including descriptions of the pathology and immunohistochemical findings. Relevant information concerning the pathogenesis of RVFV and other viral haemorrhagic diseases with a similar pathogenesis was also summarized.

The aim of the second chapter was to describe the tissue tropism and target cells of RVFV in 99 adult sheep from the 2010 South African RVF outbreak. A further aim was to determine the extent to which virus could be detected in different organs and summarize gross, histopathological and immunohistochemical findings relative to results from previous research. Multifocal-random, necrotizing hepatitis was the most distinctive lesion of RVF cases in adult sheep. Of cases where liver, spleen and kidney tissues were available 45/70 (64%) had foci of acute renal tubular epithelial injury in addition to necrosis in both the liver and spleen. In some cases, acute renal injury was the most significant RVF lesion. Concerning the diagnostic specificity of lesions in the liver, early apoptotic hepatocytes (Councilman bodies) and late apoptotic bodies with nuclear fragments and condensed cytosol were diagnostically useful. In contrast, eosinophilic intranuclear inclusions were of limited diagnostic value since they were only identified in 7/99 (7%) adult sheep. Immunolabelling for RVFV was most consistent and unequivocal in liver followed by spleen, kidney, lung and skin. It was determined in this study that the minimum set of specimens to be submitted for histopathology and IHC to confirm or exclude a diagnosis of RVF are liver, spleen and kidney. Skin from areas with visible crusts and lung could be useful additional samples.

RVF is much more acute in young lambs than in older sheep, and there appear to be important differences in the lesions and tropism. Therefore, the principle aim of the third chapter was to describe the quantitative and qualitative pathomorphology of RVF in 71 young lambs and contrast this with results for adult sheep. A further aim was to determine the diagnostic significance of different tissues and specific histologic features of RVF in young lambs. The liver lesion of RVF was much more severe in young lambs, where it caused a diffuse necrotizing hepatitis with widespread labelling of virtually every hepatocyte. A striking

diagnostic feature in lambs was multifocal liquefactive hepatic necrosis (primary foci) against a background of diffuse hepatocellular death. Primary foci were present in 59 of 71 (86%) cases, with viral antigen noticeably sparse within them. Intranuclear inclusion bodies were also diagnostically useful, and present in 27 of 71 (38%) cases. Additionally, cell death morphology in the liver in RVFV infected lambs was more heterogeneous than previously suspected whereby many hepatocytes displayed histomorphological features of lytic cell death mechanisms (cell swelling, rupture of the plasma membrane and cellular collapse) as well as apoptosis. Whereas, apoptosis was demonstrated in RVFV infected mice using terminal deoxynucleotidyl transferase dUTP nick-end labelling, the involvement other cell death mechanisms in RVF, including pyroptosis and necroptosis, should be further explored.

In young lambs, lymphocytolysis was present in all lymphoid organs except for the thymus. The kidney lesion was also much less severe than in adult sheep but viral antigen was easier to find and generally widespread. Histopathological lesions in the lungs of lambs mirrored that in adults. However, viral antigen was easy to find in lambs compared to adult sheep where viral antigen was very difficult to find in the lungs. As in adult sheep, splenic lymphocytolysis was a prominent feature, but due to a developmentally normal lack of germinal centres this was more prominent at the edge of the periarteriolar lymphoid sheaths and the red pulp in lambs. Labelling was also often seen in capillaries and small blood vessels either as non-cell-associated antigen, or as antigen in endothelial cells or intravascular cellular debris. Additionally, in the kidney viral antigen was in the peri-macular cells including the juxtaglomerular and granular extraglomerular mesangial cells. Liver and spleen specimens were the most consistently positive for RVFV antigen and were adequate to confirm or exclude a diagnosis of RVF in most cases in young lambs using IHC. Specimens from the lungs and kidneys were useful additional samples due to their characteristic histologic lesions.

There is a perception that RVF disappears in the interepidemic periods and only reappears suddenly when heavy rainfall occurs. However, RVFV infection in pregnant ewes causes a wide variety of outcomes for both ewes and foetuses and it is difficult to exclude RVF from the

list of possible differential diagnoses. Diagnosing the cause of abortions in endemic areas are further complicated by the observation that the virus seemingly does not always cross the placenta to cause lesions in the foetus. Additionally, the tropism and lesions of the placenta have not been thoroughly described. Therefore, the principle aim of the fourth chapter was to describe RVF in naturally infected foetal tissues and determine the diagnostic significance of the lesions. A total of 72 foetuses were studied of which 58 were confirmed positive for RVF. Placenta specimens were available for 35 of the foetuses. Macroscopic lesions in sheep foetuses were non-specific and included edema and hemorrhages in visceral organs, and effusions in the body cavities. Microscopically, necrotizing hepatitis was present in 48/58 (83%) of the foetuses but only severe in 20 (34%) cases. In most cases where necrotizing hepatitis was present, either primary foci or intranuclear inclusions were also present. Lymphocytolysis was present in all lymphoid organs with the exception of the thymus and Peyer's patches. The most significant histological lesion in the placenta was necrosis of trophoblasts and vascular endothelial cells in both the cotyledonary and intercotyledonary allantochorion. In the cotyledonary villi, necrosis of trophoblasts was generally diffuse with multifocal cellular debris present between the villi. RVFV antigen was most consistent in trophoblasts in the placentome. The minimum set of specimens to be submitted for histopathology include cotyledon and endometrial (particularly caruncle) samples, if available. Foetal organ samples must minimally include liver, kidney and spleen. The diagnostic investigation of abortion in RVF endemic areas must always include routine testing for the presence of RVFV and a diagnosis in the inter-epidemic periods might be missed if only limited samples are available.

Chapter 5 presents additional histochemistry and immunohistochemistry results based on further analysis of lymphoid and kidney samples from natural RVF cases. A marked reduction in the numbers of B and T lymphocytes were demonstrated in both the red and the white pulp areas of the spleen. In kidney specimens, the Jones' methenamine silver stain demonstrated a decrease in mesangial cellularity, pyknosis and karyorrhexis of vascular endothelial cells in the glomeruli and interstitial capillaries, and no disruption of the basement membranes.

Additionally, none of the spleen, lymph node or kidney specimens had convincing platelet-fibrin thrombi. These results should inform future RVFV pathogenesis study design into the role of lymphocytes, the kidney lesion and coagulopathy during RVFV infection.

In this study it was demonstrated that RVF is much more acute in young lambs than in older sheep, and that there are important differences in the lesions and tropism particularly in the liver, kidneys and lymphoid organs. Additionally, diagnosing RVF in foetuses can be challenging if samples from the ewe or the placenta are not available or a limited number of deaths and abortions occurs during an interepidemic period when the disease is not expected to be present. Therefore, continued surveillance is required in the interepidemic period, and RVF should remain a differential diagnosis in cases of abortion in endemic areas. This is especially so if only tissues from the foetus are tested and not the placenta, since the latter is often positive in the absence of viral antigen in the foetal liver or other organs.

Thesis outline:

Chapter 1 is a review of the literature. Chapters 2, 3 and 4 are written up as manuscripts for publication, and due to this there may be instances of duplication across these chapters. All publications and conference contributions are listed. Chapter 5 is a short communication of additional tests that were performed to investigate specific findings in more detail, the results of which were not reported in the aforementioned manuscripts. References and appendices are provided at the end of the thesis. The summary and conclusion are combined from the respective chapters.

RESEARCH OUTPUTS

Publications:

Odendaal L, Clift SJ, Fosgate GT, Davis AS. Lesions and cellular tropism of natural Rift Valley fever virus infection in adult sheep. Journal of Veterinary Pathology. 2019; 56(1): 61-77

Odendaal L, Davis AS, Fosgate GT, Clift SJ. Lesions and cellular tropism of natural Rift Valley fever virus infection in young lambs. Journal of Veterinary Pathology. 2019; Accepted for publication on 18 August 2019.

Conference contributions and invited lectures:

Invited lecture at the Arthropod-Borne Animal Diseases Research Unit (ABADRU), United States Department of Agriculture, Agricultural Research Service, Center for Grain and Animal Health, and at Kansas State University College of Veterinary Medicine, Section of Diagnostic Medicine/Pathobiology, Manhattan, Kansas, United States of America. November 2016: 'Rift Valley fever in South Africa'

Invited lecture at the American Society for Investigative Pathology annual meeting held at the Experimental Biology Congress, 21-25 April 2018, San Diego, California, USA: 'Tissue and cellular tropism of Rift Valley fever virus in sheep'.

Presented an abstract at the 34th World Veterinary Association Congress, 5-8 May 2018, Barcelona, Spain: **Odendaal L**, Clift SJ, Fosgate GT, Davis AS. 'Pathology and tissue tropism of natural Rift Valley fever virus infection in sheep'.

Invited lecture at the Faculty of Veterinary Medicine, Utrecht University, The Netherlands. 7 September 2018: 'Rift Valley fever: A South African Perspective'.

Poster presented at Faculty Day of the Faculty of Veterinary Science, University of Pretoria, 22 August 2019: 'Pathology and tissue tropism of natural Rift Valley fever virus infection in sheep.'

TABLE OF CONTENTS

LIST OF ABBREVIATIONS

BBB: Blood brain barrier

BUN: Blood urea nitrogen

CCHF: Crimean-Congo haemorrhagic fever

CCHFV: Crimean-Congo haemorrhagic fever virus

DHF: Dengue haemorrhagic fever

DHFV: Dengue haemorrhagic fever virus

DIC: Disseminated intravascular coagulation

d.p.i.: Days post infection

dsRNA: Double-stranded RNA

EBOV: Ebola virus

eIF2α: Eukaryotic translation initiation factor 2α

FFPE: Formalin-fixed paraffin embedded

FDPs: Fibrin/fibrinogen degradation products

G_C: Envelope glycoproteins C

G_N: Envelope glycoproteins N

EMH: Extramedullary haematopoiesis

HE: Haematoxylin and eosin

HIER: Heat-induced epitope retrieval

h.p.i.: Hours post infection

IFN: Interferon

IHC: Immunohistochemistry

IL: Interleukin

IP-10: Interferon-gamma-induced-protein-10

JMS: Jones'methenamine silver stain

L: Large segment

M: Medium segment

MIG: Monokine-induced-by-gamma-interferon

MSB: Martius scarlet blue trichrome stain

MT:	Masson trichrome stain
N:	Nucleocapsid protein
NS:	Non-structural
NSm:	Non-structural protein coded by the M-segment
NLRP3:	Nucleotide-binding domain, leucine-rich-containing family, pyrin domain-containing-3
NSs:	Non-structural protein encoded by the S-segment
PAS:	Periodic acid-Schiff stain
PALS:	Periarteriolar lymphoid sheath
PCR:	Polymerase chain reaction
PKR:	Protein kinase R also known as double-stranded RNA-dependent protein kinase
PFU:	Plaque forming units
RANTES:	Regulated-upon-activation-normal-T cell-express-sequence
RT-qPCR:	Real-time reverse transcription-polymerase chain reaction
RVF:	Rift Valley fever
RVFV:	Rift Valley fever virus
S:	Small segment
TFIIH:	Transcription factor II Human
TNFα:	Tumour necrosis factor alpha
VHF:	Viral haemorrhagic fever
VHFs:	Viral haemorrhagic fevers
WBV:	Wesselsbron virus

LIST OF FIGURES

Figure 160.	Case 55. Widespread pyknosis and karyorrhexis in a renal glomerulus with a marked decrease in the cellularity of the mesangium.	Panel 29
Figure 161.	Case 5. Deposits of red staining fibrin-related materials (arrow) in the lumen of an arteriole.	Panel 29

LIST OF TABLES

CHAPTER 1

LITERATURE REVIEW

1.1 Introduction

Rift Valley fever (RVF) virus (RVFV) is a significant veterinary and public health threat that has caused widespread outbreaks of disease in humans and livestock in most countries in Africa and the Arabian Peninsula (Pepin et al., 2010). It is caused by a mosquito-borne, single stranded RNA virus of the *Bunyavirales* order, *Phenuiviridae* family (formerly the *Bunyaviridae* family), genus *Phlebovirus* within the species *Rift Valley fever phlebovirus* (Abudurexiti et al., 2019). The virus has only one serological and immunological type and the nucleotide and amino acid sequences are highly conserved (Schmaljohn and Elliott, 2013). During years of abnormally high rainfall, extensive swarms of mosquitoes, mainly of the genera *Aedes* and *Culex*, emerge from standing water, and with sufficient numbers of susceptible unvaccinated livestock in the same area as RVFV-infected mosquitoes, epidemics start to occur (Swanepoel and Coetzer, 2004).

Most human infections with RVFV present as an uncomplicated acute febrile illness, but in a minority of patients severe hepatic disease with haemorrhagic manifestations, renal impairment, encephalitis, and ocular lesions complicate RVF (Al-Hazmi et al., 2003). Additionally, active replication of RVFV in the syncytiotrophoblast layer of the human placenta has been demonstrated, highlighting an increased risk of vertical transmission of the virus to human foetuses and miscarriage in RVFV-infected pregnant woman (McMillen et al., 2018).

The disease mainly affects sheep but cattle, goats, African buffaloes, camelids, and other wild animals are also reportedly affected (Pienaar and Thompson, 2013). Onset of disease in sheep is marked by the development of fever which may be accompanied by anorexia, weakness, listlessness, a nasal discharge, diarrhoea and occasionally haematochezia (Erasmus and Coetzer, 1981). Virtually all pregnant sheep abort if infected with wild-type RVFV and abortion

is a common sequel to recovery in pregnant animals (Daubney et al., 1931, Yedloutschnig et al., 1981, Baskerville et al., 1992). Peracute disease occurs in lambs and calves less than two weeks old, with an estimated mortality as high as 90% to 100% in lambs and 10% to 70% in calves (Bird et al., 2009). Mature livestock are significantly less susceptible to fatal disease with mortality of approximately 10% to 30% in sheep and 5% to 10% in cattle (Bird et al., 2009).

1.2 Epidemiology

A disease resembling RVF was first described in an annual report of the Government of Kenya in 1913 wherein the author, Mr Montgomery, recorded 90% mortality of new born lambs on a farm on Lake Naisvasha (Findlay, 1932). Other farms in the Rift Valley also suffered considerable losses. Post-mortem examination of lambs revealed soft friable livers and, according to Mr Montgomery, who was attending a conference concerning the newly discovered disease, other lesions identical to that described by Daubney et al. in 1931, had also been present (Daubney et al., 1931). The outbreak reported in 1931 again occurred on a farm on the shore of Lake Naisvasha, Kenya, and also caused heavy mortalities in new born lambs, a marked rise in the mortality rate of ewes, and an increased number of abortions. It was demonstrated that RVF was caused by a virus and that the disease could be reproduced by injecting healthy sheep with blood or filtered extracts from the liver or spleen of RVFV-infected sheep (Daubney et al., 1931).

Subsequently, and prior to 1977, recurrent epidemics have occurred in eastern and southern Africa with significant outbreaks in South Africa (1950–1951, 1973–1976) (Swanepoel and Coetzer, 2004, Pienaar and Thompson, 2013). Livestock trade contributes to the spread of the disease into disease-free areas thereby expanding the geographical distribution of RVF (Chevalier et al., 2010). Consequently, between 1977 and 2007 large widespread epidemics of RVF, causing many livestock deaths and human cases occurred, spreading the disease beyond east Africa into Egypt (1977-1978, 1993 and 2003), Mauritania (1998), Somalia (2007) and Sudan (2007) and resulted in re-occurrences in Kenya (2006-2007) and Tanzania (2007) (Jost et al., 2010, Hassan et al., 2011, Munyua et al., 2010, Aradaib et al., 2013, Pienaar and

Thompson, 2013, Caminade et al., 2014, Himeidan et al., 2014, Kenawy et al., 2018). The disease also spread to the Arabian peninsula and caused large epidemics in Saudi Arabia and Yemen (2000-2001) (Shoemaker et al., 2002). Rift Valley fever was also reported in Madagascar (1990) and later in the Comoros (2007) and Mayotte (2007-2008) (Morvan et al., 1991, Sissoko et al., 2009, Cêtre-Sossah et al., 2012). The most recent RVF epidemics were reported from Kenya (2018) and Mayotte (2019) and affected both humans and animals (WAHID, 2018, Eurosurveillance editorial, 2019). Experimentally competent vector species have been identified in Europe and the United States of America, and in the light of the spread of the virus to countries outside Africa, there is a risk of introduction of RVFV into these RVF-free regions (Moutailler et al., 2008, Turell et al., 2008).

The most recent outbreak of RVF in South Africa occurred over a 4-year period from 2008 to 2011 (Pienaar and Thompson, 2013). Although the Free State and the Northern Cape provinces were the worst affected, cases were identified in all nine South African provinces (Pienaar and Thompson, 2013). During this period, 18,887 animal cases were reported including 9015 animal deaths. Sheep were the worst affected species followed by cattle, goats, African buffaloes, camelids, and other wild animals (Pienaar and Thompson, 2013). Rift Valley fever virus infection was also confirmed in 302 humans with 25 deaths reported (Archer et al., 2013). Most cases, inlcuding those in humans, occurred in 2010 following heavy rainfalls across large parts of the country.

Subsequently, an isolated outbreak occurred on a sheep farm in the Free State province in April 2018 with reported cases in sheep and humans (Jansen van Vuren et al., 2018). No other outbreaks were reported between 2012 and 2017 in South Africa. However, interepidemic circulation of RVFV is suspected to occur based on seroprevalence studies in a number of African countries, as well as in ruminants in South Africa in the Free State and northern KwaZulu-Natal provinces (Ngoshe et al., 2019, van den Bergh et al., 2019). In endemic areas, maintenance of RVFV in the interepidemic periods is not well understood but data from seroprevalence studies, published for several African countries, suggests that the virus might

be maintained at low levels in the environment and sporadic clinical cases overlooked or misdiagnosed. A review of surveys conducted prior to 2000 demonstrated significant high-prevalence clusters in areas that had experienced epidemics during the late 20th century and significant low-prevalence clusters in contiguous areas of Western and Central Africa (Clements et al., 2007). In South Africa, high seroprevalence was found in cattle (34%) and goats (31.7%) in northern KwaZulu-Natal province, just south of the Mozambique border, and seroconversions to RVFV were detected throughout the year (van den Bergh et al., 2019). Seroprevalence in cattle, sheep and goats in the Free State province was estimated as 42.9%, 28.0% and 9.3% respectively and the presence of anti-RVFV IgG among domestic ruminants, born after the most recent outbreak, indicated the possibility that virus circulation had occurred during the inter-epidemic period (Ngoshe et al., 2019). In northern Kenya, antibodies to RVFV were detected in samples from children born after the outbreak in 1997–1998 indicating that low levels of transmission to humans continued in the interepidemic period (LaBeaud et al., 2008). Another notable example is Uganda, which prior to 2016 had no RVF outbreaks reported despite its proximity to Kenya and Tanzania where large epidemics in humans and animals had occurred (Nyakarahuka et al., 2019). A study involving 2700 goats in southern Uganda in 2013 reported a seroprevalence of anti-RVFV IgG of 9.8% and the presence of RVF virus neutralizing antibodies (up to 1:80), suggesting that RVF was endemic at least in goats (Magona et al., 2013). Subsequently, between 2016 and 2018 ten outbreaks of RVF were reported in Uganda, where cattle, goats, and sheep sampled in 2016 had a seroprevalence of 27%, 7% and 4% respectively (Nyakarahuka et al., 2019). Another study conducted from 2007 to 2008 on the shores of Lake Malawi in south-western Tanzania demonstrated a seroprevalence of 29.3% in 17 000 human subjects tested, with much lower rates in areas distant to the lake (Heinrich et al., 2012). A recent study of 2014 and 2015 samples from the Democratic Republic of Congo revealed a country-wide distribution of RVF with seroprevalence in cattle ranging from 16.16% in the mountainous zones to 7.34% in the forest zones (Georges et al., 2018). Although Rift Valley fever disease or outbreaks have not been observed in south-western Tanzania or the Democratic Republic of Congo, these findings

suggest that the virus is circulating and that the occasional occurrence of disease is missed (Georges et al., 2018). Therefore, sporadic clinical cases in both animals and humans may be overlooked or misdiagnosed in many countries in Africa and endemic areas of South Africa.

Sequence data demonstrates that the viruses isolated from scattered outbreaks of RVF in parts of north-eastern South Africa in 2008 clustered in Lineage C, which includes viruses isolated during a limited disease outbreak in the Kruger National Park in 1999 (Grobbelaar et al., 2011). Outbreaks were initially recorded in African buffalo in Mpumalanga and Limpopo provinces adjacent to the Kruger National Park and later in Gauteng and the North West province in humans, cattle, sheep and goats (Grobbelaar et al., 2011, Pienaar and Thompson, 2013). During February to June of 2009, viruses from the same lineage caused limited outbreaks in mostly cattle but also sheep and humans in the south of KwaZulu-Natal province (Grobbelaar et al., 2011, Pienaar and Thompson, 2013). In humans, 22 cases were diagnosed in areas where lineage C virus was active, but no deaths. During October to November 2009, lineage H virus, which had been encountered in the Caprivi Strip of Namibia in 2004, caused focal outbreaks in Northern Cape province, again in humans, cattle, sheep, goats (Grobbelaar et al., 2011, Pienaar and Thompson, 2013). The 2010 outbreak affected mostly sheep (13 117 cases reported) and was a continuation of the 2009 outbreaks in KwaZulu-Natal with isolates again clustered in lineage H (Maluleke et al., 2019). In humans, there were 26 deaths among 244 persons infected with lineage H virus (Grobbelaar et al., 2011) The outbreak continued in 2011, this time affecting mostly sheep in the Eastern Cape but also the Western and the Northern Cape provinces (Pienaar and Thompson, 2013).

Researchers hypothesize that new strains evolve in South Africa at a very slow rate due to nucleotide substitution and that they are not introduced from elsewhere outside the country (Grobbelaar et al., 2011, Maluleke et al., 2019). Previous research also suggested that translocated virus initiates smouldering infections in an area, which remain undetected until suitable climatic conditions precipitate an outbreak (Bird et al., 2007, Bird et al., 2008). Bayesian analysis of the diversity of genotypes observed in isolates from the 2008-2010

outbreaks suggest that since the major South African RVF outbreak of 1974-1976, RVFV has gradually spread throughout the interior plateau of South Africa during periods of increased rainfall and was not introduced from a distant location (Grobbelaar et al., 2011). This strengthens the hypothesis that low numbers of cases are overlooked in the interepidemic periods.

1.3 Aetiology

Rift Valley fever virus is an enveloped single-stranded RNA virus with a genome that consists of three segments, large, medium and small (L, M, and S) (Schmaljohn and Elliott, 2013). The L RNA segment codes for the viral RNA-dependent RNA polymerase while the M segment codes for the two envelope glycoproteins, carboxy terminus glycoprotein (G_C) and amino terminus glycoprotein (G_N), as well as two non-structural (NS) proteins, a 14-kDa protein (NSm1) and a 78-kDa protein (a fusion protein that contains the NSm and G_N proteins) (Suzich and Collett, 1988). The S segment codes for the viral nucleocapsid protein (N) and the nucleus-associated non-structural protein (NSs) (Struthers et al., 1984, Schmaljohn and Elliott, 2013). Rift Valley fever virus is unique amongst the *Phenuiviridae* (formally the *Bunyaviridae)* in that the NSs protein forms ribbon-like filaments in the nucleus even though the virus replicates in the cytoplasm of host cells (Struthers and Swanepoel, 1982, Struthers et al., 1984). Following replication in the cytoplasm, the three viral RNA segments form ribonucleoprotein complexes with the viral N protein and RNA polymerase (Ferron et al., 2011, Schmaljohn and Elliott, 2013). The N protein forms a filamentous coat that protects the viral RNA genome and is also required for RNA replication and transcription by the RNA polymerase (Ferron et al., 2011). Late in the infection, G_C combines with G_N to form a polyprotein which localizes to the Golgi complex where the ribonucleoprotein complexes are also recruited by the glycoproteins (Ferron et al., 2011, Schmaljohn and Elliott, 2013). The Golgi complex undergoes morphological changes with vacuolization and dispersion of small and large vesicles in the cytoplasm, which fuse with plasma membrane allowing for the release of virus into the extracellular environment (Schmaljohn and Elliott, 2013). The released virion has an

icosahedral symmetry and measures 90-110 nm in diameter (Ellis et al., 1979, Sherman et al., 2009). The cycle repeats when virus entry into a variety of cells is mediated by the glycoproteins through cellular receptors (Pepin et al., 2010). *In vitro* experiments with human monocyte-derived dendritic cells demonstrated binding and internalization of RVFV by Dendritic Cell-Specific Intercellular adhesion molecule-3-Grabbing Non-integrin (DC-SIGN) (Lozach et al., 2011). Also, RVFV interacts with DC-SIGN through the two envelope glycoproteins G_C and G_N (Phoenix et al., 2016). Therefore, DC-SIGN expressed on the surface of dermal dendritic cells possible play a critical role in the initial transmission of RVFV following an insect bite or mucosal exposure (Lozach et al., 2011). However, this remains to be confirmed under physiological conditions. Liver-Specific Intercellular adhesion molecule-3-Grabbing Non-integrin (L-SIGN) might play a role in the liver tropism of RVFV, however, L-SIGN is expressed on liver sinusoidal endothelial cells and acts as an attachment receptor rather than an endocytic receptor.(Albornoz et al., 2016, Leger et al., 2016) Therefore, the details of this interaction remain to be clarified. Additionally, RVFV infects other cells types, most of which do not express DC-SIGN or L-SIGN (e.g. hepatocytes, adrenocortical cells, renal tubular epithelial cells), another yet to be identified cellular receptor likely plays a secondary role in further rounds of RVFV infection in tissues (Lozach et al., 2011, Schmaljohn and Elliott, 2013).

The NSs protein has many biological functions in infected cells which include modulating the interferon response, facilitating efficient viral translation and acting as a general inhibitor of transcription (Ly and Ikegami, 2016). Nucleus-associated non-structural protein counteracts the host's antiviral interferon (IFN) system by preventing nuclear activation of the IFN-β gene and the cytoplasmic transcription of interferon mRNAs (Le May et al., 2004, Ikegami et al., 2009b). As a result, unrestricted viral replication is promoted. Additionally, nuclear NSs filaments binds to Sin3A Associated Protein 30 (SAP30) and to Yin Yang 1 (the activator/repressor of interferon transcription), forming a multiprotein repression complex on the IFN-β promoter and blocking interferon expression (Le May et al., 2008). The NSs protein

also allows for efficient viral translation and replication in infected cells by downregulating the activation of double-stranded RNA (dsRNA)-dependent protein kinase also known as protein kinase R (PKR) (Ikegami et al., 2009b). Protein kinase R is activated by dsRNA, introduced to cells during viral infection, and once active PKR phosphorylates eukaryotic translation initiation factor (eIF)2α, thereby suppressing viral translation. In RVFV-infected cells, NSs decreases PKR abundance and prevents eIF2α phosphorylation which augments viral replication (Ikegami et al., 2009a). The NSs protein also inhibits general transcription activity in cells by directly interacting with components of the basal transcription factor II human (TFIIH) (Le May et al., 2004, Kalveram et al., 2011). The p44 subunit of the TFIIH complex is sequestered by the NSs filamentous structure, thereby blocking assembly of TFIIH and drastically reducing transcriptional activity in RVFV-infected cells (Le May et al., 2004). In addition, NSs protein interacts with the TFIIH subunit p62 and promotes its post-translational degradation (Kalveram et al., 2011). The presence of NSs filaments in the nucleus of infected cells also induces DNA damage responses and causes cell-cycle arrest which causes the activation of p53 and apoptosis (Baer et al., 2012)

The NSm protein of RVFV suppresses apoptosis of target cells (Won et al., 2007). The NSm protein of RVFV suppresses apoptosis in target cells (Won et al., 2007). Induction of apoptosis in virus infection, and subsequent phagocytosis of virus-infected cells, is one of the host defence mechanisms that eliminates infected cells thereby limiting viral replication and spread (Nainu et al., 2017). It has been demonstrated that RVFV triggers apoptosis mainly through activation of caspase-8, specifically that the NSm protein supresses the expression of caspase-8 in infected cells thereby ensuring the efficient release of progeny RVFV within the first 24 hours after infection (Won et al., 2007). As a result, the majority of the progeny virus is released prior to virus induced apoptosis. Without the NSm protein, RVFV is not able to amplify efficiently in an infected host since the virus' presence induces a rapid progression to cell death in virtually all infected vertebrate cell types and there is not enough time for viral replication to secure efficient production of progeny virus (Won et al., 2007). Virus infected cells that undergo

transcriptional or translational suppression, as demonstrated for RVFV, may also be exposed to tumour necrosis factor alpha (TNFα) and rapidly die by apoptosis (Won et al., 2007). Most humans and animals do not develop fatal RVF disease, presumably due to variations in the host's innate immune response and exposure of the infected cells to extracellular factors, such as TNFα, that induce apoptosis prior to the completion of maximum progeny virus production (Won et al., 2007). This process may prevent severe, nearly diffuse necrosis of cells in some species or age groups preventing the death of the host and promoting the completion of the life cycle of the virus (Won et al., 2007).

1.4 Gross and histological lesions

There are several extant studies that include descriptions of RVF post-mortem lesions in sheep which are summarized in Table 1 (Daubney et al., 1931, Findlay and Daubney, 1931, Easterday et al., 1962a, Easterday et al., 1962b, Schulz, 1951, Coetzer, 1977, Coetzer and Ishak, 1982, Olaleye et al., 1996, Van Der Lugt et al., 1996, Shieh et al., 2010, Faburay et al., 2016a, Faburay et al., 2016b, Wichgers Schreur et al., 2016). Generally, the lesions in young animals are different from those observed in adult sheep (Pepin et al., 2010). The most prominent differences were noted in the liver, kidneys and lymphoid tissues (Daubney et al., 1931, Easterday et al., 1962a, Coetzer, 1977). There is no clear explanation for these differences but they may be due to age-related susceptibility of the primary target cells of RVFV (Pepin et al., 2010). Alternatively, the innate immune response to RVFV infection in young animals might be inadequate, resulting in their increased susceptibility to fatal RVF and higher viraemia levels (Pepin et al., 2010).

In adult animals, the liver has a red mottled appearance due to the presence of innumerable ill-defined necrotic foci (Daubney et al., 1931). Histologically foci of necrosis are random multifocal, focally extensive, or confluent bridging (Odendaal et al., 2014). In young lambs, the liver is paler, occasionally dull yellow with pale pinpoint foci of necrosis and subcapsular petechiae (Daubney et al., 1931). Another common finding in adult animals is a mild infiltrate of mononuclear inflammatory cells in the portal tracts and involvement of hepatocytes within

the limiting plate (Odendaal et al., 2014). In young lambs and foetuses necrotic foci coalesce and involve virtually all hepatocytes, with various studies describing the liver lesion in young lambs as massive or widespread (Findlay, 1932, Schulz, 1951, Easterday et al., 1962a, Coetzer, 1977) Liver necrosis is generally accompanied by haemorrhage and a mild to moderate infiltrate of neutrophils, lymphocytes, and macrophages (Odendaal et al., 2014). Bile stasis is not present in any of the age categories (Odendaal et al., 2014).

Injured hepatocytes often have features of apoptosis that include dissociation of cells, shrinkage and rounding, hypereosinophilic cytoplasm and karyorrhexis or karyolysis (Odendaal et al., 2014). These early apoptotic bodies are also referred to as Councilman bodies or acidophilic bodies (Coetzer, 1977). Late apoptotic bodies are present as small cytoplasmic fragments with or without intracytoplasmic nuclear fragments (Odendaal et al., 2014). Surviving hepatocytes usually have varying degrees of micro- or macrovesicular degeneration and anisokaryosis (Odendaal et al., 2014). A very distinctive feature in neonates and foetuses are randomly located foci of well circumscribed cytolysis also referred to as primary foci (Coetzer, 1977, Coetzer and Ishak, 1982, Odendaal et al., 2014). These foci vary in size and number and contain dense aggregates of hepatocellular debris, degenerate neutrophils, and sparse macrophages (Odendaal et al., 2014). Rod to oval-shaped eosinophilic intranuclear inclusions are occasionally present in injured hepatocytes, however, they are often difficult to detect in adult animals, compared to foetuses or neonates where they are often diagnostically useful (Odendaal et al., 2014). Interestingly, the hepatic lesions in human beings are similar to those in ruminants. Foci of hepatic necrosis are associated with haemorrhage and involve mid to central zones of the hepatic lobule, but often extend peripherally to the portal tracts (Van Velden et al., 1977). Typical Councilman bodies and a mild inflammatory infiltrate of predominantly lymphocytes and macrophages with a few neutrophils and a lack of bile stasis is also described in humans (Van Velden et al., 1977). Consequently, further study of RVF in ruminants may also inform our understanding of RVF liver pathogenesis in humans.

Macroscopically, sheep kidneys usually only have a few small cortical haemorrhages (Daubney et al., 1931). Microscopically, adult sheep occasionally have a severe nephrosis characterized by marked tubular epithelial degeneration and necrosis (Daubney et al., 1931, Faburay et al., 2016a, Faburay et al., 2016b). However, in lambs, the kidney lesion rarely progresses beyond tubular epithelial cell degeneration, characterized by cell swelling and nuclear fading (Daubney et al., 1931). In 1931, lesions in the kidney were deemed non-specific and a toxic degenerative change (Daubney et al., 1931). Pyknosis and karyorrhexis of cellular elements in the glomerulus of new-born lambs was reported in 1977, but also not regarded further (Coetzer, 1977). Subsequent research comparing the susceptibility of three breeds of Nigerian sheep to experimental RVFV infection reported increased blood urea nitrogen (BUN) values starting on day three post-infection and continuing until the animals died (Olaleye et al., 1996). Another recent experimental study, also reported increased BUN values and histopathological changes indicative of renal injury in several of the sheep (Faburay et al., 2016a). These findings suggest that the kidney lesion may be more significant than was previously thought. Similarly, in human patients that died of RVF, subcapsular renal haemorrhages, degeneration of proximal tubular epithelial cells and a slight infiltrate of cells in the glomeruli are described (Van Velden et al., 1977). Also, focal renal tubular epithelial necrosis in a single human kidney sample was reported as a novel finding in 2010 and the authors remarked that the validity and clinical importance of this finding warrants further investigation (Shieh et al., 2010).

Typically, RVFV-infected spleens are often described as having sub-capsular petechiae and may be normal in size or slightly enlarged (Daubney et al., 1931, Findlay and Daubney, 1931, Schulz, 1951, Coetzer, 1977, Coetzer et al., 1978). Prior to 1951, researchers had little to remark about microscopic lesions in the spleen other than occasional mentions of nuclear pyknosis and karyorrhexis in the splenic parenchyma (Daubney et al., 1931, Findlay and Daubney, 1931). Subsequent research reported extensive lymphocytolysis giving the red and the white pulp a washed-out appearance (Coetzer, 1977, Olaleye et al., 1996, Van Der Lugt

et al., 1996, Faburay et al., 2016a, Faburay et al., 2016b). In neonates, although the lymphoid tissues are not fully developed, lymphoid depletion is present histologically (Easterday et al., 1962a).

Macroscopically, lymph nodes are often described as enlarged and oedematous with scattered haemorrhages in the cortex and medulla (Daubney et al., 1931, Findlay and Daubney, 1931, Coetzer, 1977, Olaleye et al., 1996, Van Der Lugt et al., 1996). Lesions in the mesenteric lymph nodes are frequently emphasised in these reports. Additionally, haemorrhage and lymphocyte pyknosis and karyorrhexis are occasionally present microscopically. In the intestinal tract, lymphoid depletion in the lamina propria is most severe in the distal jejunum and ileum and include moderate oedema, pyknosis and karyorrhexis of mononuclear cells in the submucosa and a neutrophil infiltrate (Coetzer, 1977). Lastly, varying degrees of lymphocyte pyknosis and karyorrhexis are also present in the Peyer's patches and correspond in degree of intensity to the changes in other lymphoid tissues throughout the body (Coetzer, 1977).

Lung lesions are largely not remarked upon prior to 1951 and when mentioned, researchers report that they are normal in size and colour and lacking haemorrhages, and that the alveolar capillaries are distended with leucocytes histologically (Daubney et al., 1931, Findlay and Daubney, 1931). Subsequent reports describe macroscopic lung oedema and multifocal haemorrhages or blood in the trachea and bronchi with oedema and haemorrhage confirmed microscopically (Schulz, 1951, Coetzer, 1977, Olaleye et al., 1996). Coetzer was the first to describe single cell pyknosis and karyorrhexis in the alveolar septae and peribronchial lymphoid tissues with low numbers of neutrophils and macrophages in the interstitium (Coetzer, 1977) This pulmonary interstitial infiltrate is later characterized as mononuclear (Van Der Lugt et al., 1996). In fatal human RVF cases there is also frank haemorrhage in the lungs, with microscopic alveolar oedema and haemorrhage (Van Velden et al., 1977).

Other macroscopic lesions include hydropericardium, hydrothorax and ascites; sub-epicardial ecchymoses in the region of the coronary grooves on the ventricles of the heart, sub-

endocardial haemorrhages in the left ventricle; marked congestion of the mesenteric and omental vessels with subperitoneal petechiae and ecchymoses along the entire course of the gastrointestinal tract; haemorrhages in the abomasum and occasional enteric haemorrhage; haemorrhages in the wall of the gall bladder including occasionally blood in the lumen; cortical and medullary haemorrhages in the adrenal glands; and subcutaneous haemorrhages (Daubney et al., 1931, Findlay and Daubney, 1931, Schulz, 1951, Coetzer, 1977, Coetzer and Ishak, 1982, Olaleye et al., 1996, Van Der Lugt et al., 1996, Faburay et al., 2016a, Faburay et al., 2016b, Easterday et al., 1962a). Microscopically, there are sub-epicardial and sub-endocardial haemorrhages as well as haemorrhages in the serosa and mucosa of the gall bladder and the gastrointestinal tract (Daubney et al., 1931, Schulz, 1951, Coetzer, 1977). In the adrenal glands necrosis varies from individual cells to aggregates and is found predominantly in the zona fasciculata, although occasionally cells in the zonae glomerulosa and reticularis are also involved (Easterday et al., 1962a, Coetzer, 1977).

In foetuses, previous research into experimental and natural RVF ruminant cases reported that there were no significant macroscopic lesions other than occasional necrotizing hepatitis (Antonis et al., 2013, Baskerville et al., 1992, Daubney et al., 1931). Necrosis of the placenta has been reported in experimental RVFV infection of pregnant ewes but it is unknown if this lesion is consistently present in all ovine abortions (Antonis et al., 2013, Baskerville et al., 1992). Deposition of aggregates of calcium and an intense vasculitis involving many blood vessels have also been reported (Baskerville et al., 1992). However, the intercaruncular of the uterus and placenta were normal (Baskerville et al., 1992).

Table 1: Gross and histologic lesions for RVF reported in previously published studies.

Reference	Age and number of sheep used in study	Tissue	Gross and histologic findings for RVFV
Daubney et al., 1931	Natural disease. Lambs 3-7 days old (3500 deaths recorded) Ewes (1200 deaths recorded)	Liver:	Macroscopically in adult sheep, innumerable ill-defined necrotic foci in the liver imparting a red mottled appearance. Necrotic foci paler than the normal tissue making the rest of the liver parenchyma appear congested and haemorrhagic. In lambs, necrotic foci are more or less evenly distributed throughout the organ and may coalesce to from a diffuse necrotic lesion. Liver not enlarged. Histologically, focal degeneration of hepatocytes is closely followed by an infiltrate of predominantly neutrophils and macrophages. This could be anywhere in the lobule but is more frequently centrilobular. Infiltrating cells degenerate and lesions contain masses of granular chromatin derived from the nuclei of both infiltrating cells and necrotic hepatocytes. The cytoplasm of affected hepatocytes initially become more eosinophilic. Later, cells become contracted and rounded and more or less completely separated from one another and the nuclei undergo degeneration. The more advanced lesion may involve up to two-thirds or more of the entire lobule. The process in lambs is extremely rapid and the destruction so severe as to obscure completely the actual nature of the lesion. A few hepatocytes remain at some portion of the periphery of the lobule in lambs.
		Spleen:	Not enlarged. Petechia beneath the capsule chiefly along the free border. Microscopically the capsular haemorrhages do not extend deep into the organ. Histologically, occasional pyknosis and karyorrhexis in the pulp.

Lymph nodes:	Mesenteric lymph nodes always enlarged. They appear more moist than normal on section and often contain haemorrhages. Histologically, no distinct necrotic foci in the lymph nodes. Occasional karyorrhexis of leucocytes in areas of haemorrhage.
Lung:	Normal in size and colour and no haemorrhages present. Distention of alveolar capillaries with leucocytes, mostly neutrophils.
Kidneys:	Macroscopically, a few small ill-defined haemorrhages in the cortex. Tubular degeneration or nephrosis microscopically. Nephrosis not in lambs due to the peracute course of the disease. Adult sheep might live long enough for the development of tubular nephrosis and the actual lesion found post-mortem might depend on the length of time that they survive. Changes begin in the convoluted tubules while other tubules and the glomeruli appear normal. Later the glomeruli may contain more nuclei than normal, some of which are that of neutrophils. Karyorrhexis, thought to originate from infiltrating neutrophils also present in the glomeruli.
Heart:	Sub-epicardial ecchymoses in the region of the coronary grooves on the ventricles of the heart. Sub-endocardial haemorrhages in the left ventricle. Lesions rare in the right heart. No other lesions, other than haemorrhages, microscopically.
Mesentery:	Marked congestion always present in mesenteric and omental vessels. Described as a very characteristic feature of the disease.
Intestines:	Mucous membranes of the abomasum might be congested or on occasion have petechia. Occasionally enteric haemorrhage. Marked infiltrate of neutrophils, many of which are karyorrhectic in the interglandular tissues and particularly around the lymphoid follicles.
Brain:	No lesions apart from congestion of the meningeal vessels.

Findlay and Daubney, 1931	Experimental cases. Three lambs (one was 2 weeks old. Age of other two not mentioned). One ewe (not killed).	Liver:	Not enlarged. Paler in colour, occasionally dull yellow. Pale pinpoint foci of necrosis and tiny subcapsular haemorrhages. Complete destruction of liver lobules due to necrosis in two lambs. Random necrotic foci in the third lamb, sometimes close to the portal space or central vein, but more often midzonal. The size of the foci vary and coalesce in places. Infiltrate of predominantly neutrophils and macrophages of which many have degenerative changes.
		Spleen:	Not enlarged. Petechiae beneath the capsule and more especially near the free border. No lesions histologically.
		Lymph nodes:	Mesenteric lymph glands enlarged. Appear more moist than normal on section with haemorrhages in two lambs. Occasionally haemorrhagic foci and an infiltrate of neutrophils, many karyorrhectic.
		Lung:	No gross lesions. Congestion and many neutrophils in the interalveolar capillaries.
		Kidney:	Macroscopically congested. No significant microscopic lesions.
		Heart:	Sub-epicardial ecchymoses in the region of the coronary grooves on the ventricles of the heart. Sub-endocardial haemorrhages in the left ventricle. No lesions microscopically other than haemorrhages.
		Mesentery:	Mesenteric and omental vessels deeply engorged.
		Intestines:	Petechia in the mucous membranes of the abomasum. Numerous neutrophils, many of which are karyorrhectic, in the interglandular tissues.
		Adrenals:	No gross lesions.
		Brain:	No lesions apart from congestion of the meningeal vessels in one case.

Schulz, 1951	Natural cases. Adult sheep and newly born lambs.	Liver:	Enlarged. The surface has a mottled appearance. Focal necrosis in adult sheep and widespread, affecting most of the liver, in lambs. Necrotic foci infiltrated by neutrophils and macrophages a number of which are degenerate. Chromatin derived from the nuclei of infiltrating parenchymatous cells scattered throughout.
		Gall bladder:	Wall often hyperaemic and oedematous. Subserosal haemorrhages especially in the region of its attachment to the liver. Microscopically, subserosal and intermuscular haemorrhages.
		Spleen:	Enlarged with petechiae beneath the capsule. Cellular content of the white pulp reduced. Necrosis in the pulp.
		Lymph nodes:	Enlarged and moist on cut surface. Haemorrhages in the cortex of the mesenteric lymph glands. Necrosis in the vicinity of haemorrhages.
		Lung:	Marked hyperaemia and oedema of the lungs. Subpleural and focal pulmonary haemorrhages. Sometimes a hydrothorax. Microscopically, congestion, oedema and emphysema. Perivascular haemorrhages.
		Kidney:	Enlarged. Degenerative changes in the renal tubules.
		Heart:	Subepicardial and subendocardial ecchymoses. Hydropericardium invariably present.
		Adrenal:	Enlarged with haemorrhages in the cortex and medulla.
		Skin/subcutis:	Cutaneous and subcutaneous haemorrhages. Especially in the axillary region, the medial aspect of the hind limbs, and in the lower portions of the extremities.
		Intestines:	Subperitoneal, mucosal and submucosal haemorrhages. Oedematous and haemorrhagic mesenteric lymph nodes. Congestion and sometimes haemorrhage of the gastric and intestinal mucosa. Subperitoneal petechiae and ecchymoses along the entire course of the gastrointestinal tract. Sometimes an ascites.
		Brain:	Congestion of the meningeal vessels. Degenerative changes in neurons.

Easterday et al., 1962a	Experimental. 14 Lambs 1-5 days old	Liver:	Grey to faintly yellow pinpoint foci in the parenchyma. Irregularly congested, focally to extensively haemorrhagic, and very soft. Between 12 to 24 hours, intra- sinusoidal aggregates of neutrophils appear. Small areas of hepatocellular necrosis appear between 24 and 36 hours. These are predominantly midzonal and gradually enlarge. Precipitously, all but a few periportal parenchymal cells are destroyed. Primary foci became devoid of inflammatory cells in most. Varying amounts of haemorrhage are present.
		Spleen:	Macroscopically, not enlarged and the white pulp is depleted. Lymphoid tissues not fully developed. Lymphoid depletion histologically. Foci of cytolysis and phagocytosis of debris bordering the white pulp.
		Lymph nodes:	Minimally enlarged and turgid. Mottled pink cut surface. Lymphoid tissues not fully developed. Lymphoid depletion histologically. Foci of cytolysis and phagocytosis of debris in the sinuses.
		Lung:	No abnormalities other than a few fibrin thromboemboli in the small pulmonary arteries.
		Kidney:	No renal tubular damage.
		Heart:	Petechiae and ecchymoses in the endocardium.
		Adrenal:	Focal or diffuse haemorrhages in the cortex. Necrosis varies from individual cells to aggregates predominantly in the zona fasciculata, though in a few cases the zona glomerulosa is involved. Cortical necrosis without haemorrhage is more frequently present.
		Intestines:	Petechiae and ecchymoses in the mucosa and serosa. Mild ascites. Lymphoid depletion in the lamina propria of the small intestine. More noticeable than in the lymph nodes and spleen.
		Brain:	No lesions.

Coetzer, 1977	Natural cases. 34 lambs (8 sacrificed *in extremis*)	Liver:	Slight icterus. Necrotic foci scattered throughout. Haemorrhages, 2-3cm in diameter, in the subcapsular region and throughout the substance of the liver. Massive hepatic necrosis only preserving the portal triads. In a few cases small groups of surviving hepatocytes present in the portal triads.
		Gall bladder:	Slight to moderate oedema. Pyknosis and karyorrhexis of mononuclear cells in the lamina propria and focal haemorrhages in the serosa and lamina propria.
		Spleen:	Subcapsular petechiae. Microscopically, extensive necrosis of lymphocytes that give the red and the white pulp a washed-out appearance. Most apparent in the white pulp.
		Lymph nodes:	Enlarged, congested and oedematous. Petechiae in the cortex and medulla. Pyknosis and karyorrhexis of lymphocytes most marked in the cortex.
		Lung:	Occasional subpleural petechiae and ecchymoses with moderate emphysema and severe congestion and oedema. Histologically, mild to moderate congestion and oedema with occasional focal haemorrhages. Single cell pyknosis and karyorrhexis in the alveolar septae and peribronchial lymphoid tissues. In a few cases a mild infiltrate of neutrophils and macrophages in the interstitial tissue.
		Kidney/ urinary bladder:	Usually normal. Occasionally petechiae in the renal cortex. Infrequently small haemorrhages in the urinary bladder. Renal tubular epithelial degeneration in most lambs with necrosis in a few. Pyknosis and karyorrhexis of cellular elements within the glomeruli in 10% of cases.
		Heart	Subepicardial and subendocardial haemorrhages. Occasionally a mild hydropericardium. Except for haemorrhages no other histological changes.
		Adrenal:	Haemorrhage and necrosis in the cortex. More pronounced in the *zona fasciculata* and *zona reticularis.*

		Intestines:	Moderate ascites. Petechiae and ecchymoses on the visceral peritoneum but most marked in the mucosa of the abomasum. Histologically, changes are most severe in the distal jejunum and ileum. Pyknosis and karyorrhexis of mononuclear cells in the submucosa with moderate oedema and a neutrophil infiltrate. Varying degrees of pyknosis and karyorrhexis in lymphocytes in the Peyer's patches corresponding in degree of intensity to the changes in other lymphoid tissues in the body.
		Brain:	Slight congestion and oedema in some lambs.
		Other:	No lesions in the testis, uterus, pancreas, thyroid gland, salivary glands, thymus, tongue and skeletal muscles.
Yedloutschnig et al., 1981	Vaccine study, 58 pregnant ewes	Ewes:	A single vaccine dose did not protect the ewes against challenge with virulent (wild-type) RVFV and all the ewes either aborted or had dead foetuses in utero. Abortion between 6 and 18 d.p.i.
		Foetus:	Extensive liver necrosis reported but the numbers examined not mentioned.
Coetzer and Isak, 1982	10 new-born lambs (1 to 4 days old)	Liver:	Mild hepatocellular degeneration 6 hours post infection (h.p.i.) with RVFV, with scattered acidophilc bodies and a few neutrohils in the sinusoids. At 12-18 h.p.i., more advanced hepatocellualr degeneration with single necrotic hepatocytes and acidophilic bodies in the lobules, accompanied by a mild proliferation of macrophages and a mild infiltrate of neutrophils. At 24 h.p.i. primary foci, composed of necrotic disintegrated haptocytes and a few neutrophils, are present. These foci initially involve 5-8 hepatocytes but become larger and more circumscribed by 30-36 h.p.i. by which time they also contain abundant cellular debris and a few neutrophils and macrophages. At 48 h.p.i. most hepatocytes are necrotic and in the process of disintegration. In lambs in extremis 51-53 h.p.i. massive hepatic necrosis is present and due to cytolysis the parenchyma has a porous appreance and acidophilc bodies and few neutrophils are dispersed throughout the parenchyma. Eosinophilic filamentous or rod shaped intranuclear inlcusions are present in a low percentage of hepatocytes as well as minerilization of isolated hepatocytes.

Baskerville et al., 1992	Experimental - 20 pregnant ewes 4 infected with virulent RVFV and 16 innoculated with a avirulent vaccine strain	Foetus:	All 4 ewes infected with a virulent (wild-type) strain of RVFV aborted 9, 10 and 17 d.p.i. and 5 foetuses were recovered. The 4 ewes were killed one day after aborting and remains of another foetus were found in the uterus of 2 of the ewes and evidence of a resorbed foetus in the uterus of another ewe. No physical abnormalities in any of the foetuses with normal wool covering and hoves. Some autolysis histologically but insufficient to impair histological evaluation of tissues. No histological lesions in the liver, brain, kidneys or lungs.
		Uterus and placenta:	Intense inflammation, necrosis and an infiltrate of large numbers of neutrophils in the maternal caruncle at the level of the upper lamina propria. Distal to this zone there is complete necrosis of villi and deposition of aggregates of calcium. Intense vasculitis of many blood vessels. Necrosis also present in foetal cotyledons. Intercaruncular areas of the uterus and placenta normal.
Olaleye et al., 1996	Experimental (18 sheep between 7 to 11 months old)	Liver:	Slightly friable with pinpont areas of necrosis macroscopically. Marked coagulative hepatic necrosis.
		Spleen:	Spleen slighly enlarged in the Yankasa breed but firm and shrunken in the West African dwarf or Ouda breed. Lymphoid depletion microscopically.
		Lymph nodes:	Bronchial lymph nodes oedematous and haemorrhagic. Mesenteric lymph nodes enlarged, oedematous and hyperaemic. Lymphoid depletion microscopically.
		Nasal passages and lung:	Hyperaemic nasal turbinates. Blood clots in the trachea and bronchi of Yankasa breed of sheep but not West African dwarf or Ouda sheep. Blood in the lungs of the Yankasa breed and only red-tinged oedema in the West African dwarf or Ouda sheep. Lung oedema and haemorrhage microscopically.
		Kidney:	Pulpy and bulging on cut surface with petechiae on the serosal and cut surfaces. Microscopically, marked renal tubular degeneration.
		Heart:	Ecchymosis on the pericardium and endocardium
		Skin/mucosa/ subcutis:	Petechiae and ecchymoses on the conjunctivae, oral mucosa, anal regions and other hairless parts of the body. Subcutaneous haemorrhages.
		Intestines:	Hyperaemia and focal haemorrhages along the gastrointestinal tract. Marked ascites in the Yankasa sheep.

Van Der Lugt et al., 1996	12 new-born lambs of 1 to 4 days old (8 experimental and 4 natural)	Liver:	Hepatocellular necrosis.
		Spleen, lymph nodes:	Lymphoid necrosis.
		Lung:	Congestion and oedema with multifocal necrosis in alveolar walls and peribronchial tissue. Intravascular mononuclear cells.
		Kidney:	Sparse necrosis.
Antonis et al., 2013	Experimental infection of 11 pregnant ewes	Ewes:	No significant lesions in the organs of 4 ewes infected in the first trimester. Remnants of cotyledons and foetal membranes present.
			Necrotizing hepatitis and lung oedema in 1 of 3 ewes infected in the second trimester.
			Necrotizing hepatitis in 2 of 4 ewes infected in the third trimester.
		Foetus	No abnormalities in two live foetuses recovered from two first trimester ewes.
			Five dead foetuses and 2 live foetuses recovered from 3 second trimester ewes.
			Seven dead foetuses recovered from 4 third trimester ewes. One foetus with haemorrhages in the liver and oedema of the lymph nodes. Multifocal necrotizing hepatitis in 2 other foetuses.
		Placenta:	Focal necrosis in the cotyledons. Diffuse calcification and vascular thrombosis in a specimen from a third trimester ewe.
Odendaal et al., 2014	380 animals (119 cattle and 261 sheep) that included adults, neonates and foetuses	Liver:	Extent of liver involvement varies with age. In adult animals, foci of necrosis are random multifocal, focally extensive, or confluent bridging. In most neonates and foetuses necrosis involves almost all the hepatocytes. Haemorrhage and a mild to moderate infiltrate of neutrophils, lymphocytes, and Kupffer cells are generally present in areas of necrosis. Affected hepatocytes have features of apoptosis. Surviving hepatocytes usually have varying degrees of micro- or macrovesicular degeneration and anisokaryosis. A very distinctive feature in many cases (especially in neonates and foetuses) is randomly located foci of well circumscribed cytolysis (primary foci). Eosinophilic intranuclear inclusions are occasional present in injured hepatocytes. However, inclusion bodies are often difficult to detect and less common in the livers of adult animals compared to foetuses or neonates.

Faburay et al., 2016a	Fourteen 4–5-month-old sheep. Two mock-inoculated. Twelve inoculated with RVFV	Liver:	Hepatocellular necrosis.
		Spleen:	Lymphoid follicle depletion, red pulp necrosis and fibrin deposition. Scattered perifollicular necrosis involving the red pulp.
		Lymph nodes:	Histiocytosis.
		Lung:	Pulmonary oedema.
		Kidney:	Kidney glomeruli hypercellular in one sheep. Also, multifocal renal tubular necrosis with adjacent lymphoplasmacytic interstitial nephritis in the same sheep.
		Adrenal gland:	Multifocal adrenocortical necrosis in the zona fasciculata.
		Heart:	Foci of histiocytic and lymphoplasmacytic inflammation.
		Brain:	Occasional glial nodules in cerebral parenchyma of 2 sheep and perivascular lymphohistiocytic inflammation in the brainstem of 1 sheep.
Faburay et al., 2016b	Five vaccinated and 5 mock-vaccinated, 4-5 month old sheep	Liver:	Hepatocellular necrosis.
		Spleen:	Lymphoid follicular depletion and perifollicular red pulp necrosis.
		Lung:	Pulmonary oedema.
		Kidney:	Tubular necrosis attributable to RVFV in 1 sheep. Lymphoplasmacytic interstitial nephritis.
		Adrenal gland:	Scattered adrenocortical cell apoptosis.

Wichgers Schreur et al., 2016	Twenty-four lambs in a group of 40, between 7 and 9 weeks of age, was infected with RVFV	Liver:	Hepatocellular necrosis.
Vloet et al., 2017	Two 12-week-old sheep on which mosquitoes were allowed to feed during the viremic period of RVFV infection	Liver: Skin:	Diffuse hepatic necrosis. Extensive haemorrhages in the superficial and deep dermis at the site of mosquito bites. Blood vessels severely dilated with neutrophils and thrombocytes marginating at the periphery. Increased numbers of neutrophils and macrophages in the dermis, and hydropic degeneration of keratinocytes, acantholysis and cleft formation in the epidermis. Also, exocytosis of neutrophils with crust formation on the epidermis.

1.5 Tissue and cell tropism

Only a limited number of immunohistochemical studies of the tissue and cell tropism of RVFV infection in sheep, based on field animal samples and experimental animal specimens, exist. The findings in these studies are summarized in Table 2. Van Der Lugt et al. studied the tropism of RVFV by IHC in tissues from 8 experimentaly infected and 4 naturally infected new-born lambs (Van Der Lugt et al., 1996). Acute fatal disease with extensive hepatocyte necrosis and a progressive increase in viral antigen in the liver was reported. Viral antigen was also found in a few cells in the spleen, lymph nodes, kidneys and lungs. Shieh et al. reported that a liver specimen from one sheep and an autolysed spleen specimen from another sheep was positive for RVFV by IHC (Shieh et al., 2010). In experimentally infected 3-4 month old sheep (n = 12) viral antigen was most prominent in the liver and the spleen, with lesser amounts of antigen also present in the adrenal glands and kidney from one animal (Faburay et al., 2016a).

In a study using a RVFV vaccine candidate in sheep, positive IHC labelling was reported in the liver, spleen, kidney, lymph nodes and lungs of 2 of 5 mock-vaccinated sheep and in the adrenal glands of one sheep (Faburay et al., 2016b). Foci of hepatic necrosis were strongly positive for viral antigen in all the mock-vaccinated sheep. Two sheep had splenic lymphoid follicular depletion and perifollicular red pulp necrosis, multifocal renal tubular necrosis, lung oedema and necrosis of scattered adrenocortical cells (Faburay et al., 2016b). Viral antigen-positive macrophages or possible dendritic cells were present in circulation in the lungs and in the medullary sinuses of the mesenteric lymph nodes (Faburay et al., 2016b). There was also intravascular viral antigen in the glomeruli and rare scattered viral antigen positive cells in the adrenal cortex (Faburay et al., 2016b). A study to determine if RVFV can be transmitted from infected lambs to either immunocompetent or immunosuppressed lambs, reported RVFV antigen in hepatocytes and in mononuclear phagocytes in the liver, spleen and lymph nodes (Wichgers Schreur et al., 2016). One lamb exhibited intense positive staining of endothelial cells lining both smaller and larger veins in the spleen, tonsil and lymph nodes. The location

of the RVFV-infected mononuclear phagocytes was not further characterized in this study. The most recent experimental study reports intense labelling of RVFV antigen in endothelial cells of dermal blood vessels, macrophages, smooth muscle cells, lipocytes, keratinocytes and fibroblasts in skin exposed to RVFV-infected mosquitos (Vloet et al., 2017).

Table 2: Immunohistochemical results reported for RVFV antigen in previously published studies.

Study	Age of sheep and number in study	Tissue	Immunohistochemical result
Van Der Lugt et al., 1996	12 new-born lambs	Liver:	Positive hepatocytes in all the lambs.
		Spleen, lymph nodes:	Scattered positive cells in the red pulp of the spleen in three lambs, and in the cortex, paracortex and medullary cords of lymph nodes in two lambs.
		Lung:	Labelling in a small number of unidentified cells in alveolar walls and in alveolar macrophages in three lambs.
		Kidney:	Viral antigen in mesangial cells in the renal glomeruli.
Shieh et al., 2010	Two sheep of unknown age	Liver:	Positive hepatocytes in one sheep.
		Spleen:	Specimen autolysed but positive in one sheep. No attempt to identify cells.
Faburay et al., 2016a	Fourteen 4 to 5-month-old sheep. Two mock-inoculated. Twelve inoculated with RVFV	Liver:	Positive hepatocytes and macrophages in 6 sheep.
		Spleen:	Viral antigen in three sheep. No data about labelling cells.
		Lymph nodes:	Labelled histiocytes in the sinusoids.
		Lung:	Negative for viral antigen.
		Kidney:	Kidney glomeruli positive for viral antigen in one sheep. The same sheep had viral antigen in tubular epithelial cells and luminal debris.
		Adrenal gland:	Foci of necrosis in the zona fasciculata were positive for RVFV antigen in 1 sheep
		Heart:	Negative for viral antigen.
		Brain:	Negative for viral antigen.

Faburay et al., 2016b	Five vaccinated and 5 mock-vaccinated, 4-5-month-old sheep	Liver:	Labelling in the cytoplasm of hepatocytes and in intralesional macrophages in all mock-vaccinated sheep.
		Spleen:	Viral antigen in 2 sheep, mostly perifollicular.
		Lymph nodes:	Scattered positive sinusoidal histiocytes in 2 sheep
		Lung:	Viral antigen in macrophages or possible dendritic cells in circulation in 2 sheep.
		Kidney:	Evidence of glomerular filtration of viral antigen in 2 sheep.
		Adrenal gland:	Rare viral antigen positive cells in 1 sheep
Wichgers Schreur et al., 2016	Twenty-four lambs in a group of 40, between 7 and 9 weeks of age, was infected with RVFV	Liver:	Labelling of hepatocytes and mononuclear phagocytes.
		Spleen, lymph nodes:	Viral antigen in mononuclear phagocytes. Data about locality of labelling cells not provided. One lamb with labelling of endothelial cells lining veins.
		Tonsils:	Labelling of endothelial cells lining veins.
Vloet et al., 2017	Two 12-week-old sheep on which mosquitoes were allowed to feed during the viraemic period of RVFV infection	Skin:	Strong labelling of RVFV antigen in endothelial cells of dermal blood vessels, smooth muscle cells, lipocytes, keratinocytes and fibroblasts in mosquito-exposed skin. RVFV antigen is also associated with the margination of thrombocytes in the blood vessels and present in the cytoplasm of infiltrating macrophages but not in neutrophils. In the epidermis, localized areas of positively stained keratinocytes are present in the stratum basale, stratum spinosum and stratum granulosum.

1.6 Pathogenesis

Rift Valley fever virus is one of many RNA viruses that causes viral haemorrhagic fever (VHF). The designation VHF is given to severe febrile illnesses that cause marked vascular dysregulation and vascular damage (Paessler and Walker, 2013). Many of these viruses are zoonotic, including RVFV, making them of particular concern from both a veterinary science and public health perspective (Basler, 2017). In human medicine haemorrhagic fever viruses are classified into four taxonomic families namely the *Arenaviridae* (e.g. Lassa fever virus), *Bunyaviridae* (e.g. Crimean-Congo haemorrhagic fever virus and RVFV), *Filoviridae* (Ebola and Marburg viruses) and the *Flaviviridae* (Dengue haemorrhagic fever virus and Yellow fever virus) (Gould and Solomon, 2008). There appear to be many similarities between the pathology and pathogenesis of all the viral haemorrhagic fevers (Paessler and Walker, 2013). Therefore, some of what is unknown about the pathogenesis of RVF can be deduced from studies concerning other VHF viruses such as Ebola virus (EBOV), Crimean-Congo haemorrhagic fever (CCHF) virus (CCHFV), Dengue haemorrhagic fever (DHF) virus (DHFV), Marburg haemorrhagic fever virus or Lassa fever virus. This is not a comprehensive review of the considerable data on all these agents but rather a comparison of a few of the better studied diseases. A review of the similarities between the pathogenesis of the various viral haemorrhagic fevers (VHFs), descriptions of the virus-cell interactions and the participation of the immune response help us understand the nature of the resulting disease.

All VHFs are characterized by a broad spectrum of clinical manifestations ranging from asymptomatic cases to mild and severe symptomatic cases with malaise, fever, vascular permeability, decreased plasma volume, coagulation abnormalities and varying degrees of haemorrhage (Basler, 2017). Common amongst the VHFs are liver damage, lymphocyte depletion and abundant proinflammatory cytokine and chemokine production leading to systemic inflammatory response syndrome (Geisbert and Jahrling, 2004, Paessler and Walker, 2013, Basler, 2017). This may result in increased endothelial cell permeability with oedema, impairment of the coagulation system (as evidenced by thrombocytopenia, consumption of

clotting factors, increased levels of fibrin degradation and bleeding), hypotension and multiorgan failure (including kidney failure), culminating in circulatory shock in the terminal stages of disease (Wauquier et al., 2010, Basler, 2017).

Detailed models representing our current understanding of VHF have been proposed. Studies in nonhuman primates and rodents experimentally infected with EBOV, CCHFV, and DHFV, suggest that some of the antigen presenting cells are early targets of these viruses (Geisbert et al., 2003a, Connolly-Andersen et al., 2009). Antigen presenting cells are specialized to capture microbial antigens, break them into small peptides, and display these to the appropriate T lymphocytes thereby inciting the adaptive immune response (Kumar et al., 2007). Antigen presenting cells include dendritic cells of the dermis, spleen and lymph nodes, Langerhans' cells in the epidermis, macrophages including perisinusoidal macrophages (Kupffer cells) of the liver, B lymphocytes, and type II and type III epithelioreticular cells of the thymus (Kumar et al., 2007). It is thought that early in the infection virus is endocytosed by antigen presenting cells in the mucosa or the skin (Geisbert and Jahrling, 2004, Basler, 2017). Virus gains entry via the bite of an infected insect (e.g. RVFV, CCHFV or DHFV), breaks in the skin (e.g. EBOV), or through exposure to excreta of infected rodents (e.g. Lassa fever virus) (Basler, 2017). Virus replicates in the cytoplasm of macrophages or dendritic cells at the site of viral entry and is then conveyed via lymphatic capillaries to the regional lymph nodes and to the parenchymal cells in the liver, kidney, adrenal cortex and other organs, promoting systemic dissemination and resulting in necrosis of many cells (Geisbert and Jahrling, 2004, Basler, 2017). Presumably tissue macrophages and vascular endothelial cells become secondarily infected and systemic inflammatory response syndrome, accompanied by vascular dysregulation and vascular damage with circulatory shock follows (Geisbert and Jahrling, 2004).

Hepatocellular necrosis is common for all VHFs (Geisbert and Jahrling, 2004). The pathogenic mechanism for RVFV induced necrotizing hepatitis includes apoptosis that was demonstrated in mice using terminal deoxynucleotidyl transferase dUTP nick-end labelling (Smith et al.,

2010). Additionally, the presence of NSs filaments in the nucleus induces p53 activation and apoptosis (Baer et al., 2012). However, RVFV also induces the formation of nucleotide-binding domain, leucine-rich-containing family, pyrin domain-containing-3 (NLRP3) inflammasomes that activate Caspase-1 leading to the maturation of interleukin 1β and interleukin-18 and the induction of pyroptosis (Ermler et al., 2013). The latter is a lytic cell death mechanism characterized by cell swelling, rupture of the plasma membrane and cellular collapse (Belizário et al., 2015, Nailwal and Chan, 2018).

In some cases of VHF fulminant hepatic failure follows, however, hepatocellular lesions are often not significant enough to cause death (Geisbert and Jahrling, 2004). Acute renal dysfunction may also play a role in the pathogenesis VHFs with a fatal outcome. In a clinical study of severe illness due to RVFV in 165 human patients in Saudi Arabia, 69 were diagnosed with hepatic failure alone, 55 with both hepatic and renal failure and 13 with renal failure alone of which respectively 12, 39 and 3 patients died (Al-Hazmi et al., 2003). Acute renal failure associated with RVF was also described in human patients in Sudan where 85 patients had signs and symptoms of renal failure without hepatic involvement (El Imam et al., 2009). In the recent EBOV outbreak in Sierra Leone patients had evidence of both hepatocellular damage and impaired kidney function that were characterized by increased levels of liver enzymes, creatinine, blood urea nitrogen, and other markers (Schieffelin et al., 2014). Increased deviation from normal values for BUN, aspartate aminotransferase, and creatinine predicted a fatal outcome. In Marburg haemorrhagic fever, renal dysfunction presenting as proteinuria, with pale swollen kidneys in fatal cases, is frequently observed (Mehedi et al., 2011).

Renal dysfunction is also occasionally a serious complication of fulminant liver failure secondary to the development of portal hypertension which then leads to splanchnic and systemic vasodilatation (Betrosian et al., 2007). Vasodilatation, mediated by nitric oxide and other vasodilators, causes relative hypovolemia and reduced effective central blood volume (Betrosian et al., 2007). However vascular damage with plasma leakage causing non-dependant oedema and fluid sequestration in the body cavities may also exacerbate

hypovolaemia and contribute to the development of renal failure. In DHF, the most severely affected children develop Dengue shock syndrome due to excessive depletion of intravascular volume as a result of plasma leakage, accompanied by only minor bleeding manifestations, most commonly skin petechiae or bruising (Wills et al., 2002). In Lassa fever, vascular damage with capillary leakage is also more prominent than haemorrhage and results in pleural effusion, pericardial oedema, and hydropericardium in severe cases (Callis et al., 1982). Hypovolaemia may also be further exacerbated by reduced synthesis of albumin by the liver and impaired secretion of steroid synthesizing enzymes by virus infected adrenal cortical cells (Geisbert and Jahrling, 2004). Adrenal cortical cells are permissive to infection by many VHF viruses including RVFV (Faburay et al., 2016b, Faburay et al., 2016a). Reduced albumin leads to reduced plasma oncotic pressure and contributes to plasma leakage, whereas reduced levels of steroid synthesizing enzymes from the adrenal glands may contribute to hypotension and sodium loss (Geisbert and Jahrling, 2004). However, renal impairment may also occur as a result of direct virus-related injury of kidneys, which has been demonstrated in both ovine and human RVFV infections (Daubney et al., 1931, Coetzer, 1977, Van Der Lugt et al., 1996, Al-Hazmi et al., 2003, Shieh et al., 2010, Faburay et al., 2016a, Faburay et al., 2016b).

The VHFs also cause a diversity of coagulation disorders (Paessler and Walker, 2013). Haemorrhage, presenting as petechiae, ecchymoses and mucosal haemorrhages, usually occur but is often not life threatening (Paessler and Walker, 2013). Infection of vascular endothelial cells has been linked to tissue damage, and would presumably contribute to haemorrhagic diathesis, but is seemingly not to a primary cause of pathology (Geisbert et al., 2003b). Ebola virus infection studies in cynomolgus monkeys demonstrated that secondarily infected vascular endothelial cells undergo cytolysis but extensive disruption of the architecture of the vascular endothelium does not occur (Geisbert et al., 2003b). Instead, the concomitant release of pro-inflammatory cytokines and chemokines from virus infected endothelial cells and monocyte/macrophages causes inflammation which normally shifts the haemostatic system in favour of thrombosis (Esmon, 2004, Paessler and Walker, 2013). The combination

of endothelial injury and inflammation cause a marked increase in the activation of the coagulation cascade accompanied by platelet aggregation and consumption (thrombocytopenia) (Paessler and Walker, 2013). Hepatic necrosis may also decrease the production of coagulation factors (Paessler and Walker, 2013). Depending on the combination of viral virulence factors and a variety of physiologic factors intrinsic to the patient, changes in coagulation may range from limited detectable laboratory deviations to disseminated intravascular coagulation (DIC). Whether or not classical (thrombotic) DIC always occurs in VHFs is a subject of much debate (Geisbert and Jahrling, 2004).

Disseminated intravascular coagulation can be classified as either enhanced-fibrinolytic-type DIC (fibrinolytic DIC) or suppressed-fibrinolytic-type DIC (thrombotic DIC) (Asakura, 2014). In thrombotic DIC (e.g. in sepsis) multiple microthrombi form in circulation due to coagulation cascade activation (Asakura, 2014). However, because plasminogen activator inhibitor is overexpressed in the vascular endothelium, due to the action of lipopolysaccharide and cytokines, fibrinolysis is suppressed and many microthrombi remain causing multi-organ failure (Asakura, 2014). Laboratory findings include an elevation in thrombin-antithrombin complex (TAT), a coagulation activation marker, and only mildly elevated plasmin-α2 plasmin inhibitor complex (PIC), a fibrinolysis activation marker. Fibrin/fibrinogen degradation products (FDPs) and D-dimer levels are also elevated and bleeding complications are relatively mild in thrombotic DIC. In contrast, in fibrinolytic DIC microthrombi are histologically difficult to demonstrate due to enhanced fibrinolytic activation (Asakura, 2014). Laboratory findings include a steep increase in PIC, but only a mild increase in the activity of plasminogen activator inhibitor, the fibrinolytic inhibitory factor (Asakura, 2014). Additionally, levels of TAT, D-dimers and FDPs, which reflect dissolution of microthrombi, are also elevated. Bleeding symptoms in enhanced fibrinolytic DIC are severe, and life-threatening bleeding may occur (Asakura, 2014).

In a Saudi Arabian human prospective clinical study of severe illness due to RVFV haemorrhagic manifestations were reported in 32 of 165 (19.4%) patients (Al-Hazmi et al., 2003). Symptoms included haematemesis, haemoptysis, vaginal bleeding, bleeding from the

gums in addition to petechial rashes and ecchymoses of the skin (Al-Hazmi et al., 2003). The occurrence of DIC in human RVF cases has been reported but was inadequately characterized to enable classification as either fibrinolytic or thrombotic (Madani et al., 2003, Al-Hazmi et al., 2003). In DHF, it was demonstrated that levels of FDPs are not elevated to a degree consistent with thrombotic DIC (Wills et al., 2002). Instead, fibrinolytic DIC occurs in DHF wherein degradation of fibrinogen prompts secondary activation of procoagulant homeostatic mechanisms (Marchi et al., 2009, Asakura, 2014). Patients with fatal infections of CCHF have petechial rashes and haemorrhagic symptoms such as epistaxis, haematemesis, and melena accompanied by thrombocytopenia and markedly elevated FDPs, possible consistent with fibrinolytic DIC (Swanepoel et al., 1989). In sheep, experimentally infected with RVFV, melena, blood in the airways and gastrointestinal tract, and haemorrhages in the heart have been reported (Olaleye et al., 1996). Thrombocytopenia and prolonged prothrombin and clotting times are present and plasma fibrinogen levels fluctute during the period of RVFV infection (Olaleye et al., 1996). In a wild-type RVFV rhesus macaque infection study 3 of 15 animals had petechiae, ecchymoses and bleeding from the nares, gums or venipuncture sites accompanied by thrombocytopenia, prolonged prothrombin and clotting times and significant decreases in FDPs and fibrinogen levels, again consistent with fibrinolytic DIC (Cosgriff et al., 1989).

In human patients infected with RVFV, levels of proinflammatory cytokine interleukin-1β and TNF-α were very low or absent (Jansen van Vuren et al., 2015). Interestingly in sepsis, interleukin-1 and TNF are increased and cause the production of large amounts of tissue factor from monocytes/macrophages and the vascular endothelium, thus leading to thrombotic DIC and microcirculatory dysfunction (Asakura, 2014). Consequently, it seems unlikely that microthrombi will play a significant role in the pathogenesis of RVF. However, prior research concerning experimental RVF in lambs mentions a few fibrin thromboemboli in the small pulmonary arteries in one study and thrombosis of the central veins in 3 of 34 lambs in another study (Easterday et al., 1962a, Coetzer, 1977). Also, coronary thrombosis was reported in one

human patient in 1951, but cardiovascular disease was not excluded in this patient who also had a 'tight feeling over the chest' and refused hospitalization (Mundel and Gear, 1951). In contrast, lesions that were described in four patients that died from RVF during the outbreak in 1975 in South Africa did not mention microthrombi in any of the tissues (Van Velden et al., 1977). Therefore, evidence of thrombosis in RVF is limited and there is also no study that explicitly looks at the role of coagulopathy in RVF.

Dysregulation of the inflammatory response also contributes to a fatal outcome in VHF. Wild-type RVFV infection of human monocyte-derived macrophages can lead to a productive infection and inhibition of the innate immune response via decreased expression of IFN-α2, IFN-β and TNF-α (McElroy and Nichol, 2012). In human patients infected with RVFV, interleukin-8 (IL-8) and interleukin-6 (IL-6) levels were increased and were at similar levels in fatal cases and survivors (Jansen van Vuren et al., 2015). Interleukin-8 is a pro-inflammatory chemokine produced by macrophages in response to infection, while IL-6 is an important mediator of fever and of the acute phase response (Jansen van Vuren et al., 2015). Serum levels of monokine-induced-by-gamma-interferon (MIG), interferon-gamma-induced-protein-10 (IP-10) and interleukin-10 (IL-10) were significantly increased while the chemokine RANTES (regulated-upon-activation-normal-Tcell-express-sequence) was significantly decreased in fatal human RVFV cases relative to survivors and controls (Jansen van Vuren et al., 2015). This suggests an imbalance in the immune response in fatal RVFV cases because MIG, IP-10 and RANTES are pro-inflammatory chemokines whereas IL-10 is immunosuppressive. This imbalance would contribute to failure of adaptive immune responses to clear infection in fatal cases and explain why RVFV replicates to significantly higher levels in patients with fatal outcomes, but the details of such a model remain to be worked out (Njenga et al., 2009, Jansen van Vuren et al., 2015).

Interestingly none of the VHF viruses infect lymphocytes. However, their rapid loss by apoptosis is a prominent feature of these diseases and lymphocytolysis is often noted (Wauquier et al., 2010, Geisbert et al., 2000, Basler, 2017). In Ebola subtype Zaire and MARV

infection, lymphoid depletion affects the centres of B-cell follicles in lymph nodes (Geisbert et al., 2000). Fatal outcomes in humans infected with Ebola subtype Zaire are also characterized by very low levels of circulating cytokines produced by T lymphocytes and by massive loss of peripheral CD4+ and CD8+ lymphocytes causing a profound suppression of the adaptive immune responses (Wauquier et al., 2010). However, the innate immune responses are also impaired by Ebola subtype Zaire infection which is characterized by hypersecretion of numerous proinflammatory cytokines, chemokines and growth factors, and by the significant absence of type I interferon production (Wauquier et al., 2010).

Encephalitis, a complication of RVF in humans, has been experimentally reproduced in mice and rats, but has not been described in sheep or any other ruminants (Al-Hazmi et al., 2003, Dodd et al., 2014, Busch et al., 2015). Neurologic disease has also been described in other VHFs such as Lassa fever, DHF and Marburg haemorrhagic fever (Okokhere et al., 2018, Madi et al., 2014, Mehedi et al., 2011). Meningoencephalitis associated with RVFV infection was described in 7 of 165 patients in Saudi Arabia and accompanied by either retinitis (n = 5), hepatitis (n = 3), or kidney failure (n = 1) (Al-Hazmi et al., 2003). Previously, in fatal human RVF cases, focal necrosis with an infiltrate of mononuclear cells and perivascular cuffing in the CNS has been described (Van Velden et al., 1977). This finding together with the delayed-onset encephalitis and/or retinitis in humans suggests inadequate adaptive immunity (Dodd et al., 2013, Al-Hazmi et al., 2003). Additionally, an increased mortality rate is seen in human patients infected with both RVFV and human immunodeficiency virus (HIV), and all these patients present with CNS symptoms (Mohamed et al., 2010). Trafficking of virus across the blood-brain barrier (BBB), a layer of vascular endothelial cells reinforced by tight junctions between the cells and supported by astrocytes and pericytes, might be blocked by RVFV-neutralizing antibodies (Dodd et al., 2014). (Dodd et al., 2014). Experiments in wild-type mice variously depleted of CD4+, CD8+ or B lymphocytes and infected with NSs deleted RVFV, demonstrated that a robust IgG and a neutralizing antibody response were critical for mediation of viral clearance and protection from neurological disease (Dodd et al., 2013). One third of

CD4-deleted mice develop neurologic signs by 12 to 36 days post infection (d.p.i.) and have a reduced antibody response and increased viral RNA titres following infection with NSs deleted RVFV (Dodd et al., 2013). The hypothesis is that activation of CD4+ T lymphocytes is required to augment RVFV antibody affinity maturation and class switching in B lymphocytes (Harmon et al., 2018). Therefore, individuals with CD4+ T lymphocyte dysfunction might be at an increased risk of developing severe RVF, including encephalitis.

However, it has not been established exactly how RVFV crosses the BBB. Aerosol or intranasal exposure might be necessary, since encephalitis occurs in laboratory animals exposed to RVFV via this route rather than via subcutaneous injection (Smith et al., 2010, Bales et al., 2012, Reed et al., 2012). Also, although RVFV is mosquito-transmitted, consuming or handling products from sick animals, including slaughtering sick livestock and handling dead foetuses is associated with severe disease or death (Madani et al., 2003, Anyangu et al., 2010, Mutua et al., 2017). Therefore, RVFV might infect peripheral sensory and motor neurons in the eyes or oronasal mucosa directly, causing encephalitis and retinitis via these routes (McGavern and Kang, 2011). Immunocompetent Lewis rats exposed to wild-type RVFV by aerosolization develop lethal encephalitis and also have low levels of viral RNA in their eyes (Caroline et al., 2015). Lethal disease in the Lewis rats is also accompanied by increases in monocyte chemoattractant protein-1 (MCP-1), macrophage colony-stimulating factor (M-CSF), keratinocyte chemoattractant/human growth-regulated oncogene (Gro/KC), RANTES, and IL-1β, all evident in the serum before the onset of clinical disease, and these increases are followed by inflammatory derangement in the brain during clinical illness (Caroline et al., 2015). It has been hypothesised that these chemokines may be actively recruiting monocytes, macrophages, and neutrophils into the CNS (Caroline et al., 2015). Additionally, aerosol exposure of rats with wild-type RVFV has demonstrated that neurological symptoms commence concomitant with increased vascular permeability and possible brain oedema, and that virus replication occurs in the brain several days before vascular leakage is detected (Walters et al., 2019). Therefore, in some species at least, it would seem that RVFV gains

entry into the CNS via peripheral neurons where replication of virus causes inflammation and increased vascular permeability, with concomitant release of chemokines that attract mononuclear cells to the CNS and cause neurological symptoms. Unfortunately though, this still doesn't explain why ruminants have never been reported to develop encephalitis, since it seems likely that they would come into contact with aborted foetuses and placentas.

In previous publications, a clear distinction was made between the susceptibility to, and progression of disease in young animals when compared to adults. There is no clear explanation in the literature why these differences are present but they may be due to age-related susceptibility of the primary target cells of RVFV (Pepin et al., 2010). Alternatively the innate immune response to virus infection in young animals might be inadequate, making them more susceptible to fatal RVFV infection with very high viraemia (Pepin et al., 2010). Therefore, the principle aim of this study was to summarize gross, histopathological and immunohistochemical findings, relative to results from previous research, for three age groups: adult sheep, young lambs and foetuses. The tissue tropism and target cells of RVFV in a large number of naturally infected sheep was reported separately to determine if the target cells and organs were different in the three age groups. Specifically tissues from 99 adult sheep, 71 young lambs and 58 foetuses from the 2010-2011 South African RVFV outbreak were examined. Further aims were to ascertain the extent to which virus was present in different organs and establish the diagnostic significance of certain tissues and specific histologic features of RVFV in the various age groups. Additionally, results for 34 placenta specimens were reported and the diagnostic usefulness of this organ, compared to other organs, and which section of the placenta, if any, was most useful for a diagnosis.

CHAPTER 2

LESIONS AND CELLULAR TROPISM OF NATURAL RIFT VALLEY FEVER VIRUS INFECTION IN ADULT SHEEP

This paper was published: Odendaal L, Clift SJ, Fosgate GT, Davis AS. Lesions and cellular tropism of natural Rift Valley fever virus infection in adult sheep. *Veterinary Pathology*. 2019; 56(1): 61-77. Copied here with permission.

2.1 Summary

Rift Valley fever is a mosquito-borne disease that affects both ruminants and humans, with epidemics occurring more frequently in recent years in Africa and the Middle East, probably as a result of climate change and intensified livestock trade. Sheep necropsied during the 2010 RVF outbreak in South Africa were examined by histopathology and IHC. A total of 124 sheep were available for study of which 99 cases were positive for RVF. Multifocal-random, necrotizing hepatitis was confirmed as the most distinctive lesion of RVF cases in adult sheep. Of cases where liver, spleen and kidney tissues were available 45 of 70 had foci of acute renal tubular epithelial injury in addition to necrosis in both the liver and spleen. In some cases, acute renal injury was the most significant RVF lesion. Immunolabelling for RVFV was most consistent and unequivocal in liver followed by spleen, kidney, lung and skin. Rift Valley fever virus antigen-positive cells included hepatocytes, adrenocortical epithelial cells, renal tubular epithelial cells, macrophages, neutrophils, epidermal keratinocytes, microvascular endothelial cells and vascular smooth muscle. The minimum set of specimens to be submitted for histopathology and IHC to confirm or exclude a diagnosis of RVFV are liver, spleen and kidney. Skin from areas with visible crusts and lung could be useful additional samples. In endemic areas, cases of acute renal tubular injury should be investigated further if other more common causes of renal lesions have already been excluded. RVFV can also cause an acute infection in the testis, which requires further investigation.

2.2 Introduction

Rift Valley fever virus was first reported in sheep in 1931 in the Rift Valley of Kenya and is a zoonotic disease that causes considerable morbidity and mortality in ruminants and occasionally humans (Daubney et al., 1931, Pepin et al., 2010). It is caused by a mosquito-borne, single stranded RNA virus of the *Bunyavirales* order, *Phenuiviridae* family (formerly the *Bunyaviridae* family), genus *Phlebovirus* within the species *Rift Valley fever phlebovirus* (Abudurexiti et al., 2019). Epidemics of RVF are more and more frequent in Africa and the Middle East and generally occur during years of abnormally high rainfall when sufficient numbers of susceptible livestock congregate in areas containing RVFV-infected mosquitoes (Gear et al., 1955, Swanepoel and Coetzer, 2004, Chevalier et al., 2010). Livestock trade contributes to the spread of the disease into disease-free areas thereby expanding the geographical distribution of RVF (Chevalier et al., 2010). Susceptibility to RVFV varies with age, with mortality rates typically 90% or higher in young lambs, and 20 to 30% in older lambs and ewes (Erasmus and Coetzer, 1981). Adult sheep often die without showing any definite signs, and abortion in ewes is often the only indication of infection in a flock (Erasmus and Coetzer, 1981).

Few studies of the gross and histopathological lesions in sheep that died of natural RVFV infection have been published (Daubney et al., 1931, Schulz, 1951, Coetzer, 1977, Van Der Lugt et al., 1996, Shieh et al., 2010). These studies reported that sheep, including lambs that die from natural RVFV infection have the most significant lesions in the liver, but that lesions can also occur in other organs including the spleen, lymph nodes, kidneys, lungs, heart, adrenal glands, gall bladder, skin, and digestive tract (Daubney et al., 1931, Schulz, 1951, Coetzer, 1977, Van Der Lugt et al., 1996). Necrotic foci are distributed more or less evenly throughout the liver and can coalesce to form diffuse necrotic lesions in lambs (Daubney et al., 1931). Additionally, adult sheep occasionally have marked renal tubular epithelial degeneration and necrosis (Daubney et al., 1931, Olaleye et al., 1996, Faburay et al., 2016a, Faburay et al., 2016b). Schultz reported that the lesions of RVF in South African sheep differed from those

previously described by Daubney and others (Daubney et al., 1931, Schulz, 1951). Daubney et al. had little to remark about microscopic lesions in the spleen and lungs whereas Schultz reported necrosis in the white pulp of the spleen and oedema, emphysema and haemorrhages in the lungs of the South African cases (Daubney et al., 1931, Schulz, 1951).

Schultz also reported cortical and medullary haemorrhages in the adrenal glands and subcutaneous haemorrhages whereas Daubney et al. did not mention adrenal or subcutaneous lesions. However, neither Daubney et al. or Schulz reported the total number of animals or the numbers in the various age groups that were examined (Daubney et al., 1931, Schulz, 1951). The cellular tropism of RVFV was studied using IHC in 8 experimentaly infected and 4 naturally infected new-born lambs, wherein extensive hepatocyte necrosis and a progressive increase in viral antigen in the liver was reported (Van Der Lugt et al., 1996). Viral antigen was also reported in a few cells in the spleen, lymph nodes, kidneys and lungs. In a study of naturally infected sheep, RVFV antigen was identified by IHC in liver from one sheep and autolysed spleen from another sheep (Shieh et al., 2010). In a single experimentally infected 3-4 month old sheep, viral antigen was most prominent in the liver and the spleen, with lesser amounts also detected in the adrenal glands and within renal tubular epithelial cells and luminal debris in the kidney (Faburay et al., 2016a). In a trial of a RVFV vaccine candidate, viral antigen was reported in the liver, spleen, lymph nodes, kidney, lungs and adrenal glands of the unvaccinated sheep (Faburay et al., 2016b). Viral antigen-positive macrophages or dendritic cells were detected in the lungs and medullary sinuses of mesenteric lymph nodes. There was also evidence of viral antigen in renal glomeruli and rarely in the adrenal cortex. In a study involving 40 lambs, of which 24 were experimentally infected with RVFV, antigen was observed in hepatocytes and mononuclear phagocytes in the liver, spleen and lymph nodes as well as endothelial cells in lymphoid organs (Wichgers Schreur et al., 2016). Rift Valley fever virus antigen has also been observed in the skin of 2 experimentally infected sheep (Vloet et al., 2017). Notwithstanding, in all these studies the tropism and target cells of RVFV was only partly revealed, making future observations in similar studies difficult to contextualize.

The aim of this study was to describe the tissue tropism and target cells of RVFV in a large number of naturally infected sheep, specifically 99 sheep from the 2010 South African RVFV outbreak. A further aim was to determine the extent to which virus can be detected in different organs and summarize gross, histopathological and immunohistochemical findings in the present study relative to results from previous research.

2.3 Materials and methods

2.3.1 Case selection

All specimens originated from the carcasses of naturally infected sheep necropsied during the 2010 RVF outbreak in South Africa. This work was done in agreement with the Animal Ethics Committee of the University of Pretoria (clearance certificate V096-16). Supplementary material in support of the results presented in this article is available from the authors upon request.

Tissue specimens were collected from hundreds of sheep during the outbreak and submitted to the Agriculture Research Council-Onderstepoort Veterinary Institute for testing including RT-qPCR on 1617 specimens. Tissues collected in formalin from 1034 necropsied animals were submitted for histopathological examination. These necropsies were conducted by employees of the South African State Veterinary Services and private veterinary practitioners. With permission from the State Veterinary Services, the principal author (Lieza Odendaal) conducted necropsies on 97 animals that included 37 adult sheep. Tissue specimens from these cases were collected in 10% neutral buffered formalin and paraffin embedded. Ultimately, FFPE tissue specimens were available from 306 adult sheep. From this collection, cases were excluded when the level of autolysis was severe or when only one organ was available for study. A total of 124 cases were suitable for study of which 99 cases were classified positive for RVF with one or more positive test results for histopathology, RT-qPCR and/or IHC. Sheep that died of natural infections during the outbreak and examined for RVFV as part of the government campaign to monitor the spread of RVF, but tested negative, were included as controls (n = 25). Immunohistochemistry has a sensitivity and specificity of 97.6%

and 99.4%, histopathology of 94.6% and 92.3% and RT-qPCR of 97.4% and 71.7%, respectively.(Odendaal et al., 2014) A parallel interpretation of tests was chosen to maximize sensitivity and therefore, any animal with at least one positive test result was selected for study.

2.3.2 Diagnostic tests

Nucleic acid extractions and RT-qPCR on fresh liver for 81 of the cases were performed at the Biotechnology PCR Laboratory of the Agriculture Research Council- Onderstepoort Veterinary Institute as described previously (Odendaal et al., 2014). Embedding, sectioning and HE of formalin-fixed tissues were done according to the standard operating procedures of the Section of Pathology, Department of Paraclinical Sciences, Faculty of Veterinary Science, University of Pretoria. Immunohistochemical labelling for the detection of RVFV antigen was performed using polyclonal hyperimmune mouse ascitic fluid (National Institute for Communicable Diseases, Johannesburg, SA) as described previously (Odendaal et al., 2014). Previously, 40 controls were tested that included 8 RT-qPCR and IHC positive RVF cases that occurred in 2009, and 32 additional negative tissue controls that died from aetiologies that cause liver pathology resembling RVF (Odendaal et al., 2014). The controls were tested with a range of relevant and irrelevant antibodies namely RVFV antibody, polyclonal mouse ascitic fluid to Wesselsbron virus (WBV), monoclonal mouse ascitic fluid to bovine herpes virus-1, and rabbit polyclonal antiserum to equine herpes virus-1 (Odendaal et al., 2014).

Briefly, the immunoperoxidase method included microwave antigen retrieval in citrate buffer (pH 6.0), incubation with the anti-RVFV primary antibody at 1:500 dilution for 1 hour and rabbit anti-mouse secondary antibody (F0232, DakoCytomation, Glostrup, Denmark) followed by detection with a standard avidin-biotin peroxidase system, Vectastain® Elite® ABC-HRP Kit (PK-6100, Vector Laboratories, Inc., Burlingame, CA, USA), NovaRED peroxidase substrate (SK-4800, Vector Laboratories, Inc.) and haematoxylin counterstain.

2.3.3 Examination of tissues

Histomorphological features in all available organs were systematically recorded and reviewed within the context of lesions associated with RVFV infection. The number and types of non-

hepatic organs available for study varied considerably by case with liver (n = 124), spleen (n = 110) and kidney (n = 102) being the specimens most often submitted. In some cases, additional tissue specimens were available: 87 lung, 67 heart, 40 gastrointestinal tract, 23 gall bladder, 20 lymph node, 13 skin, 13 brain, 11 adrenal, 10 uterus and 2 testis specimens. Gastrointestinal tract specimens included forestomach (n = 5), abomasum (n = 24), small intestine (n = 20), large intestine (n = 2) and tongue (n = 12).

Lesion severity in the liver, spleen and kidney was scored using a qualitative scale as mild, moderate or severe (Table 3, 4 and 5). Immunolabelling for RVFV antigen was scored on a semi-quantitative scale as isolated, scattered or widespread labelling. In the liver, spleen and kidney an area of tissue measuring approximately 5mm^2 was evaluated. For all other tissues where labelling tended to be isolated (gall bladder, lung, heart, intestines, tongue, adrenal glands, skin, lymph nodes, uterus and testis) all the available tissue was examined. Isolated labelling was defined as positive signal that was only rarely present in the organ parenchyma and involved a total cell count of less than 20. These could be single cells or multifocal groups of cells. In cases with scattered labelling, positive signal was occasionally present in single cells or groups of cells and the total cell count was between 21 and 100. Widespread labelling was defined as positive signal involving greater than 100 cells in the examined area of tissue.

2.3.4 Statistical analysis

Categorical data were described as frequencies, proportions, and 95% mid-P exact confidence intervals (CI). Semi-quantitative data were described using the median and interquartile range. Paired categorical data were compared using McNemar's chi-square tests. Semi-quantitative data were compared between the liver and all other organs using Wilcoxon rank sum tests. Correlations between semi-quantitative variables were estimated using Spearman's Rho (ρ). Statistical analyses were performed in available software (Epi Info, version 6.04, CDC, Atlanta, GA and IBM SPSS Statistics Version 23, International Business Machines Corp., Armonk, NY, USA) and results interpreted at the 5% level of significance.

Table 3. Histopathology scoring of liver lesions in sheep naturally infected with RVFV.

Score	Description
None	No evidence of hepatocellular death, inflammation or hemorrhage.
Mild	One third or less of the examined parenchyma affected. Foci of hepatocellular death are associated with a mild to moderate infiltrate of predominantly neutrophils with fewer macrophages. Hemorrhage often present in areas of cell death.
Moderate	Areas of hepatocellular death in between 1/3 and 2/3 of the examined parenchyma. Hemorrhage and an inflammatory infiltrate as described above.
Severe	Areas of hepatocellular death in more than 2/3 of the examined parenchyma, with hemorrhage and an inflammatory infiltrate as described above.

Table 4. Histopathology scoring of lesions in the spleen of sheep naturally infected with RVFV.

Score	Description
None	No appreciable lymphocyte necrosis or depletion.
Mild	Necrosis present in the germinal centre of the follicles. Sparing of lymphocytes in the mantle zone, marginal zone and the PALS, with many small to medium lymphocytes remaining in these areas. Scattered tingible-body macrophages present in the white pulp mostly in the germinal centres and marginal zone. No or sparse lymphocytolysis in the red pulp.
Moderate	Necrosis present in the germinal centre of the follicles. Mild to moderate depletion of the mantle zone accompanied by scattered lymphocytolysis in the marginal zone and the peripheral zone of the PALS. In some cases, the mantle zone is no longer discernible. Sparing of lymphocytes in the PALS adjacent to the central artery of the white pulp. Tingible-body macrophages especially prominent in the marginal zone. Occasionally mild to moderate lymphocytolysis in the red pulp.
Severe	Necrosis present in the germinal centre with disintegration of the mantle zone. Broad zone of necrosis present in the marginal zone and in the peripheral zone of the PALS with the PALS in most cases reduced to a narrow band of small to medium lymphocytes adjacent to the tunica media of the central artery. Many tingible-body macrophages present in the remains of the germinal centres and the marginal zone. Mild to moderate lymphocytolysis in the red pulp.

Table 5. Histopathology scoring of renal lesions in sheep naturally infected with RVFV.

Score	Description
None	No lesions attributable to acute tubular or glomerular injury detected.
Mild	Scattered or aggregates of degenerating or necrotic tubules in only a few (≤5 out of 10) low power fields (10x objective) examined. Lesions in necrotic tubules are characterized by tubular epithelial cell pyknosis, karyorrhexis, and karyolysis accompanied by intratubular cellular and proteinaceous debris and detachment of the epithelium from the basement membrane. Round desquamated cells with homogenous eosinophilic cytoplasm sometimes present within the lumens of a tubules, particularly in the superficial cortex and medullary rays. Intermittently, tubules are lined by attenuated epithelial cells, causing the tubular lumens to appear dilated. Scattered pyknosis and karyorrhexis present in the glomeruli with occasional attendant neutrophils.
Moderate	Scattered or aggregates of degenerating or necrotic tubules in most (>5 out of 10) low power fields (10x objective) examined. Characteristics of tubular and glomerular injury as described above. Occasionally granular or cellular casts present within the tubules.
Severe	Acute tubular injury or necrosis in most of the tubules with characteristics as described above in all of the low power fields (10x objective) examined.

2.4 Results

2.4.1 Overview

Immunolabelling for RVFV was most consistent and unequivocal in liver followed by spleen, kidney, lung and skin (Table 6). Positive labelling was cytoplasmic and typically fine diffuse to coarse granular. Labelling was widespread in 68 of 82 (83%) liver specimens that tested positive for RVFV by IHC. In comparison, labelling in the spleen, kidney and lung was only widespread in 9 of 63 (14%), 11 of 55 (20%) and 6 of 40 (15%) IHC-positive cases respectively and difficult to find in many cases. Notably, 6 of 11 (55%) skin specimens were positive for RVFV antigen. Neither histological lesions nor RVFV antigen were detected in any tissues from the central nervous system (n = 13), nor in any tissues of the 25 cases included as negative controls.

Table 6. Frequency of viral antigen in different organs and comparison to quantity of immunolabelling in liver, for 99 sheep with RVFV infection.

Organ	Proportion with immunolabelling		Quantity of immunolabelling	
	Positive/ Total	Percentage (95% CI)	Median (IQR)*	*P* value†
Liver	82/99	83 (74, 89)	Widespread (widespread, widespread)	NA
Gallbladder	8/22	36 (19, 58)	Isolated (isolated, scattered)	<0.001
Spleen	63/86	73 (63, 82)	Scattered (isolated, scattered)	<0.001
Lymph nodes	7/19	37 (18, 60)	Scattered (isolated, scattered)	0.001
Kidney	55/83	66 (56, 76)	Isolated (isolated, scattered)	<0.001
Adrenal glands	4/10	40 (14, 71)	Scattered (isolated, widespread)	0.039
Lung	40/70	57 (45, 68)	Isolated (isolated, scattered)	<0.001
Heart	8/57	14 (7, 25)	Isolated (isolated, isolated)	<0.001
Rumen	0/5	0 (0, 45)	None	0.074
Abomasum	0/24	0 (0, 12)	None	<0.001
Small intestine	7/19	37 (18, 60)	Isolated (isolated, isolated)	0.011
Large intestine	0/2	0 (0, 78)	None	0.480
Tongue	2/10	20 (3, 52)	Scattered (isolated, scattered)	0.010
Skin	6/11	55 (26, 81)	Isolated (isolated, isolated)	0.010
Uterus	2/10	20 (3, 52)	Isolated (isolated, isolated)	0.006
Testis	2/2	100 (22, 100)	Widespread (scattered, widespread)	0.317
Brain	0/13	0 (0, 21)	None	0.003

Positive/Total = number with positive immunolabelling for RVFV antigen out of the total number of tissues examined. CI = confidence interval. IQR = interquartile range. NA = not applicable. *Calculated only for the cases with positive labelling; the categories in parentheses are the interquartile range of antigen quantity in the sample set. †Based on Wilcoxon rank sum tests comparing the quantity of positive immunolabelling to the quantity of labelling in liver samples. P value corresponds to McNemar's chi-square test comparing the proportions of positive immunolabelling when no slides had detectable labelling.

2.4.2 Liver

Macroscopically, the liver often had a mottled red appearance (Fig. 1) due to the presence of innumerable ill-defined necrotic foci. Microscopically, necrotic foci were situated irregularly throughout the lobule and their distribution varied from multifocal to focally extensive to confluent bridging. Necrosis was generally accompanied by haemorrhage (Fig. 2) and a mild to moderate infiltrate of neutrophils and macrophages. Typically, the portal tract interstitium was expanded by mild oedema and low numbers of mononuclear cells exhibiting occasional karyorrhexis (Fig. 3). The bile ducts were uninvolved. Many hepatocytes had features of apoptosis (Figs. 3 and 4) that included dissociation of cells, cellular shrinkage and rounding, hypereosinophilic cytoplasm, pyknosis and karyorrhexis, and fragmentation of cells into multiple smaller apoptotic bodies. Adjacent hepatocytes often had varying degrees of micro- or macro-vesicular degeneration and anisokaryosis. Scattered hyperplastic Kupffer cells were occasionally present within adjacent sinusoids. Filamentous or oval eosinophilic intranuclear inclusions associated with nuclear chromatin marginalization were unequivocally observed in the hepatocytes of only 7 cases (Fig 4).

Necrosis was absent in the liver specimens from 10 of 99 (10%) cases. Of these, 7 were positive by RT-qPCR. Notably, for the other 3 cases, no histological lesions or immunohistochemical labelling were present in the liver, or in the spleen of 2 cases with available specimens; however, scattered (n = 2) or widespread (n = 1) RVFV antigen and acute tubular injury were present in the kidneys, and 2 of these 3 cases were also positive by RT-qPCR of the liver.

The severity and distribution of hepatic necrosis varied considerably among cases with 34, 23 and 32 specimens classified as mild, moderate or severe necrosis respectively. Most often the patterns of necrosis (Table 7) were predominantly centrilobular (27 of 99), predominantly confluent centrilobular to midzonal (27 of 99) or multifocal random (23 of 99). However, necrosis was never limited to one particular zone and was found in multiple zones whenever

necrosis was recorded. Instead, there could be confluent centrilobular necrosis with a few midzonal and periportal foci, or patchy involvement of the centrilobular zones with prominent necrosis midzonally and in the periportal areas, or a random distribution of necrotic foci throughout the lobule, or massive necrosis involving the entire hepatic lobule. Additionally, foci of necrosis were invariably present in one or more of the periportal zones, specifically affecting hepatocytes of the limiting plate.

Hepatocytes were the predominant target of RVFV infection in the liver (Fig. 5) with IHC labelling widespread to scattered (82 of 99) and easily identified in most cases. Diffuse, fine to coarse granular labelling was present in the cytoplasm of hepatocytes, and viral antigen-positive cytoplasmic fragments were frequently present within the sinusoids and central veins. Areas of hepatocellular death were thought to become devoid of immunolabelling as lesions became more extensive. Positively labelled Kupffer cells and degenerate neutrophils were sparse. Immunolabelling was not detected in nuclei or in association with intranuclear inclusion bodies.

Table 7. Predominant histologic patterns of liver necrosis in 99 sheep with RVF infection.

Pattern of liver necrosis	Proportion	Percentage (95% CI)
Number of specimens with necrosis	89/99	90 (83, 95)
Confluent centrilobular to midzonal	28/99	28 (20, 38)
Centrilobular	27/99	27 (19, 37)
Multifocal random	23/99	23 (16, 32)
Midzonal	9/99	9 (5, 16)
Diffuse	2/99	2 (0, 7)

Proportion = number affected out of the total number of tissues examined. CI = confidence interval.

Panel 1: Figures 1-6. Rift Valley fever virus, liver, adult sheep.

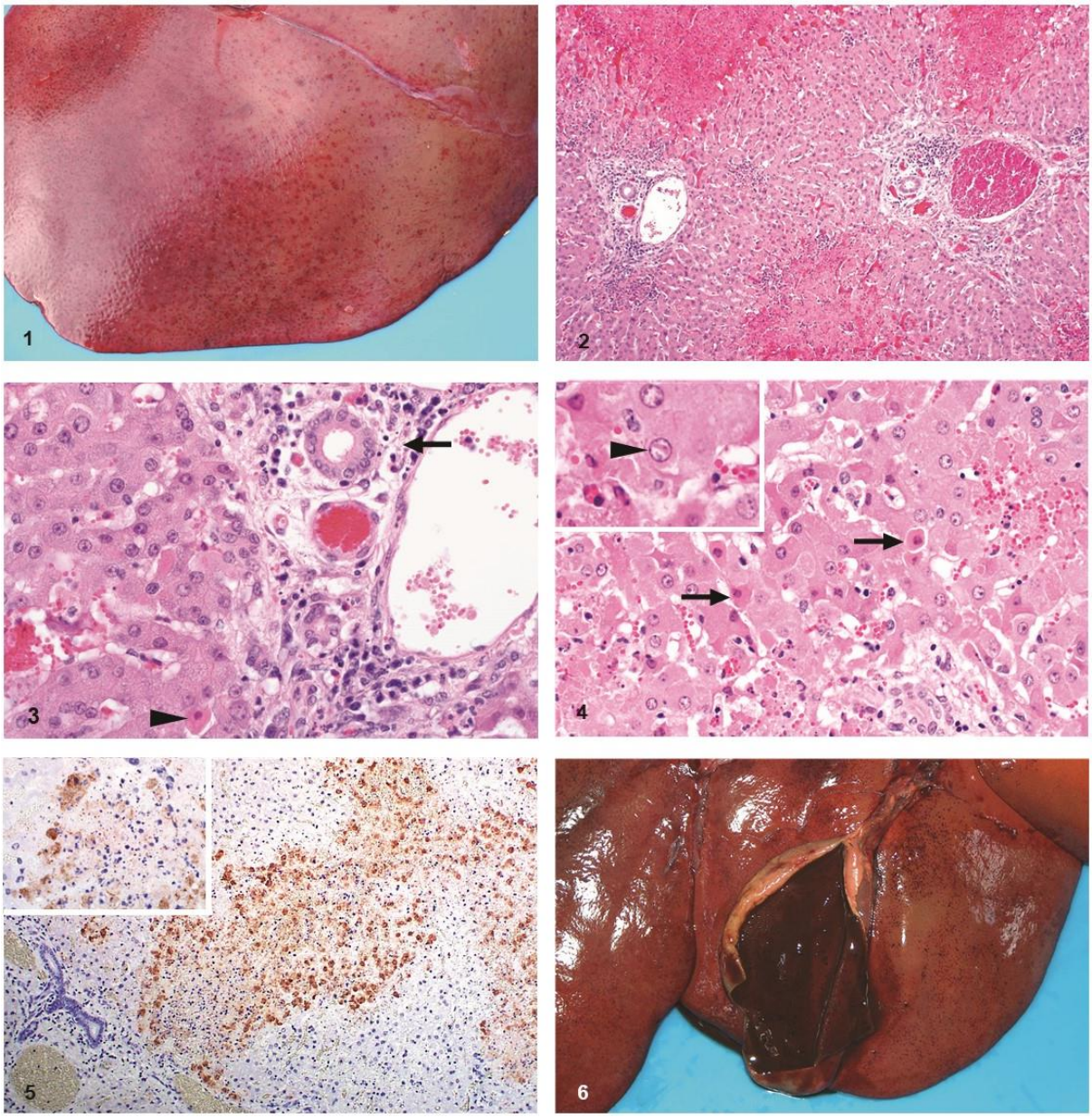

Figure 1. Case 57. Multifocal to coalescing haemorrhage and necrosis. **Figure 2.** Case 32. Multifocal random hepatocellular haemorrhage and necrosis. Haematoxylin and eosin (HE). **Figure 3.** Case 32. Mild oedema and mononuclear cell inflammation with karyorrhexis (arrow) in the portal area. Early apoptotic body (arrowhead) also referred to as a Councilman body. HE. **Figure 4.** Case 49. Early apoptotic bodies (arrows) characterized by shrinkage of affected cells with acidophilic cytoplasm and pyknosis. **Inset:** Rod-shaped acidophilic intranuclear inclusion in the nucleus of a hepatocyte (arrowhead). HE. **Figure 5.** Case 46. RVFV antigen in areas of hepatocellular death. **Inset:** Fine granular labelling in the cytoplasm of injured hepatocytes and cytoplasmic fragments. IHC for RVFV. **Figure 6**. Case 61. Haemorrhage in the wall of the gall bladder.

2.4.3 Gall bladder

Haemorrhage and oedema were occasionally present macroscopically in the gall bladder (Fig. 6). Microscopically, 10 of 22 (45%) cases with available specimens had foci of necrosis and haemorrhage. Typically, haemorrhage was prominent in the serosa or adventitia but sometimes it extended into the muscularis externa or the lamina propria. Foci of necrosis, present in the lamina propria, serosa, or adventitia had a mild to moderate infiltrate of mononuclear cells and degenerate neutrophils. There was no significant correlation between liver necrosis and gall bladder necrosis ($\rho = 0.132$; $P = 0.549$).

Immunolabelling for RVFV antigen was present in 8 of 22 (36%) cases. The labelling was generally in or around capillaries or small blood vessels and included cellular debris, neutrophils or mononuclear cells. Areas of necrosis did not contain viral antigen in 3 of 22 cases, and in 1 of 22 cases the labelled cells were not within areas of necrosis.

2.4.4 Spleen

Gross lesions were uncommon in the spleen with capsular and subcapsular petechiae present occasionally. Microscopically, there were varying degrees of necrosis in the white and red pulp. This was a prominent feature in 64 of 86 (74%) cases giving the majority of the specimens a paucicellular appearance histologically (Fig. 7). Necrosis was most apparent in the germinal centres, mantle zones, marginal zones and peripheral zones of the periarteriolar lymph sheaths (PALS) of the white pulp and was characterized by the presence of cellular debris and tingible-body macrophages (Fig. 8). Necrosis was mild (21 of 63) mainly involving the follicular germinal centres, or moderate (25 of 63) with prominent necrosis of the germinal centres and the mantle zone and some involvement of the marginal zone and peripheral zone of the PALS, or severe (18 of 63) with prominent involvement of the follicles, marginal zones and peripheral zones of the PALS. Necrosis was never prominent in the T-cell rich area of the PALS adjacent to the tunica media of the central artery. Lymphocytolysis in the red pulp was typically far less prominent and generally occurred as single cell necrosis.

Splenic infection with RVFV was detected by IHC in 63 of 86 (73%) cases with available specimens. Viral antigen was either isolated (n = 30), scattered (n = 24) or widespread (n = 9) and the quantity of labelling was significantly associated with the degree of splenic necrosis (ρ = 0.505, $P < 0.001$). Viral antigen was mainly in cellular debris or in large mononuclear cells that had abundant, often clear cytoplasm, and oval to polygonal, often slightly eccentric nuclei, histomorphologically identified as macrophages (Fig. 9). Positive labelling was observed more readily in the white pulp, particularly in the marginal zone, which was positive in 59 of 63 (94%) cases with IHC-positive spleen specimens (Table 8). The red pulp was positive in 58 of 63 (92%) cases with IHC-positive spleen specimens. Interestingly, viral antigen was absent from the white pulp in four specimens and instead was widespread only in the red pulp in these cases. In 21 of 63 (33%) cases with IHC-positive specimens, sparse labelling was present in cells in the follicles. These cells were polygonal with abundant cytoplasm and large nuclei and contained phagocytosed cellular debris in the cytoplasm, consistent with tingible-body macrophages (Fig. 10). However, not all cells identified as tingible-body macrophages contained RVFV antigen.

Notably, splenic necrosis was absent from 22 of 86 (26%) cases classified as positive for RVF. Test results for these cases varied with 13 testing negative for viral antigen by IHC but positive on RT-qPCR and/or liver histology. Of these cases, 4 of 22 had either widespread (n = 3) or isolated (n = 1) positive labelling for RVFV antigen in the spleen as well as widespread necrosis and viral antigen in the liver. A further 2 of 22 cases had no detectible necrosis or viral antigen in the liver or the spleen but were IHC-positive in the kidney. The remaining 3 cases with no detectible necrosis or labelling in the spleen had necrosis and viral antigen in the liver

Panel 2: Figures 7-12. Rift Valley fever virus, spleen and lymph node, adult sheep.

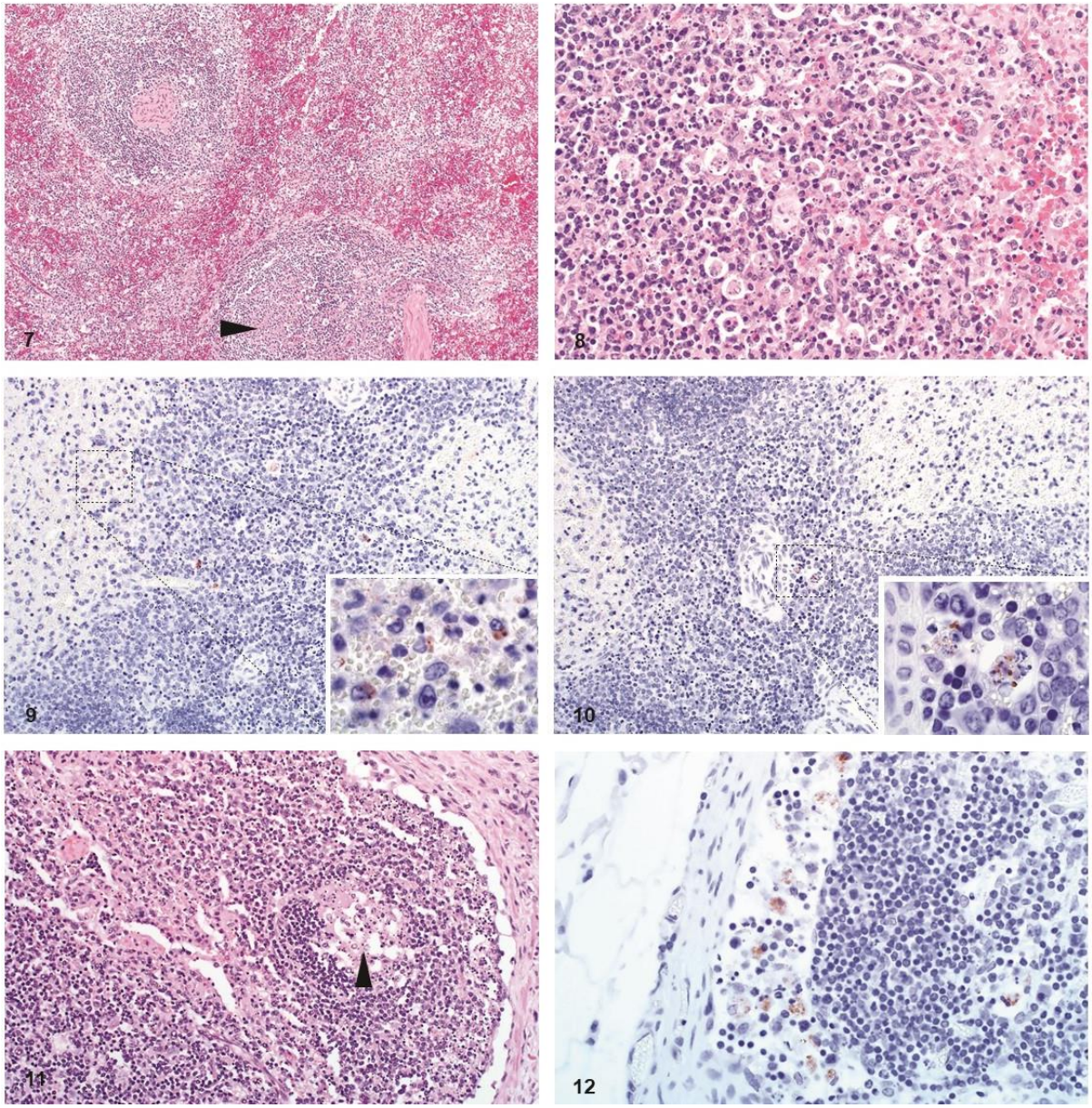

Figure 7. Case 47. Spleen. Necrosis in the follicular germinal centre (arrowhead). The various zones within the white pulp are indistinct. HE. **Figure 8.** Case 48. Spleen. Prominent tingible-body macrophages and lymphocyte apoptosis in a splenic germinal centre. HE. **Figure 9.** Case 58. Spleen. Multifocal distribution of RVFV antigen. **Inset:** Viral antigen in macrophages. IHC for RVFV. **Figure 10.** Case 58. Spleen. Sparse RVFV antigen in the white pulp**. Inset:** Cells containing phagocytosed cellular debris in the cytoplasm, consistent with tingible-body macrophages. Also, coarse granular labelling for RVFV in the cytoplasm. IHC for RVFV. **Figure 11.** Case 58. Lymph node. Necrosis in the germinal centre of a follicle (arrowhead). HE. **Figure 12.** Case 46. Lymph node. Viral antigen within macrophages in the subcapsular sinus. IHC for RVFV.

Table 8. Distribution of viral antigen in different zones of the spleen, for specimens with positive immunolabelling for RVFV in sheep.

Splenic zone	Proportion	Percentage (95% CI)
Marginal zone	59/63	94 (85, 98)
Red pulp	58/63	92 (83, 97)
Marginal zone and red pulp	55/63	87 (77, 94)
Only red pulp	4/63	6 (2, 15)
Only white pulp	5/63	8 (3, 17)
Germinal centre and mantle zone	21/63	33 (23, 46)
Periarteriolar lymphatic sheath	11/63	17 (10, 28)

Proportion = number of positive spleen specimens over the total number of spleen specimens examined, based on immunohistochemistry for RVFV antigen. CI = confidence interval. The data do not include specimens with negative immunolabelling.

2.4.5 Lymph nodes

Macroscopically, lymph nodes were enlarged, oedematous and congested. Mesenteric lymph nodes were often especially affected. Microscopically, there was lymphoid necrosis characterized by varying degrees of follicular lymphocytolysis and cortical lymphoid depletion in 10 of 19 (53%) cases with available specimens. Necrosis in lymph nodes was significantly associated with splenic necrosis ($\rho = 0.532$, $P = 0.023$). In most cases and similar to the spleen, lymphocytes within follicular germinal centres were especially depleted (Fig. 11). In some cases, there was also mild to moderate depletion of the mantle zone lymphocytes accompanied by scattered lymphocytolysis in the interfollicular cortex and the paracortex. In severe cases, the entire cortex was depleted and no distinction could be made between follicles, interfollicular cortex and paracortex.

Of the cases with available lymph node specimens, 7 of 19 (37%) were positive for RVFV antigen. Viral antigen was present in scattered mononuclear cells histomorphologically consistent with macrophages in the subcapsular, paratrabecular and medullary sinuses (Fig. 12).

2.4.6 Kidney

Gross lesions in the kidney were uncommon other than occasional capsular or cortical petechiae or ecchymoses. Microscopically, multifocal acute tubular epithelial injury lacking significant associated inflammation was frequently present (68 of 83 cases). Severe injury was present in 30 of 83 (36%) cases while moderate and mild injury occurred in 14 of 83 (17%) and 24 of 83 (29%), respectively. There were no lesions in the remaining 15 kidney cases even though 6 of these tested positive by IHC. Occasionally, haemorrhages were present in the glomeruli or the interstitium. Scattered nuclear pyknosis and karyorrhexis was present in the glomeruli and accompanied by occasional neutrophils in 63 of 83 (76%) cases (Fig. 13). Glomeruli often appeared less densely cellular than normal. Acute tubular injury was significantly associated with the degree of pyknosis and karyorrhexis in the glomeruli (ρ= 0.267, P = 0.015) and with the amount of viral antigen detected (ρ = 0.227, P = 0.039). Similar to the glomeruli, nuclear debris was often present in the interstitial capillaries. Tubular injury was characterized by tubular epithelial cell pyknosis, karyorrhexis and karyolysis, with detachment of these cells from the basement membrane (Fig. 14).

RVFV antigen was present in the kidney of 55 of 83 (66%) cases with available specimens. In the positive cases, viral antigen was typically in the cortex with 41 of 55 (75%) having antigen in the glomeruli, 33 of 55 (60%) in the tubules and 22 of 55 (40%) in both (Table 9). More specifically, viral antigen was in glomerular and interstitial capillaries, tubular epithelial cells and vascular smooth muscle cells (Figs. 15 and 16). In the glomeruli, viral antigen was in mononuclear cells, neutrophils, cellular debris or extracellularly in the capillaries. Viral antigen was present in the interstitial capillaries in 36 of 41 (88%) cases where glomerular labelling was also present, and labelling in the glomerular capillaries was significantly associated with labelling in the interstitial capillaries (ρ = 0.789, P < 0.001). In the interstitial capillaries, viral antigen was present in mononuclear cells, cellular debris, or extracellularly. Within tubules, labelling was in the cytoplasm of epithelial cells and predominately in the proximal convoluted tubules (Table 10). Labelling in the interstitial capillaries was significantly associated with

labelling in tubular epithelial cells (ρ = 0.282, *P* = 0.010). There was also an association between labelling in the glomerular capillaries and tubular epithelial cell labelling (ρ = 0.281, *P* = 0.010). Necrotic cells in areas of acute tubular injury were not consistently positive for viral antigen. Labelling was never present simultaneously in both proximal tubules and collecting tubules. In 3 cases, viral antigen was not present in the glomeruli or the proximal convoluted tubules but instead occurred predominantly in collecting tubules.

Table 9. Distribution of viral antigen in different areas of the kidney, for specimens with positive immunolabelling for RVFV in sheep.

Anatomical location	**Proportion**	**Percentage (95% CI)**
Glomeruli	41/55	75 (62, 85)
Interstitial capillaries	36/55	65 (52, 77)
Only glomeruli	3/55	5 (1, 14)
Only interstitial capillaries	0/55	0 (0, 5)
Glomeruli and interstitial capillaries	34/55	62 (49, 74)
Tubules	33/55	60 (47, 72)
Only tubules	11/55	20 (11, 32)
Glomeruli and tubules	22/55	40 (28, 53)
Collecting ducts	9/51*	18 (9, 30)
Only collecting ducts	0/51*	0 (0, 6)
Vascular smooth muscle	5/55	9 (3, 19)

Proportion = number of positive tissues over the total number of tissues examined, based on immunohistochemistry for RVFV antigen. * = Medulla not sampled in 4 cases. CI = confidence interval. The data do not include specimens with negative immunolabelling.

Table 10. Predominant location of viral antigen within renal tubules, for specimens with positive immunolabelling for RVFV in renal tubules.

Anatomical location	Proportion	Percentage (95% CI)
Proximal convoluted tubules	19/33	58 (40, 73)
Proximal straight tubules	3/33	9 (2, 23)
Loop of Henle	0/31*	0 (0, 9)
Distal straight tubules	1/33	3 (0, 14)
Distal convoluted tubules	4/33	12 (4, 27)
Collecting tubules	6/29*	21 (9, 38)

Proportion = number of positive tissues over the total number of tissues examined, based on immunohistochemistry for RVFV antigen. * = Medulla not sampled in four cases. CI = confidence interval. The data do not include specimens with negative immunolabelling in renal tubules.

2.4.7 Adrenal gland

Macroscopically, occasional cortical petechiae were present in the adrenal glands. Microscopically, 5 of 11 (45%) cases with available specimen had multifocal adrenocortical necrosis and haemorrhage. Necrosis involved individual cells to aggregates of cells predominantly in the zona fasciculata (Fig. 17). In one case, groups of cells in the zona glomerulosa were also involved. In four of the cases with necrosis, RVFV antigen was present in secretory cells of the zona fasciculata and in the cytoplasm of necrotic cells (Fig. 18). Labelling was focally disseminated in areas of necrosis or in single cells or small groups of cells that were not necessarily necrotic. One case with adrenocortical necrosis had no observable viral antigen labelling. Lesions and viral antigen were absent from the adrenal medulla.

Panel 3: Figures 13-18. Rift Valley fever virus, kidney and adrenal gland, adult sheep.

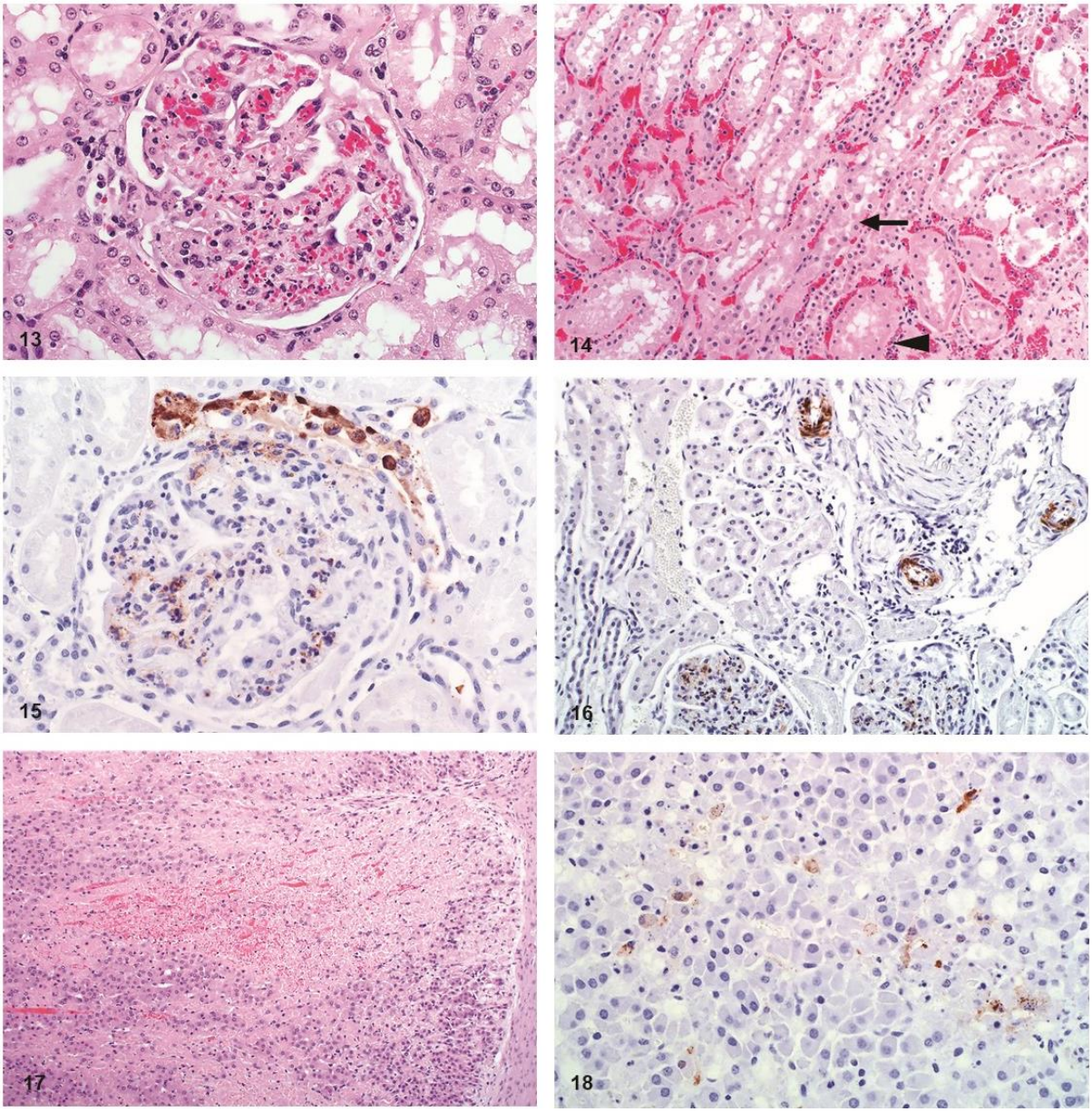

Figure 13. Case 55. Kidney. Scattered pyknosis and karyorrhexis in a renal glomerulus with sparse degenerate neutrophils. HE. **Figure 14.** Case 47. Kidney. Pyknosis in renal tubular epithelial cells (arrowhead) with detachment of the epithelium from the basement membrane (arrow). HE. **Figure 15.** Case 3. Kidney. Viral antigen in mononuclear cells, neutrophils and cellular debris in the glomerulus and in renal tubular epithelial cells. IHC for RVFV. **Figure 16**. Case 3. Kidney. Viral antigen within smooth muscle cells in small arteries at the cortico-medullary junction. IHC for RVFV. **Figure 17.** Case 55. Adrenal gland. Haemorrhage and focal disseminated necrosis in the cortex. HE. **Figure 18.** Case 46. Adrenal gland. Viral antigen within secretory cells in the zona fasciculata. IHC for RVFV.

2.4.8 Lung

Marked lung oedema and congestion were a consistent macroscopic finding (Fig. 19). The lungs were wet and heavy with fluid oozing from the cut surfaces and copious amounts of foam filling the trachea and bronchi. This was accompanied by mild to moderate hydrothorax. Microscopic examination revealed congestion, occasional haemorrhage, emphysema and intra-alveolar and interstitial oedema in 51 of 70 (73%) cases (Fig. 20). Inflammation, varying from mild to severe was present in the alveolar capillaries in all cases, and consisted of predominantly mononuclear cells accompanied by fewer neutrophils. Single cell pyknosis and karyorrhexis was occasionally present in the alveolar septa and peribronchial lymphoid tissues (Fig. 20). Haemorrhage was present in 9 of 70 (13%) cases.

RVFV antigen was present in lung specimens of 40 of 70 (57%) cases. Labelling was generally difficult to identify and was classified as isolated in 24 of 40 (60%) positive cases. Scattered and widespread viral antigen was present in 10 of 40 (25%) and 6 of 40 (15%) positive cases respectively. RVFV antigen was present in interstitial mononuclear cells histomorphologically consistent with pulmonary intravascular macrophages, or in the capillaries associated with cellular debris (Fig. 21). Labelling was absent from alveolar macrophages and pulmonary epithelial cells.

2.4.9 Heart

Macroscopically, epicardial- and endocardial haemorrhages and mild to moderate hydropericardium were present in most cases. Sub-epicardial ecchymoses were common in the coronary grooves and occasionally also present in paraconal and subsinuosal grooves. Sub-endocardial haemorrhages were generally in the left ventricle. Microscopically, there were focal haemorrhages in the endo- and epicardium in 13 of 57 (23%) cases. Histomorphological lesions attributable to RVFV infection were not present in the myocardium of any case.

Panel 4: Figures 19-23. Rift Valley fever virus, lung and heart, adult sheep.

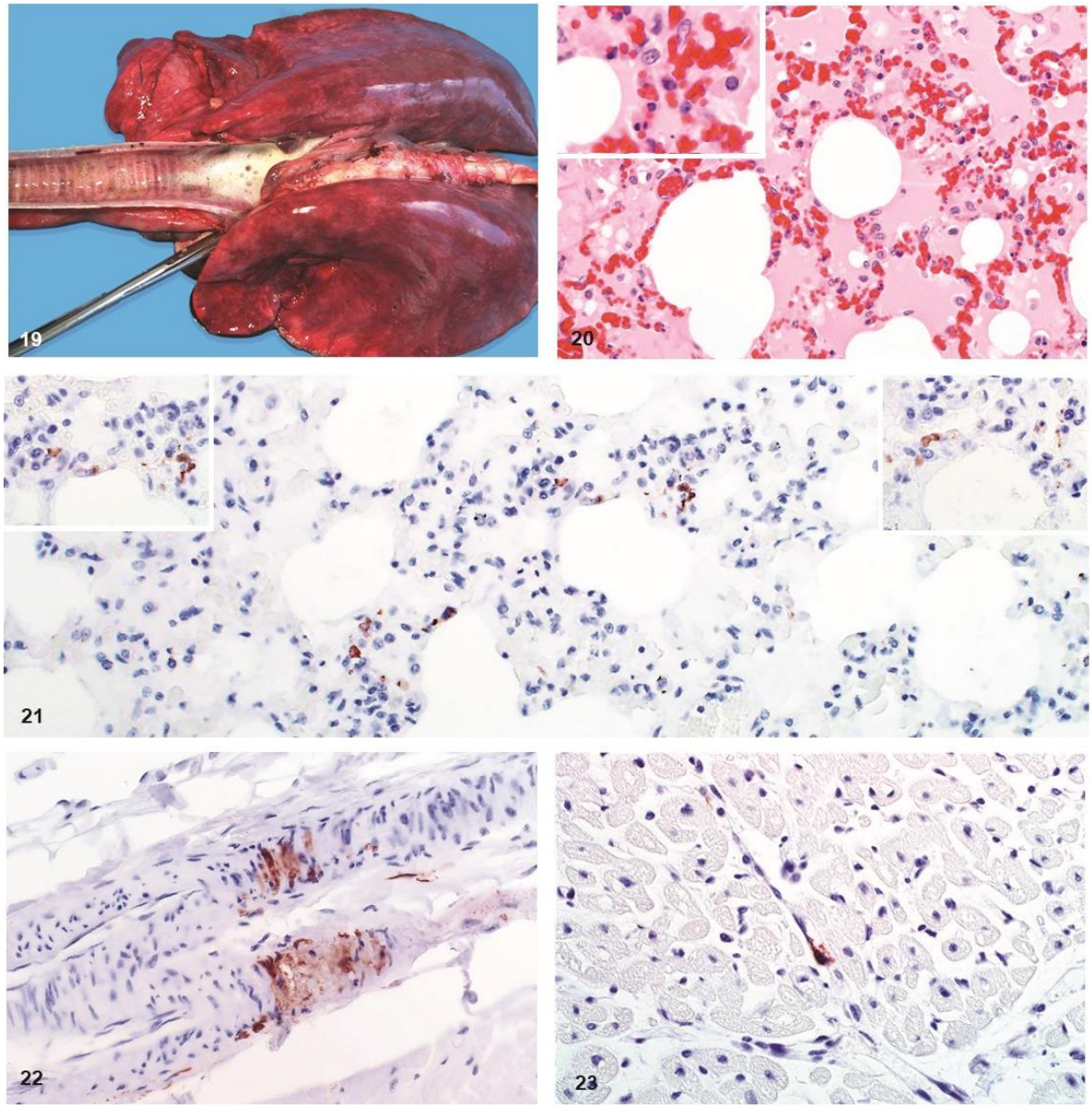

Figure 19. Case 48. Lung. Marked pulmonary oedema and congestion. **Figure 20.** Case 29. Lung. Marked pulmonary oedema with congestion, and a mild mononuclear inflammation accompanied by smaller numbers of neutrophils in the interstitial capillaries. **Inset:** Pyknosis and karyorrhexis in the pulmonary interstitium. HE. **Figure 21.** Case 9. Lung. Sparse viral antigen in the pulmonary interstitium. **Insets:** RVFV antigen in macrophages. IHC for RVFV. **Figure 22.** Case 3. Heart. RVFV antigen in vascular smooth muscle cells in a small artery. IHC for RVFV. **Figure 23.** Case 85. Heart. Positive labelling of endothelial cells in a capillary. IHC for RVFV.

Of the cases with available heart specimens only 8 of 57 (14%) were positive for RVFV antigen. Immunolabelling was either isolated (n = 7) or scattered (n = 1) and in the interstitium around capillaries or small blood vessels in association with cellular debris. In two cases, viral antigen was present in vascular smooth muscle cells within small blood vessels (Fig. 22). Viral antigen was also present in vascular endothelial cells (Fig. 23) or in circulation in association with cellular debris. Cardiomyocytes and intravascular mononuclear cells were negative for viral antigen.

2.4.10 Gastrointestinal tract

Although multifocal serosal haemorrhages could be present anywhere along the course of the gastrointestinal tract, they were often prominent on the surfaces of the rumen and abomasum. Occasionally, haemorrhages were also in the mucosa and submucosa. Peritoneal haemorrhages were sometimes present along the entire length of the major abdominal blood vessels. Mild to moderate serosanguinous ascites was also frequently present.

Necrosis was present in the lamina propria of the small intestine in 8 of 19 (42%) cases. However, autolysis was severe in 5 of 19 (26%) of these cases and as a result, the prevalence of necrosis related to RVFV infection in the small intestine was likely underestimated. Small necrotic foci were sporadically present between the intestinal crypts and at the base of the villi. Necrotic foci were comprised of cellular debris and a mild to moderate infiltrate of degenerate neutrophils and mononuclear cells. In some of the specimens a heavy infiltrate of eosinophils, likely unrelated to RVFV infection, was also present. Submucosal haemorrhage was present in one case.

Two cases had necrosis of the gut-associated lymphoid tissue, and consequently the Peyer's patches (like other lymphoid tissues) appeared depleted of lymphocytes. In other cases, nuclear and cellular debris were present in capillaries and in the connective tissue of the lamina propria.

Panel 5: Figures 24-29. Rift Valley fever virus, small intestine, tongue, skin and testis, adult sheep.

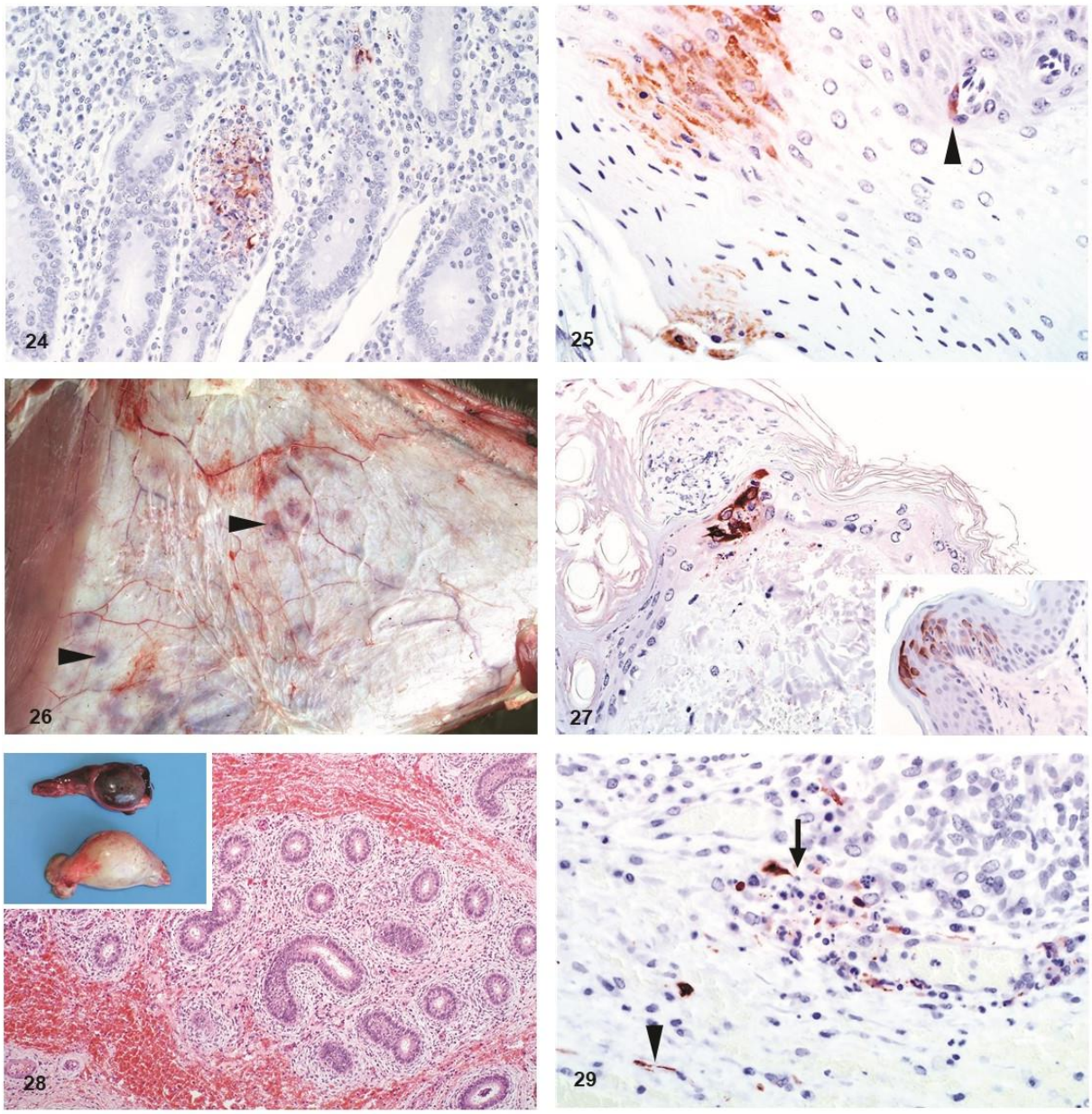

Figure 24. Case 55. Small intestine. Viral antigen in foci of necrosis in the lamina propria. IHC for RVFV. **Figure 25.** Case 48. Tongue. Positive labelling in the epithelium, and in an endothelial cell (arrowhead) in the submucosa. IHC for RVFV. **Figure 26.** Case 46. Skin, flank. Multifocal subcutaneous haemorrhages (arrowheads). **Figure 27.** Case 61. Skin. Viral antigen in keratinocytes below a cellular crust. **Inset:** Case 48. Skin. Abundant viral antigen in the cytoplasm of keratinocytes. IHC for RVFV. **Figure 28.** Case 49. Testis. Haemorrhage in the loose connective tissue surrounding the efferent ductules. **Inset:** Petechiae in the tunica albuginea of one testis and suffusive haemorrhage in another testis. HE. **Figure 29.** Case 49. Testis. RVFV antigen in intravascular cell fragments (arrow) and endothelial cells (arrowhead) in small blood vessels in the connective tissue surrounding an efferent ductule. IHC for RVFV.

RVFV antigen was present in the small intestine of 7 of 19 (37%) cases. Most positive labelling was present in necrotic foci, either associated with cellular debris or on rare occasions in the cytoplasm of cells histomorphologically consistent with macrophages (Fig. 24). Viral antigen was not present in epithelial cells. Lesions and immunolabelling were also absent from all rumen (n = 5), abomasum (n = 24) and large intestine (n = 2) specimens. Two of 10 examined tongue specimens had scattered groups of positive epithelial cells and one had positive endothelial cell labelling (Fig. 25).

2.4.11 Skin

Macroscopically, haemorrhages were commonly present in the subcutis and mucous membranes (Fig. 26). Crusts, presumably caused by insect bites, were often on the nose and ears. Histological lesions in the cases with available specimens (11) were minimal with scattered foci of haemorrhage and necrosis in 2 cases. Multifocal cellular crusts overlying areas of mild eosinophilic inflammation, interpreted as insect bite hypersensitivity, were present in a further 2 cases.

RVFV antigen was present in the skin of 6 of 11 (55%) cases. Typically, it was in the epidermis in the cytoplasm of keratinocytes (Fig. 27) and in 2 cases antigen was present below cellular crusts. Less frequently (2 of 11), viral antigen was present in the superficial dermis in association with cellular debris. In one case, viral antigen was in the epithelium of a hair bulb and in another in sebaceous gland epithelium.

2.4.12 Reproductive organs

Two young rams had multifocal petechiae to suffusive haemorrhages in the testis. Microscopically, haemorrhage was in the tunica albuginea and in the connective tissue surrounding the seminiferous tubules, efferent ductules, and duct of the epididymis (Fig. 28). Viral antigen was present multifocally within the connective tissue surrounding these structures in a variety of cell types including vascular smooth muscle and endothelial cells and possibly macrophages and fibroblasts (Fig. 29). Viral antigen was also present in cell fragments and

neutrophils in the blood vessels. Viral antigen was absent from the seminiferous tubules, efferent ductules, or the duct of the epididymis.

Ten uterine specimens were available for evaluation but unfortunately, most were of insufficient diagnostic quality. Haemorrhage was in the perimetrium and myometrium of 3 of 10 cases. Isolated viral antigen was in cellular debris or mononuclear cells in 2 of 10 cases.

2.5 Discussion

The aims of this study were to describe the tissue tropism and target cells of RVFV in a large number of naturally infected sheep, and to summarize gross, histopathological and immunohistochemical findings relative to results from previous research. The 2010 RVF outbreak in South Africa provided a valuable opportunity to study the pathology and cellular tropism of RVFV in sheep and compare this with previous reports. Liver, spleen, kidney and lungs were the specimens most often submitted. A fairly high number of gall bladder specimens (n = 23) were present, not surprisingly, since historically in South Africa much emphasis has been placed on oedema and haemorrhage of the gall bladder as a typical RVF lesion (Mundel and Gear, 1951, Erasmus and Coetzer, 1981). Similarly, many abomasal specimens were included (n = 24) due to the perceived importance of oedema and haemorrhages in the wall of this organ (Erasmus and Coetzer, 1981, Swanepoel and Coetzer, 2004). It should be noted that since organs were not consistently sampled in these field cases, the frequencies of lesions and immunolabelling could be an overestimate of the general population of RVF cases if there was a tendency to sample grossly abnormal organs.

Macroscopically, necrosis and haemorrhage of the liver was accompanied by lesions suggestive of vascular endothelial injury including, mild hydropericardium, hydrothorax and ascites, marked and diffuse pulmonary congestion and oedema, congestion and oedema of lymph nodes, and haemorrhages in many organs. The exact mechanism for haemorrhage and plasma leakage in RVFV infection in sheep has not been elucidated. However, the mechanisms of increased vascular permeability in viral haemorrhagic fever have often been

attributed to direct viral infection or damage of vascular endothelial cells, endothelial activation and dysfunction, infection of macrophages causing the production of pathologic concentrations of cytokines and other mediators, and thrombocytopenia (Paessler and Walker, 2013). Haemorrhage and necrosis in organs other than the liver have also been ascribed to activation of the coagulation cascade accompanied by depressed production of coagulation factors due to severe hepatic necrosis, which may cause disseminated intravascular coagulation (Paessler and Walker, 2013). Previously, thrombocytopenia, and prolonged prothrombin and clotting times have been demonstrated in sheep (Olaleye et al., 1996). In the present study RVFV antigen was present in endothelial cells and microscopic foci of necrosis were sporadically identified in various organs like the gall bladder, small intestines, skin, heart and testis. However, there was no convincing evidence of vascular fibrinoid necrosis or microvascular fibrin thrombi in any organ. Their absence may be attributable to hyperfibrinolysis or enhanced-fibrinolytic-type disseminated intravascular coagulation, which was described in Dengue haemorrhagic fever (Marchi et al., 2009, Asakura, 2014). Therefore, direct infection and injury of endothelial cells accompanied by enhanced activation of coagulation with consumption of platelets and coagulation factors could play a role in the pathogenesis of RVFV in sheep. However, the formation of fibrin thrombi might be inhibited by increased clot lysis causing widespread bleeding. Therefore, direct infection and injury of endothelial cells accompanied by enhanced activation of coagulation with consumption of platelets and coagulation factors could play a role in the pathogenesis of VHF (Paessler and Walker, 2013).

Microscopically, multifocal-random, necrotizing hepatitis was confirmed as the most distinctive histopathological feature of RVF cases in adult sheep. Experimental studies in adult sheep and lambs wherein animals were examined at known days post-infection have reported a sequence of events for the liver (Daubney et al., 1931, Findlay, 1932, Easterday et al., 1962a, Coetzer and Ishak, 1982). The earliest change affected either a single hepatocyte or groups of two to five hepatocytes randomly distributed in the lobule. Daubney et al. observed that hepatocytes in the central zone were more frequently infected first whereas Findlay and Easterday et al. reported that initial lesions were more frequently midzonal (Daubney et al.,

1931, Easterday et al., 1962a, Findlay, 1932). Focal degeneration of hepatocytes was closely followed by infiltration of the lesion with chiefly neutrophils and macrophages. These cells became degenerate and lesions evolved into foci consisting of karyorrhectic debris derived from the nuclei of both hepatocytes and infiltrating cells (Daubney et al., 1931). More advanced lesions might involve up to two-thirds or more of the entire lobule. In the present study a single pattern of necrosis could not be discerned. Instead, necrosis was distributed irregularly throughout the lobule. The severity and pattern of necrosis could also vary considerably between different liver specimens from the same animal.

Concerning the diagnostic specificity of lesions in the liver, early apoptotic hepatocytes (also referred to as Councilman bodies or acidophilic bodies) and late apoptotic bodies with nuclear fragments and condensed cytosol, in areas of hepatocellular damage, are diagnostically useful. In contrast, characteristic eosinophilic intranuclear inclusions are of limited diagnostic value since they are rare in older animals and often not clearly identifiable or confused with pseudo-inclusions. They are however, very useful in neonates and especially in foetuses where liver necrosis is often very subtle. Hepatocyte injury due to other concurrent causes such as hepatotoxic plants or hypoxia due to severe anaemia might also complicate hepatic histopathological interpretation. However, one consistent finding in this study was that, unlike the necrosis caused by hepatotoxic plants or hypoxia, RVFV invariably caused foci of necrosis in one or more of the periportal zones, specifically affecting hepatocytes of the limiting plate.

Sheep breeds might differ in their response to RVFV infection with an associated variation in lesions that could explain why previous reports concerning splenic, lung and skin lesions are inconsistent. Daubney et al. reported that the spleen was not enlarged, while Schulz reported splenomegaly (Daubney et al., 1931, Schulz, 1951). Daubney et al. reported that the lungs were normal in size and colour and did not exhibit haemorrhages. Subsequent researchers described pulmonary congestion, oedema and emphysema with occasional haemorrhagic foci that are consistent with the findings of the present study (Schulz, 1951, Coetzer, 1977, Van Der Lugt et al., 1996, Faburay et al., 2016a, Faburay et al., 2016b). Another study comparing

the susceptibility of three breeds of sheep to experimental infection reported that the spleen of the Yankasa breed of sheep was enlarged while that of West African Dwarf and Ouda sheep were shrunken and firm (Olaleye et al., 1996). All three breeds exhibited lung oedema with haemorrhages and oedema in the bronchial lymph nodes, but pulmonary haemorrhage was more severe in the Yankasa breed. Petechiae and ecchymoses were reported in the visible mucous membranes and hairless areas of the skin of the Yankasa sheep but not in the West African Dwarf and Ouda sheep (Olaleye et al., 1996). The results of the present study confirmed the findings of previous reports concerning RVF in South Africa whereby subcutaneous haemorrhages were observed in the axillary region, the medial aspect of the hind limbs, and in the lower portions of the extremities (Schulz, 1951, Erasmus and Coetzer, 1981). Although Merino and Dorper are the most common breeds of sheep in South Africa, ascribing the lesions reported here to these breeds is not possible since breed was rarely recorded on laboratory submission forms.

Differences in lesions among published studies could also be ascribed to differences in viral genes, viral strains, or inoculum route (Peters and Anderson, 1981, Bales et al., 2012). The physiological state of the animal, diet, rearing practices, and concurrent infection with other pathogens might also account for differing responses to viral infections in general (Peters and Anderson, 1981, Bales et al., 2012). However, studies in rats suggest that host genetic background and host immunological response might play a more important role than viral virulence and inoculum size on the clinical outcome of RVFV infection (Peters and Anderson, 1981, Hartman et al., 2014, Busch et al., 2015). Genetically resistant rats treated with an immunosuppressive drug and challenged with up to 5 x 10^6 PFU were more resistant to infection than healthy rats bearing a susceptibility gene and challenged with 5-50 PFU (Peters and Anderson, 1981). Genetic resistance might also explain why naturally occurring encephalitis, a complication of RVF in humans that has been experimentally reproduced in mice and rats, has not been described in sheep (Van Velden et al., 1977, Al-Hazmi et al., 2003, Dodd et al., 2014, Busch et al., 2015). Whether genetic resistance is more important than viral virulence for the outcome of RVFV infection in sheep should be further explored.

Microscopically, lymphoid necrosis in the spleen and other lymphoid tissues was mentioned in previous studies but was not described in detail (Coetzer, 1977, Olaleye et al., 1996, Van Der Lugt et al., 1996, Shieh et al., 2010, Faburay et al., 2016a, Faburay et al., 2016b). The results of the present study confirmed that necrosis occurs in the spleen and lymph nodes of adult sheep and that splenic necrosis was significantly associated with necrosis in the lymph nodes. Previous research reported that lymphocytes in the Peyer's patches had varying degrees of pyknosis and karyorrhexis, corresponding in degree of intensity to similar lesions in other lymphoid tissues and that pyknosis and karyorrhexis also occasionally occurred in the bronchus-associated lymphoid tissues (Coetzer, 1977). Additionally, in the intestines karyorrhexis of cells in the interglandular tissues and particularly around the lymphoid follicles submucosa has been reported (Daubney et al., 1931). In the present study, severe changes were observed in the gut associated lymphoid tissues in the small intestine that mirrored changes in the lymph nodes. Scattered lymphocytolysis was also noted in the lamina propria of the small intestine, the periportal areas of the liver and occasionally in the bronchus-associated lymphoid tissues. Previous reports also described marked pyknosis and karyorrhexis of mononuclear cells in the distal jejunum and ileum in lambs (Coetzer, 1977). Unfortunately, this finding was not corroborated in the current study since the different anatomical regions of the small intestine could not be reliably identified. Therefore, all lymphoid tissues and anatomical locations where lymphocytes often occur should be meticulously examined since pyknosis and karyorrhexis of lymphocytes seem to be typical for RVFV infection.

The present study also identified lymphocytolysis as being prominent in the B-cell rich areas of lymphoid organs, suggesting that B lymphocytes were preferentially targeted. The pathogenic mechanism of lymphocytic depletion in sheep is likely apoptosis as demonstrated in mice using terminal deoxynucleotidyl transferase dUTP nick-end labelling (Smith et al., 2010). Also, tingible-body macrophages, described in this study, are by definition cells that phagocytose fragments of apoptotic bodies (Aguzzi et al., 2014). However, further examination

of lymphocyte subsets with cell markers would clarify which cells undergo lymphocytolysis and elucidate pathogenic mechanisms.

In the present study multifocal acute renal tubular injury was present in most of the cases (68 of 83; 82%). Daubney et al. made the astute inference that renal tubular degeneration (nephrosis) was absent in lambs due to the peracute course of the disease in that age group. The same authors surmised that infected adult sheep might live long enough for kidney damage to develop, and whether lesions are observed or not depended on the length of time that sheep survived, hence the variable lesion severity observed in the present study (Daubney et al., 1931). Daubney et al. also observed that renal changes in adult sheep that died acutely occured in the convoluted tubules while other tubules appeared normal. In less acute cases, the tubular injury was less advanced and affected all the tubular epithelial cells in the cortex (Daubney et al., 1931). In the present study changes were in the convoluted, straight and collecting tubules in the cortex but not in the loops of Henle or in the medulla.

Furthermore, scattered pyknotic and karyorrhectic nuclear and cellular debris was present in the glomeruli. The origin of this debris could not be ascertained with certainty but it often appeared to be present within capillary lumens and hence could originate from leucocytes or endothelial cells. The fragments could also be remnants of necrotic leucocytes or vascular endothelial cells from distant tissues, trapped within the capillary beds of an end-artery organ. Similar to the renal glomerular findings, cellular debris was also observed in the renal interstitial capillaries and in the pulmonary alveolar septa Coetzer also reported the latter (Coetzer, 1977). Comparable findings have been made in DHF where apoptosis of leucocytes was demonstrated in the pulmonary microvasculature and apoptosis of vascular endothelial cells in pulmonary and intestinal tissues (Limonta et al., 2007). High levels of circulating endothelial cells were demonstrated in fatal human DHF cases (Cardier et al., 2006). Therefore, in RVF cases in sheep it seems likely that nuclear and cellular debris in the renal glomerular capillaries, renal interstitial capillaries and in the pulmonary alveolar septa all have the same

origin, namely necrotic vascular endothelial cells or leucocytes. This futher supports the proposed mechanism of observed haemorrhage and plasma leakage in RVFV infection.

Immunolabelling for RVFV was most unequivocally positive in the liver, with labelling in the cytoplasm of injured hepatocytes and cytoplasmic fragments. Labelling was also readily identified in spleen, although positive labelling was observed more readily in the white pulp, particularly in the marginal zone. In the kidney, viral antigen was more often in the cortex within glomerular and interstitial capillaries, tubular epithelial cells and vascular smooth muscle cells. Additionally, viral antigen might first appear in the glomerular and peritubular capillaries, second in proximal convoluted tubular epithelial cells and then gradually move through the more distal tubules and the collecting ducts of individual nephrons, progressively clearing from the glomeruli and more proximal aspects until the virus completely disappears from the kidney or the animal dies. This interpretation was supported by our observation of a stronger correlation between glomerular and interstitial labelling than between glomerular and tubular labelling.

Lung specimens were often positive for RVFV antigen but labelling was generally sparse and difficult to identify. Viral antigen in the adrenal glands was in adrenocortical cells in the zona fasciculata. RVFV antigen was also present in macrophages in lymph nodes; epithelial cells and a vascular endothelial cell in the tongue; in foci of necrosis in the gall bladder and small intestine; and within vascular smooth muscle cells and vascular endothelial cells in heart specimens. Viral antigen has been previously detected in lymph node but not in gall bladder, small intestine, tongue or heart (Van Der Lugt et al., 1996, Faburay et al., 2016b, Wichgers Schreur et al., 2016).

Skin specimens might be useful diagnostically since a surprisingly high percentage (55%) were IHC positive. However, viral antigen was rarely present in skin specimens taken from areas with subcutaneous haemorrhages. We suspect that specimens from the nose and ears or other areas with crusting due to insect bites, might be more useful diagnostically. A study to determine the competance of *Culex pipiens* as a vector of RVFV supports this conclusion

(Vloet et al., 2017). In this study RVFV was absent in skin specimens not exposed to mosquitoes. Instead, antigen was detected in mosquito-exposed skin in macrophages, vascular endothelial cells, smooth muscle cells, lipocytes, keratinocytes and fibroblasts.

To our knowledge this is the first report of lesions and RVFV antigen detection in the testis of sheep. However, the successful passaging of RVFV in lamb testis cell cultures was previously reported (Coackley, 1965). In the present study, RVFV antigen was not within the seminiferous tubules, efferent ductules, or the duct of the epididymis and was instead only in the connective tissue surrounding these structures. However, there is still a risk that RVFV might be transmitted through semen. RVFV genomic RNA was detected by RT-PCR in the semen of a human kidney transplant recipient for up to 4 months after onset of symptoms (Haneche et al., 2016). RVFV antigen and antibodies were also detected using ELISA and AGID in the semen of bulls 1-3 weeks after vaccination with a live attenuated RVFV vaccine (Saad et al., 1997). Currently, international trade rules do not require the screening of ruminant semen for RVFV (OIE., 2017). Therefore, a study of RVFV-infected ruminants should be performed that attempts to detect viable virus from semen to determine concentrations and duration of shedding.

Macrophages were positive for RVFV antigen in this study, and based on morphology, microanatomical location and comparisons with descriptions of these cells in mice and humans we consider these to include Kupffer cells in the liver; marginal zone, metallophilic, tingible-body and red pulp macrophages in the spleen; sinus macrophages in the lymph nodes; pulmonary intravascular macrophages; lamina proprial macrophages in the intestinal tract; intravascular macrophages in the renal interstitium and glomerular tuft; and testicular interstitial macrophages. RVFV antigen was also reported to occur in macrophages in the skin of experimentally infected sheep (Vloet et al., 2017).

Vascular smooth muscle cells and endothelial cells were also positive for RVFV antigen in this study. One common feature of tissue macrophages, vascular smooth muscle cells and endothelial cells is that they all express class AI scavenger receptors (SCARA1) (Zani et al.,

2015). In mice, tissue macrophages expressing SCARA1 were detected in the red pulp and marginal zone of the spleen, subcapsular region of lymph nodes, the lamina propria of the intestines, Kupffer cells in the liver and macrophages of the lung (Hughes et al., 1995). In human tissues, anti-scavenger receptor class A antibodies have been shown to recognize macrophages such as Kupffer cells in the liver, pulmonary macrophages, macrophages in lymphoreticular organs, macrophages in the lamina propria of the intestines and interstitial macrophages in kidney and testis (Tomokiyo et al., 2002). This corresponds with the distribution of RVFV immunolabelled macrophages detected in sheep in the present study. Scavenger receptors are membrane-bound pattern recognition receptors that bind to a variety of ligands including endogenous proteins and pathogens and have been classified into 10 eukaryote families, defined as Classes A-J (Zani et al., 2015). It has been shown that the uptake of adenovirus 5, herpes simplex virus type 1 and vaccinia virus is mediated via class A scavenger receptors (Haisma et al., 2009, MacLeod et al., 2013, MacLeod et al., 2015). Although class B scavenger receptors differ from the class A scavenger receptors in terms of structure and function, a number of them have been identified as receptors for viruses such as enterovirus 71, coxsackie virus and hepatitis C virus (Scarselli et al., 2002, Yamayoshi et al., 2009, Yamayoshi et al., 2012). The finding that diverse viruses exploit scavenger receptors, and that the cellular tropism demonstrated for RVFV in sheep might coincide with the distribution of SCARA1 in tissues, should be explored in future studies.

The minimum set of specimens to be submitted for histopathology and IHC to confirm or exclude a diagnosis of RVFV should include liver, spleen and kidney with lung and skin useful additional samples (Table 11). Characteristic microscopic lesions occur in the liver, spleen, kidney and lungs. These lesions include necrosis of limiting plate hepatocytes with apoptosis; marked lymphocytolysis in B-lymphocyte dependent areas of the spleen; acute renal tubular epithelial injury; and nuclear pyknosis and karyorrhexis in the capillaries of the glomeruli and pulmonary interstitium. A definitive diagnosis of RVFV can be obtained by performing IHC on FFPE liver, spleen and kidney.

Table 11. Preferred diagnostic specimens for investigation of RVF using histopathology and immunohistochemistry.

Diagnostic specimen in order of importance	Recommended number of samples and location	Justification
Liver	Sections from at least two liver lobes	Typical hepatocyte injury and apoptotic bodies. Fine diffuse to coarse granular labelling in the cytoplasm of injured hepatocytes and in cytoplasmic fragments in most cases. Sections from different areas in the liver may differ completely, with one section having extensive labelling and lesions and another having few or none.
Spleen	At least one section	Typical lymphocytolysis in the white pulp which is most apparent in the germinal centres, mantle zones, marginal zones and peripheral zones of the periarteriolar lymph sheaths and characterized by the presence of cellular debris and tingible-body macrophages. RVFV antigen positive macrophages can include those in the in the marginal zone and red pulp of the spleen and tingible-body macrophages in the white pulp.
Kidneys	One section from both kidneys that includes cortex and medulla	Acute renal tubular epithelial injury favouring the more proximal aspects of the nephron. Also, nuclear pyknosis and karyorrhexis in the glomerular capillaries in most cases. Possible hitherto-unrecognized renal form of RVF in sheep.
Skin	From the ears and other areas with visible crusts due to insect bites	In mosquito-exposed skin, virus is present in a variety of cells including keratinocytes and infiltrating macrophages. Biopsy samples from the ears of live animals could be useful to demonstrate infection.
Lung	One section	Pyknosis and karyorrhexis in the pulmonary interstitial capillaries in most cases. Also, RVFV antigen-positive macrophages present in the pulmonary interstitium, but difficult to identify in most specimens.

However, when typical liver and spleen lesions are absent but renal tubular epithelial injury is apparent, IHC should be performed to exclude a possible renal form of RVFV. In the present study, 3 cases had acute renal tubular injury with labelling for RVFV in the kidney, but no histological lesions or immunohistochemical labelling in the liver, or in the spleen of 2 cases with available specimens. This result could simply be a reflection of inadequate sampling since often only a single specimen from the liver and/or the spleen and/or the kidney was submitted to diagnostic laboratories. However, these cases could represent an atypical form of RVF in sheep. Acute renal failure associated with RVF was described in human patients in Saudi Arabia and Sudan where 13 and 85 patients respectively had signs and symptoms of renal failure without hepatic involvement (Al-Hazmi et al., 2003, El Imam et al., 2009). Therefore, in RVF-endemic areas, routine screening of acute renal tubular epithelial injury for RVFV antigen presence should be considered, especially when other common causes (e.g. pulpy kidney disease and, nephrotoxic plants and antimicrobials) have already been excluded.

2.6 Conclusion

This large investigation of RVFV pathology and tropism in sheep provides a comprehensive description of lesion distribution at the tissue and cellular level. Liver necrosis was confirmed as the most distinctive feature of RVF cases in adult sheep. Furthermore, 45 of 70 (64%) cases where liver, spleen and kidney tissues were available also had foci of acute renal tubular epithelial injury in addition to necrosis in both the liver and spleen. Acute renal tubular and glomerular injury was the most frequent RVF lesion in some cases suggesting that an atypical renal form of RVF might occur in sheep. The liver was most consistently positive for RVFV antigen followed by the spleen, kidneys, lung and skin. Antigen-positive cells included hepatocytes, renal tubular epithelial cells, adrenocortical cells, macrophages, neutrophils, vascular smooth muscle cells, and vascular endothelial cells.

In most cases, a diagnosis of RVF can be confirmed using histopathology of the liver, kidney and spleen. Skin with crusting due to insect bites and lung could be useful additional samples. However, we recommend that in endemic areas, cases of acute renal tubular injury be investigated further using IHC if other more common causes have already been excluded. The fact that RVFV can cause an acute infection in the testis requires further investigation with possible revisions to international trade rules to include testing of semen for RVFV using PCR and virus isolation.

CHAPTER 3

LESIONS AND CELLULAR TROPISM OF NATURAL RIFT VALLEY FEVER VIRUS INFECTION IN YOUNG LAMBS

This paper was accepted for publication: Odendaal L, Davis AS, Fosgate GT, Clift SJ. Lesions and cellular tropism of natural Rift Valley fever virus infection in young lambs. *Veterinary Pathology*. Manuscript ID: VET-19-FLM-0002.R2. Copied here with permission. An additional panel (No. 15) and related text in the results was added to this chapter.

3.1 Summary

A clear distinction can be made regarding the susceptibility to, and the severity of lesions in young lambs when compared to adult sheep. In particular, there are important differences in the lesions and tropism of Rift Valley fever virus (RVFV) in the liver, kidneys and lymphoid tissues of young lambs. A total of 84 lambs (< 6 weeks old), necropsied during the 2010-2011 RVF outbreak in South Africa were examined by histopathology and immunohistochemistry (IHC). Of the 84 lambs, 71 were positive for RVFV. The most striking diagnostic feature in infected lambs was diffuse necrotizing hepatitis with multifocal liquefactive hepatic necrosis (primary foci) against a background of diffuse hepatocellular death. Lymphocytolysis was present in all lymphoid organs except for the thymus. Lesions in the kidney rarely progressed beyond hydropic change and occasional pyknosis or karyolysis in renal tubular epithelial cells. Viral antigen was diffusely present in the cytoplasm of hepatocytes but this labelling was noticeably sparse in primary foci. Immunolabelling for RVFV in young lambs was also detected in macrophages, vascular smooth muscle cells, adrenocortical epithelial cells, renal tubular epithelial cells, renal peri-macular cells and cardiomyocytes. RVFV immunolabelling was also often present in capillaries and small blood vessels either as non-cell-associated viral antigen, as antigen in endothelial cells or intravascular cellular debris. Specimens from the liver, spleen,

kidney and lungs were adequate to confirm a diagnosis of RVF. Characteristic lesions were present in these organs with the liver and spleen being the most consistently positive for RVFV by IHC.

3.2 Introduction

Rift Valley fever is a viral haemorrhagic disease caused by a single stranded RNA virus of the *Bunyavirales* order, *Phenuiviridae* family. The virus, first isolated in 1931 during an investigation into an outbreak among sheep in the greater Rift Valley of Kenya, causes severe disease in both humans and animals (Daubney et al., 1931). Subsequently, epidemics have been reported in most countries in Africa (Pepin et al., 2010). The disease also spread to the Arabian peninsula and caused large epidemics in Saudi Arabia and Yemen (Shoemaker et al., 2002). RVF was also reported in Madagascar and later in the Comoros and Mayotte (Cêtre-Sossah et al., 2012, Morvan et al., 1991, Sissoko et al., 2009). The disease mainly affects sheep but cattle, goats, African buffaloes, camelids, and other wild animals are also reportedly affected (Pienaar and Thompson, 2013). The virus is primarily transmitted by mosquitoes and experimentally competent vector species have been identified in Europe and the United States of America, raising concern about the risk of introduction of RVFV into these RVF-free regions (Moutailler et al., 2008, Turell et al., 2008).

The first description of RVF in Kenya reported heavy mortalities in new-born lambs, a marked rise in the mortality rate of ewes and an increase in abortions (Daubney et al., 1931). The authors remarked that the liver lesions in young lambs were much more severe than in adult sheep and that extensive hepatic necrosis only rarely occurred in adult sheep. Daubney et al. also noted that lesions in the kidneys of young lambs differed from those of adult sheep (Daubney et al., 1931). Multifocal acute renal tubular injury (nephrosis) in adult sheep with RVF was confirmed in subsequent research (Daubney et al., 1931, Faburay et al., 2016b, Faburay et al., 2016a, Odendaal et al., 2019, Olaleye et al., 1996, Ragan et al., 2019). However, in lambs, the kidney lesion rarely progresses beyond tubular epithelial cell degeneration,

characterized by cell swelling and karyolysis (Daubney et al., 1931). In addition to diffuse hepatic necrosis, studies of natural infections in young lambs also reported gall bladder oedema, pleural effusions, lung oedema, and widespread haemorrhages in many organs including occasional enteric haemorrhage (Coetzer, 1977, Daubney et al., 1931, Schulz, 1951). Varying degrees of pyknosis and karyorrhexis in lymphoid tissues of new-born lambs that died of RVF were also reported (Coetzer, 1977).

Experimentally, the incubation period of RVF in 1 to 5 day old lambs is 12-24 hours (Easterday et al., 1962a). This is followed by a marked febrile response (41-42 ^{O}C), and rapid progression to death within 24 to 72 hours (Easterday et al., 1962a). The initial lesion in the liver of 1 to 5 day old lambs consists of small aggregates of neutrophils in the sinusoids that develop between 12 and 24 hours after inoculation (Easterday et al., 1962a). Between 24 and 36 hours, small random foci of hepatocellular necrosis, referred to as primary foci, develop (Easterday et al., 1962a). These foci involve only a few hepatocytes at 24 hours after exposure and evolve into larger, more circumscribed areas of liquefactive necrosis in the ensuing 6 to 12 hours (Coetzer, 1977). Within primary foci, the hepatocytes and infiltrating leucocytes disintegrate completely causing a loss of tissue and cellular profiles, and present as fine basophilic karyorrhectic particles against a background of homogenous eosinophilic debris (Coetzer, 1977, Easterday et al., 1962a). Shortly after development of the primary foci, diffuse destruction of the remaining hepatocytes occur (Coetzer, 1977). A number of authors have described primary foci in young lambs and concluded that it is pathognomonic for RVFV (Coetzer, 1977, Easterday et al., 1962a, Erasmus and Coetzer, 1981).

The cellular tropism of naturally occuring RVFV has only been studied using IHC in 4 new-born lambs wherein viral antigen was reported in the liver, spleen, lymph nodes and lungs (Van Der Lugt et al., 1996). Previously, we described the lesions and reported the cellular tropism of natural RVFV infection in adult sheep from the same outbreak in South Africa (Chapter 2). RVF is much more acute in young lambs than in older sheep, and there are important

differences in the lesions and tropism in particularly the liver, kidneys and lymphoid organs of young lambs. Therefore, the principle aim of the present study was to describe the quantitative and qualitative pathomorphology of RVFV infection in diverse organs from a large number of naturally infected lambs and contrast this with previously published results for adult sheep as described in chapter 2. Further aims were to ascertain the extent to which virus can be detected in different organs and establish the diagnostic significance of certain tissues and specific histologic features of RVFV in young lambs.

3.3 Materials and methods

3.3.1 Case selection

All specimens originated from the carcasses of naturally infected lambs necropsied during the 2010-2011 RVF outbreak in South Africa that affected mainly sheep (Pienaar and Thompson, 2013). This work was done with approval from the Animal Ethics Committee of the University of Pretoria (clearance certificate V096-16). Supplementary material in support of the results presented in this article is available from the authors upon request.

Tissue samples were collected from sheep including young lambs as described previously (Chapter 2). Briefly, tissues from 1034 necropsied animals were collected by government officials and the principle investigator (Lieza Odendaal), preserved in 10% neutral buffered formalin, embedded in paraffin, and haematoxylin and eosin-stained histologic sections were routinely prepared. Included were at least 173 young lambs up to 6 weeks of age. From this collection, cases were excluded when the level of autolysis was severe, when only one organ was submitted, or when the liver was not available for study. A total of 84 cases were suitable for study of which 71 cases were classified positive for RVF based on results of histopathology, RT-qPCR and/or IHC. A parallel interpretation of tests was chosen to maximize sensitivity and therefore, any animal with at least one positive test result was selected for study. Additionally, animals that died as part of the outbreak and were shown to be infected with RVFV were

presumed to have died of RVF even if lesions were absent. The negative controls were 13 lambs that died of natural infections during the outbreak and were examined for RVFV as part of the government campaign to monitor the spread of RVF, but tested negative.

3.3.2 Diagnostic tests

Nucleic acid extractions and RT-qPCR on fresh liver specimens for 46 of the cases from the 2010 outbreak were performed at the Biotechnology PCR Laboratory of the Agriculture Research Council-Onderstepoort Veterinary Institute as described previously (Odendaal et al., 2014). None of the cases included from the 2011 outbreak (n = 16) were tested using RT-qPCR.

Immunohistochemistry with additional controls was performed as described in the original validation study (Odendaal et al., 2014). Briefly, labelling for the detection of RVFV antigen was performed using polyclonal antibody to RVFV (mouse ascitic fluid), prepared at the National Institute for Communicable Diseases (Johannesburg, South Africa) as described (Sartorelli et al., 1966, Swanepoel et al., 1986). Previously, 40 controls were tested that included 8 RT-qPCR- and IHC-positive RVF cases that occurred in 2009, and 32 additional negative tissue controls that that had liver lesions that resembled RVF but resulted from other causes (Odendaal et al., 2014). The controls were tested with a range of relevant and irrelevant antibodies namely: polyclonal antibody to RVFV, polyclonal antibody (mouse ascitic fluid) to WBV (antibody to WBV), monoclonal antibody (mouse ascitic fluid) to bovine herpesvirus-1, and rabbit polyclonal antiserum to equine herpesvirus-1 (Odendaal et al., 2014). The antibody to WBV, which was used as the negative reagent control antibody in this study, was similarly prepared at the National Institute for Communicable Diseases and validated for IHC at the Faculty of Veterinary Science, University of Pretoria (Sartorelli et al., 1966, van der Lugt et al., 1995). Additionally, to confirm that intravascular immunoreactivity observed in this study was due to RVFV antigens, tissue sections were sequentially tested with the antibodies to RVFV and WBV.

The immunohistochemistry method included microwave antigen retrieval in citrate buffer (pH 6.0), blocking of endogenous peroxidases with 3 % hydrogen peroxide, incubation with the anti-RVFV primary antibody at 1:500 dilution for 1 hour, and rabbit anti-mouse secondary antibody (F0232, DakoCytomation, Glostrup, Denmark) followed by detection with a standard avidin-biotin peroxidase system, Vectastain® Elite® ABC-HRP Kit (PK-6100, Vector Laboratories, Inc., Burlingame, CA, USA), NovaRED peroxidase substrate (SK-4800, Vector Laboratories, Inc.) and haematoxylin counterstain.

3.3.3 Examination of tissues

Histomorphological features in all available organs were systematically recorded and reviewed within the context of lesions associated with RVFV infection. Lesion severity in the liver, spleen and kidney was scored using a qualitative scale as mild, moderate or severe. The number of primary foci in the liver specimens were scored on a semi-quantitative scale as isolated (<5), scattered (between 6 and 10) or widespread (>10). All liver samples measuring between approximately 5 mm^2 and 20 mm^2 were examined. Immunolabelling for RVFV antigen was scored on a semi-quantitative scale as isolated, scattered or widespread labelling, as previously described (Section 2.3.3)

The number and types of organs available for study varied considerably by case with liver (n = 84; inclusion criterion), spleen (n = 64), lung (n = 63) and kidney (n = 56) being the specimens most often submitted. Additional tissue specimens included 40 heart, 30 gastrointestinal tract, 21 lymph node, 19 brain, 10 thymus, 8 adrenal, 3 gall bladder and 3 skin specimens. Gastrointestinal tract specimens included tongue (n = 5), forestomach (n = 3), abomasum (n = 15), small intestine (n = 19) and large intestine (n = 1).

3.3.4 Statistical analysis

Categorical data were presented as proportions and 95% mid-P confidence intervals. Data from ordinal scales were described using the median and interquartile range (25th to 75th percentiles). Results for the ordinal scales were compared between the liver and other organs using Wilcoxon signed rank tests. Correlations between scaler data were estimated using Spearman's rho and categorical data using Cohen's kappa. Statistical analyses were performed in freeware (Epi Info, version 6.04, CDC, Atlanta, GA, USA) and commercial statistical software (IBM SPSS Statistics Version 25, International Business Machines Corp., Armonk, NY, USA). Significance was set as $P < 0.05$.

3.4 Results

3.4.1 Overview

The organs most consistently positive for RVFV by IHC were liver and spleen (Table 12). Viral antigen was also easily identified in lung, kidney, brain, lymph node, thymus, and small intestine. Positive labelling was typically fine diffuse to coarse granular cytoplasmic labelling. Vascular labelling was especially prominent in blood vessels, both as non-cell-associated antigen, as well as cell-associated antigen in endothelial cells and vascular smooth muscle cells. Endothelial/non-cell-associated intravascular viral antigen was often present in the brain, lymphoid organs and the lung (Table 13), whereas labelling in vascular smooth muscle cells was most commonly present in the kidney (Table 14). Immunolabelling was not observed in sequential slides incubated with antibody to WBV instead of RVFV (Figs. 30-41). Additionally, typical histological lesions and RVFV antigen were not detected in any of the tissues from the 13 cases included as negative tissue controls (Figs. 42-65). Immunohistochemistry was negative for RVFV antigen in all samples from negative control cases.

Table 12. Frequency of viral antigen in different organs and comparison to quantity of immunolabelling in liver, for 71 young lambs with natural RVFV infection.

Organ	Proportion with Immunolabelling		Quantity of Immunolabelling	
	Positive/ Total[a]	Percentage (95% CI)	Median (IQR)[b]	P value[c]
Liver	67/71	94 (87, 98)	Widespread (widespread, widespread)	NA
Gallbladder	2/3	67 (13, 98)	Widespread (widespread, widespread)	0.317
Spleen	48/53	91 (80, 96)	Widespread (scattered, widespread)	<0.001
Lymph nodes	14/17	82 (59, 95)	Widespread (widespread, widespread)	0.066
Thymus	8/9	89 (56, 99)	Widespread (scattered, widespread)	0.157
Kidney	40/46	87 (75, 95)	Widespread (scattered, widespread)	<0.001
Adrenal glands	3/5	60 (18, 93)	Widespread (widespread, widespread)	1.0
Lung	46/52	88 (78, 95)	Widespread (widespread, widespread)	0.003
Heart	27/36	75 (59, 87)	Widespread (scattered, widespread)	0.001
Rumen	1/3	33 (2, 87)	Isolated (NA)	0.102
Abomasum	9/13	69 (41, 89)	Widespread (widespread, widespread)	0.066
Small intestine	12/14	86 (60, 98)	Widespread (isolated, widespread)	0.026
Large intestine	0/1	0 (0, 95)	NA	NA
Tongue	3/5	60 (18, 93)	Scattered (isolated, widespread)	0.180
Skin	2/3	67 (13, 98)	Scattered (scattered, widespread)	0.317
Brain	17/19	89 (69, 98)	Widespread (scattered, widespread)	0.014

[a]Positive/Total represents number with positive immunolabelling for RVFV antigen out of the total number of tissues examined. CI, confidence interval; IQR, interquartile range; NA, not applicable. [b]Calculated only for the cases with positive labelling; the categories in parentheses are the IQR of antigen quantity in the sample set. [c]Based on Wilcoxon signed rank tests comparing the quantity of positive immunolabelling to the quantity of labelling in liver samples.

Table 13: Frequency of non-cell-associated viral antigen in blood vessels or antigen in vascular endothelial cells or intravascular cellular debris, for young lambs with natural RVFV infection.

Organ	Positive/total[a]	Percentage (95% CI)[b]
Gallbladder	2/3	67 (13, 98)
Spleen	43/53	81 (69, 90)
Lymph node	14/17	82 (59, 95)
Thymus	8/9	89 (56, 99)
Kidney	35/46	76 (62, 87)
Adrenal glands	3/5	60 (18, 93)
Lung	42/52	81 (68, 90)
Heart	27/36	76 (60, 88)
Gastrointestinal tract	17/22	77 (57, 91)
Tongue	3/5	60 (18, 93)
Skin	2/3	67 (13, 98)
Brain	17/19	89 (69, 98)

[a] Positive/total represents number with positive immunolabelling for RVFV antigen out of the total number of tissues available for examination. [b] CI, confidence interval.

Table 14. Frequency of viral antigen in vascular smooth muscle in the organs of young lambs with natural RVFV infection.

Organ	Positive/total[a]	Proportion-% (95% CI)[b]
Spleen	1/53	2 (0, 9)
Kidney	26/46	57 (42, 70)
Lung	1/52	2 (0, 9)
Heart	3/36	8 (2, 21)
Gastrointestinal tract	1/22	5 (0, 20)

[a] Positive/total represents number with positive immunolabelling for RVFV antigen out of the total number of tissues available for examination. [b] CI, confidence interval.

Panel 6: Figures 30-32. Rift Valley fever virus, liver, young lambs. Sequential testing of tissue sections with antibodies to RVFV and WBV.

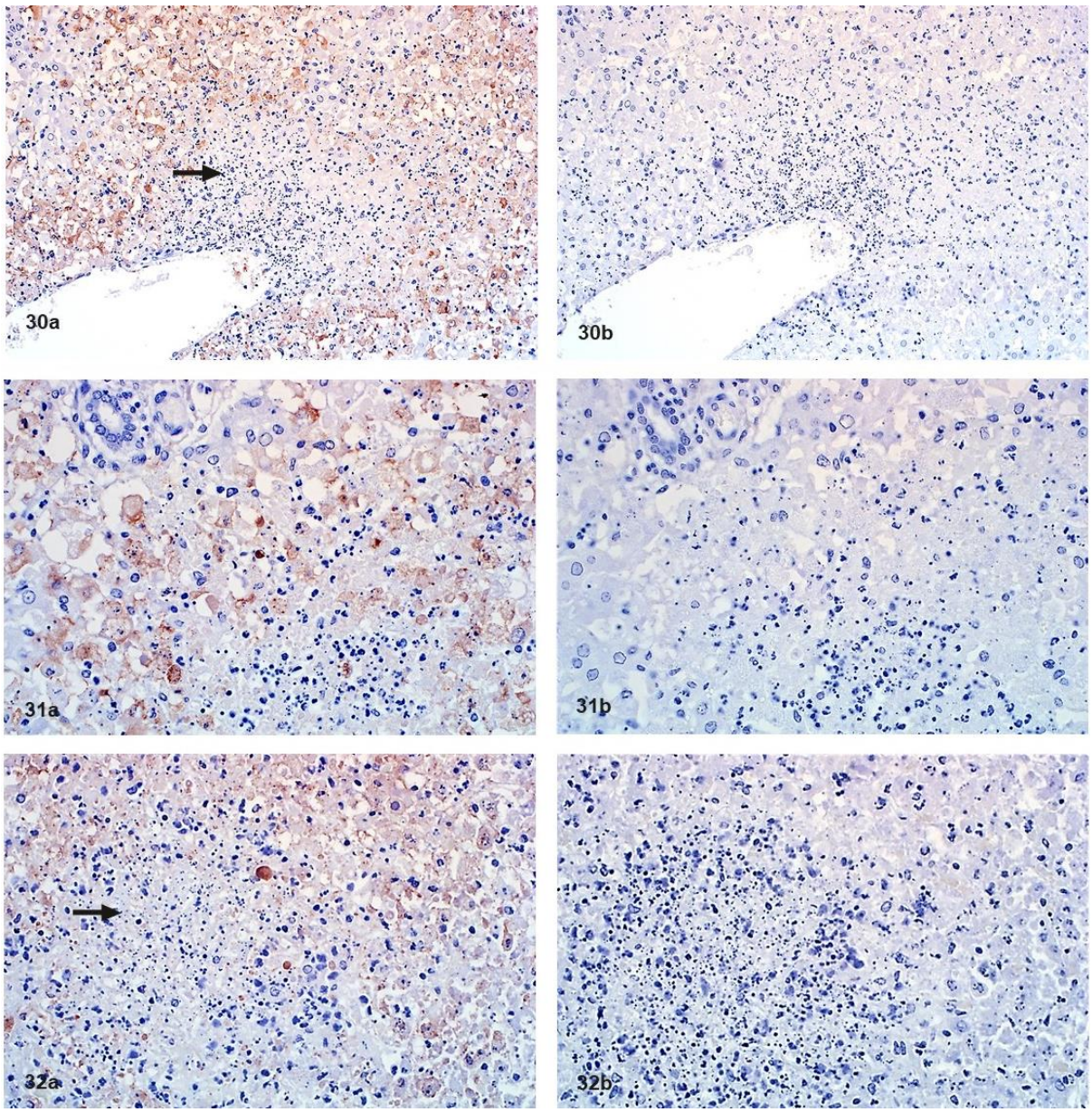

Figure 30a. Case 3. Sparse viral antigen in a primary focus (arrow) adjacent to the central vein, accompanied by intense labelling in the surrounding liver parenchyma. IHC for RVFV. **Figure 30b.** Case 3 sequential slide. Negative for viral antigen. IHC for WBV. **Figure 31a.** Case 54. RVFV antigen in the cytoplasm of necrotic hepatocytes adjacent to a portal canal. IHC for RVFV. **Figure 31b.** Case 54 sequential slide. Negative for viral antigen. IHC for WBV. **Figure 32a.** Case 32. Labelling in the cytoplasm of necrotic hepatocytes and sparse labelling in a midzonal primary focus (arrow). IHC for RVFV. **Figure 32b.** Case 32 sequential slide. Negative for viral antigen. IHC for WBV.

Panel 7: Figures 33-35. Rift Valley fever virus, spleen, lymph node and thymus, young lambs. Sequential testing of tissue sections with antibodies to RVFV and WBV.

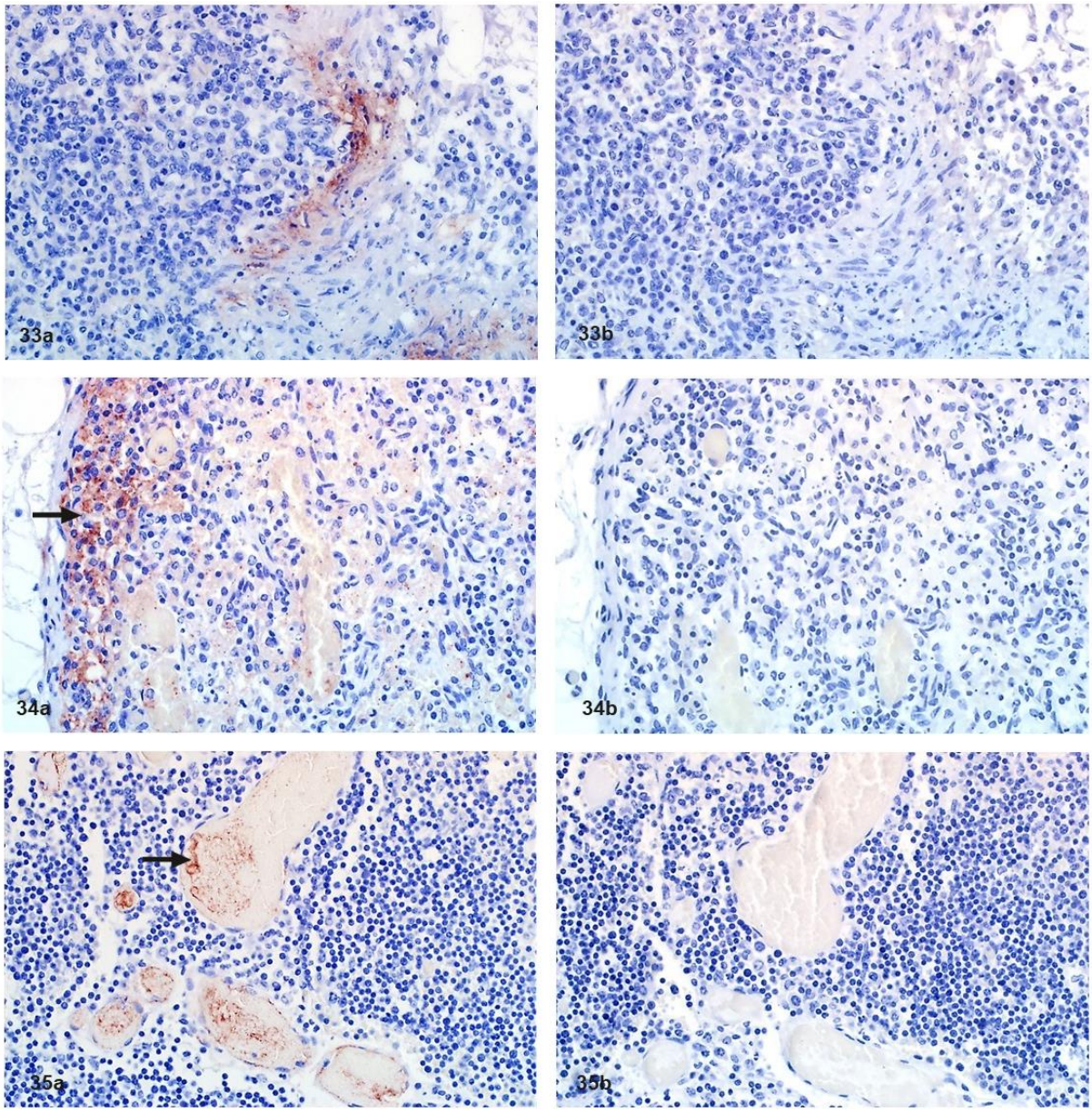

Figure 33a. Case 56. Spleen. RVFV antigen in the capsule. IHC for RVFV. **Figure 33b.** Case 56 sequential slide. Spleen. Negative for viral antigen. IHC for WBV. **Figure 34a.** Case 33. Lymph node. Prominent viral antigen in the subcapsular sinus (arrow). Also, widespread labelling in the superficial cortex. IHC for RVFV. **Figure 34b.** Case 33 sequential slide. Lymph node. Negative for viral antigen. IHC for WBV. **Figure 35a.** Case 33. Thymus. Non-cell-associated viral antigen in interstitial blood vessels (arrow) and RVFV antigen in endothelial cells. IHC for RVFV. **Figure 35b.** Case 33 sequential slide. Thymus. Negative for viral antigen. IHC for WBV.

Panel 8: Figures 36-38. Rift Valley fever virus, kidney and lung, young lambs. Sequential testing of tissue sections with antibodies to RVFV and WBV.

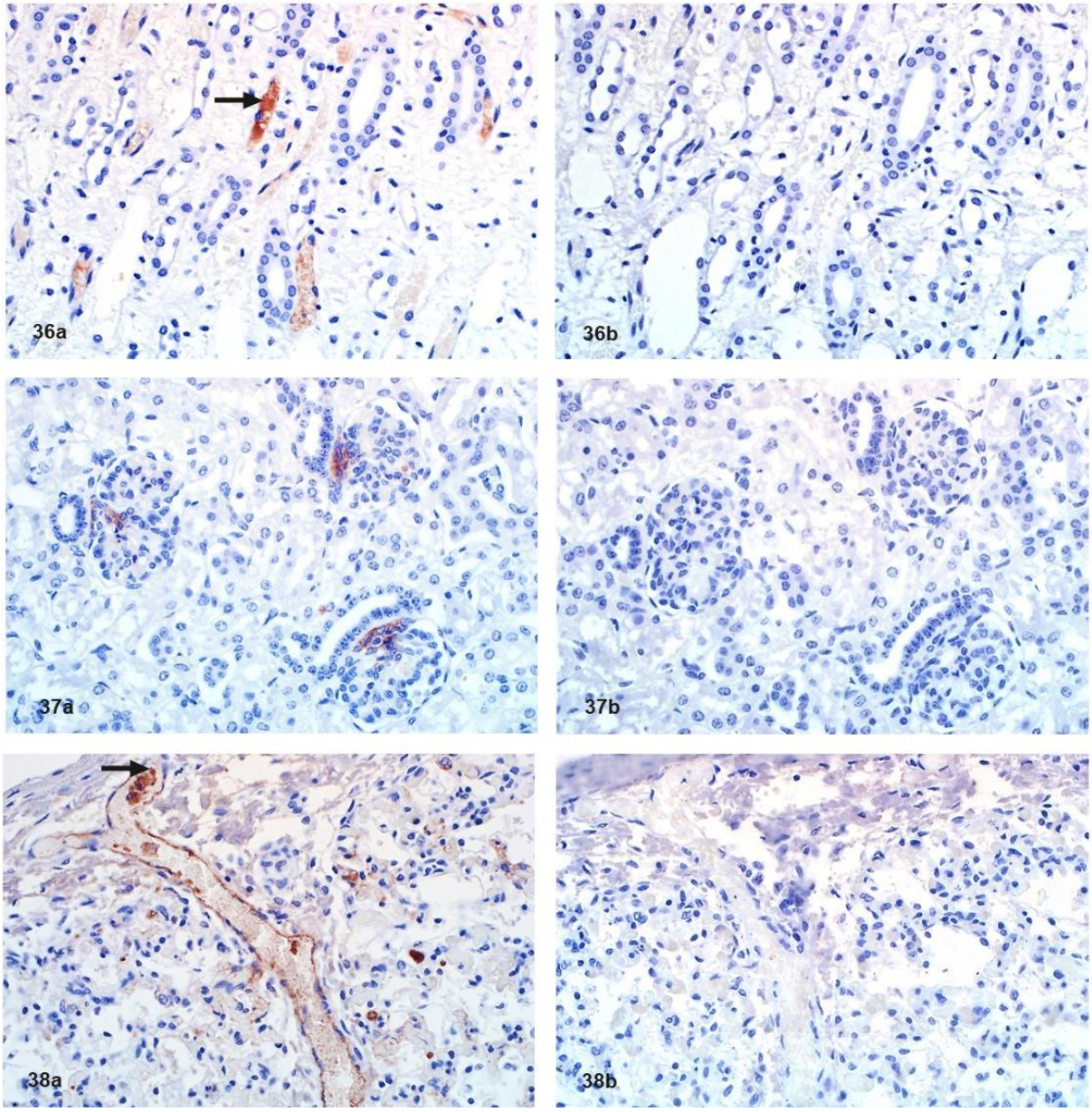

Figure 36a. Case 17. Kidney. Non-cell-associated viral antigen in interstitial blood vessels in the medulla (arrow). IHC for RVFV. **Figure 36b.** Case 17 sequential slide. Kidney. Negative for viral antigen. IHC for WBV. **Figure 37a.** Case 57. Kidney. RVFV antigen opposite the macula densa in juxtaglomerular cells and extraglomerular mesangial cells in the glomeruli. IHC for RVFV. **Figure 37b.** Case 57 sequential slide. Kidney. Negative for viral antigen. IHC for WBV. **Figure 38a.** Case 33. Lung. Non-cell-associated viral antigen in an interstitial blood vessel (arrow) and RVFV antigen in endothelial cells and intravascular cell fragments. Also, widespread viral antigen in the pulmonary interstitium. IHC for RVFV. **Figure 38b.** Case 33 sequential slide. Lung. Negative for viral antigen. IHC for WBV.

Panel 9: Figures 39-41. Rift Valley fever virus, heart and cerebrum, young lambs. Sequential testing of tissue sections with antibodies to RVFV and WBV.

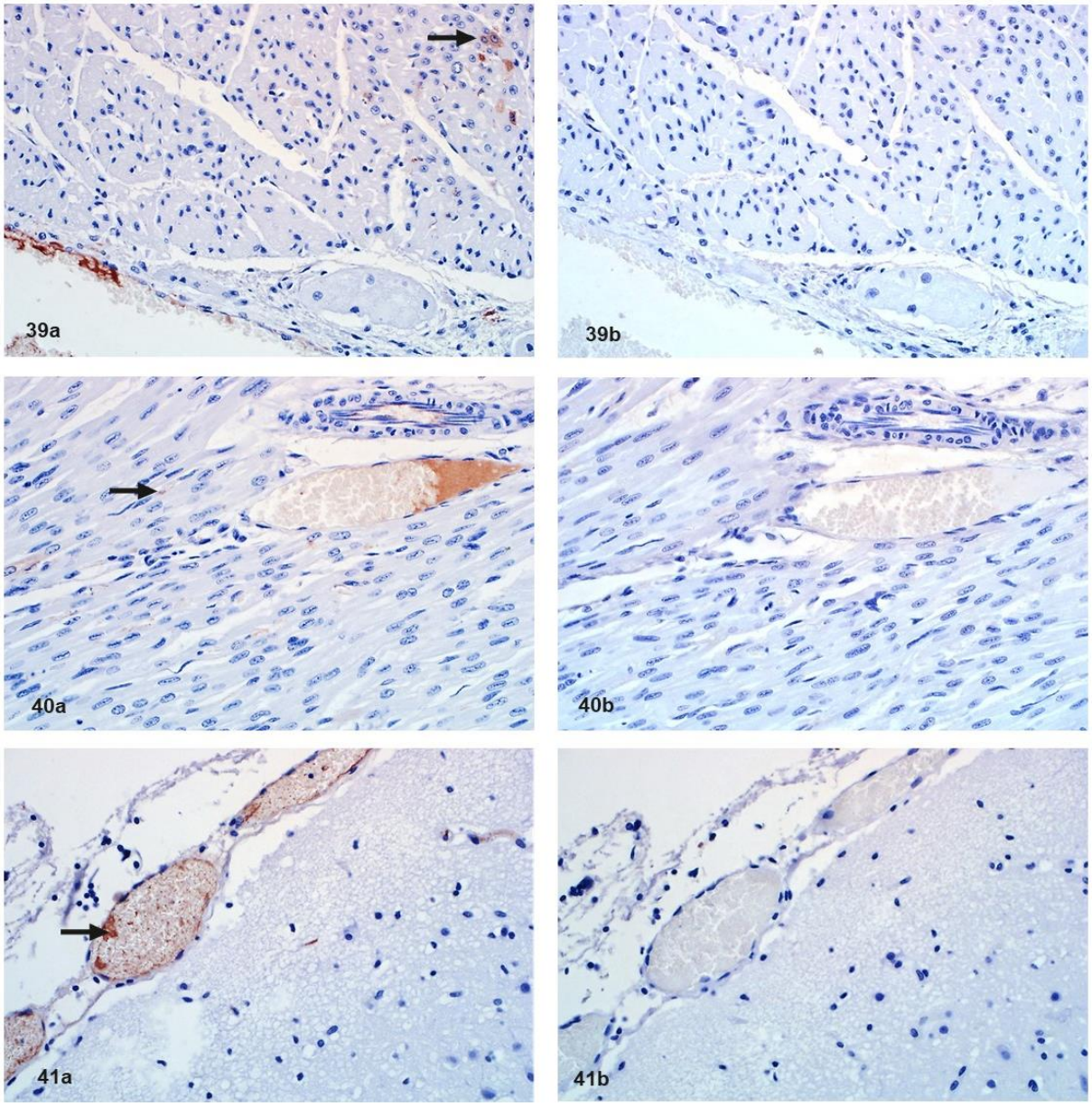

Figure 39a. Case 39. Heart. RVFV antigen in scattered cardiomyocytes (arrow). Also, non-cell-associated viral antigen in a blood vessel and in endothelial cells. IHC for RVFV. **Figure 39b.** Case 39 sequential slide. Heart. Negative for viral antigen. IHC for WBV. **Figure 40a.** Case 39. Heart. Non-cell-associated viral antigen in a blood vessel and labelling in interstitial capillaries (arrow). IHC for RVFV. **Figure 40b.** Case 39 sequential slide. Heart. Negative for viral antigen. IHC for WBV. **Figure 41a.** Case 30. Cerebral cortex. Non-cell-associated viral antigen in a vein in the pia mater (arrow) and RVFV antigen in endothelial cells. Also, labelling in capillaries in the substance of the cerebral cortex. IHC for RVFV. **Figure 41b.** Case 30 sequential slide. Cerebral cortex. Negative for viral antigen. IHC for WBV.

Panel 10: Figures 42-47. Negative tissue controls (non-infected, age-matched), liver and spleen, young lambs. IHC for RVFV.

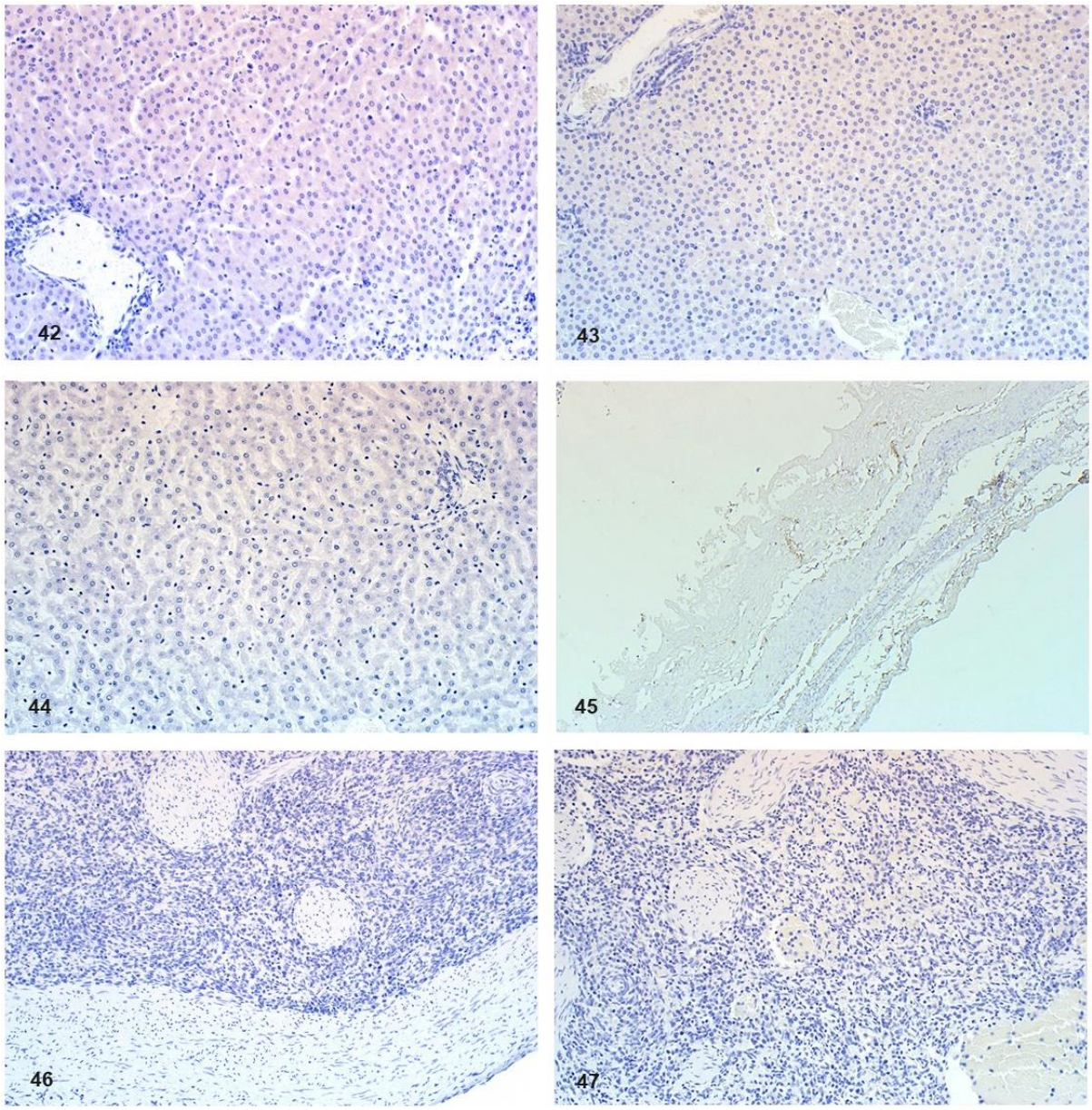

Figure 42. Control 4. Liver. Parenchyma and blood vessels negative for viral antigen. **Figure 43.** Control 9. Liver. Negative for viral antigen. **Figure 44.** Control 12. Liver. Negative for viral antigen. **Figure 45.** Control 1. Gall bladder. Negative for viral antigen. **Figure 46.** Control 12. Spleen. Capsule and subcapsular red pulp. Negative for viral antigen. **Figure 47.** Control 1. Spleen. Red and white pulp with large blood vessels and trabeculae negative for viral antigen.

Panel 11: Figures 48-53. Negative tissue controls (non-infected, age-matched), lymph node, thymus, kidney and adrenal, young lambs. IHC for RVFV.

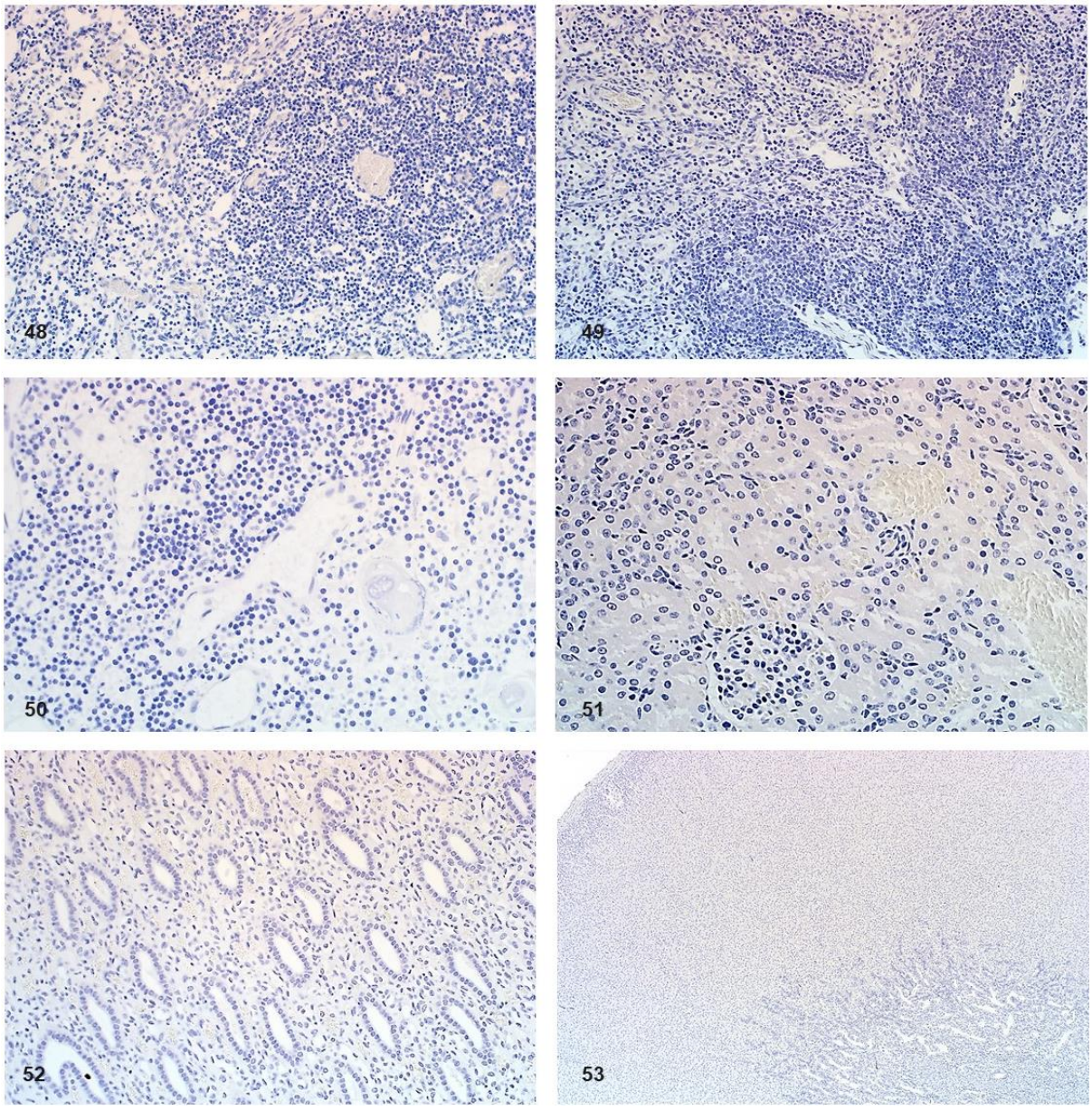

Figure 48. Control 4. Lymph node. Cortex and medulla negative for viral antigen. **Figure 49.** Control 9. Lymph node. Capsule, cortex and medulla negative for viral antigen. **Figure 50.** Control 2. Thymus. Negative for viral antigen. **Figure 51.** Control 6. Kidney. Cortex negative for viral antigen. **Figure 52.** Control 9. Kidney. Medulla negative for viral antigen. **Figure 53.** Control 1. Adrenal. Capsule and cortex negative for viral antigen.

Panel 12: Figures 54-59. Negative tissue controls (non-infected, age-matched), lung, heart, abomasum and small intestine, young lambs. IHC for RVFV.

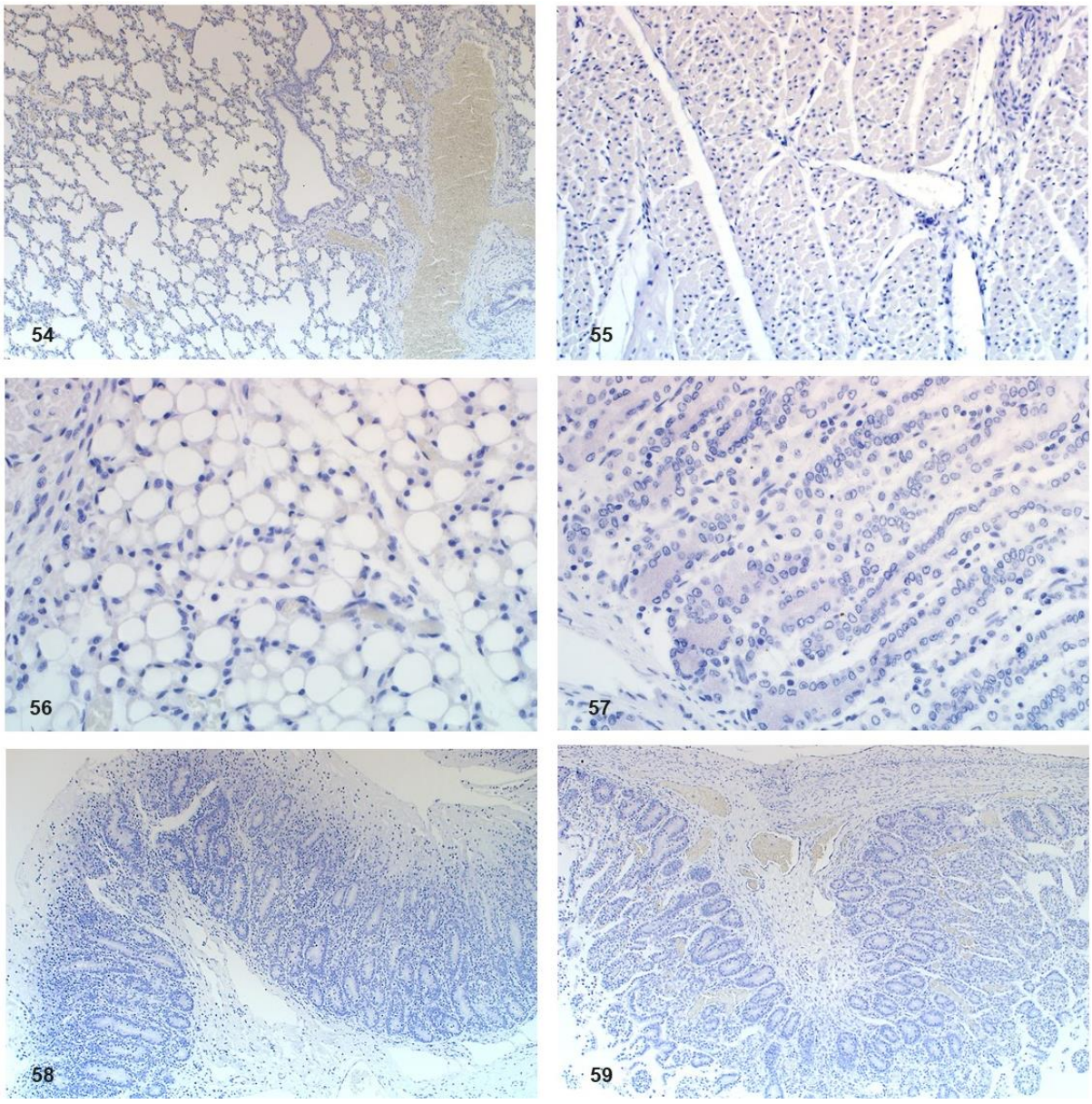

Figure 54. Control 9. Lung. Negative for viral antigen. **Figure 55.** Control 3. Heart. Myocardium with blood vessels and Purkinje fibres negative for viral antigen. **Figure 56.** Control 13. Pericardial fat. Negative for viral antigen. **Figure 57.** Control 4. Abomasum. Negative for viral antigen. **Figure 58.** Control 1. Small intestine. Negative for viral antigen. **Figure 59.** Control 8. Small intestine. Negative for viral antigen.

Panel 13: Figures 60-65. Negative tissue controls (non-infected, age-matched), ileum, tongue, skin, cerebrum and cerebellum, young lambs. IHC for RVFV.

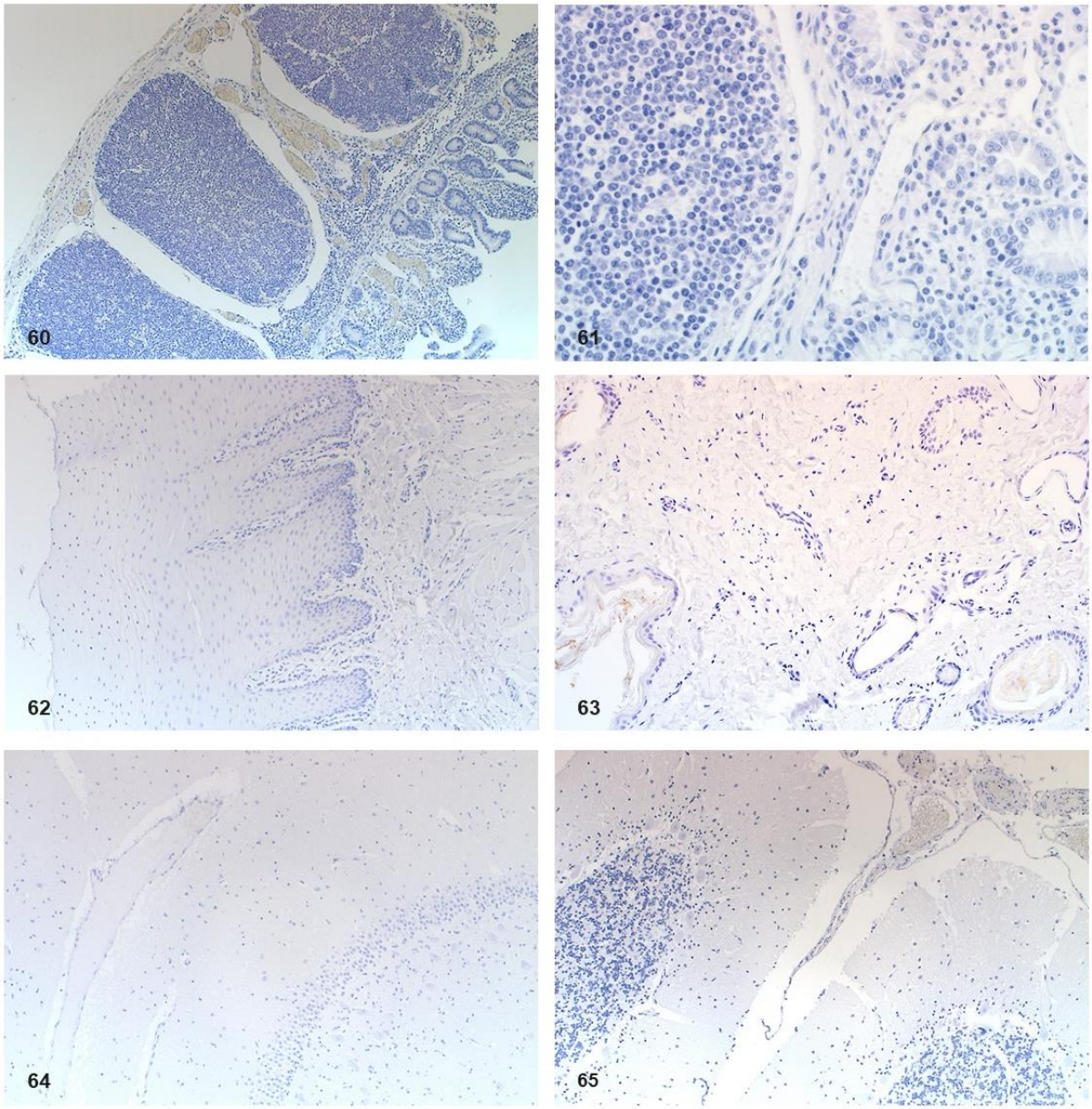

Figure 60. Control 8. Ileum. Peyer's patches, blood vessels and layers of the ileum negative for viral antigen. **Figure 61.** Control 12. Ileum. Edge of a Peyer's patch and mucosa negative for viral antigen. **Figure 62.** Control 1. Tongue. Epithelium and underlining tissues negative for viral antigen. **Figure 63.** Control 1. Skin. All structures in the epidermis and dermis negative for viral antigen. **Figure 64.** Control 13. Cerebrum. Cortex negative for viral antigen. **Figure 65.** Control 13. Cerebellum. Negative for viral antigen.

3.4.2 Liver

Macroscopically, the livers were often swollen and friable. They were either light yellow or yellowish-brown due to diffuse necrosis, or dark red due to severe congestion (Fig. 66). Necrotic foci could be distinguished in some while in other cases congestion or diffuse colour changes masked necrosis.

Microscopically, diffuse necrosis accompanied by an infiltrate of predominantly degenerate neutrophils with fewer macrophages, was present in 65 of 71 (92%) cases with available specimens. Primary foci were present in the liver specimens from 60 of 71 (85%) cases and were either isolated (30 of 71), scattered (16 of 71) or widespread (13 of 71). These foci were randomly distributed, well demarcated areas of liquefactive necrosis, consisting of remnants of completely disintegrated hepatocytes, fine nuclear fragments, and a sparse infiltrate of degenerate neutrophils and macrophages in a collapsed reticular network (Figs. 30, 31, 32, 67, 68, 76, 77).

Few surviving hepatocytes were present and invariably these showed degenerative (hydropic) changes. The orderly arrangement of hepatocytes into plates was markedly disrupted and sinusoids were difficult to discern. Hepatocytes with condensed hypereosinophilic cytosol and pyknosis or karyorrhexis (Councilman bodies or acidophilic bodies) were present (Fig. 69). Other hepatocytes were swollen and rounded with the nucleus completely disintegrated (karyolysis) or only small nuclear fragments remaining (karyorrhexis) (Fig. 70). Some hepatocytes appeared to have collapsed due to rupture of the cell membrane. Limiting plate hepatocytes were necrotic and the connective tissue in the portal tracts was often disrupted. Haemorrhage or severe congestion featured prominently in most cases. Intranuclear inclusion bodies (Figs. 69 and 70) were identified in 27 of 71 (38%) specimens and mineralization of hepatocytes (Fig. 71) in 15 of 71 (21%). Necrosis in the liver was positively correlated with necrosis in the lymph nodes (ρ=0.515; P=0.034) but not the spleen (ρ=0.116; P=0.409).

Panel 14: Figures 66-73. Rift Valley fever virus, liver, young lambs.

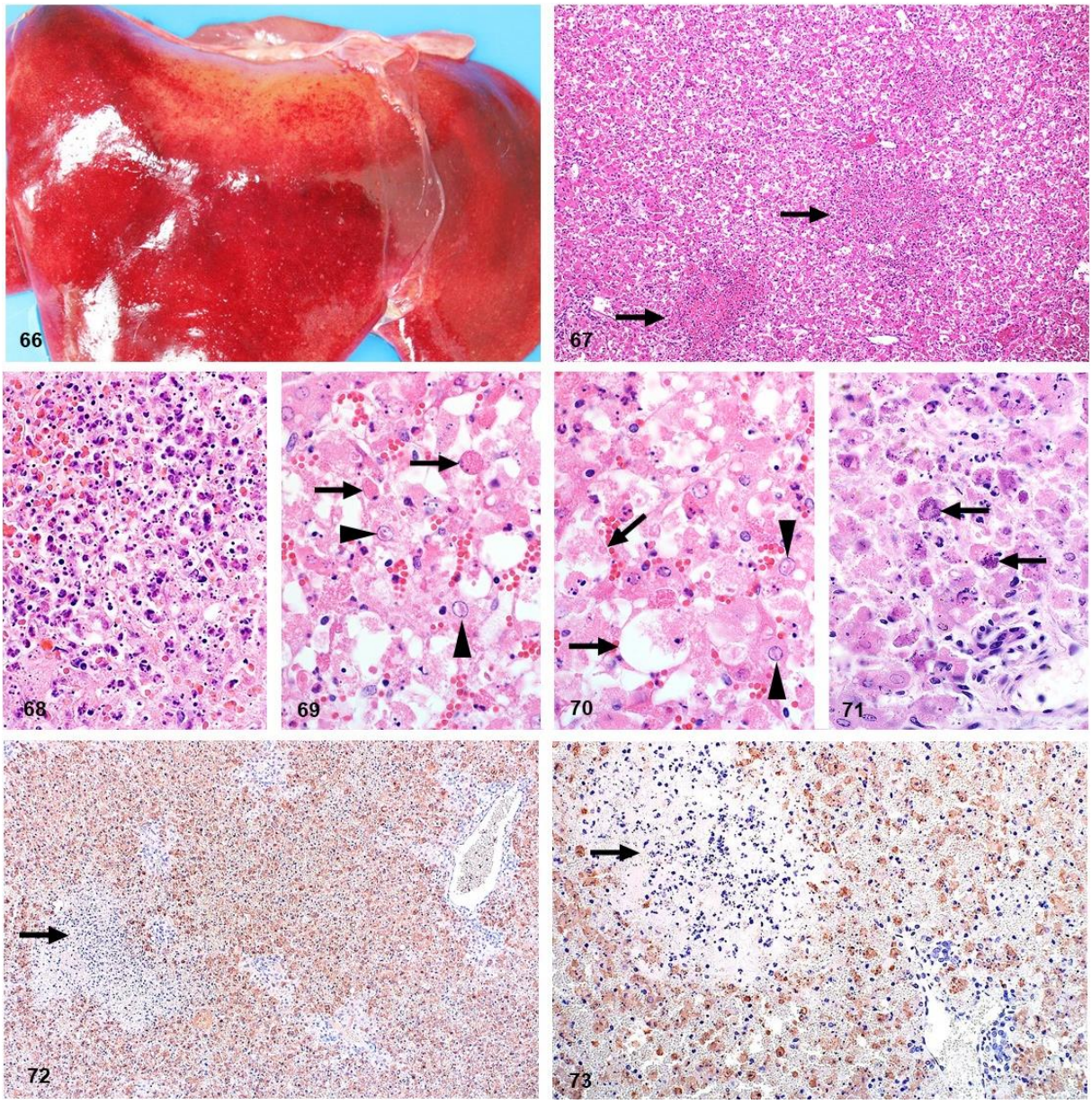

Figure 66. Case 30. Hepatic necrosis and haemorrhage. **Figure 67.** Case 11. Multifocal liquefactive hepatic necrosis (arrows) also referred to as primary foci. HE. **Figure 68.** Case 11. Edge of a primary focus with nuclear fragments and remnants of completely disintegrated hepatocytes and leucocytes. HE. **Figure 69.** Case 3. Diffuse necrotizing hepatitis with a mild infiltrate of degenerate neutrophils. Hepatocytes display features suggesting apoptosis including shrinkage of affected cells, acidophilic cytoplasm and karyorrhexis (arrows). Rod-shaped, acidophilic viral inclusion bodies are present in the nucleus of some hepatocytes (arrowheads) HE. **Figure 70**. Case 3. Hepatocytes with features suggesting lytic cell death (arrows) including severe cell swelling and karyorrhexis. Also present are intranuclear inclusion bodies (arrowheads). HE. **Figure 71.** Case 12. Mineralized hepatocytes (arrows). HE. **Figure 72.** Case 2. Sparse viral antigen in a primary focus (arrow) compared to the intense labelling in the surrounding liver parenchyma. IHC for RVFV. **Figure 73**. Case 15. Labelling in the cytoplasm of necrotic hepatocytes and sparse labelling in a primary focus (arrow). IHC for RVFV.

Panel 15: Figures 74-77. Liver. Young lambs. Gordon and Sweets' silver stain for reticular fibres.

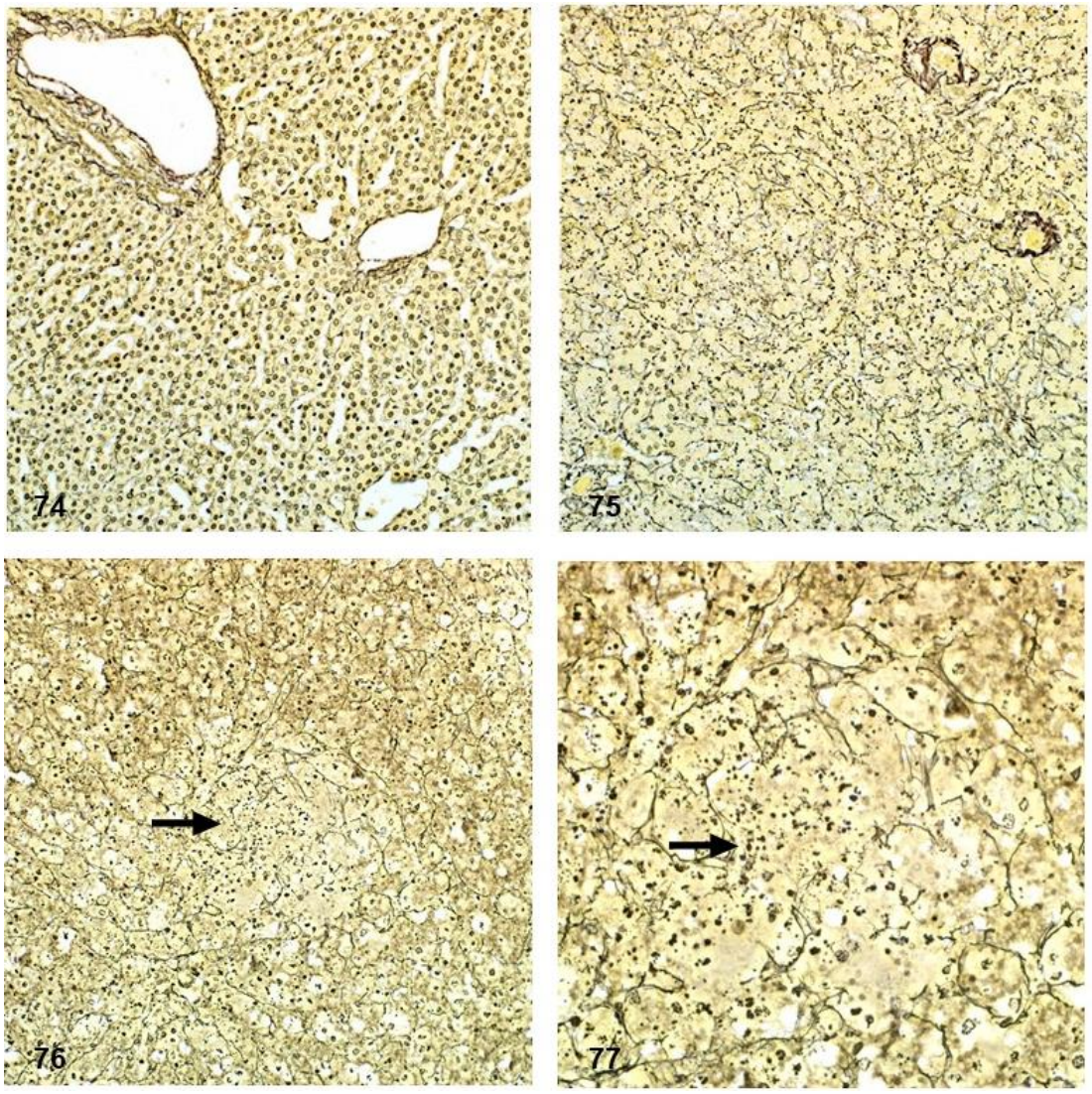

Figure 74. Case 9. Liver. Negative tissue control (non-infected, age-matched)**. Figures 75-77.** Liver. RVFV-infected young lambs. Gordon and Sweets' silver stain. **Figure 75.** Case 5. The orderly arrangement of hepatocytes into plates is markedly disrupted with sinusoids difficult to discern and reticulin fibres in disarray. **Figure 76.** Case 10. Diffuse necrotizing hepatitis with a primary focus (arrow). **Figure 77.** Case 10. Higher magnification view of the same primary focus in the previous figure, with nuclear fragments and remnants of reticulin fibres present in an area of liquefactive necrosis (arrow).

RVFV antigen was widespread and easily identified in 67 of 71 (94%) cases. Most RVFV immunolabelling in the liver was within hepatocytes (Fig. 72). Within primary foci, labelling was primarily present in scattered cellular debris. Additionally, viral antigen was always sparse in primary foci compared to the intense labelling in the surrounding liver parenchyma (Fig. 73).

Four cases, positive by RT-qPCR, were negative by IHC in all the available organs. Mild hepatocellular injury with severe acute renal tubular injury was present in one of these cases while another had moderate centrilobular hepatic necrosis that was considered to have resulted from anaemia. In this latter case, haemonchosis was mentioned in the records. Lesions were absent from the liver and the kidneys of the other 2 cases.

3.4.3 Gallbladder

Oedema and occasional haemorrhages were present macroscopically in the examined gall bladders. Histologically, in 2 of the 3 cases with available specimens, IHC labelling was present in capillaries and small blood vessels either as non-cell-associated viral antigen or as antigen in endothelial cells or intravascular cellular debris.

3.4.4 Spleen

Gross lesions were uncommon in the spleen with capsular and subcapsular haemorrhages only occasionally present. Microscopically, splenic necrosis was a prominent feature in 50 of 53 (94%) cases and was either mild (n = 9), moderate (n = 15) or severe (n = 26). Generally, the PALS was a narrow zone of clearly identifiable cells, while in most cases (51 of 53) follicular germinal centres, mantle cell layers and marginal zones were poorly developed (Fig. 78). The latter was interpreted as developmentally normal for young lambs. Therefore, necrosis mainly involved lymphocytes in the red pulp and the peripheral aspects of the PALS (Fig. 78). Necrosis was present in both the red and white pulp in 47 of 48 (98%) cases that tested positive for RVFV antigen by IHC, and characterized by the prominent presence of cellular debris in addition to occasional tingible-body macrophages. In the red pulp, necrosis was mild, moderate and severe in 7 of 48 (15%), 17 of 48 (35%) and 23 of 48 (48%) cases respectively.

Necrosis in the white pulp was graded as mild, moderate or severe in 18 of 48 (38%), 14 of 48 (29%) and 15 of 48 (31%) of the IHC positive cases, respectively.

Splenic infection with RVFV was detected by IHC in 48 of 53 (91%) cases and antigen was either widespread (n = 33), scattered (n = 9) or isolated (n = 6). Viral antigen was commonly present in the red pulp in association with cellular debris (Table 15). In 41 of 53 (77%) cases, labelling was especially prominent in the subcapsular red pulp and in small blood vessels or smooth muscle within the capsule (Figs. 33a, 79). Non-cell-associated antigen and antigen in endothelial cells and cellular debris was also often present in small blood vessels. Mononuclear cells, morphologically consistent with macrophages, in the red pulp or at the periphery of the PALS were also positive in 45 of 53 (85%) cases. Occasionally, cells identified as tingible-body macrophages (Fig. 79) contained RVFV antigen (14 of 53 cases).

3.4.5 Lymph nodes

Macroscopically, lymph nodes were enlarged, oedematous and congested. Mesenteric lymph nodes were especially affected. Microscopically, there were variable degrees of lymphocytolysis and lymphoid depletion in 15 of 17 (88%) cases. Similar to the spleen, follicular germinal centres were not well developed in most cases and apoptotic lymphocytes were scattered throughout the cortex and the medullary cords (Fig. 80). In the cases that tested positive for RVFV antigen, lymphocytolysis was mild, moderate, and severe in 2 of 14 (14%), 8 of 14 (57%) and 4 of 14 (29%) cases respectively. Necrosis in lymph nodes was positively correlated with splenic necrosis (ρ=0.577; P=0.050)

Of the cases with available lymph node specimens, 14 of 17 (82%) were positive for RVFV antigen with widespread labelling in most cases (n = 11). Viral antigen was present in small blood vessels and capillaries in endothelial cells (Fig. 81) or as non-cell-associated virus (Fig. 34a). In the sinusoids, mononuclear cells, morphologically consistent with macrophages, were also positive for viral antigen (Fig. 81).

Panel 16: Figures 78-83. Rift Valley fever virus, lymphoid tissues, young lambs.

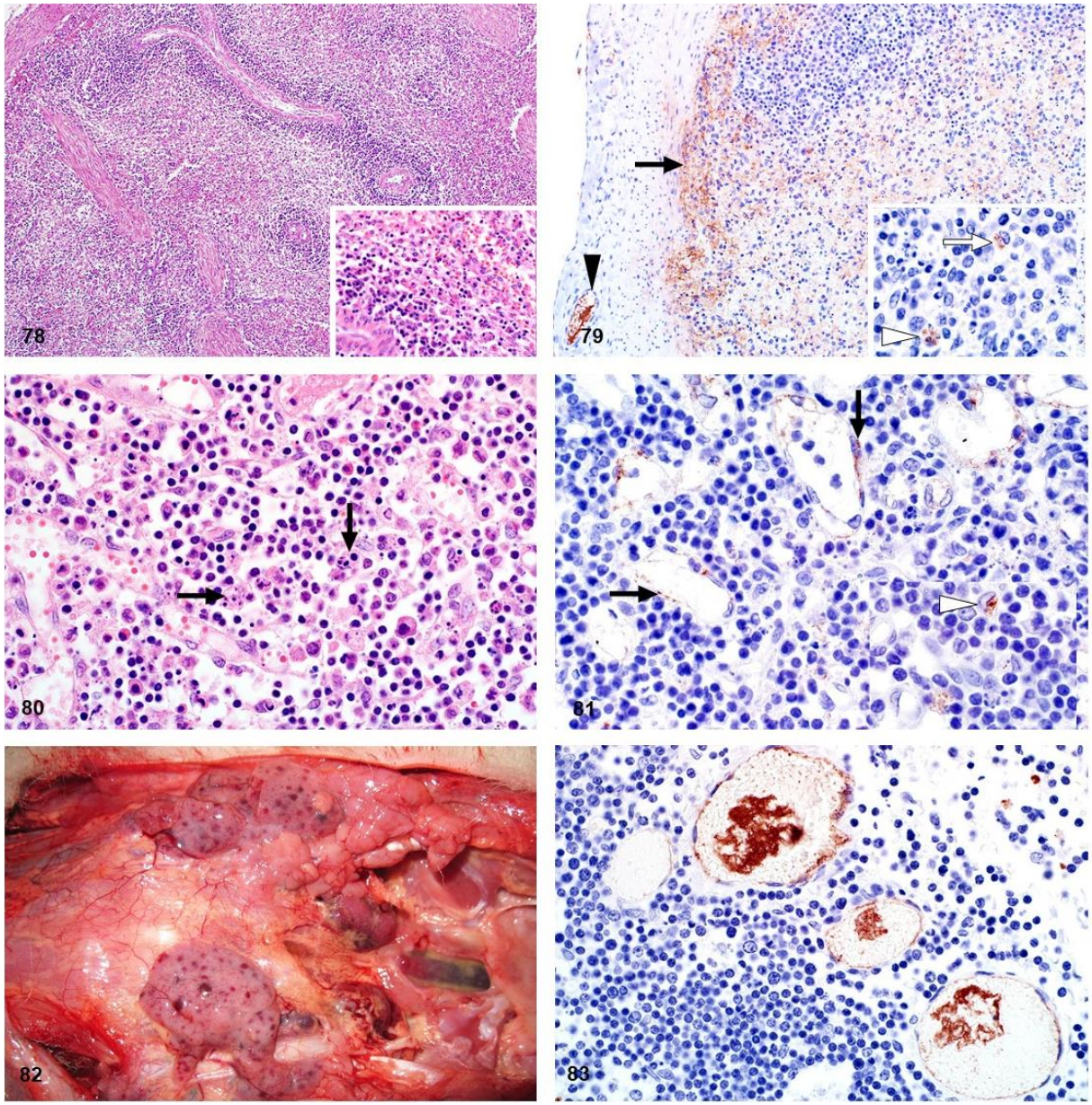

Figure 78. Case 3. Spleen. Depletion of the red pulp with an absence of follicular germinal centres. Mantle and marginal zones are poorly developed, interpreted as developmentally age-appropriate. **Inset:** Lymphocytolysis in the red pulp and the periarteriolar lymphoid sheath. HE. **Figure 79.** Case 8. Spleen. Prominent viral antigen in the subcapsular red pulp (black arrow) and in a small blood vessel in the capsule (black arrowhead)**. Inset:** RVFV antigen in a mononuclear cell, morphologically consistent with a macrophage (white arrow) and a tingible-body macrophage (white arrowhead). IHC for RVFV. **Figure 80.** Case 9. Lymph node. Lymphocytolysis and occasional tingible-body macrophages (arrows) in the medulla. HE. **Figure 81.** Case 9. Lymph node. Endothelial cells positive for RVFV antigen (arrows) in the medulla**. Inset:** Viral antigen in a mononuclear cell, morphologically consistent with a macrophage (white arrowhead). IHC for RVFV. **Figure 82.** Case 31. Thymus. Multifocal petechiae. **Figure 83.** Case 16. Thymus. Non-cell-associated viral antigen in interstitial blood vessels and RVFV antigen in endothelial cells. IHC for RVFV.

Table 15. Distribution of viral antigen in different zones of the spleen, for specimens with positive immunolabelling for RVFV in young lambs.

Splenic zone	Proportion[a]	Percentage (95% CI)[b]
Marginal zone	35/48	73 (59, 84)
Red pulp	47/48	98 (90, 100)
Marginal zone and red pulp	35/48	73 (59, 84)
Only white pulp	0/48	0 (0, 6)
Only intravascular	1/48	2 (0, 10)
Germinal centre and mantle cell layers	0/48	0 (0, 6)
Periarteriolar lymphatic sheath	0/48	0 (0, 6)
Subcapsular red pulp and/or capsular vasculature	41/48	85 (73, 93)

a Proportion = number of positive spleen specimens over the total number of spleen specimens examined, based on immunohistochemistry for RVFV antigen. b CI = confidence interval. The data do not include specimens with negative immunolabelling.

3.4.6 Thymus

Petechiae or ecchymoses present in the thymus (Fig. 82) were confirmed microscopically as being in the interstitium in 3 of 9 (33%) cases with available specimens. However, lymphocytolysis that was frequently present in the other lymphoid organs, was absent in the thymus. Additionally, viral antigen was confined to capillaries and small blood vessels as non-cell-associated viral antigen, antigen in endothelial cells or intravascular cellular debris (Figs. 35a, 83).

3.4.7 Kidney

Gross kidney lesions were uncommon other than occasional capsular or cortical petechiae or ecchymoses. Microscopically, severe multifocal acute tubular epithelial injury lacking significant associated inflammation was present in 11 of 46 (24%) cases. Mild or moderate injury occurred in 5 of 46 and 4 of 46 cases respectively. Characteristic degenerative changes in tubular epithelial cells included fine vacuolation and swelling as well as impingement of the tubular lumen. This was occasionally accompanied by pyknosis or karyolysis, with detachment

of a few cells from the basement membrane. Marked acute renal tubular epithelial necrosis was absent. There were no tubular epithelial lesions in the remaining 26 of 46 (57%) kidney specimens even though 23 of these tested positive by IHC. Additionally, the glomeruli appeared less densely cellular than normal and scattered pyknosis and karyorrhexis was present within the glomeruli of 37 of 46 (80%) cases (Fig. 84). Nuclear debris was also often present in the interstitial capillaries, and pyknosis and karyorrhexis in the glomeruli were positively correlated (ρ=0.896, P<0.001) with the presence of nuclear debris in the interstitial capillaries. The presence of pyknosis and karyorrhexis in the glomeruli was also significantly associated with the detection of viral antigen in the glomeruli (ρ= 0.309, P= 0.0346).

Of the cases with available kidney specimens, 40 of 46 (87%) were positive for RVFV antigen. In the positive cases, labelling was present in both the cortex and medulla. Glomerular labelling was present in 37 of 40 (93%) cases. Viral antigen was often present at the vascular pole of the glomerulus opposite the macula densa, within a small group of cells that are likely juxtaglomerular and extraglomerular mesangial cells (lacis cells) (Figs. 37a, 85). Cells of the macula densa were not affected. Labelling was also present in smooth muscle cells in the efferent or afferent arteriole (Fig. 86) or vascular endothelial cells (Fig. 87). In 26 of 40 (65%) cases viral antigen was also present in smooth muscle cells of small blood vessels in the cortex or at the corticomedullary junction (Fig. 88). Labelling of tubular epithelium was present in 8 of 40 (20%) IHC positive cases and viral antigen was isolated (n = 6) or scattered (n = 2). Labelling was predominantly in proximal tubules (n = 6), less frequently in distal tubules (n = 3) and absent from any other levels of the nephron. Labelling in the glomeruli was significantly associated with the presence of viral antigen in the tubules (ρ=0.112; P=0.099)

Viral antigen was present in the cortical interstitial capillaries in 32 of 46 (70%) cases where glomerular labelling was also present, and this association was significant (ρ=0.715; P<0.001). Viral antigen was also present in the medullary interstitial capillaries (Figs. 36a, 89) in 31 of 46 (67%) cases and the presence of viral antigen in the cortical interstitium was

significantly associated with presence of viral antigen in the medullary interstitium (ρ=0.748; P<0.001). In both cortical and medullary interstitial capillaries, viral antigen was present as non-cell-associated antigen, in vascular endothelial cells or within cellular debris. In interstitial cortical capillaries, viral antigen was also present in mononuclear leucocytes. In 2 cases, viral antigen was not present in the glomeruli, tubules or the cortical interstitial capillaries but instead occurred predominantly in medullary interstitial capillaries. Viral antigen was also present in capillaries and small blood vessels in the perirenal adipose tissue (Fig. 90).

3.4.8 Adrenal gland

Lesions were infrequent with a few necrotic cells present in the zona fasciculata in only 1 of 5 cases. RVFV antigen was present in secretory cells in all zones of the cortex in 3 of 5 cases (Fig. 91). Labelling was also present in capillaries and small blood vessels in the capsule and in periadrenal adipose tissues. Lesions and viral antigen were absent from the adrenal medulla.

3.4.9 Lung

Marked pulmonary oedema and congestion accompanied by mild to moderate hydrothorax were common findings (Fig. 92). Microscopically, intra-alveolar and interstitial oedema was present in 39 of 52 (75%) cases (Fig. 93). Inflammation, varying from mild to severe was present in the alveolar capillaries in all cases, and consisted of predominantly mononuclear cells. Pyknosis and karyorrhexis were often present in the alveolar septa and pulmonary blood vessels (Fig. 93). Haemorrhage was present in 5 of 52 (10%) cases.

Labelling was widespread and easily identifiable in 46 of 52 (88%) cases (Fig. 94). Viral antigen was present in mononuclear cells, histomorphologically consistent with macrophages, within the interstitial capillaries of 43 of 52 (83%) cases (Fig. 95). Labelling was also present as non-cell-associated antigen, or antigen associated with endothelial cells or cellular debris in small blood vessels and capillaries in 42 of 53 (79%) cases (Figs. 38a, 94). Antigen was also present in pulmonary vascular smooth muscle cells in 1 case.

Panel 17: Figures 84-91. Rift Valley fever virus, kidney and adrenal, young lambs.

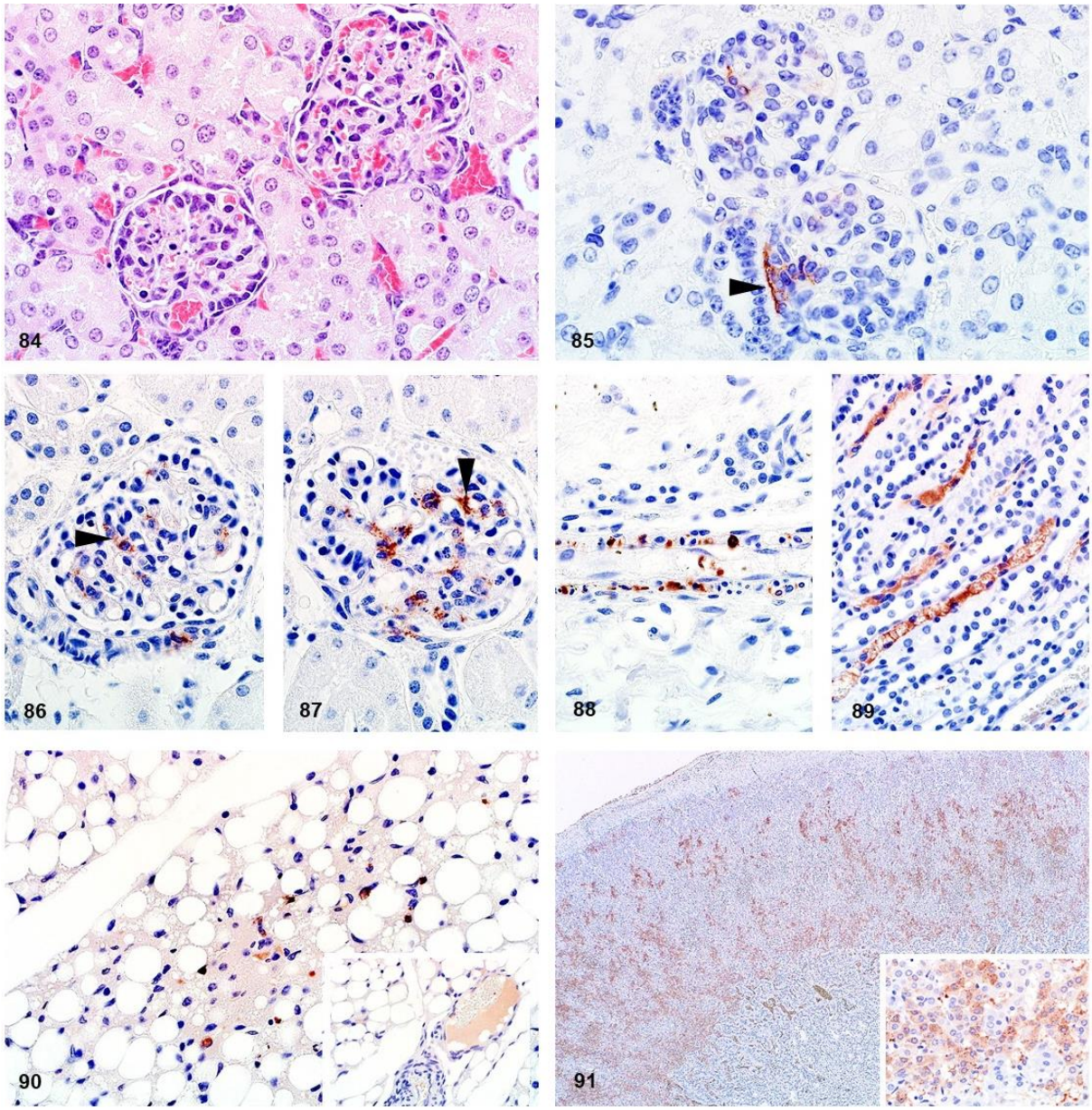

Figure 84. Case 38. Kidney. The renal glomeruli are less densely cellular than normal with scattered pyknosis and karyorrhexis. HE. **Figure 85.** Case 56. Kidney. RVFV antigen opposite the macula densa in juxtaglomerular cells and extraglomerular mesangial cells (flat and elongated cells located near the macula densa). IHC for RVFV. **Figure 86.** Case 7. Kidney. Labelling of a smooth muscle cell (arrowhead) in the efferent or afferent arteriole and viral antigen in mononuclear cells in the glomerulus. IHC for RVFV. **Figure 87**. Case 7. Kidney. Labelling of endothelial cells (arrowhead) and mononuclear cells in the glomerulus. IHC for RVFV. **Figure 88.** Case 3. Kidney. Viral antigen within smooth muscle cells in a small artery at the cortico-medullary junction. IHC for RVFV. **Figure 89.** Case 7. Kidney. Non-cell-associated viral antigen and antigen in vascular endothelial cells in medullary interstitial capillaries. IHC for RVFV. **Figure 90.** Case 23. Peri-renal adipose tissue. RVFV antigen present in capillaries and small blood vessels. IHC for RVFV. **Inset:** Non-cell-associated antigen in a small blood vessel. IHC for RVFV. **Figure 91.** Case 36. Adrenal gland. Widespread RVFV antigen in the cortex. **Inset:** RVFV antigen within secretory cells. IHC for RVFV.

Panel 18: Figures 92-97. Rift Valley fever virus, thymus, liver, lung, and heart, young lambs.

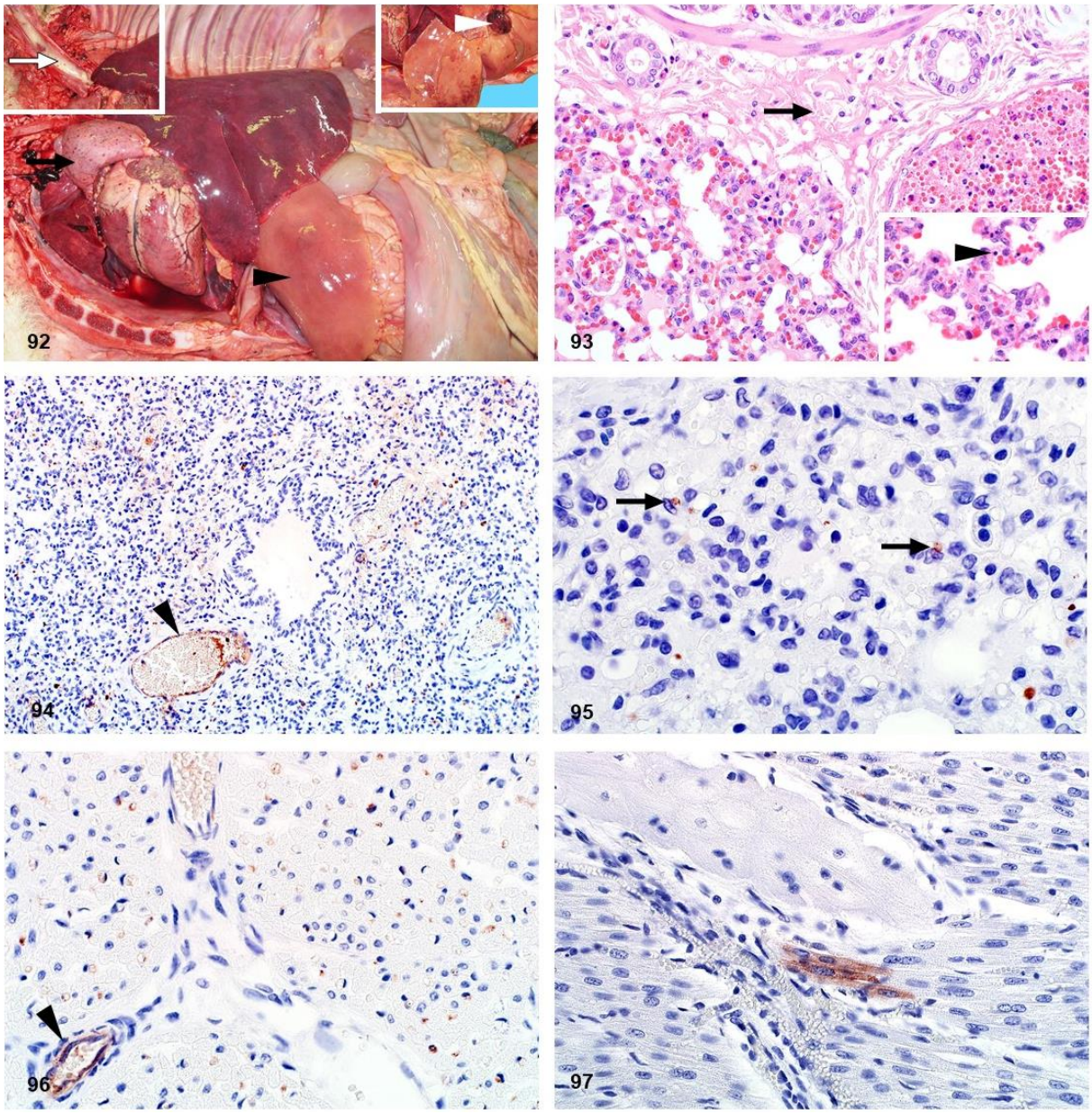

Figure 92. Case 32. Thymic (black arrow) and pericardial petechiae, and diffuse hepatic necrosis (black arrowhead). The lungs are uncollapsed with a wet appearance. **Left inset:** Opened trachea. Foamy fluid in the trachea (white arrow). **Right inset:** Visceral surface of the liver. Diffuse hepatic necrosis, multifocal ecchymoses, and haemorrhage in the hepatic lymph node (white arrowhead) **Figure 93.** Case 3. Lung. Marked pulmonary interstitial oedema (arrow) with moderate interstitial mononuclear inflammation. **Inset:** Pyknosis and karyorrhexis (arrowhead) in the interstitium. HE. **Figure 94.** Case 54. Lung. Widespread viral antigen in the pulmonary interstitium and in blood vessels with labelling of endothelial cells (arrowhead). IHC for RVFV. **Figure 95.** Case 9. Lung. RVFV antigen in mononuclear cells (arrows), morphologically consistent with macrophages, in the pulmonary interstitium. IHC for RVFV. **Figure 96.** Case 66. Heart. Positive labelling of endothelial cells in capillaries and a small blood vessel (arrowhead). IHC for RVFV. **Figure 97.** Case 16. Heart. RVFV antigen in cardiomyocytes. IHC for RVFV.

3.4.10 Heart

Macroscopically, epicardial- and endocardial haemorrhages as well as mild to moderate hydropericardium were present in most cases. However, histomorphological lesions attributable to RVFV infection were not present in the cardiac parenchyma in any of the cases with available specimens.

RVFV antigen was present in the heart of 27 of 36 (75%) cases. Viral antigen was typically non-cell-associated or within endothelial cells of the small blood vessels and capillaries (Figs. 39a, 40a, 96) and widespread in most cases (19 of 27). This included capillaries in pericardial adipose tissue. In three cases, viral antigen was also present in the smooth muscle cells of small blood vessels, and in five cases single or small aggregates of cardiomyocytes were positive for viral antigen (Figs. 39a, 97). In one case viral antigen was present in Purkinje fibres.

3.4.11 Gastrointestinal tract

Peritoneal and abomasal mucosal haemorrhages were occasionally noted macroscopically. Microscopically, blood was sometimes present in the lumen of the abomasum (27%; 4 of 15) and the small intestine (11%; 2 of 19). Rare foci of necrosis were present in the lamina propria of the small intestine. In contrast, karyorrhexis of cells in the lamina propria, probably lymphocytes, was common. Karyorrhexis and pyknotic cellular debris was also present in lymphoid follicles in the Peyer's patches (Fig. 98).

Viral antigen was present in vascular endothelial cells in small blood vessels and capillaries in the rumen, abomasum, small intestine and tongue (Figs. 99, 100). In the small intestine, labelling was also associated with cellular debris in the lamina propria and present in small groups of mucosal epithelial cells.

Panel 19: Figures 98-103. Rift Valley fever virus, gastrointestinal tract, skin and nervous tissue, lambs.

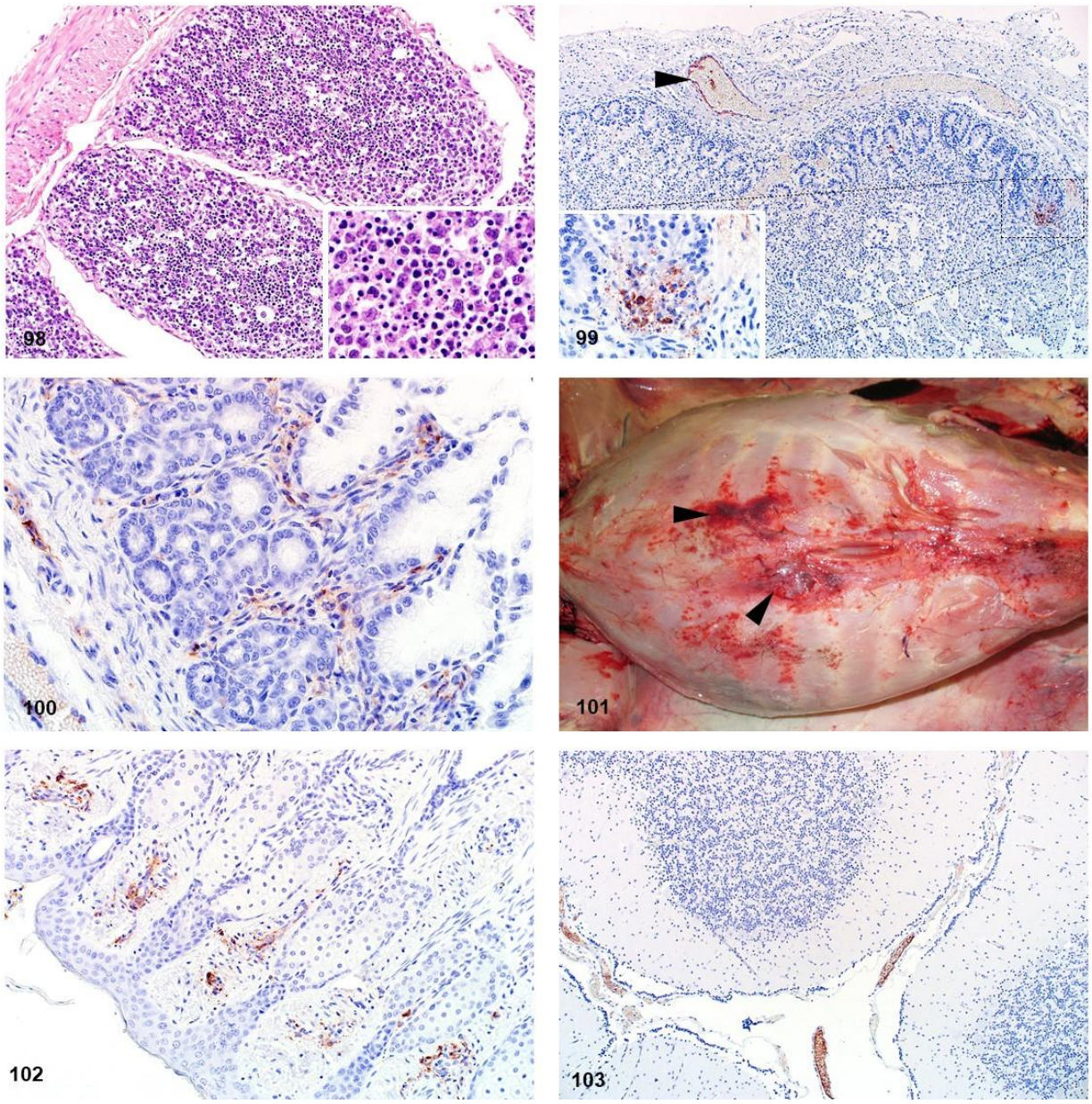

Figure 98. Case 51. Ileum, Peyer's patches. Marked lymphocytolysis in both lymphoid nodules. **Inset:** Pyknosis and karyorrhexis of lymphocytes. HE. **Figure 99.** Case 24. Small intestine. RVFV antigen in a focus of necrosis in the lamina propria, and in vascular endothelial cells (arrowhead) in the muscularis externa. **Inset:** Focus of necrosis with karyorrhexis and cells morphologically consistent with macrophages containing viral antigen. IHC for RVFV. **Figure 100.** Case 23. Abomasum. Viral antigen in vascular endothelial cells in the lamina propria and in the muscularis mucosae. IHC for RVFV. **Figure 101.** Case 31. Subcutaneous tissue, abdomen. Multifocal subcutaneous haemorrhages (arrowheads). **Figure 102.** Case 23. Skin. Viral antigen in capillaries in the dermal papillae. IHC for RVFV. **Figure 103.** Case 16. Cerebellum. Viral antigen in blood vessels in the cerebellar folds. IHC for RVFV.

3.4.12 Subcutis and skin

Macroscopically, haemorrhages were commonly present in the subcutis (Fig. 101). Viral antigen was present in the superficial dermis in association with cellular debris or mononuclear cells. Positive labelling was also present intravascularly associated with cellular debris or vascular endothelial cells (Fig. 102).

3.4.13 Nervous system

The only histological lesion present in tissues from the central nervous system was mild to moderate oedema. Viral antigen was detected in 17 of 19 (89%) cases with available specimens. Positive labelling was mainly present in vascular endothelial cells or cellular debris in capillaries and small blood vessels in the meninges (Figs. 41a, 103). Occasionally, viral antigen was present in capillaries in the white or grey matter but never within the brain parenchymal cells. Non-cell-associated viral antigen was often present within lumens of blood vessels. Peripheral nerve bundles, occasionally encountered in tissue sections, had viral antigen in their capillary endothelial cells; antigen was absent from nerve fibres in these locations.

3.5 Discussion

The severity and pathomorphology of RVF in young lambs are different from that in adult sheep. In particular, the lesions in the liver, kidneys and lymphoid tissues differ remarkably. Additionally, the distribution of RVFV antigen differs from that previously reported in adult sheep from the same outbreak as discussed in chapter 2. Therefore, the principle aims of this study were to describe the tissue tropism and target cells of RVFV in diverse organs from a large number of naturally infected young lambs less than 6 weeks old, and to summarize the gross, histopathological and immunohistochemical findings relative to results discussed in chapter 2. A further aim was to determine the extent to which virus can be detected in different organs, establish the diagnostic importance of different tissues and characterize specific histologic features of RVF in lambs. The 2010-2011 RVF outbreak in South Africa provided a

valuable opportunity to study the pathology and cellular tropism of RVFV in 71 young lambs and compare findings with previous reports. Similar to the adult cases published previously, the frequencies of lesions and immunolabelling could be an overestimate of the general population of RVF cases since organs were not consistently sampled in these field cases and there might have been a tendency to sample grossly abnormal organs. Another limitation is that the exact age at which the pathomorphological appearance of lesions in young lambs begin to resemble those seen in adults is not known. In this study, the oldest lamb with histologic lesions and immunolabelling resembling that of young lambs was 6 weeks old. Unfortunately, there were no lambs with ages recorded as 7 or 8 weeks. The age at which lesions become less severe probably depends on the maturity of the immune system, nutritional status of the lamb, breed, farming practices and perhaps the virus strain. Therefore, pathologists confronted with cases of RVF could encounter variations in the relationship between animal age, and the lesions and pattern of immunolabelling.

Early in the 2010 outbreak, it was reported that veterinarians conducting necropsies on a number of lambs did not recognize the possibility of RVF until they came upon a carcass with clearly distinguishable miliary necrotic foci in the liver or hemorrhages in the abomasum, because these lesions are important features of RVF in South Africa (personal communication). Macroscopic lesions can be non-specific in young lambs with RVF, because the characteristic liver lesions are sometimes obscured by congestion or discolouration of the liver due to diffuse necrosis or autolysis. Lesions suggestive of vascular endothelial injury can include hemorrhages in many organs including the subcutis; hydropericardium, hydrothorax and ascites; marked diffuse pulmonary congestion and edema; and edema in other organs including the lymph nodes, gall bladder, or the mucosa of the abomasum. Previous research has reported that necrotic foci in the liver of 1 to 5 day old lambs infected with RVFV can be obscured by general hepatic discolouration (Easterday et al., 1962a). In that study, hemorrhages appeared late in the disease course and the only other lesions were lymphadenomegaly and histologically appreciated depletion of the white pulp of the spleen.

Therefore, circumspection is required when conducting necropsies on young lambs in RVFV endemic areas.

Previous research also reported that liver lesions do not occur in young lambs prior to 24 hours after virus exposure, but that virus can be detected in blood and liver samples as early as 12 hours post exposure (Coetzer and Ishak, 1982, Easterday et al., 1962a). Four lambs in the present study tested positive on RT-qPCR of the liver but were negative on IHC. The necrotizing hepatitis typical of RVF in young lambs was also absent in these cases. These lambs were possibly infected with RVFV and developed a viraemia but died from other complications (e.g. systemic inflammatory response syndrome) before lesions could develop in the liver and virus became detectable by IHC. Whatever the reason for the disparate test results, this demonstrates that the investigator, when confronted with high mortalities, should examine and sample multiple lambs if possible and might, on occasion, encounter discordant test results.

The pathogenic mechanism for RVFV-induced necrotizing hepatitis, is likely hepatocellular death and the death of Kupffer cells or infiltrating macrophages by both apoptosis and lytic cell death mechanisms, including pyroptosis and necroptosis. The histomorphological changes in hepatocytes, described in previous research, concur with modern descriptions of apoptosis, and apoptosis was demonstrated in mice using terminal deoxynucleotidyl transferase dUTP nick-end labelling (Coetzer, 1977, Coetzer and Ishak, 1982, Daubney et al., 1931, Easterday et al., 1962a, Smith et al., 2010). Additionally, the presence of NSs filaments in the nucleus induces DNA damage responses and causes cell-cycle arrest, p53 activation, and apoptosis (Baer et al., 2012). However, in the present study many hepatocytes in RVFV-infected lambs also displayed histomorphological features of lytic cell death mechanisms which are characterized by cell swelling, rupture of the plasma membrane and cellular collapse (Belizário et al., 2015, Nailwal and Chan, 2018). Research has shown that RVFV induces the formation of nucleotide-binding domain, leucine-rich-containing family, pyrin domain-containing-3 (NLRP3) inflammasomes that activate caspase-1 leading to the maturation of interleukin 1β

and interleukin-18 and the induction of pyroptosis (Ermler et al., 2013). However, pyroptosis is considered a primary cellular response following the sensing of potentially damaging insults whereas necroptosis is mostly observed as a backup cell death defence mechanism that is triggered when apoptosis is hindered (Frank and Vince, 2019). It has been demonstrated that RVFV triggers apoptosis mainly through activation of caspase-8, but that the NSm protein of the virus suppresses apoptosis of target cells to ensure the efficient release of progeny virus within the first 24 hours after infection (Won et al., 2007). Therefore, the majority of the progeny virus is released prior to virus-induced apoptosis. Influenza A virus infection elicits concomitant activation of parallel pathways of mixed lineage kinase domain-like protein (MLKL)-driven necroptosis and Fas-associated protein with death domain (FADD)-mediated apoptosis, while the NLRP3 inflammasome promotes host immune defense against influenza A virus infection causing pyroptosis of infected epithelial cells, macrophages, and dendritic cells in the lung (Nogusa et al., 2016, Owen and Gale, 2009). Macrophages also undergo NLRP3 inflammasome-mediated pyroptosis in other viral infections including dengue virus and hepatitis C (Shrivastava et al., 2016, Wu et al., 2013). Macrophages play an important role in RVFV pathogenesis and conceivably, some of the cellular debris seen in necrotic foci in RVFV infection is composed of the remnants of macrophages. Therefore, it would seem that cell death morphology in the liver in RVFV-infected lambs is more heterogeneous than previously suspected, and the possibility that multiple cell death pathways are involved should be further explored.

Diagnostically, foci of liquefactive hepatic necrosis, referred to as primary foci in previous reports, are a very useful feature of RVFV infection in young lambs (Coetzer, 1977, Easterday et al., 1962a). The term liquefactive necrosis is preferred since the primary foci are not typical of coagulative necrosis where the architecture of the hepatic plates is preserved, and features of other recognized forms of necrosis are absent. Previous research reported that lesions in the liver of lambs commenced as small aggregates of neutrophils in the sinusoids followed by the death of small groups of hepatocytes (Easterday et al., 1962a). In lambs, this occurred at

24 to 36 hours after inoculation. Cell death progressed to the point where only remnants of completely lysed hepatocytes remained within a collapsed reticulum framework. Myriads of small nuclear remnants were scattered throughout the lesion and infiltrating neutrophils and macrophages underwent degenerative changes and likewise disintegrated. The areas of necrosis enlarged but remained discrete or rarely became confluent, and were accompanied by an infiltrate of more neutrophils and macrophages. Previous research also reported that between 36 and 48 hours post-infection, lesions were absent from the remainder of the liver parenchyma and hepatocytes outside the primary foci were histologically normal (Easterday et al., 1962a). Precipitously though, during the ensuing hours all but a few hepatocytes underwent cell death so that the primary foci were a prominent feature against a background of widespread cell death. From previous research it would seem that the initial sequence of events in adult sheep is the same and histomorphologically random foci of cell death in adult sheep also consist of disintegrated hepatocytes and leucocytes, with infiltrating neutrophils and macrophages (Chapter 2). However, diffuse hepatocellular death rarely occurs in adult sheep. Qualitatively, lytic cell death with collapse of the reticulum framework was also less apparent in adult sheep (Chapter 2). Therefore, primary foci against a background of diffuse hepatocellular death is a striking diagnostic feature in young lambs. Additionally, the mild portal edema and inflammation, characteristic of RVF in adult sheep, was not observed in young lambs likely due to disruption of the portal tract connective tissue by diffuse hepatic necrosis (Chapter 2).

Previous research reported that the primary foci were more useful diagnostically than intranuclear inclusion bodies, with primary foci found in 100% of cases and nuclear inclusions in only 49% (Coetzer, 1977). The present study had a similar ratio of 2:1 for primary foci (59 of 71; 83%) and nuclear inclusions (27 of 71; 38%). However, primary foci were only present in 86% of the cases in the present study. In most cases only one liver specimen was submitted and only a single mixed-organ paraffin block was prepared for most cases to limit costs, so the liver specimens were often quite small. Also, it was previously reported that lesions in the liver

can differ between specimens taken from the same animal (Chapter 2). Easterday et al. also reported that primary foci were difficult to find in some lambs (Easterday et al., 1962a). It is less likely that necrosis would be absent or overlooked but primary foci might be missed if only one very small specimen is available for histologic examination. Therefore, sampling multiple liver lobes and combining fewer organs in a block might improve the odds of identifying this very useful diagnostic feature in naturally infected lambs.

Lymphocytolysis was present in all lymphoid organs except for the thymus where resident T lymphocytes were completely unaffected in all cases. This strengthens a previous hypothesis that B lymphocytes, although not directly infected, are preferentially targeted in RVF. An alternative explanation is that developing lymphocytes in the thymus might be protected from the effects of RVFV infection by the blood-thymus barrier. Lesions and labelling in the spleen of young lambs also differed considerably from that of adult sheep. Research results from this study demonstrated that adult sheep generally had mature secondary follicles and necrosis was most obvious in the germinal centres, mantle cell layers, marginal zones and peripheral zones of the PALS of the white pulp (i.e. B-cell rich areas) (Chapter 2). Lymphoid follicles were poorly developed (age-appropriate in lambs) and necrosis primarily involved lymphocytes in the red pulp with fewer necrotic lymphocytes observed in the peripheral zones of the PALS. However, lymphocytolysis occurred in both white and red pulp at an equal frequency. Previously in adult sheep, positive labelling was observed more readily in the white pulp, particularly in the marginal zone. In young lambs labelling was widespread and easily identifiable in the red pulp and the splenic capsule. In most of the lamb cases, labelling was observed in small blood vessels in the capsule and foci of intense labelling were often present in the subcapsular red pulp. Labelling in or beneath the capsule was not seen in any of the adult cases sampled during the same outbreak (Chapter 2). Therefore, part of the splenic capsule should always be included in samples from young lambs.

Multifocal acute renal tubular injury, characterized by tubular epithelial cell pyknosis, karyorrhexis, and karyolysis and accompanied by intratubular cellular and proteinaceous

debris and detachment of the epithelium from the basement membrane, which has been previously reported in adult sheep, was absent in young lambs (Chapter 2). Instead, in agreement with earlier research, some lambs (20 of 46) had varying degrees of degenerative (hydropic) changes in tubular epithelial cells (Coetzer, 1977, Daubney et al., 1931) Daubney et al. also reported that death ensues too rapidly following RVFV infection in lambs to permit the development of extensive lesions (Daubney et al., 1931). In contrast, the previously reported pyknosis and karyorrhexis present in the glomeruli and interstitial capillaries, similar to previous findings in adult sheep, was a useful diagnostic feature (Chapter 2).

In RVFV antigen-positive adult sheep, labelling was often present in the renal tubules (33 of 55; 60%), and widespread in 9 of these, whereas labelling was isolated or scattered when present at all in lambs (8 of 40; 20%) (Chapter 2). Conversely, in the kidneys, viral antigen was more often present in vascular smooth muscle cells in young lambs (28 of 46; 61%) compared to adult sheep (5 of 83; 6%) (Chapter 2). In young lambs, smooth muscle labelling was present in small arteries in the cortex, in the efferent or afferent arterioles, and in arcuate arteries at the corticomedullary junction. In the adult cases, the labelling was only present in the muscular tunic of arcuate arteries at the corticomedullary junction (Chapter 2). Viral antigen was also more commonly observed in endothelial cells in capillaries and small blood vessels in the young lambs than in adult sheep. Possibly young lambs do not survive long enough for virus to spread much beyond the blood vasculature in the kidney; and due to the much higher viraemia in lambs, RVFV seemingly infects smooth muscle cells and endothelial cells more extensively.

Another prominent feature in the kidney, was viral antigen in a small group of cells opposite the macula densa. This was interpreted as antigen occurring in the peri-macular cells that include juxtaglomerular and granular extraglomerular mesangial cells. Smooth muscle cells in the afferent arterioles transition into granular extraglomerular mesangial cells at this location. Juxtaglomerular mesangial cells have also been demonstrated to be modified smooth muscle cells capable of contracting or relaxing in response to vasoactive agents (Schlondorff, 1987).

Kidney specimens from 2 of 83 adult sheep examined retrospectively had a similar pattern of labelling (Chapter 2). Additionally, van der Lugt et al.(Van Der Lugt et al., 1996) also found RVFV antigen in mesangial cells in 2 of 12 new-born lambs. In mice, it was experimentally demonstrated that adeno-associated virus 9 exclusively targets the juxtaglomerular apparatus and specifically cells opposite the macula densa (Xiao et al., 2015). It is possible that vascular smooth muscle cells and the renal peri-macular cells share receptors that make them both permissible for RVFV infection.

Infection of granular extraglomerular mesangial cells might suppress renin production which could have a deleterious effect on the regulation of glomerular filtration rate and renal blood flow. Infection of aldosterone secreting cells in the zona glomerulosa of the adrenal gland could potentiate this effect. RVFV infection of secretory cells in all zones of the adrenal cortex seemed to be more pronounced in young lambs compared to adult sheep where it was most prominently seen in secretory cells of the zona fasciculata (Chapter 2). The normal physiologic response to hypotension might be suppressed due to RVFV infection, and combined with vascular leakage, could exacerbate shock. In Dengue haemorrhagic fever, the most severely affected children develop dengue shock syndrome due to excessive depletion of intravascular volume as a result of plasma leakage, accompanied by only minor bleeding manifestations (Wills et al., 2002). Furthermore, RVFV infection of glucocorticoid producing cells in the zona fasciculata of the adrenal gland could also decrease the metabolic availability of glucose and fatty acids and further increasing the likelihood of a fatal outcome. However, additional studies would be needed to validate these speculations.

Previous research reported that the peak level of virus in the blood of young lambs is consistently greater than in adults (Easterday et al., 1962b). This concurs with the present investigation where viral antigen was generally widespread and easily detectable in the vasculature of young lambs; while in adult sheep labelling could be difficult to find in organs other than the liver (Chapter 2). Previous research in young lambs also reported that by 24 hours post-infection virus titers were high in the liver, spleen, lymph nodes, kidneys, lungs and

brain, and the authors inferred that the virus in the tissues was largely in the blood of these organs (Easterday et al., 1962a). Findings in the present study support that conclusion, since viral antigen was often present in capillaries and small blood vessels as non-cell-associated viral antigen or antigen associated with intravascular cell fragments. This was especially noticeable within the splenic capsule; interstitial tissues of the kidney, heart, lungs and lymphoid tissues; meninges of the brain; adipose tissue; and in the lamina propria and submucosa of the abomasum and small intestine. Therefore, samples from the liver and spleen should be sufficient to confirm a diagnosis of RVFV in young lambs using PCR or IHC (Table 16). Samples from the lung and kidney would be useful additional samples for histopathology, because pyknosis and karyorrhexis in the capillaries of the glomeruli and pulmonary interstitium were often present. Samples from the thymus and brain, although likely to test positive for viral antigen via IHC in RVFV-infected lambs, do not have any characteristic histologic lesions and therefore were not considered essential for confirming the diagnosis.

Table 16. Preferred diagnostic specimens for young lambs for investigation of RVF using histopathology and immunohistochemistry.

Diagnostic specimen in order of importance	Recommended number of samples and location	Justification
Liver	Sections from at least two liver lobes	Multifocal liquefactive hepatic necrosis (primary foci) present against a background of diffuse hepatocellular death. Fine diffuse to coarse granular labelling in the cytoplasm of necrotic hepatocytes and in cytoplasmic fragments in most cases. Sections from different areas in the liver may differ, with one section having primary foci and another having none.
Spleen	At least one section with capsule	Typically, lymphocytolysis that is most apparent as cellular debris in red pulp. RVFV antigen is particularly prominent in cellular debris in the red pulp, the subcapsular red pulp and in small blood vessels in the capsule.
Kidneys	One section that includes both cortex and medulla	Pyknosis and karyorrhexis in the glomerular capillaries in most cases. In some cases, tubuler epithelial cells (typically in the cortex), have hydropic change. Viral antigen is prominent in mononuclear, vascular smooth muscle, vascular endothelial, juxtaglomerular and extraglomerular mesangial cells.
Lung	One section	Pyknosis and karyorrhexis in the pulmonary interstitial capillaries in most cases. Antigen-positive macrophages in the pulmonary interstitium and labelling of endothelial cells or non-cell-associated viral antigen in the blood vessels in most cases.

3.6 Conclusion

The principal histologic lesion observed in young lambs naturally infected with RVFV was diffuse necrotizing hepatitis with prominent foci of liquefactive necrosis (primary foci). Hepatic lesions were typically accompanied by lymphocytolysis in lymphoid tissues with the notable exception of thymus as well as pyknosis and karyorrhexis in the glomerular and pulmonary interstitial capillaries. Additionally, lesions in the kidney rarely progressed beyond hydropic change and occasional pyknosis or karyolysis of tubular epithelial cells. Therefore, histological review of tissues from lamb deaths has an important role in RVF diagnosis.

Liver and spleen specimens were the most consistently positive for RVFV antigen and were adequate to confirm or exclude a diagnosis of RVFV in most cases using either PCR or IHC. Specimens from the lungs and kidneys were useful additional samples due to their characteristic histologic lesions. Rarely, PCR- positive lambs did not have typical histological lesions or viral antigen detectible by IHC in their tissues. However, RVFV causes high mortality in young lambs, and provided adequate samples are taken from multiple cases, the diagnosis should be straightforward.

The presence of RVFV antigen in vascular smooth muscle cells, vascular endothelial cells, adrenocortical epithelial cells and renal peri-macular cells was more prominent in the young lambs in this study compared to the adult sheep cases from the same outbreak that were studied previously. We hypothesize that these cells are more permissible to RVFV infection in very young animals, which would worsen clinical outcomes such as hepatic and renal failure, and shock, and contribute towards an increased likelihood of a fatal outcome to infection.

CHAPTER 4

OVINE FOETAL AND PLACENTAL LESIONS AND CELLULAR TROPISM IN NATURAL RIFT VALLEY FEVER VIRUS INFECTION

This chapter has been prepared for submission to *Veterinary Pathology*.

4.1 Summary

Infection with RVFV causes abortion storms and a wide variety of outcomes for both ewes and foetuses. Sheep foetuses and placenta specimens were examined during the 2010-2011 RVF outbreak in South Africa. A total of 72 foetuses were studied of which 58 were confirmed positive for RVF. Placenta specimens were available for 35 of the foetuses. Macroscopic lesions in foetuses were non-specific and included effusions in the body cavities and oedema and haemorrhages in visceral organs. Microscopically, necrotizing hepatitis was present in 48 of 58 cases with councilman bodies, primary lytic foci and eosinophilic intranuclear inclusions in hepatocytes useful diagnostic features. Lymphocytolysis was present in lymphoid organs examined with the exception of the thymus and Peyer's patches, and pyknosis or karyorrhexis was often present in the renal glomeruli. The most significant histological lesion in the placenta was necrosis of trophoblasts and endothelial cells in the cotyledonary and intercotyledonary allantochorion. Immunolabelling for RVFV was most consistent in trophoblasts of the cotyledon or caruncle. Other antigen-positive cells included hepatocytes, renal tubular epithelial, juxtaglomerular and extraglomerular mesangial cells, vascular smooth muscle and endothelial cells, cardiomyocytes, Purkinje fibers, adrenocortical cells and macrophages. Fetal organ samples must minimally include liver, kidney and spleen. From the placenta, the minimum recommended specimens for histopathology include the cotyledonary units and caruncles from the endometrium, if available. The diagnostic investigation of abortion in endemic areas should

always include routine testing for RVFV and a diagnosis during inter-epidemic periods might be missed if only limited specimens are available for examination.

4.2 Introduction

Rift Valley fever virus causes disease in both livestock and humans, and frequent epidemics in eastern and southern Africa with significant outbreaks in South Africa between 1950 and 2011 (Swanepoel and Coetzer, 2004). The disease is caused by infection with RVFV, an arthropod-borne virus of the family *Phenuiviridae*, genus *Phlebovirus*. Previously, we reported that a clear distinction can be made between the lesions and cellular tropism of natural RVFV infections in young lambs and adult sheep (Chapters 2 and 3). The disease is uncommon in non-pregnant sheep but virtually all pregnant sheep abort when infected with a wild-type strain of RVFV (Swanepoel and Coetzer, 2004). Rift Valley fever is also an important zoonosis with most human infections presenting as an acute self-limiting febrile illness (Al-Hazmi et al., 2003, Madani et al., 2003, El Imam et al., 2009). However, in a minority of human patients, severe hepatic disease with widespread haemorrhages, renal impairment, encephalitis, or ocular lesions can develop (Madani et al., 2003, Al-Hazmi et al., 2003, El Imam et al., 2009). Additionally, virus replication in the human placenta and vertical transmission of RVFV to human foetuses resulting in an increased risk of miscarriage have also been reported (Arishi et al., 2006, Adam and Karsany, 2008, Baudin et al., 2016, McMillen et al., 2018).

Experimental RVFV infection in pregnant ewes causes a wide variety of outcomes. In a study by Antonis and co-workers, four of 11 pregnant ewes experimentally inoculated with RVFV developed a viraemia and succumbed or had to be euthanized before the end of the experiment (Antonis et al., 2013). Three of these ewes developed multifocal necrotizing hepatitis and the fourth had a moderate-to-severe hepatitis. Four of the 7 surviving ewes, euthanatized at 21-23 days post infection, developed neither detectable viraemia nor clinical signs. These ewes also failed to seroconvert and lacked lesions typical of RVF at post mortem examination. In contrast, the other 3 surviving ewes developed a detectable viraemia and

seroconverted but had no significant lesions at post mortem examination. Interestingly, the liver specimens from all 11 ewes and brain specimens from 9 of 11 were positive for viral RNA. Lesions in the brain were not described.

Reports concerning the development of lesions and detection of viral RNA in foetal organs and placenta in experimental cases also varies within the literature. Viral RNA was detected in liver or brain samples of all 18 foetuses obtained from 9 experimentally infected ewes (Antonis et al., 2013). Multifocal necrotizing hepatitis was reported for 2 of the foetuses and placental lesions were identified in 3 of 11 specimens. There were $10^{8.33}$ RNA copies per gram in the liver of one foetus whereas viral RNA was undetectable in the liver of 5 other foetuses. A ewe inoculated intradermally with the virulent van Wyk RVFV strain aborted after infection and a viral load of $10^{6.2}$ virus per gram was measured in the placenta using the mouse intraperitoneal median lethal dose (mouse lethal doses) technique (Easterday et al., 1962b). However, minimal virus was identified in foetal blood, and virus could not be detected in foetal liver, lungs or spleen. In a RVFV vaccine study, a single vaccine dose did not protect ewes against challenge with virulent RVFV and at necropsy all 58 ewes had either aborted or had dead foetuses (Yedloutschnig et al., 1981). A RVFV concentration of $10^{2.5}$ to $10^{4.5}$ mouse lethal doses per gram was obtained from foetal spleen, liver and brain specimens.

The lesions and cellular tropism of naturally occuring RVFV in sheep foetuses and placenta have not been described in previous published research. There is the perception that RVF disappears in the interepidemic periods and only reappears suddenly when heavy rainfall occurs. However as mentioned, experimental studies have demonstrated a wide variety of outcomes for pregnant ewes and foetuses infected with RVFV. Therefore, excluding RVF from the list of possible differential diagnoses in endemic areas might be difficult given the paucity of information concerning the gross, histopathological and immunohistochemical findings in naturally occurring abortions caused by RVFV. Therefore, the principle aim of this fourth chapter was to describe RVFV infection in naturally infected foetal tissues and determine the diagnostic significance of the lesions. A second aim was to compare the diagnostic usefulness

of the placenta compared to other organs and to determine which section of the placenta, if any, is most useful for a diagnosis.

4.3 Materials and methods

4.3.1 Case selection

Tissue specimens were collected from sheep and foetuses as described previously (Section 2.3.1). Briefly, tissues from 1034 necropsied animals were collected by government officials and the principle investigator (Lieza Odendaal), preserved in 10% neutral buffered formalin, embedded in paraffin, and haematoxylin and eosin-stained histologic sections were routinely prepared. Included were tissues from at least 122 ovine foetuses. From this collection, cases were excluded when the level of autolysis was severe or only a single organ was available for study. Cases without available liver specimens were also excluded.

A total of 72 ovine foetus cases were suitable for study of which 58 cases tested positive for RVFV based on results of histopathology, RT-qPCR and/or IHC. Also included in this study were placenta and uterus (caruncle) from 8 ewes that tested positive for RVF. Matching foetal organs (included in the 72 foetus cases) were available for 3 of these ewes. Placenta specimens were available for 35 of the cases. Animals that died as part of the outbreak and were shown to be infected with RVFV based on a parallel interpretation of one or more tests (histopathology, RT-qPCR, and IHC) were presumed to have died of RVF even if macrospopic or histologic lesions were absent. The negative controls tissues for the study were 14 aborted foetuses from the same outbreak that tested negative for RVFV.

4.3.2 Diagnostic tests

Nucleic acid extractions and RT-qPCR on fresh tissue specimens from 54 of the cases were performed at the Biotechnology PCR Laboratory of the Agriculture Research Council-Onderstepoort Veterinary Institute as described previously (Odendaal et al., 2014).

Immunohistochemistry labeling with additional controls for the detection of RVFV antigen was performed using polyclonal antibody to RVFV (mouse ascitic fluid) as described in the original validation study (Odendaal et al., 2014). Briefly, the method included microwave antigen retrieval in citrate buffer (pH 6.0), blocking of endogenous peroxidases with 3% hydrogen peroxide, incubation with the anti-RVFV primary antibody at 1:500 dilution (National Institute for Communicable Diseases, Johannesburg, South Africa) for 1 hour and, rabbit anti-mouse secondary antibody (F0232, DakoCytomation, Glostrup, Denmark) followed by detection with a standard avidin-biotin peroxidase system, Vectastain® Elite® ABC-HRP Kit (PK-6100, Vector Laboratories, Inc., Burlingame, CA, USA), NovaRED peroxidase substrate (SK-4800, Vector Laboratories, Inc.) and hematoxylin counterstain.

4.3.3 Examination of tissues

Histomorphological lesions in all available organs were systematically recorded within the context of lesions associated with RVFV infection. As described in Chapter 3, lesion severity in the liver, kidney and spleen was scored using a qualitative scale as mild, moderate or severe. The number of primary foci in the liver specimens were scored on a semi-quantitative scale as isolated (<5), scattered (between 6 and 10) or widespread (>10). Immunolabelling for RVFV antigen was also scored on a semi-quantitative scale as isolated, scattered or widespread labelling, as previously described (Section 2.3.2). The severity of autolysis was qualitatively graded as mild, moderate or severe as previously described (Odendaal et al., 2014). Briefly, autolysis was mild when cells were intact and organ architecture was distinct. Autolysis was moderate when cytoplasmic borders were still distinct, but some cells showed fading of nuclei and/or tissues stained uniformly eosinophilic. Severe autolysis was classified by loss of basophilia, indistinct cytoplasmic borders, nuclear fading, complete lysis of red blood cells and the presence of many putrefactive bacteria in the tissues.

The number and types of foetal organs available for study varied with liver (n = 72), lung (n = 61), spleen (n = 59) and kidney (n = 58) being the specimens most often submitted.

Additional tissue specimens included 47 heart, 17 gastrointestinal tract, 4 lymph node, 32 brain, 27 thymus, 6 adrenal, and 3 skin specimens. Gastrointestinal tract specimens included tongue (n = 7), forestomach (n = 7), abomasum (n = 5), small intestine (n = 15) and large intestine (n = 2).

Placenta specimens were available for 30 of the 72 foetuses included in this study. Another 5 placenta specimens had matching maternal organ samples but no other foetal tissues. For the 35 available placenta specimens, cotyledon was included in 30 of 35 with a portion of the chorioallantoic membrane connected to cotyledonary villi in 21 of 35 cases. Intercotyledonary allantochorion was available in 11 of 35 cases and in 2 cases this was the only placenta specimen available. For 7 of the 8 ewes classified as positive for RVFV, caruncle with myometrium and varying amounts of chorioallantoic villi were available. Additionally, there was one caruncle specimen with myometrium attached that had matching foetal organs but other tissues from the ewe were not available. Uterus specimens with intact endometrium, myometrium and perimetrium were available for 4 of 8 ewe cases. For 4 of 30 of the foetal cases, maternal caruncle with myometrium and varying numbers of cotyledonary villi were also available. The negative control specimens included placenta for 4 of the 72 foetuses.

4.3.4 Statistical analysis

Dichotomous data were described using proportions and 95% mid-P confidence intervals. Scalar data were descriptively presented using the median and interquartile range (25^{th} to 75^{th} percentiles). Data from ordinal scales were compared between the liver and other organs using Wilcoxon signed rank tests. Bivariate correlations between scaler data variables were evaluated using Spearman's rho. Agreement between dichotomous variables was estimated using the kappa statistic. Freeware (Epi Info, version 6.04, CDC, Atlanta, GA, USA) and commercial statistical software (IBM SPSS Statistics Version 25, International Business Machines Corp., Armonk, NY, USA) were used to perform statistical analyses. Statistical results were evaluated at the 5% level of significance.

4.4 Results

4.4.1 Overview

Macroscopic lesions most often reported in examined fetuses included edema and hemorrhages in visceral organs and effusions in the body cavities (Fig. 104). Reported post-mortem changes were occasional moderate to advanced autolysis with increased friability of tissues and hemoglobin imbibition that made it difficult to discern lesions. Before excluding cases due to severe autolysis or lack of sufficient organs for examination, autolysis was classified in histological specimens as mild, moderate or severe in 48, 36 and 15 of the total number of RVFV positive cases (n = 99), respectively. From the subset of RVFV positive cases included in the study (n = 58), autolysis was classified as mild or moderate in 31 (53%) and 27 (47%) cases, respectively.

Other than lung edema, typical histological lesions for RVF were absent from the organs of the fetuses included as RVFV negative controls. Placenta lesions in the negative controls included multifocal hemorrhages, varying degrees of karyorrhexis and karyolysis of trophoblasts and the presence of cellular debris between the chorionic villi.

Viral antigen was easily observed and widespread in most organs including liver, kidney, lymphoid organs, lung, heart, brain and placenta (Table 17). Positive labelling was typically fine diffuse to coarse granular cytoplasmic labelling or non-cell-associated antigen. In blood vessels, labelling was especially prominent as non-cell-associated antigen but also as cell-associated antigen in endothelial cells (Table 18). Viral antigen was also commonly present in vascular smooth muscle cells in multiple organs but particularly in the kidney (Table 19).

Non-cell-associated antigen was also often present in the capsules of organs or in the loose connective tissue around the gall bladder, intestines, adrenals or the thymus. The reticulin framework in the liver and spleen, and the basement membranes in the kidney cortex, apex of the renal papilla and the heart were also occasionally delineated by the presence of non-cell-associated antigen. This was not considered to be an IHC artefact because viral antigen was always absent from epithelial cells, and their associated basement membranes, in the medulla

of the kidney, thymic cortex, T-cell areas of the gut-associated lymphoid tissue (GALT) in the ileum, the brain parenchyma, and mesenchymal connective tissues of the placenta. Additionally, RVFV antigen were not present in any of the tissues from the 14 cases included as negative tissue controls.

Table 17. Frequency of viral antigen in different organs and comparison to quantity of immunolabelling in liver, for 58 sheep foetuses with RVFV infection.

Organ	Tropism		Staining intensity	P value[c]
	Positive/ total[a]	Percentage (95% CI)	Median (IQR)[b]	
Liver	47/58	81 (69, 90)	Widespread (widespread, widespread)	NA
Gallbladder	4/4	100 (47, 100)	Widespread (widespread, widespread)	1.0
Kidney	40/49	82 (69, 91)	Widespread (widespread, widespread)	0.157
Spleen	40/48	83 (71, 92)	Widespread (widespread, widespread)	0.026
Lung	40/51	78 (66, 88)	Widespread (scattered, widespread)	0.002
Heart	34/40	85 (71, 94)	Widespread (widespread, widespread)	0.157
GI tract	8/13	62 (34, 84)	Widespread (widespread, widespread)	0.285
Rumen	3/5	60 (18, 93)	Widespread (widespread, widespread)	0.317
Abomasum	2/3	67 (13, 98)	Widespread (widespread, widespread)	0.317
Small intestine	7/11	64 (34, 87)	Widespread (widespread, widespread)	0.655
Large intestine	0/2	0 (0, 78)	NA	0.317
Tongue	4/4	100 (47, 100)	Widespread (scattered, widespread)	0.157
Adrenal glands	2/4	50 (9, 91)	Widespread (scattered, widespread)	0.317
Skin	1/2	50 (3, 97)	Scattered (NA)	1.0
Thymus	18/21	86 (66, 96)	Widespread (widespread, widespread)	1.0
Lymph nodes	3/4	75 (24, 99)	Widespread (widespread, widespread)	0.317
Brain	22/29	76 (58, 89)	Widespread (scattered, widespread)	0.007
Placenta	25/26	96 (82, 100)	Widespread (widespread, widespread)	0.046

[a]Positive/total represents the number with positive immunolabelling for RVFV antigen out of the total number of tissues examined. CI, confidence interval; IQR, interquartile range; NA, not applicable. [b]Calculated only for the cases with positive labelling; the categories in parentheses are the interquartile range of antigen quantity in the sample set. [c]Based on Wilcoxon rank sum tests comparing the quantity of positive immunolabelling to the quantity of labelling in liver samples.

Table 18: Frequency of non-cell-associated viral antigen in blood vessels or antigen in vascular endothelial cells or intravascular cellular debris for 58 sheep foetuses with RVFV infection.

Organ	Positive/total[a]	Percentage (95% CI)[b]
Gallbladder	4/4	100 (47, 100)
Kidney	35/49	71 (58, 83)
Spleen	36/48	75 (61, 86)
Lung	35/51	69 (55, 80)
Heart	34/40	85 (71, 94)
Intestine	8/13	62 (34, 84)
Tongue	4/4	100 (47, 100)
Adrenal glands	1/4	25 (1, 76)
Skin	1/2	50 (3, 97)
Thymus	18/21	86 (66, 96)
Lymph node	3/4	75 (24, 99)
Brain	22/29	76 (58, 89)

[a] Positive/total represents number with positive immunolabelling for RVFV antigen out of the total number of tissues available for examination. [b] CI, confidence interval.

Table 19. Frequency of viral antigen in vascular smooth muscle in the organs of 58 sheep foetuses with RVFV Infection.

Organ	Positive/total[a]	Proportion-% (95% CI)[b]
Gallbladder	1/4	25 (1, 76)
Kidney	37/49	76 (62, 86)
Spleen	25/48	52 (38, 66)
Lung	11/51	22 (12, 34)
Heart	21/40	53 (37, 68)
Small intestine	1/13	8 (0, 32)
Tongue	2/4	50 (9, 91)
Adrenal gland	1/4	25 (1, 76)
Thymus	3/21	14 (4, 34)
Brain	3/29	10 (3, 26)

[a] Positive/total represents number with positive immunolabelling for RVFV antigen out of the total number of tissues available for examination. [b] CI, confidence interval.

Other than lung oedema, typical histological lesions for RVFV were absent from the organs of the foetuses included as RVFV negative controls. Placenta lesions in the negative controls included multifocal haemorrhages, varying degrees of karyorrhexis and karyolysis of trophoblasts and the presence of cellular debris between the chorionic villi.

4.4.2 Liver

Macroscopically, affected livers were often swollen and friable and either yellow or dark red (Fig. 104). Foci of necrosis or haemorrhage were not seen. Microscopically, the severity of hepatic necrosis varied considerably among cases with 10 of 58 (17%), 18 of 58 (31%) and 20 of 58 (34%) of specimens classified as mild, moderate or severe necrosis respectively. Necrosis in the liver was positively correlated with necrosis in the spleen (ρ=0.511; P<0.001). Descriptively, severity of liver necrosis was also correlated with necrosis in lymph nodes (ρ=0.949) but the sample size was only 4 and the association was not significant (P=0.051).

There was no discernible pattern of necrosis in the liver. Instead, random hepatocyte necrosis or dropout of hepatocytes from the reticulin framework was present. Councilman bodies or acidophilic bodies, with condensed hypereosinophilic cytosol and marginalized chromatin, pyknosis or karyorrhexis, were also often present. In mild cases, the normal architecture of the liver was largely intact with hepatocyte plates and sinusoids easily distinguishable. Randomly scattered cells had undergone necrosis showing karyolysis or karyorrhexis with occasional dropout of hepatocytes from the reticulin framework. In moderate cases, histomorphologically normal appearing hepatocytes were present in clumps or short strings of up to 10 cells, with scattered intervening hepatocyte necrosis and aforementioned hepatocyte dropout (Figs. 105, 106). The orderly arrangement of hepatocytes into plates was indistinct and sinusoids were sometimes difficult to distinguish. In severe cases, surviving hepatocytes were present in small clumps or short strings of up to 5 cells with most nuclei in the majority of the high-power fields lost due to karyorrhexis or karyolysis accompanied by hepatocytes dropout (Figs. 107, 108). In a few severe cases there was complete dissociation of all the remaining hepatocytes and the sinusoids were difficult to distinguish from the empty spaces that followed due to

hepatocytes dropout. Portal areas were also difficult to identify in these severe cases. Irrespective of the degree of necrosis, haemorrhage or pooling of blood in necrotic spaces was rare and inflammation was either absent or sparse and predominantly neutrophilic. Macrophages were inconspicuous whereas oedema was often present in the portal areas and haematopoiesis (Fig. 107) was present in most cases.

Primary foci were present in the liver specimens from 26 of 58 (45%) cases and were either isolated (20 of 58), scattered (3 of 58) or widespread (3 of 58). Necrosis in the liver was positively correlated with the number of primary foci (ρ=0.296; P=0.024). Intranuclear inclusion bodies (Fig. 106) were identified in 36 of 58 (62%) cases and mineralization of hepatocytes in 2 of 58 (3%). All three features were absent from 5 of 58 (9%) cases that had mild (n = 1), moderate (n = 1) or severe (n = 3) necrosis. In a further 10 of 58 (17%) cases there were no lesions in the liver. For 5 of these 10 cases, matched placenta specimens were IHC positive. For another case, the placenta was positive by RT-qPCR but negative by IHC. There were no placenta samples for the other 4 cases.

RVFV antigen was widespread and easily identified in 47 of 58 (81%) cases. Hepatocytes were the predominant target of RVFV (Fig. 109). Viral antigen was sparse in primary foci and when present associated with scattered cellular debris (Fig. 109). Occasionally the entire reticulin framework was delineated by the presence of non-cell-associated viral antigen accompanied by intense labelling of the tunica intima of hepatic veins (Fig. 110).

4.4.3 Gall bladder

Microscopic lesions were absent in the available specimens. However, moderate to severe autolysis was present in all 4 specimens. Viral antigen was widespread in the capillaries and small blood vessels either as non-cell-associated viral antigen or as antigen in endothelial cells or intravascular cellular debris. Labelling was present in vascular smooth muscle cells in blood vessels of the adventitia and serosa in one case. No involvement of gall bladder epithelium was seen.

Panel 20: Figures 104-110. Rift Valley fever virus, sheep foetuses.

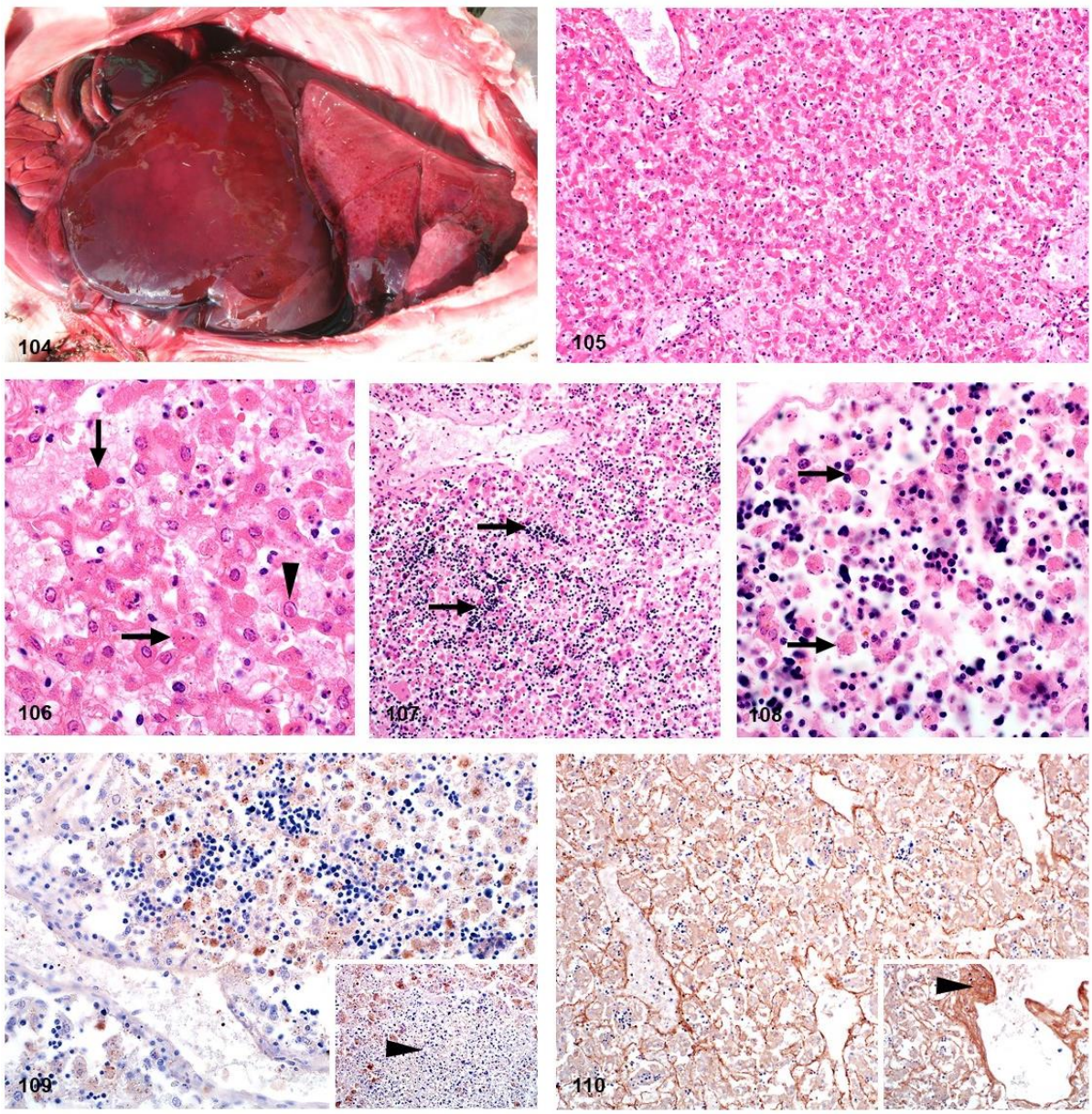

Figure 104. Case 15. Hepatomegaly, multifocal to coalescing haemorrhages in the lungs, and serosanguinous effusions in the thorax. **Figure 105.** Case 7. Liver. The orderly arrangement of hepatocytes into plates is indistinct. HE. **Figure 106.** Case 7. Liver. Councilman bodies (arrows), scattered neutrophils and rod-shaped, acidophilic viral inclusion in the nucleus of a hepatocyte (arrowhead). HE. **Figure 107.** Case 1. Liver. Diffuse necrotizing hepatitis with widespread extramedullary haematopoiesis (arrows). HE. **Figure 108.** Case 1. Liver. Disassociation of necrotic hepatocytes (arrows). HE. **Figure 109.** Case 35. Liver. Viral antigen in the cytoplasm of necrotic hepatocytes. **Inset:** Case 3. Liver. A primary focus (arrowhead) with nuclear fragments and remnants of completely disintegrated hepatocytes and leucocytes. IHC for RVFV. **Figure 110.** Case 28. Liver. Delineation of the reticulin framework by viral antigen. **Inset:** Intense labelling of the tunica intima of a large vein. IHC for RVFV.

4.4.4 Spleen

Microscopically, lymphocytolysis was present in 42 of 48 (88%) RVF cases and was either mild (n = 14), moderate (n = 16) or severe (n = 12). Generally, the periarteriolar lymphatic sheaths comprised a narrow zone of lymphocytes, and follicular germinal centres and mantle zones were not developed, which was considered age-appropriate in foetuses. Lymphocytolysis was present in both the red and white pulp in all spleen specimens that tested positive for RVFV antigen by IHC, and was characterized by the presence of cellular debris and occasional tingible body macrophages.

Splenic infection with RVFV was present in 40 of 48 (83%) cases and antigen was either widespread (n = 33), scattered (n = 3) or isolated (n = 4). Viral antigen was predominantly present in the red pulp and mostly non-cell-associated or associated with cellular debris. Positively labelled mononuclear cells, morphologically consistent with macrophages, were seen within the red pulp in 31 of 40 (78%) and the white pulp in 19 of 40 (48%) cases. Tingible body macrophages labelled only rarely.

In 36 of 40 (90%) RVFV positive cases, labelling was prominent in small blood vessels and capillaries as non-cell-associated antigen and antigen in endothelial cells and cellular debris (Fig. 111). In 25 of 40 (63%) cases, RVFV antigen was also present in smooth muscle cells in blood vessels in the capsule or in the central arteries (Figs. 111, 112). The serosa, smooth muscle cells in the capsule and the reticulin framework of the red pulp labelled intensely in some cases.

4.4.5 Lymph nodes

There were no gross lesions in the lymph nodes. Microscopically, there were variable degrees of lymphocytolysis in 3 of the 4 available lymph node specimens. In these, cellular debris was present in both the cortex and medulla. Similar to the spleen, follicular germinal centres were not developed.

Panel 21: Figures 111-117. Rift Valley fever virus, spleen and kidney, sheep foetuses.

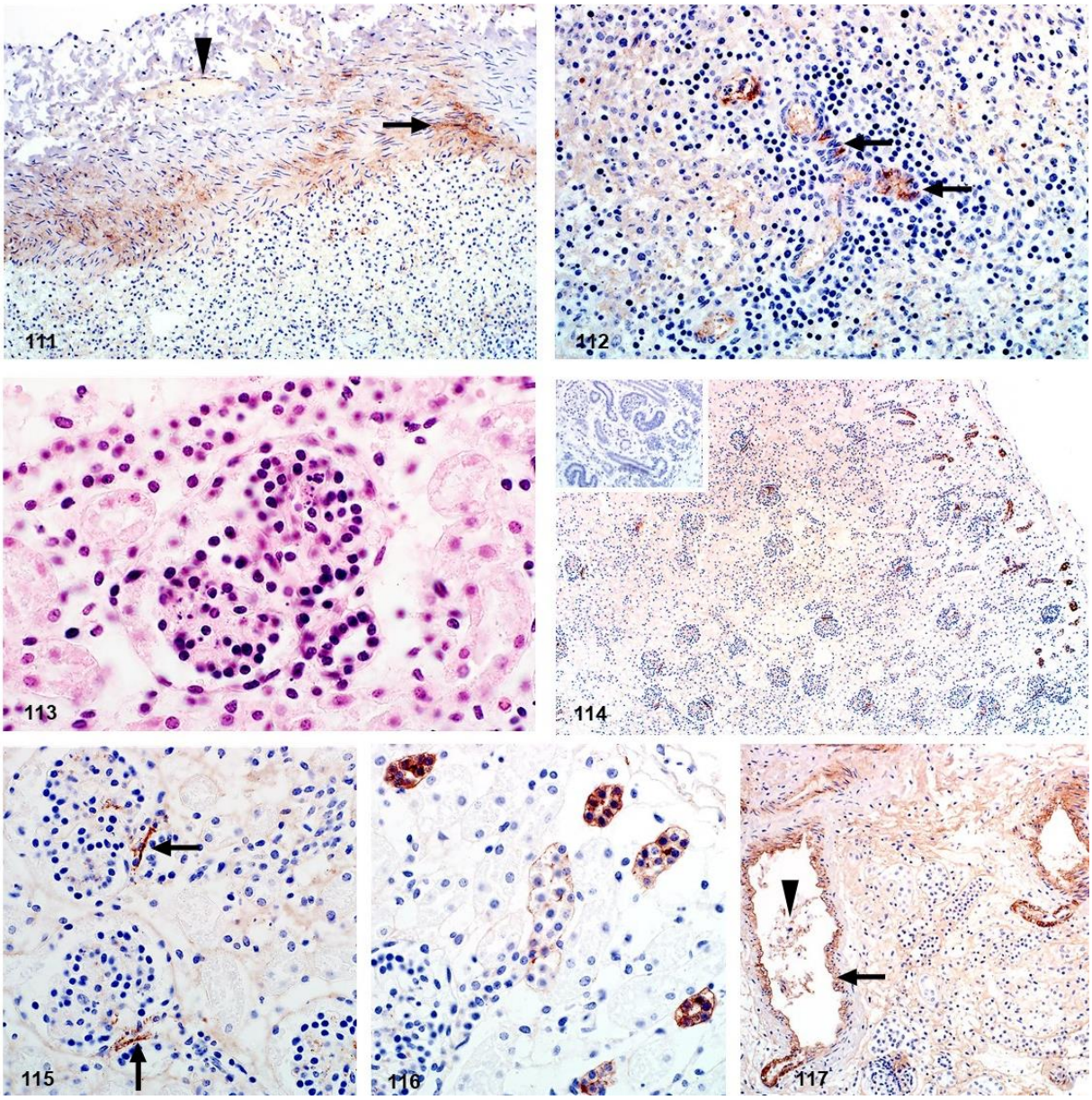

Figure 111. Case 34. Spleen. Viral antigen in smooth muscle cells (arrow) and small blood vessels (arrowhead) in the capsule. IHC for RVFV. **Figure 112:** Case 56. Spleen. Viral antigen in smooth muscle cells in a central artery (arrows). IHC for RVFV. **Figure 113.** Case 26. Kidney. Scattered pyknosis and karyorrhexis in a renal glomerulus. HE. **Figures 114-117.** Kidney. IHC for RVFV. **Figure 114.** Case 26. Widespread viral antigen in the glomeruli, renal tubules in the superficial cortex and in the interstitium. **Inset:** Negative control tissue (uninfected) with no antigen in the interstitium or immature renal corpuscles or tubules. **Figure 115.** Case 26. Labelling of juxtaglomerular cells opposite the macula densa (arrows). **Figure 116.** Case 26. Viral antigen in immature tubules in the superficial cortex. **Figure 117.** Case 54. Viral antigen in smooth muscle (arrow) and in cell debris in a blood vessel (arrowhead). Also, delineation of the reticulin framework by viral antigen.

Viral antigen was present in all 3 cases with lymphoid necrosis. Labelling was present in the capillaries and small blood vessels either as non-cell-associated viral antigen or as antigen in endothelial cells or intravascular cellular debris. In the sinusoids, mononuclear cells, morphologically consistent with macrophages, were also positive for viral antigen. In 2 specimens, non-cell-associated virus was present in the capsular blood vessels, and in one of these cases the loose connective tissue surrounding the capsule was also diffusely positive.

4.4.6 Thymus

No gross or microscopic lesions were observed in the thymus. The lymphocytolysis present in other lymphoid organs was absent. Viral antigen, present in 18 of 21 (86%) available specimens, was often present in capillaries and small blood vessels as non-cell-associated viral antigen or as antigen in endothelial cells or intravascular cellular debris. Viral antigen was also present in vascular smooth muscle cells in 2 of 21 (10%) cases.

4.4.7 Kidney

Gross lesions were not present in the kidney. Microscopically, severe multifocal acute tubular epithelial injury lacking significant associated inflammation was present in only 3 of 49 (6%) cases with kidney specimens. This was characterized by karyolysis of proximal tubular epithelial cells and the presence of cellular debris and round desquamated cells with homogenous eosinophilic cytoplasm in the lumens of tubules, particularly in the superficial cortex and medullary rays. Haemorrhage was present in the cortical interstitium or below the capsule in some cases. Glomeruli often appeared less densely cellular than normal with pyknosis or karyolysis in 43 of 49 (88%) cases (Fig. 113). Nuclear debris was often present in interstitial capillaries in 37 of 49 (76%) cases and the amount of pyknosis and karyorrhexis in the glomeruli was positively correlated ($\rho = 0.617$, $P < 0.001$) with the quantity of nuclear debris in the interstitial capillaries. Pyknosis and karyorrhexis in the glomeruli was also significantly associated with the presence of viral antigen in the glomeruli ($\rho = 0.705$, $P < 0.001$).

RVFV antigen was present in 40 of 49 (82%) cases with available kidney specimens. In the positive cases, labelling was present in the cortex in 40 of 40 (100%) cases (Fig. 114) and in both the cortex and the medulla in 26 of 40 (65%) cases. RVFV antigen was most prominent in the glomeruli and was present in 39 of 40 (98%) positive cases. Interpretation of cellular tropism in foetal glomeruli was often hindered by the presence of intense granular labelling in most of the glomerular tufts; however, in some cases antigen could be localized specifically to either vascular endothelial cells or mononuclear cells. Viral antigen was often present at the vascular pole of the glomerulus opposite the macula densa, in a small group of cells that are likely juxtaglomerular cells and extraglomerular mesangial cells (Fig. 115). In 11 of 40 cases, labelling was also present in tubules in the cortex (Fig. 116). In contrast, labelling was absent in tubules in the medulla.

Labelling was also occasionally present in smooth muscle cells in the efferent or afferent arterioles or in small blood vessels in the cortex including arcuate blood vessels in the corticomedullary junction in 37 of 40 (93%) cases (Fig. 117). Non-cell-associated antigen or antigen in vascular endothelial cells or cellular debris was often present in blood vessels or interstitial capillaries in both the cortex and the medulla.

Labelling was more prominent in the interstitial capillaries of the cortex compared to the medulla. Viral antigen was present in the cortical interstitial capillaries in 32 of 40 (80%) positive cases and labelling in the glomerulus was significantly associated with labelling in these interstitial capillaries ($\rho=0.551$; $P<0.001$). Viral antigen was also present in the medullary interstitial capillaries in 23 of 40 (58%) cases and the presence of viral antigen in the cortical interstitium was significantly associated with the presence of viral antigen in the medullary interstitium ($\rho=0.609$; $P<0.001$). Finally, viral antigen was occasionally present in the capillaries and small blood vessels of the perirenal adipose tissue.

4.4.8 Adrenal gland

Two of 4 cases for which specimens were available were positive for RVFV antigen. However, significant histological lesions were not discernible in either case. One sample was in fairly good condition and viral antigen was in cortical epithelial cells in all three zones as well as in vascular endothelial cells in the capsule, cortex and medulla. Autolysis was advanced in the second specimen and only the capsule and cortex were available for examination; however, labelling was clearly discernible in scattered cortical epithelial cells and also in vascular smooth muscle cells in the capsule. Labelling was also present as non-cell-associated antigen or antigen associated with endothelial cells in the periadrenal adipose tissues.

4.4.9 Lung

Macroscopic haemorrhages were occasionally present in the lungs and a serosanguineous effusion was common in the thoracic cavity. Microscopically, pulmonary interstitial oedema was present in 44 of 51 (86%) cases with available specimens and was classified as moderate to severe in 29 of 51 (57%) cases (Fig. 118). This oedema expanded the connective tissue surrounding blood vessels, bronchi or bronchioles and was present in the pulmonary septa. Intra-alveolar oedema could not be assessed since a mild accumulation of liquid in foetal airways is considered to be age-appropriate. A few lung specimens were clearly aerated (6 of 51). Mild expansion of the alveoli was often noted but interpreted as attributable to the loss of liquid during processing and not the presence of air. Haemorrhage was present in the pulmonary septa or the visceral pleura in 21 of 51 (24%) cases. Mild pyknosis and karyorrhexis were often present in the alveolar septa and pulmonary blood vessels.

Labelling was present in 40 of 51 (78%) cases (Fig. 119). Viral antigen was present in mononuclear cells, histomorphologically consistent with macrophages, in the interstitial capillaries in 38 of 40 (95%) of RVFV positive cases. Labelling was also present as non-cell-associated antigen or antigen associated with endothelial cells or cellular debris in small blood vessels and capillaries in 35 of 40 (88%) positive specimens. In 11 of 40 (28%) positive specimens, viral antigen was present in vascular smooth muscle cells.

Panel 22: Figures 118-123. Rift Valley fever virus, lung and heart, sheep foetuses.

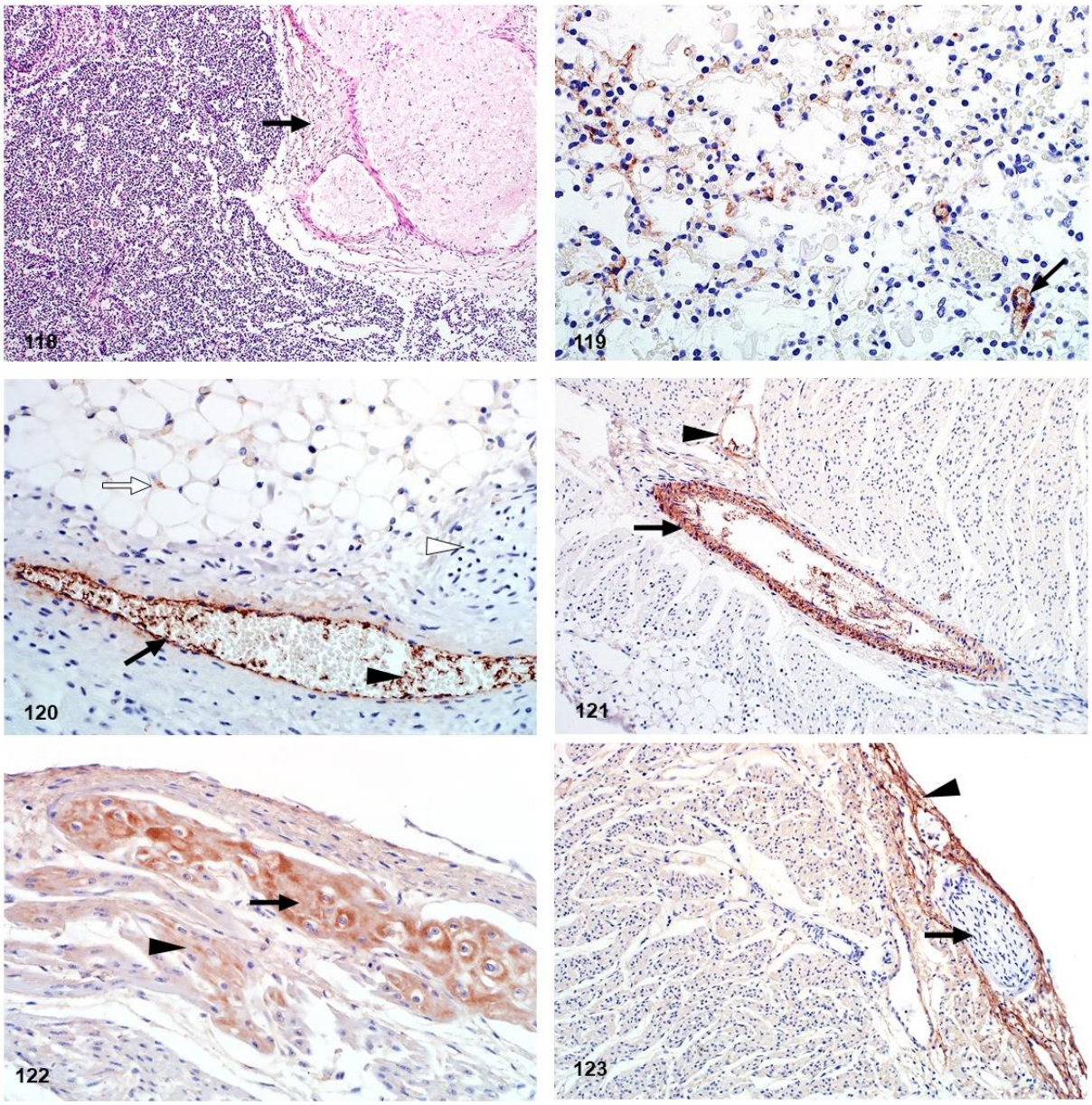

Figure 118. Case 26. Lung. Interstitial oedema (arrow). HE. **Figure 119.** Case 7. Lung. Non-cell-associated viral antigen in the interstitial capillaries and in endothelial cells (arrow). IHC for RVFV. **Figures 120-123.** Heart. IHC for RVFV. **Figure 120.** Case 55. Viral antigen in endothelial cells (arrow) and non-cell-associated antigen (arrowhead) in the blood vessels. Labelling is also present in capillaries in the pericardial fat (white arrow). Viral antigen is absent from the nerve fiber (white arrowhead). **Figure 121.** Case 26. Viral antigen in vascular smooth muscle (arrow) and endothelial cells (arrowhead). **Figure 122.** Case 4. Viral antigen in Purkinje fibres (arrow) and in cardiomyocytes (arrowhead). **Figure 123.** Case 24. Intense labelling in the subepicardium with antigen absent from the nerve fiber (arrow).

4.4.10 Heart

Macroscopic and histopathological lesions were absent in the cardiac parenchyma apart from one case where sub-epicardial haemorrhage was present. RVFV antigen was present in heart specimens of 34 of 40 (85%) cases. Viral antigen was present as non-cell-associated antigen or antigen associated with endothelial cells or cellular debris in small blood vessels and capillaries in all RVFV cases (Fig. 120) and widespread in most instances (31 of 34). Labelling was also present in vascular smooth muscle cells in 21 of 34 (62%) RVFV positive specimens (Fig. 121). Purkinje fibres were available for examination in 35 of the heart samples. In 22 of these (63%) the Purkinje fibres labelled intensely positive (Fig. 122). Viral antigen was also present in cardiomyocytes in 13 of 34 (38%) positive cases (Fig. 122). Diffuse labelling of the myocardium, not considered to be artefactual immunolabelling, and intense subepi- and endocardial labelling was occasionally observed (Fig. 123). Rarely, viral antigen was also present in capillaries in the pericardial adipose tissue (Fig. 120).

4.4.11 Gastrointestinal tract

Macroscopically, blood or blood-stained mucoid fluid was present in the abomasum. A serosanguineous effusion was often present in the peritoneal cavity. Microscopically, rare foci of necrosis were present in the lamina propria of the small intestine. Cellular debris, likely due to lymphocytolysis of GALT was observed sporadically in the lamina propria of the small intestine. Karyorrhexis was also present in the connective tissue between the Peyer's patches whereas lymphocytes within the Peyer's patches were not affected (Fig. 124).

Viral antigen was present in 8 of 13 cases with specimens from the intestinal tract. Commonly, labelling was present in the vascular endothelial cells of small blood vessels and capillaries in the rumen, abomasum, small intestine and tongue (Figs. 125, 126). Labelling within the lamina propria was more pronounced in the small intestine. Occasional labelling was also present as non-cell-associated antigen or antigen associated with cellular debris in small blood vessels in the muscularis mucosa or the serosa. In one case, labelling was also observed in vascular smooth muscle cells in a small blood vessel in the serosa. In another case, fine diffuse labelling

was present throughout all layers of the small intestine including the connective tissue adjacent to the serosa and smooth muscle cells in the tunica muscularis. Positively labelled cellular debris was also present in the lumen of the small intestine in this case and in the rumen of another case.

Viral antigen was present as non-cell-associated antigen or antigen associated with endothelial cells or cellular debris in the small blood vessels of 4 of 4 (100%) cases with tongue specimens. In two of these cases, fine diffuse labelling was present in the connective tissue and in the skeletal myofibres (Fig. 126).

4.4.12 Skin

Only 2 samples were available for histological examination of which one was positive for RVFV antigen. Labelling was prominent in vascular endothelial cells or cell debris in capillaries (Fig. 127). There was also diffuse viral antigen in the epidermis.

In the case where the skin sample was RVFV antigen negative, all the other available visceral organs from the foetus (liver, spleen, lymph node, thymus, kidney, lung, heart and intestines) also tested negative. However, samples from the placenta and visceral organs of the ewe (liver, gall bladder, spleen, lymph node, kidney, adrenal, lung, and skin) were positive while the uterus specimen was negative.

4.4.13 Nervous system

Other than oedema, no lesions were present in any tissues from the central nervous system. Labelling was present in capillaries and small blood vessels of the meninges in 22 of 29 (76%) cases either as non-cell-associated antigen or antigen associated with vascular endothelial cells or cellular debris (Figs. 128, 129). Occasionally, viral antigen was present in vascular smooth muscle cells (3 of 11; 27%) or in capillaries in the white or grey matter but never within the brain parenchymal cells (Fig. 130). Peripheral nerve bundles, occasionally encountered in tissue sections, had viral antigen in the capillaries. However, antigen was absent from nerve fibres (Figs. 123, 126).

Panel 23: Figures 124-130. Rift Valley fever virus, intestinal tract, skin and brain, sheep foetuses.

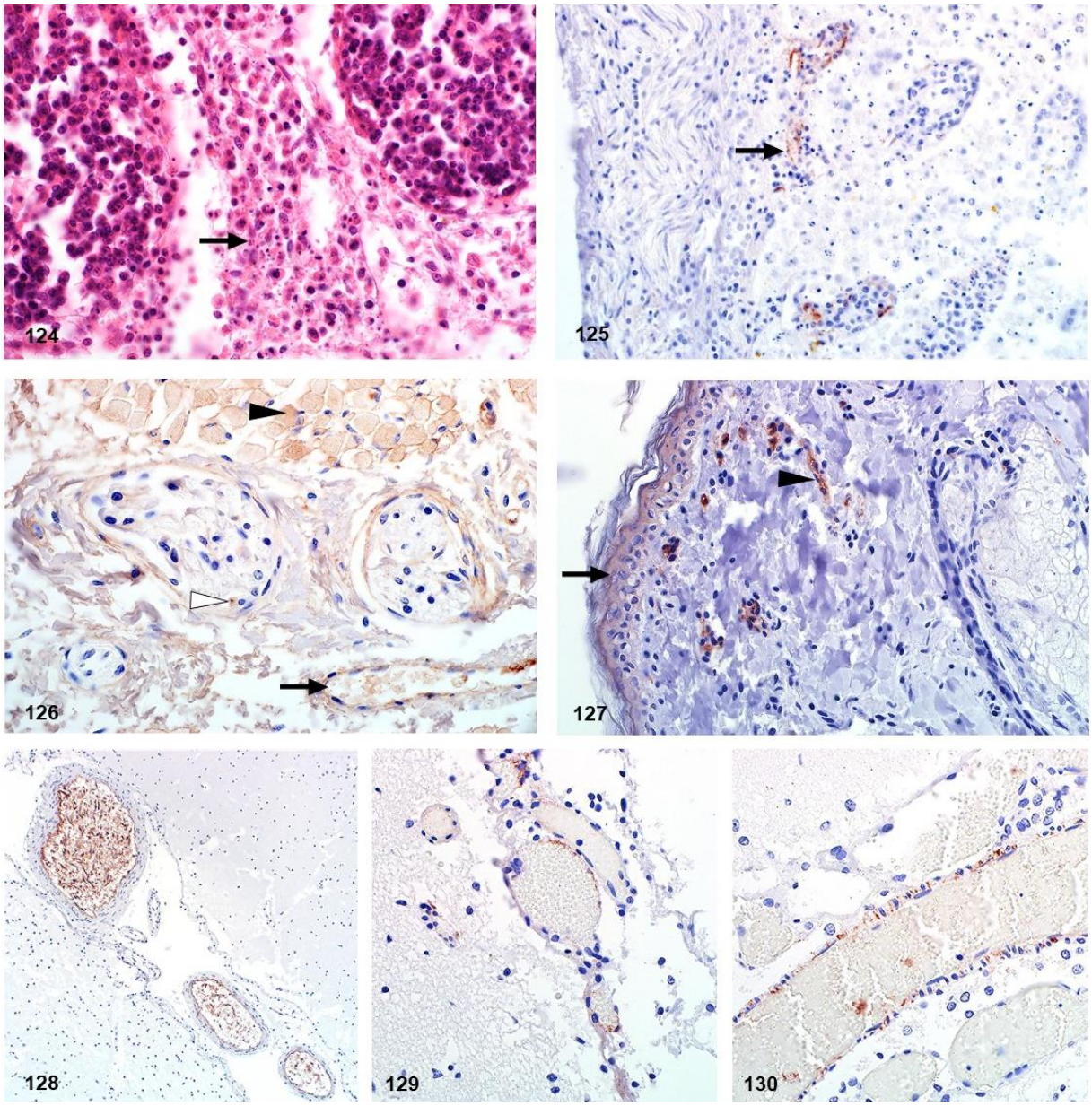

Figure 124. Case 4. Ileum. Lymphocytolysis (arrow) in the lamina propria between the Payer's patches. HE. **Figures 125-130.** IHC for RVFV. **Figure 125.** Case 16. Small intestine. Viral antigen in capillaries in the lamina propria **Figure 126.** Case 47. Tongue. Labelling in vascular endothelial cells (arrow) and in skeletal muscle fibres (arrowhead). Viral antigen is likely absent from nerve fibres in the nerve bundles and instead in the capillaries (white arrowhead). IHC for RVFV. **Figure 127.** Case 3. Skin. Diffuse labelling in the epidermis (arrow). There is also viral antigen present in the capillaries of the dermis (arrowhead). **Figure 128.** Case 4. Meningeal blood vessels. Intense labelling of cellular debris in the blood vessels. **Figure 129.** Case 35. Meningeal blood vessels. Viral antigen in endothelial cells **Figure 130:** Case 35. Meningeal blood vessels. Viral antigen in smooth muscle cells.

4.4.14 Placenta

Macroscopically, there was intercotyledonary oedema and the placentomes were congested and necrotic (Fig. 131). Oedema was confirmed microscopically and was prominent in the cotyledonary allantochorion (Fig. 132). The most significant histological lesion however, was necrosis of trophoblasts and endothelial cells in both the cotyledonary and intercotyledonary allantochorion (Figs. 133, 134). In the cotyledonary villi, necrosis of trophoblasts was generally diffuse with multifocal cellular debris present between the villi (Fig. 133). Other histological changes in the placenta, possibly normal physiological changes, included haemorrhage and mineralization. In the RVFV positive cases, haemorrhage was present in 8 of 26 (31%) placenta specimens with matching foetal tissues and 4 of 5 (75%) placenta specimens where other maternal tissues were available but no foetal tissues. Multifocal haemorrhage was most often adjacent to chorioallantoic villi (10 of 12). Occasionally haemorrhage was present in the myometrium (3 of 9) or the perimetrium (1 of 4). Course blue granules, possible mineral, was present in multiple single trophoblasts or aggregates of trophoblasts in the chorioallantoic villi in 9 of 31 (26%) cases. Occasionally, a blue finely granular to amorphous material was present in the chorioallantoic villi (4 of 30) that was possibly glycosaminoglycans or mineral and was considered to be a normal physiological change. Intravascular cellular debris and severe congestion were often present. Necrotizing vasculitis was rare (n = 1) and there were no thrombi in any of the placenta specimens.

RVFV antigen was present in 28 of 31 (90%) RVFV positive foetus and ewe cases where placenta was available. Labelling was predominantly in trophoblasts and cellular debris in the cotyledonary allantochorion. Most of the viral antigen positive trophoblasts were mononuclear cells, but occasionally binucleate and multinucleated syncytial cells were also positive (Figs. 135, 136). However, not all necrotic trophoblasts were positive for RVFV antigen. Labelling was generally sparse in the intercotyledonary placenta, with rare intercotyledonary trophoblasts positive in 4 of 10 (40%) cases.

Viral antigen was also associated with vascular endothelial cells, intravascular cellular debris or non-cell-associated in 16 of 31 (52%) positive foetus and ewe cases (Fig. 136). Labelling was present in foetal blood vessels in the chorioallantoic membranes in 15 of 26 (58%) available specimens and also prominent in the cotyledonary allantochorion in 4 of these cases. Viral antigen was also present in blood vessels in 3 of 9 (33%) myometrium specimens. Labelling was always absent from the endometrium, squamous mesothelial cells lining the allantoic cavity, and chorionic and allantoic mesenchyme.

In 11 of 58 (19%) foetal cases, all the available organ specimens were IHC negative. Placenta was available for 7 of these cases of which 6 tested IHC positive. In one case, all available foetal organs were negative but the placenta was PCR positive and IHC negative. In this case, only a small portion of the chorioallantoic membrane was available to examine histologically. Karyorrhexis and karyolysis of trophoblasts were present, although only a few could be reliably identified.

Viral antigen was present in the placenta specimens of 6 of 8 RVFV positive adult sheep. For one adult case liver tested negative with both IHC and RT-qPCR but the placenta and the adult kidney labelled positive by IHC. A foetus was not available for testing in this case. In another adult case the liver tested positive but the placenta was negative. For a further 3 adult cases foetal tissues were also available. Liver specimens from the ewes tested positive in all 3 cases. Foetal liver specimens tested positive by RT-qPCR but were IHC negative, and the placenta specimens were IHC positive. Another 2 adult ewes were RT-qPCR and IHC positive. In one case liver was IHC positive but intercotyledonary placenta and uterus specimens that included caruncle were all negative. In the third case maternal liver, kidney, spleen and lung tested IHC positive but the perimetrium, myometrium, endometrium and severely autolysed caruncle containing many trophoblasts were IHC negative.

Histological and immunohistochemical findings in the placenta and uterus are summarized in table 20. Detailed results for the uterus are discussed in Section 2.4.12.

Panel 24: Figures 131-136. Rift Valley fever virus, sheep placenta.

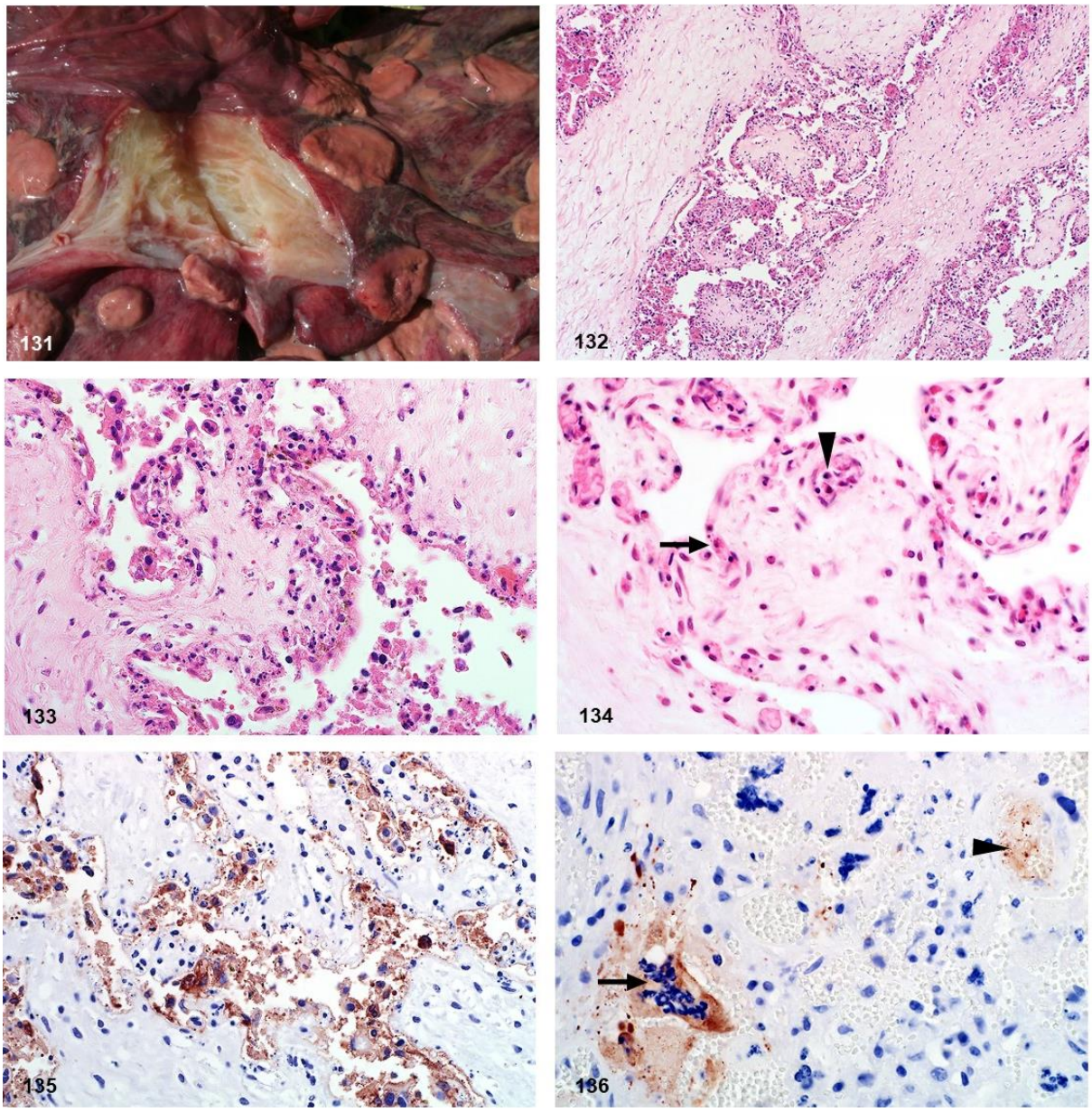

Figure 131. Adult case 46. Marked intercotyledonary oedema and congestion and necrosis of the cotyledons. **Figure 132.** Case 30. Foetal cotyledon. Oedema of the cotyledonary villi (arrows) and cellular debris between the villi. HE. **Figure 133.** Diffuse necrosis of trophoblasts. HE. **Figure 134.** Case 23. Chorioallantoic membrane. Necrosis of chorionic trophoblasts (arrow) and endothelial cells (arrowhead). HE. **Figure 135.** Case 30. Foetal cotyledon. RVFV antigen in trophoblasts and cellular debris. IHC for RVFV. **Figure 136.** Case 15. Maternal caruncle. RVFV antigen in a multinucleated syncytiotrophoblast (arrow) and non-cell-associated viral antigen in a blood vessel (arrowhead). IHC for RVFV.

Table 20. Lesions and immunohistochemical labelling in placenta specimens obtained from ewes and/or foetuses with natural RVFV infection.

	Case number	RVFV infection status	Anatomical section of placenta and/or uterus available for study	Histopathology	Tissues or cells positive by immunohistochemistry
1.	Foetal case 1	PCR[a] and IHC[b] positive.	Section of foetal cotyledon from what had been the hilus of the placentome (hereafter referred to as the hilus) with a portion of the chorioallantoic membrane containing prominent chorioallantoic blood vessels. Adequate chorionic villi, covered by trophoblasts.	Severe diffuse karyorrhexis and karyolysis of trophoblasts covering the foetal vascular mesenchyme of the chorionic villi. Intravascular debris in the large foetal chorionic blood vessels that contain many pyknotic nuclei and nuclear fragments.	Many necrotic trophoblasts in the foetal cotyledon (including binucleated and multinucleated cells). Cellular debris between the chorionic villi in the cotyledon and in apoptotic cells in the cotyledon. Vascular endothelial cells and intravascular cellular debris in the chorioallantoic membrane.
2.	Foetal case 4	IHC positive.	Section of foetal cotyledon from the hilus with a portion of the chorioallantoic membrane containing prominent chorioallantoic blood vessels.	Severe diffuse karyorrhexis and karyolysis of trophoblasts covering the foetal vascular mesenchyme of the chorionic villi. Also, karyorrhexis and karyolysis of trophoblasts covering intercotyledonary chorion.	Many necrotic trophoblasts in the foetal cotyledon (including binucleated and multinucleated cells). Vascular endothelial cells and intravascular cellular debris in the intercotyledonary chorion.

			Sections of intercotyledonary placenta with trophoblast covered villi on the one side (chorion) and squamous mesothelial cells on the allantoic side.	Multifocal haemorrhages (with some consisting of only haemolysed blood and some a combination of haemolysed and non-haemolysed blood) between the chorionic villi in the placentome. Course blue granules, possible mineral, in isolated trophoblasts.	
3.	Negative foetal tissue control 2	PCR and IHC negative.	Sections of intercotyledonary placenta.	Some autolysis and cellular debris. Most trophoblasts covering the chorionic villi appear normal.	None.
4.	Foetal case 8	IHC positive.	Multiple sections of foetal cotyledon from the hilus with a portion of the chorioallantoic membrane with prominent chorioallantoic blood vessels. Adequate chorionic villi included.	Severe diffuse karyorrhexis and karyolysis of trophoblasts covering foetal vascular mesenchyme of the chorionic villi. Moderate oedema of the mesenchyme of the chorionic villi.	Many necrotic trophoblasts in the foetal cotyledon including a few positive binucleate cells.
5.	Foetal case 13	IHC positive.	Mostly intercotyledonary placenta. Tiny section of foetal cotyledon containing chorionic villi. Mostly chorioallantoic membrane from the hilus where it transitions into intercotyledonary placenta.	Karyorrhexis and karyolysis of trophoblasts in both the intercotyledonary placenta and the cotyledon.	Isolated trophoblasts in the foetal cotyledon and in the intercotyledonary placenta.

6.	Foetal case 15 and adult case 46 [c]	PCR and IHC positive.	Full thickness placentome. Maternal caruncle with myometrium (mostly the inner layer and only a small section of outer layer). Foetal cotyledon from the hilus with a small section of the chorioallantoic membrane containing small foetal blood vessels. No perimetrium.	Scattered karyorrhexis and karyolysis of trophoblasts. Multifocal haemorrhage in both the myometrium and between the maternal caruncular villi. Severe congestion as well.	Many necrotic trophoblasts in the placentome at all levels, including binucleated cells and multinucleated syncytial (maternal-foetal hybrid) cells. Small amount of non-cell-associated viral antigen in a few blood vessels in the myometrium. Isolated vascular endothelial cells in the myometrium. Also, cell debris and non-cell-associated virus in capillaries of the villi of the placentome. Maternal organ samples positive for RVFV (liver, kidney, spleen, lung, lymph node).
7.	Foetal case 18 and adult case 54 [c]	PCR and IHC positive.	Full thickness placentome. Maternal caruncle with myometrium (mostly the inner layer). Foetal cotyledon from the hilus with a small section of the chorioallantoic membrane containing small and large chorioallantoic blood vessels. Section of the uterus with myometrium, endometrium, perimetrium and intercotyledonary placenta.	Scattered karyorrhexis and karyolysis of trophoblasts. Mild congestion. Moderate oedema of the foetal mesenchyme especially noticeable in the chorioallantoic membrane.	Many necrotic trophoblasts in the placentome at all levels, including binucleated cells and multinucleated syncytial (maternal-foetal hybrid) cells. Small amount of non-cell-associated viral antigen in a few blood vessels in the myometrium. Also, cell debris and non-cell-associated viral antigen in capillaries of the villi of the placentome.

					Maternal organ samples positive (liver, kidney, uterus).
8.	Foetal case 19 and adult case 55 [c]	PCR and IHC positive.	Full thickness placentome. Maternal caruncle with myometrium (mostly the inner layer). A large sample of intercotyledonary placenta. Also, a section with intercotyledonary placenta opposed to the endometrium. Sections that are likely allantoamnionic membrane.	Severe diffuse karyorrhexis and karyolysis of trophoblasts in the placentome and trophoblasts covering the intercotyledonary placenta. Course blue granules, possible mineral, in scattered trophoblasts. Also possible mineralization in the adventitia of a few blood vessels in the placentome and intercotyledonary placenta.	Isolated necrotic trophoblasts in the intercotyledonary placenta opposed to the endometrium. Small amount of non-cell-associated viral antigen in a few blood vessels in the intercotyledonary placenta and in the myometrium. Also, a few vascular endothelial cells in small blood vessel in the intercotyledonary placenta. None in the allantoamnionic membrane. Maternal organ samples positive (liver, kidney, spleen, lung, intestine).
9.	Foetal case 20	PCR and IHC positive.	Full thickness placentome. Maternal caruncle with myometrium. A large sample of intercotyledonary placenta. Also, a section with intercotyledonary placenta opposed to the endometrium. Sections that are possibly allantoamnionic membrane.	Severe diffuse karyorrhexis and karyolysis of trophoblasts in the placentome and trophoblasts covering the intercotyledonary placenta. Myriads of bacteria, and fungal hyphae in one section of the intercotyledonary placenta.	Many necrotic trophoblasts in the placentome at all levels. Many trophoblasts in the intercotyledonary placenta. Vascular endothelial cells, intravascular cellular debris and non-cell-associated virus in the intercotyledonary chorion. Intravascular cellular debris and non-cell-associated viral antigen in tissues that are possibly allantoamnionic membrane.

10.	Foetal case 23	PCR and IHC positive.	Sections of foetal cotyledons from the hilus with a portion of the chorioallantoic membrane containing large foetal blood vessels. Adequate chorionic villi included.	Severe diffuse karyorrhexis and karyolysis of trophoblasts in both the intercotyledonary placenta and the cotyledon. Multifocal haemorrhages between the chorionic villi. Also, foci of haemolysed blood (tested negative for fibrin). Blue finely granular material, possible mineral, multifocal in the foetal mesenchyme in the cotyledon.	Many necrotic trophoblasts in the cotyledon. No convincing labelling of trophoblasts in the intercotyledonary placenta. Vascular endothelial cells, intravascular cellular debris and non-cell-associated virus in the intercotyledonary chorion. Isolated positive debris in the lumen of small blood vessels on the chorionic side of the chorioallantoic membrane.
11.	Foetal case 29	PCR and IHC positive.	Section of foetal cotyledon. Moderately autolysed.	Severe diffuse karyorrhexis and karyolysis of trophoblasts. Course blue granules, possible mineral, in many trophoblasts. Blue finely granular material, possible mineral, in the foetal mesenchyme of the cotyledon. Severe congestion.	Cellular debris in the cotyledon.
12.	Foetal case 30	PCR and IHC positive.	Section of foetal cotyledon from the hilus with a portion of the chorioallantoic membrane containing large foetal blood vessels. Adequate chorionic villi included.	Severe diffuse karyorrhexis and karyolysis of trophoblasts. Multifocal haemorrhages with haemolysis between the chorionic villi in the placentome.	Many necrotic trophoblasts in the foetal cotyledon (including many binucleated cells). Cellular debris between the chorionic villi in the cotyledon.

					Many round cells with features consistent with apoptosis in the cotyledon. Vascular endothelial cells and intravascular cellular debris in the chorioallantoic membrane.
13.	Foetal case 32	PCR and IHC positive.	Section of foetal cotyledon. No chorioallantoic membrane.	Severe diffuse karyorrhexis and karyolysis of trophoblasts. Course blue granules, possible mineral, in many trophoblasts. Blue finely granular material, possible mineral, in the foetal mesenchyme of the cotyledon.	Scattered necrotic trophoblasts in the foetal cotyledon.
14.	Foetal case 33	PCR and IHC positive.	Section of foetal cotyledon from the hilus with a small portion of the chorioallantoic membrane.	Severe diffuse karyorrhexis and karyolysis of trophoblasts. Moderate oedema of foetal mesenchyme in the cotyledon.	Many necrotic trophoblasts in the foetal cotyledon. A few multinucleated cells and cellular debris between the chorionic villi.
15.	Foetal case 35	PCR and IHC positive.	Section of foetal cotyledon from the hilus with a small portion of the chorioallantoic membrane. Very few chorionic villi included.	Severe diffuse karyorrhexis and karyolysis of trophoblasts. Moderate oedema of foetal mesenchyme in the cotyledon.	A few necrotic trophoblasts in the foetal cotyledon. Vascular endothelial cells and intravascular cellular debris in the chorioallantoic membrane.

16.	Foetal case 40	PCR and IHC positive.	Section of foetal cotyledon from the hilus with a small portion of the chorioallantoic membrane. Adequate chorionic villi included.	Severe diffuse karyorrhexis and karyolysis of trophoblasts. Multifocal haemorrhages with haemolysis (tested negative for fibrin) between the chorionic villi in the placentome.	Many necrotic trophoblasts in the foetal cotyledon. Cellular debris between the chorionic villi.
17.	Foetal case 41	PCR and IHC positive.	Section of foetal cotyledon from the hilus with a small portion of the chorioallantoic membrane. Adequate chorionic villi included.	Severe diffuse karyorrhexis and karyolysis of trophoblasts. Multifocal haemorrhages with haemolysis (tested negative for fibrin) between the chorionic villi in the placentome. Severe oedema of foetal mesenchyme in the cotyledon. Course blue granules, possible mineral, in scattered trophoblasts.	Many necrotic trophoblasts in the foetal cotyledon. Cellular debris between the chorionic villi. Vascular endothelial cells and intravascular cellular debris in the chorioallantoic membrane.
18.	Negative tissue control 6 [c]	PCR and IHC negative.	Section of foetal cotyledon from the hilus with a small portion of the chorioallantoic membrane. Adequate chorionic villi included. Matching maternal organs on the slide.	Mild karyorrhexis and karyolysis of trophoblasts. (Likely normal apoptosis of trophoblasts). Moderate oedema of the chorioallantoic membrane. Multifocal haemorrhage in the chorioallantoic membrane with haemolysed blood clots.	None. Organs from the ewe also negative for RVFV.

19.	Foetal case 43	PCR and IHC positive.	Poor sample. Gravel in the sample caused severe fragmentation of the tissues during cutting. Only small pieces of chorionic villi recognizable.	Severe diffuse karyorrhexis and karyolysis of trophoblasts.	Many necrotic trophoblasts in the bits and pieces of foetal cotyledon.
20.	Negative foetal tissue control 8	PCR and IHC negative.	Section of foetal cotyledon from the hilus with a small portion of the chorioallantoic membrane. Adequate chorionic villi included.	Severe diffuse karyorrhexis and karyolysis of trophoblasts. Multifocal haemorrhages between the large foetal arteries in the chorioallantoic membrane just above the chorionic villi.	None.
21.	Negative foetal tissue control 9	PCR and IHC negative.	Section of foetal cotyledon from the hilus with a small portion of the chorioallantoic membrane. Adequate chorionic villi included.	Severe diffuse karyorrhexis and karyolysis of trophoblasts. Myriads of small coco-bacilli between the villi.	None.
22.	Foetal case 45	PCR and IHC positive.	Section of foetal cotyledon from the hilus with a small portion of the chorioallantoic membrane. Adequate chorionic villi included.	Severe diffuse karyorrhexis and karyolysis of trophoblasts. Severe oedema of the chorioallantoic membrane and foetal mesenchyme in the cotyledon.	Many necrotic trophoblasts in the foetal cotyledon. Cellular debris between the chorionic villi. Vascular endothelial cells and intravascular cellular debris in the chorioallantoic membrane

23.	Foetal case 46	PCR negative and IHC positive	Section of foetal cotyledon from the hilus with a small portion of the chorioallantoic membrane. Adequate chorionic villi included.	Scattered karyorrhexis and karyolysis of trophoblasts. Severe oedema of the foetal mesenchyme in the cotyledon.	Isolated necrotic trophoblasts in the foetal cotyledon.
24.	Foetal case 47	PCR negative and IHC positive.	Section of foetal cotyledon from the hilus with a small portion of the chorioallantoic membrane. Adequate chorionic villi included.	Severe diffuse karyorrhexis and karyolysis of trophoblasts. Severe oedema of foetal mesenchyme in the cotyledon. Course blue granules, possible mineral, in many trophoblasts. Blue finely granular material, possible mineral, in the foetal mesenchyme of the cotyledon.	Many necrotic trophoblasts in the foetal cotyledon. Cellular debris between the chorionic villi. Vascular endothelial cells and intravascular cellular debris in the chorioallantoic membrane.
25.	Foetal case 48	Only placenta PCR positive. All foetal tissues IHC negative.	Only a small portion of the chorioallantoic membrane.	Myriads of small coccoid bacteria.	None. Inadequate sample.
26.	Foetal case 51	IHC positive.	Section of foetal cotyledon from the hilus with a small portion of the chorioallantoic membrane. Very few chorionic villi included.	Severe diffuse karyorrhexis and karyolysis of trophoblasts. Severe oedema of foetal mesenchyme in the cotyledon and the chorioallantoic membrane.	Isolated necrotic trophoblasts in the foetal cotyledon.

				Widespread proliferation of small coccoid bacteria.	
27.	Foetal case 52	IHC positive.	Section of foetal cotyledon from the hilus with a small portion of the chorioallantoic membrane. Adequate chorionic villi included. A lot of intercotyledonary placenta.	Severe diffuse karyorrhexis and karyolysis of trophoblasts. Many trophoblasts show marked cell swelling. Multifocal haemorrhages between the chorionic villi.	Scattered necrotic trophoblasts in the foetal cotyledon labelling. Most of the necrotic trophoblasts not labelling. Isolated vascular endothelial cells and intravascular cellular debris in the chorioallantoic membrane.
28.	Foetal case 53	PCR and IHC positive.	Section of foetal cotyledon from the hilus with a small portion of the chorioallantoic membrane. Also, a section of intercotyledonary placenta.	Severe diffuse karyorrhexis and karyolysis of trophoblasts. Severe oedema of foetal mesenchyme in the cotyledon and the chorioallantoic membrane.	Many necrotic trophoblasts in the foetal cotyledon labelling. Cellular debris between the chorionic villi. Also, many necrotic trophoblasts in the intercotyledonary placenta.
29.	Foetal case 54	PCR and IHC positive.	Section of foetal cotyledon from the hilus with a small portion of the chorioallantoic membrane.	Severe diffuse karyorrhexis and karyolysis of trophoblasts. Multifocal haemorrhages between the chorionic villi. Severe oedema of foetal mesenchyme in the cotyledon. Also, moderate congestion of the tissues.	Many necrotic trophoblasts in the foetal cotyledon labelling. Cellular debris between the chorionic villi. Vascular endothelial cells and intravascular cellular debris in the chorioallantoic membrane and in the chorionic villi.

30.	Foetal case 58	PCR and IHC positive.	Section of foetal cotyledon from the hilus with a small portion of the chorioallantoic membrane.	Severe diffuse karyorrhexis and karyolysis of trophoblasts.	Many necrotic trophoblasts in the foetal cotyledon labelling. Cellular debris between the chorionic villi. Vascular endothelial cells and intravascular cellular debris in the chorioallantoic membrane.
31.	Adult case 8 [d]	Placenta IHC negative. Other tissues PCR and IHC positive.	Section of the uterus with perimetrium, myometrium and endometrium. Epithelium of the endometrium mostly lost in processing. Section of maternal caruncle with myometrium and a few chorionic villi included. Small section of intercotyledonary placenta. Other foetal tissues not available.	Mild karyorrhexis and karyolysis of some trophoblasts. Most trophoblasts appear normal. Multifocal haemorrhages between the villi in the placentome. Severe oedema of the chorionic villi.	None in the placenta or the uterus. Many adult sheep tissues positive (liver, spleen, lung, adrenal, skin, lymph node).
32.	Adult case 40 [d]	Placenta IHC negative. Other tissues PCR and IHC positive.	Section of the uterus with perimetrium, myometrium and endometrium. Very autolysed and congested section of caruncle with some trophoblasts remaining.	Karyorrhexis and karyolysis of trophoblasts. Multifocal haemorrhages between the villi and course blue granules, possible mineral, in many trophoblasts.	None in placenta. Other adult sheep tissues positive (liver, kidney, spleen, lung).
33.	Adult case 42 [d]	PCR and IHC positive.	Section of the uterus with perimetrium, myometrium and endometrium.	Multifocal haemorrhages in the myometrium and perimetrium.	Many necrotic trophoblasts. Also, many binucleates and multinucleated trophoblasts.

			Section of maternal caruncle with myometrium and a few chorionic villi included. Section of foetal cotyledon from the hilus with a small portion of the chorioallantoic membrane.	Moderate to severe (differs between sections) karyorrhexis and karyolysis of trophoblasts. Severe congestion of placentome tissue. Course blue granules, possible mineral, in many trophoblasts.	The only adult tissue that was positive was kidney (liver heart, lung, spleen and uterus negative). Vascular endothelial cells and intravascular cellular debris in the chorioallantoic membrane and chorionic villi.
34.	Adult case 43 [d]	PCR and IHC positive.	Section of maternal caruncle with myometrium and a few chorionic villi included	Severe diffuse karyorrhexis and karyolysis of trophoblasts.	Scattered necrotic trophoblasts positive. Many adult sheep tissues positive (liver, spleen, kidney lung).
35.	Adult case 47 [d]	PCR and IHC positive.	Section of the uterus with myometrium and endometrium. Perimetrium lost. Section of placentome with many chorionic villi. Section of intercotyledonary placenta.	Multifocal haemorrhages in the myometrium. Severe diffuse karyorrhexis and karyolysis of trophoblasts.	Scattered necrotic trophoblasts positive. Many necrotic cells not labelled.

a RT-qPCR on fresh tissues. b Immunohistochemistry on formalin-fixed paraffin-embedded tissues. c Foetus that had matching maternal tissues and placenta specimens (n = 4). d Tissues from adult animals that included placenta and in some cases uterus (n = 5)

4.5 Discussion

Infection with RVFV has a wide variety of outcomes for both ewes and foetuses and limited information is available concerning the lesions in foetal organs, including the placenta. Therefore, the principle aim of this study was to summarize gross, histopathological and immunohistochemical findings and evaluate the diagnostic utility of different tissues and specific histologic features of RVFV in foetuses and the placenta. A further aim was to compare the distribution of viral antigen in foetal organs and cells with previous results in adult sheep and young lambs from the same outbreak (Chapter 2 and 3). As with the results for the adult sheep and the young lambs, a limitation of this study is that the frequencies of lesions and immunolabelling could be an overestimate of the general population of RVF cases. This is due to the fact that organs were not consistently sampled in these field cases and non-specific macroscopic lesions in most foetal organs might have exacerbated this shortcoming. Another limitation was that the stage of gestation or the length of foetuses was not known and usually foetuses could not be paired with the dams or placentas. It was not uncommon for multiple dead ewes, lambs, foetuses and the occasional placenta from the same flock to be presented for necropsy on the same day. In the present study, only four foetuses could be matched with the dam and a placenta specimen.

In the 2010-2011 RVFV outbreak in South Africa, farmers typically reported the near simultaneous abortion of large numbers of pregnant ewes. This was accompanied by dystocia, the death of up to 100% of young lambs, and the deaths of a significant number of adult ewes. Some pregnant ewes were found dead or died after having aborted. Other pregnant ewes aborted without showing clinical signs and recovered. During the outbreak in Kenya in 1931, it was reported that the ewes had been bred to lamb in July and August and that abortions started to occur in the latter part of June (Daubney et al., 1931). By mid-July there was a marked increase in the number of abortions on the farm and also high mortality of ewes with coincident high mortality in lambs (Daubney et al., 1931). By the end of July mortality in ewes and lambs was more extensive but abortions among the ewes had almost ceased with the situation much

the same by mid-August (Daubney et al., 1931). Ewes were either found dead without having shown symptoms or succumbed a few hours after having a mucopurulent nasal discharge, inappetence and occasional vomition and haematochezia. Some ewes that aborted however, were not visibly ill with the exception of a few that developed metritis or peritonitis. Additional experiments demonstrated that abortion was also a common sequel to recovery in pregnant animals (Daubney et al., 1931). In an experimental study in the Netherlands to determine the susceptibility of pregnant animals (n = 11) of a native breed of sheep to RVFV, 3 of 4 ewes infected in the third trimester had to be euthanized due to severe clinical signs and 1 of 3 ewes in the second trimester of gestation died (Antonis et al., 2013). Four other ewes in the study, euthanized on 21- and 23-days post-infection, did not develop clinical signs or viraemia but post-mortem examination revealed one dead foetus in a third trimester ewe, and live twin foetuses in the uterus of 2 first trimester ewes and one second trimester ewe. In 2 of 4 first trimester ewes euthanized at 22 days post-infection, there were remnants of gestation in the uterus (Antonis et al., 2013). The study was terminated and all the surviving ewes (7 of 11) euthanized at 21-23 days post-infection. Therefore, it is unknown how many of the ewes may have aborted and survived the infection. However, it would seem from the data provided by Daubney et al. and the experiment by Antonis et al. that ewes in the later stages of pregnancy are more susceptible to lethal disease and might die before aborting whereas ewes in the earlier stages of pregnancy might abort or resorb the foetus and survive the infection. However, additional studies would be needed to validate these speculations.

In the present study, macroscopic lesions in foetuses with RVF were non-specific and autolysis was categorised as mild or moderate in most cases (84 of 99; 86%). Similar observations were made in other field cases and in experimental studies (Antonis et al., 2013, Baskerville et al., 1992, Daubney et al., 1931). In a trial of a RVFV vaccine candidate, it was reported that none of 7 foetuses recovered from 4 ewes infected with the virulent strain of RVFV had gross lesions (Baskerville et al., 1992). Autolysis was also described as insufficient to impair examination of tissues histologically. Another study examining the susceptibility of pregnant sheep to a strain

of virus from the 1974 RVF outbreak in the Free State province of South Africa reported that macroscopic lesions were absent in 18 foetuses recovered and autolysis was present in 6 of 12 foetuses that had died in-utero (Antonis et al., 2013). Since the lungs of at least 6 of 58 foetuses in the present study were aerated, seemingly some RVFV-infected ovine foetuses might be born alive. Therefore, a significant number of pregnant ewes infected with RVFV might expel a foetus without severe autolysis. Additionally, in endemic areas a differential diagnosis of RVF in aborted foetuses should always be considered during interepidemic periods even if lesions are absent in the foetus and the ewe does not show any clinical signs.

In agreement with the present study, fetal malformations have not been reported in natural cases of RVF or in experimental cases using wild-type virus (Antonis et al., 2013, Baskerville et al., 1992, Daubney et al., 1931). However, a number of live-attenuated RVF vaccine stains cause fetal malformations of the central nervous system and the musculoskeletal system. The MP 12 vaccine strain administered during the first (28, 35 and 42 days) and second trimester (49 and 56 days) of pregnancy was reported to cause spinal hypoplasia, hydranencephaly, brachygnathia inferior and arthrygryposis (Hunter et al., 2002). An overdose of Clone 13 vaccine strain (6.8 $\log_{10}$ $TCID_{50}$, s.c.) administered during the first trimester of pregnancy caused malformation in 7 of 20 foetuses that included hydranencephaly, hypoplasia of the cerebrum, cerebellum, and spinal cord, brachygnathia, arthrogryposis and scoliosis (Makoschey et al., 2016). Vaccination of ewes between 42 and 74 days of pregnancy with the Smithburn attenuated RVF virus resulted in abortion and arthrogryposis, hydranencephaly or micrencephaly in 3 of 7 fetuses (Coetzer and Barnard, 1977). Therefore, natural RVFV infection is not on the list of differential diagnoses when fetal malformations are encountered. However, ill-advised use of live attenuated vaccines in ewes in the first or second trimester of pregnancy should be investigated if fetal malformations are reported.

Microscopically, necrotizing hepatitis with primary lytic foci and eosinophilic intranuclear inclusions in hepatocytes were useful diagnostic features in foetuses, but were not present in all cases in the present study. Liver lesions were absent in 10 of 58 (17%) cases, and were

subtle in another 10 of 58 (17%) cases. However, in most of the cases where necrosis was present, either primary foci or intranuclear inclusions were also present (43 of 48; 90%) with intranuclear inclusions present in 62% of foetal liver specimens. Cases where both primary foci and intranuclear inclusions are absent might present a diagnostic challenge if other specimens, particularly foetal cotyledon or maternal caruncle, are not available. There were 4 such cases identified in this study. Additionally, absence of necrosis, primary foci or nuclear inclusions in the liver does not necessarily exclude a diagnosis of RVF.

Whereas intranuclear inclusions were detectable in HE stained sections in 62% of foetal liver specimens, it was previously reported that they were present in 38% of young lambs and only in 7% of adult sheep cases (Section 2.4.2 and 3.4.2). Notable, unlike the pleomorphic intranuclear inclusions in mice experimentally infected with RVFV that have variably distinct borders and no or only an equivocal halo, unequivocal inclusions in sheep, including foetuses are rod-shaped or filamentous and have a distinct halo (Ulrich, 2019). Further investigations are needed to clarify why intranuclear inclusions are fairly common in foetuses and neonates but are rarely found in adult animals. Intranuclear inclusions in RVFV-infected hepatocytes are initially ribbon-like structures formed by the nucleus-associated non-structural (NSs) protein of RVFV (Struthers and Swanepoel, 1982, Struthers et al., 1984) The NSs protein counteracts the antiviral interferon (IFN) system by supressing the nuclear activation of the IFN-β gene and the cytoplasmic transcription of interferon mRNAs thereby blocking interferon expression and promoting unrestricted viral replication (Le May et al., 2004, Ikegami et al., 2009b). Additionally, nuclear NSs filaments bind to SAP30 and to Yin Yang 1, forming a multiprotein repression complex on the IFN-β promoter (Le May et al., 2008). The NSs protein also downregulates the activation of PKR, which prevents the phosphorylation of eIF2α (Ikegami et al., 2009b). In the absence of NSs protein efficient viral replication is prevented since phosphorylated eIF2α supresses viral translation. Results of this study concur with those of previous studies in adult sheep and young lambs that have shown that RVF is much more severe in young animals when compared to adult animals (Chapters 2 and 3). Also, it was

semi-quantitatively demonstrated that there is significantly more viral antigen in the tissues of foetuses and young lambs than in adult sheep. We hypothesize that complete or insufficient formation of the NSs protein might be hindered by an unknown mechanism in adult animals, and less so in very young animals and foetuses. Whether increased formation of NSs filaments in the nucleus might result in more severe disabling of the antiviral interferon response and therefore much higher viraemia should be further explored.

The lack of a fully developed adaptive and innate immune system in young or unborn animals may also lead to higher morbidity and mortality in young animals and foetuses than in older animals (Zhao et al., 2008). Previous research demonstrated that neonatal mice exposed to toll-like receptor stimuli (lipopolysaccharide, polyinosinicacid:polycytidylic acid and murine hepatitis virus-A59) suffer from uncontrolled proinflammatory innate responses related to their low numbers of T lymphocytes (Zhao et al., 2008). Additionally, after LPS treatment the proinflammatory cytokines TNF, MCP-1, and IL-6 in serum gradually decrease as the age of the mice increase (Zhao et al., 2008). Large numbers of naive T lymphocytes, present in adult animals, might be required to temper the early innate responses and reduce the secretion of proinflammatory cytokines (Zhao et al., 2008). Moreover, children infected with Dengue haemorrhagic fever virus often have minimal bleeding manifestations but develop severe shock due to excessive plasma leakage and severe depletion of intravascular volume (Wills et al., 2002). In the present study haemorrhages in foetuses were minimal but plasma leakage with effusions in body cavities, accompanied by brain and lung oedema, was very common. Consequently, young or unborn animals might suffer severe microcirculatory dysfunction and shock due to a lack of sufficient numbers of T lymphocytes to keep the proinflammatory innate responses under control.

Other histological lesions in foetuses were generally far subtler than those previously reported in young lambs and adult sheep, and could be easily overlooked (Chapter 2 and 3). Lymphocytolysis was present in all lymphoid organs except for the thymus and Peyer's patches where resident T lymphocytes were unaffected. In the spleen, follicular germinal

centres and mantle zones were undeveloped, deemed to be age-appropriate, and necrosis was generally most obvious in the red pulp. Acute renal tubular injury was rare but nuclear pyknosis and karyorrhexis in the glomeruli, and to a lesser extent in the interstitial capillaries, were useful diagnostic features. Additionally, mild pyknosis and karyorrhexis were often present in the alveolar septa and pulmonary blood vessels.

Foetal liver specimens were not consistently positive for RVFV antigen. It was previously observed for adult sheep and young lambs that most RVFV immunolabelling was in the liver (Chapters 2 and 3). In foetuses, the cotyledon and caruncle seem to be the more reliable specimens for diagnostic testing, with viral antigen present in the trophoblasts of 28 of 30 RVF cases (Table 21). A recent study investigating vertical transmission of RVFV in rats also found that the placenta had a higher viral load than the liver and other maternal organs (McMillen et al., 2018). High levels of infectious virus were obtained from the placenta regardless of the time of infection, and one placenta specimen obtained from a surviving rat on the day of delivery had over 10^9 PFU/ml. The same study also reported that RVFV has a preference for reproductive tissues including the uterus, ovary, placenta, and mammary glands (McMillen et al., 2018). Therefore, in RVFV-infected foetuses or ewes, specimens from the cotyledonary placenta or endometrial specimens (caruncle), if available, are more likely to yield a positive test result than foetal liver samples.

Previous research has shown that brain specimens from foetuses test positive by PCR and virus isolation, more often that the liver (Antonis et al., 2013, Shone, 1958). However, in the present study the heart was more frequently positive by IHC than brain specimens. In the brain viral antigen was most often present in the meningeal blood vessels, occasionally in capillaries in the white or grey matter but never within brain parenchymal cells. In the heart, viral antigen was often present in myocardial Purkinje fibres, cardiomyocytes and vascular smooth muscle cells. It was previously reported that labelling was occasionally present in these cells in young lambs whereas in adult sheep viral antigen was only sporadically found in vascular smooth muscle cells and never in cardiomyocytes or myocardial Purkinje fibres (Chapters 2 and 3).

We therefore recommend that heart samples should be collected in studies involving foetuses or very young lambs and when specimens from the brain are collected these must include meninges.

Remarkably high viraemias of $10^{8.33}$ RNA copies per gram in the liver using RT-qPCR, and $10^{6.2}$ virus per gram in the placenta using the mouse lethal doses technique have been reported in foetuses, and in the present study viral antigen was present in capillaries and blood vessels as non-cell-associated virus or within vascular endothelial cells (Easterday et al., 1962b, Antonis et al., 2013). Viral antigen also appeared to have diffused into the capsule and connective tissue stroma of organs in some foetuses giving the impression that transudates in the thorax and abdomen might have contained extremely high viral loads. A study in rats demonstrated RVFV in the amniotic sac (McMillen et al., 2018). Therefore, the amniotic fluid might contain high viral loads in some cases. Further support for this included diffusely present viral antigen in the epidermis of one foetus. However, further studies are needed to investigate if these assertions are accurate.

Table 21. Preferred foetal diagnostic specimens for investigation of RVF using histopathology and immunohistochemistry.

Diagnostic specimen in order of importance	Recommended number of samples and location	Justification
Cotyledon or caruncle	At least one section	Severe, diffuse karyorrhexis and karyolysis of trophoblasts. RVFV antigen is prominent in trophoblasts but often also present as non-cell-associated antigen or antigen associated with endothelial cells or cellular debris in placental or endometrial blood vessels.
Liver	Sections from at least two liver lobes	Random necrotizing hepatitis with dropout of hepatocytes from the reticulin framework of variable severity. Multifocal liquefactive hepatic necrosis (primary foci) and eosinophilic intranuclear inclusions. Fine diffuse to coarse granular labelling in the cytoplasm of necrotic hepatocytes and in cytoplasmic fragments in most cases. Sections from different areas in the liver may differ, with one section having primary foci and another having none.
Spleen	At least one section with capsule	Typically, lymphocytolysis, is most apparent in the red pulp. RVFV antigen is particularly prominent in cellular debris in the red pulp and in vascular smooth muscle cells and endothelial cells in small blood vessels in both the capsule and the parenchyma.
Kidneys	One section that includes both cortex and medulla	Pyknosis and karyorrhexis in glomeruli in most cases. Viral antigen is prominent in mononuclear, vascular smooth muscle, vascular endothelial and juxtaglomerular and extraglomerular mesangial cells.

4.6 Conclusion

Although many species are susceptible to RVFV infection, sheep are often the most severely affected. This is particularly true for pregnant sheep. RVFV infection in pregnant ewes causes a wide variety of outcomes for both ewes and foetuses and it may be impossible to exclude RVF from the list of possible differential diagnoses even if sampling is adequate. Some ewes show no clinical signs, do not seroconvert and do not have a detectable viraemia (Antonis et

al., 2013). Macroscopic lesions in most foetuses are also absent or non-specific. Microscopically, the liver often has characteristic lesions but in a small percentage of cases the necrosis can be mild and diagnostic features such as primary foci and inclusion bodies might be absent.

RVFV antigen-positive cells included hepatocytes, renal tubular epithelial cells, juxtaglomerular cells and extraglomerular mesangial cells, vascular smooth muscle and endothelial cells, skeletal muscle cells, cardiomyocytes, myocardial Purkinje fibres, adrenocortical cells, macrophages and occasionally neutrophils. However, cotyledonary placenta or endometrial samples are often positive whereas the foetal organs might be negative for viral antigen. Therefore, for routine histopathology and IHC, liver specimens should be examined together with specimens from at least the cotyledonary placenta with foetal spleen and kidney being useful additional samples. If available, specimens from the endometrium (caruncle) are also very useful. Additional testing should be performed in endemic areas even if histological lesions are absent and RVFV IHC is negative. It is recommended that if testing using PCR is contemplated, samples tested should include heart in addition to liver and brain since heart was positive by IHC more frequently than the brain in the present study. However, even when multiple samples are tested using multiple techniques and a negative result is obtained, RVF should remain a differential diagnosis when more abortions occur in endemic areas.

CHAPTER 5

INVESTIGATIONS INTO LYMPHOCYTOLYSIS, KIDNEY LESIONS AND THROMBOSIS IN NATURAL RIFT VALLEY FEVER VIRUS INFECTION

5.1 Summary

A number of interesting questions regarding the pathogenesis of RVFV in the kidney and lymphoid organs were raised in the preceding chapters. Lymphocytolysis appeared to be more prominent in the B-cell rich areas of lymphoid organs. To investigate this further, immunohistochemistry was performed on samples from RVFV infected sheep using anti-CD3 and anti-CD20 antibody. A marked reduction in the numbers of B and T lymphocytes were demonstrated in both the red and the white pulp areas of the spleen. B lymphocyte areas were collapsed and many more T cells than normally expected were present in the collapsed germinal centres. It should be investigated if lymphocyte subsets decrease simultaneously or if B lymphocytes are affected more severely initially with a drop in T lymphocytes later in the course of fatal disease. In kidney specimens, the Jones' methenamine silver stain demonstrated a decrease in mesangial cellularity and pyknosis and karyorrhexis of vascular endothelial cells in the glomeruli and interstitial capillaries. There was no disruption of basement membranes. The Masson trichrome and periodic acid-Schiff stains confirmed a decrease in mesangial cellularity. Possible hypoxia related to hypotension plays a role in the development of this lesion. Lastly, convincing platelet-fibrin thrombi could not be demonstrated in any of the tissues examined, using the Martius scarlet blue trichrome stain. Fibrinolysis and the formation of fibrin thrombi might occur concomitantly in RVFV infection so that thrombosis does not occur. The results presented here, using the RVF natural disease case material, should inform future RVFV pathogenesis study design into the role of lymphocytes, development of kidney pathology and aspects of coagulopathy during RVFV infection.

5.2 Introduction

In chapter 2, necrosis in the spleen of adult sheep was reported. Lymphocytolysis identified on HE stained sections was most prominent in the B-cell rich areas of lymphoid organs, suggesting the preferential targeting of B lymphocytes. Further examination of lymphocyte subsets with cell surface markers might provide more insight into this lesion

Multifocal acute renal tubular injury (nephrosis) was present in most of the adult sheep and scattered pyknotic and karyorrhectic nuclear and cellular debris was present in the glomeruli (Chapter 2). Pyknosis and karyorrhexis of cellular elements in the glomerulus can be immune complex–mediated, characterized by mesangial hypercellularity with thickening of the basement membranes, double contours of the walls of the capillary loops and increased leukocytes (Cianciolo et al., 2016, Rao et al., 2006). Further examination of the kidney with histochemical stains that highlight basement membranes and capillary loops in glomeruli may provide more insight into this lesion.

There was also no convincing evidence of microvascular fibrin thrombi in any organ in HE stained sections. Their absence may be attributed to hyperfibrinolysis or enhanced-fibrinolytic-type disseminated intravascular coagulation, which has been described in Dengue haemorrhagic fever (Marchi et al., 2009, Asakura, 2014). The formation of fibrin thrombi might be inhibited by increased clot lysis causing widespread bleeding. However, application of histochemical stains that reveal the presence of fibrin thrombi may confirm or disprove the observations made previously in HE stained sections.

5.3 Materials and methods

Convenience sampling was used to select RVFV infected cases to study. The selected FFPE tissues had minimal acid haematin and autolysis and demonstrated the lesion of interest. Fourteen kidney specimens from RVFV infected adult sheep, with varying degrees of nephrosis and glomerular pyknosis and karyorrhexis, were selected. Additionally, 10 spleen specimens with known lymphocytolysis were selected to study lymphocyte subsets. Lymph

node specimens from 2 cases and kidney specimens from 3 cases were also in the tissue blocks that contained the spleen.

Tissue sectioning and staining with HE, Martius scarlet blue trichrome (MSB), Jones' methenamine silver (JMS), Masson trichrome (MT) and periodic acid-Schiff stain (PAS) of FFPE tissues were done according to the standard operating procedures of the Section of Pathology, Department of Paraclinical Sciences, Faculty of Veterinary Science, University of Pretoria. These histochemical stains were chosen to preferentially stain basement membranes, the mesangium of glomeruli and the tubulointerstitium. Negative tissue controls included tissues from two uninfected sheep. Positive controls for the histochemical and immunohistochemical tests described next were those routinely used in the Section of Pathology (e.g. a case of canine babesiosis with fibrin in the kidney and lymph nodes for the MSB).

T and B lymphocytes were identified by IHC using polyclonal rabbit anti-CD3 antibody (A0452, DakoCytomation, Glostrup, Denmark) and polyclonal rabbit anti-CD20 antibody (PA5-16701, ThermoFisher Scientific, Illinois, USA) at 1:600 and 1:800 dilutions respectively. Blocking of endogenous peroxidases was followed by either microwave heat epitope retrieval in citrate buffer (pH 6.0) at 96 °C for 14 min and incubation with anti-CD3 for 1 hour at room temperature or similar retrieval in Tris-EDTA buffer (pH 9.0) at 96 °C for 21 min and incubation with anti-CD20 for 2 hours. For both antibodies rabbit specific horseradish peroxidase micro-polymer detection kit with 3,3'-diaminobenzidine (DAB) chromogen (ab236466, Abcam, Massachusetts, USA) and haematoxylin counterstaining were used to visualize labelled cells according to the instructions of the manufacture.

5.4 Results

5.4.1 Further investigation of lymphocytolysis

Anti-CD3 and anti-CD20 immunohistochemistry demonstrated a marked difference in the morphology of the spleen in a normal sheep (Figs. 137, 138, 139) when compared to RVFV

infected sheep (Figs. 141, 142, 144, 145). The numbers of B and T lymphocytes in the spleen were visibly reduced in both the red and the white pulp in RVFV infected cases. B lymphocyte areas had collapsed in 7 of 10 (70%) of the specimens and there was an abnormal distribution of T lymphocytes in the white pulp. Many more T cells than normally expected were present in the collapsed germinal centres. It was not possible to accurately categorise lymphocyte depletion as mild, moderate or severe in either B cell or T cell areas. The antibodies also cannot differentiate between viable lymphocytes and dead or dying lymphocytes. Germinal centres were often necrotic (8 of 10; 80%) (Figs. 140, 143) and the remaining cellular debris was often anti-CD20 positive (Figs. 142, 145).

5.4.2 Further investigation of the glomerular damage

The JMS stain (Figs. 146, 147, 148, 149) was the most informative of the histochemical stains applied to the kidney in demonstrating a decrease in mesangial cellularity. Interestingly, the stain also showed that there was no disruption of basement membranes.

Pyknosis and karyorrhexis were present in the glomeruli and in the interstitium in 12 of 14 (86%) cases tested. In 5 of 14 (36%) kidney specimens there was pyknosis and karyorrhexis of vascular endothelial cells in the glomeruli and interstitial capillaries (Fig. 147) with a mild to moderate decrease in the cellularity of the mesangium (Figs. 147, 148). Severe necrosis of mesangial cells with a marked decrease in the cellularity of the mesangium was present in 6 of 14 (43%) cases (Fig. 149). Both the PAS and MT stains confirmed a decrease in mesangial cellularity (Figs. 150, 151, 152, 153).

Interestingly, anti-CD3 and anti-CD20 labelled debris was present in the glomerular capillaries of 2 of 3 specimens.

5.4.3 Further investigation concerning fibrin formation

None of the spleen or lymph node specimens (Figs. 154, 155, 156, 157) or kidney specimens (Fig. 158, 159, 160, 161) had convincing platelet-fibrin thrombi with the MSB stain. However, small amounts of fibrin-like material (Fig. 161) were present in the capillaries of 5 of 14 (36%) of the kidney cases.

Panel 25: Figures 137-145. Spleen, adult sheep. Sequentially sections stained with HE and incubated with anti-CD3 and anti-CD 20 antibodies for T and B lymphocytes.

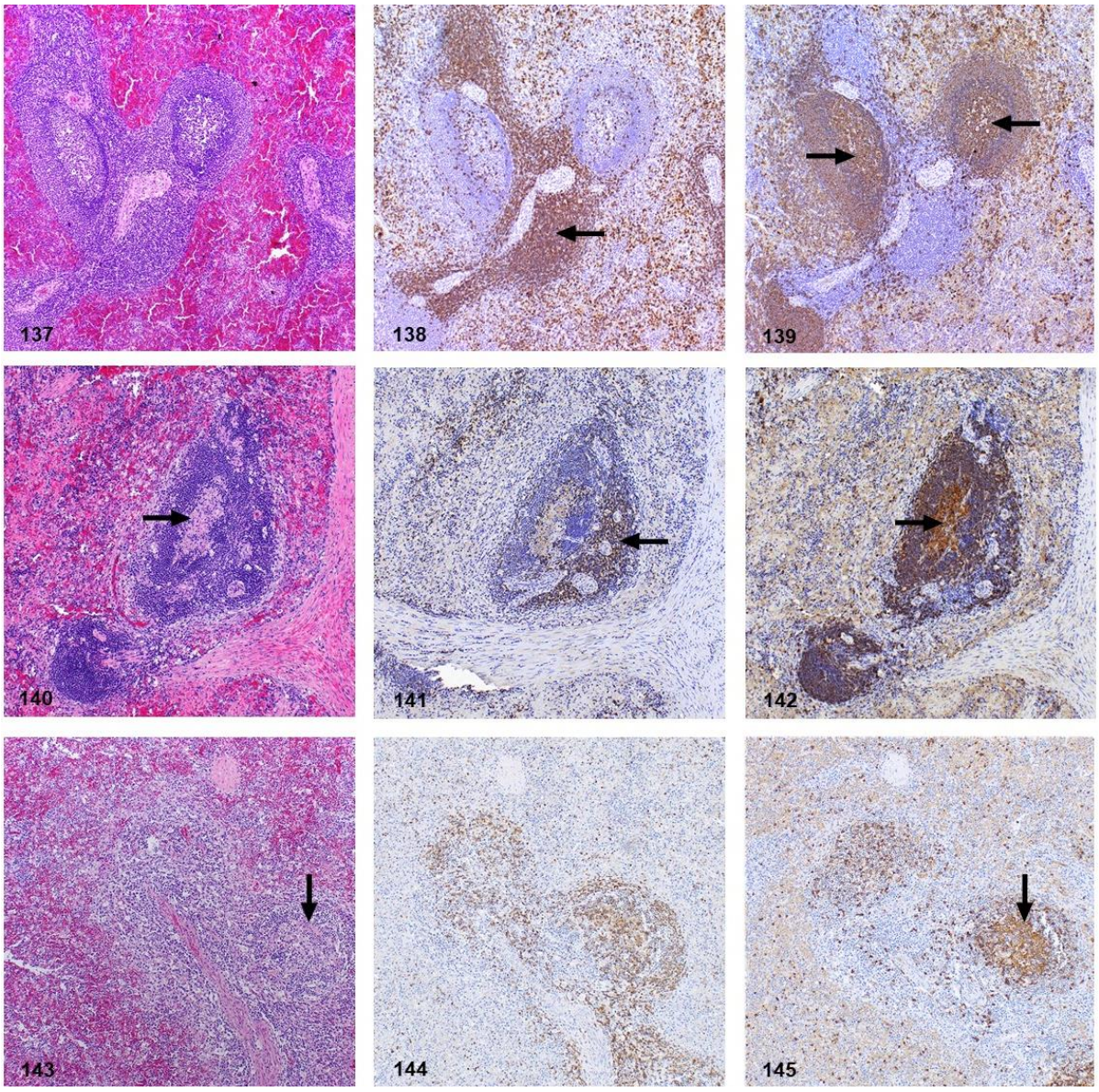

Figures 137-139. Sequential spleen sections from an uninfected control sheep. **Figure 137.** Normal morphology of the white pulp. HE. **Figure 138.** PALS with many T lymphocytes (arrow). Anti-CD3 IHC. **Figure 139.** Splenic germinal centres (arrows) containing many B lymphocytes. Anti-CD20 IHC. **Figures 140-145.** Case 55. Sequential spleen sections from a RVFV infected sheep. **Figure 140.** Necrosis in a germinal centre (arrow). HE. **Figure 141.** Scattered T lymphocytes in the red pulp and moderate depletion of the PALS (arrow). Anti-CD3 IHC. **Figure 142.** Anti-CD20 positive necrotic debris in a germinal centre (arrow) with many B lymphocytes in the mantle layer, marginal zones, peripheral zones of the PALS and in the red pulp. Anti-CD20 IHC. **Figure 143-145.** Case 47. Sequential spleen sections for a RVFV infected sheep. **Figure 143.** A marked loss of lymphocytes gives the specimens a paucicellular appearance. There is also necrosis in a germinal centre (arrow). HE. **Figure 144.** Scattered T lymphocytes in the red pulp and severe depletion of the PALS. Anti-CD3 IHC. **Figure 145.** Anti-CD20 positive necrotic debris in the germinal centre (arrow) with a few residual B lymphocytes in the marginal zones of the PALS and in the red pulp. Anti-CD20 IHC.

Panel 26: Figures 146-149. Kidney, RVFV-infected adult sheep. Jones' methenamine silver stain (JMS).

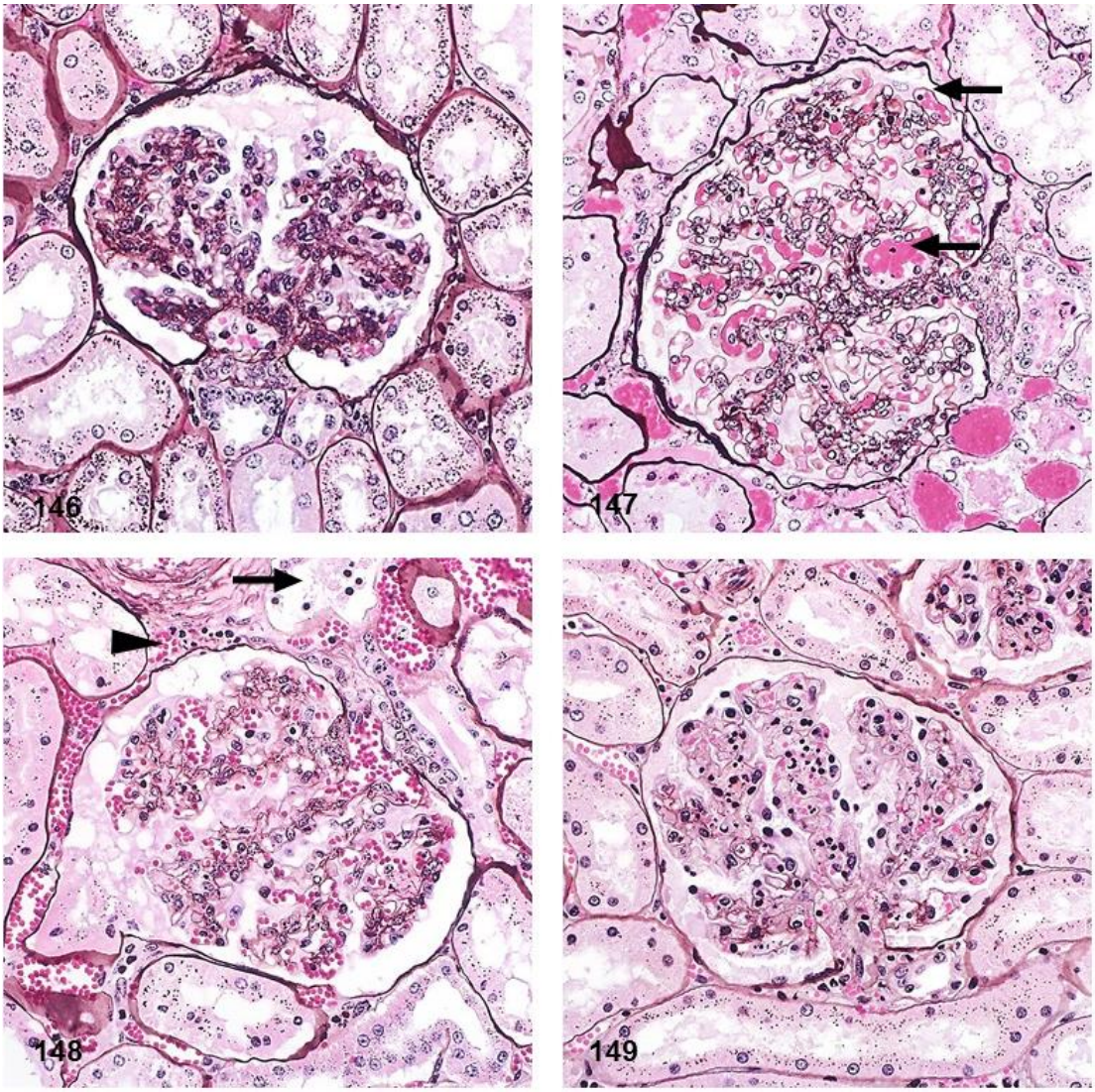

Figure 146. Case 60. Normal glomerulus, renal tubules and tubulointerstitium in an adult sheep not infected with RVFV, sectioned at 3 µm thickness. JMS. **Figures 146-147.** Kidney of RVFV-infected adult sheep, sectioned at 3 µm thickness. JMS. **Figure 147.** Case 5. Congestion in the glomerulus and interstitium with nuclear fragments and pyknosis in (arrows) in the capillaries. **Figure 148.** Case 18. Pyknosis in renal tubular epithelial cells (arrow) with a mild decrease in mesangial cellularity. There is also congestion with pyknosis in the interstitium (arrowhead). **Figure 149.** Case 48. Widespread pyknosis and karyorrhexis in a renal glomerulus with a marked decrease in mesangial cellularity. Pyknosis is also present in the interstitium.

Panel 27: Figures 150-153. Kidney, RVFV-infected adult sheep. Masson trichrome (MT) and periodic acid-Schiff (PAS) stains.

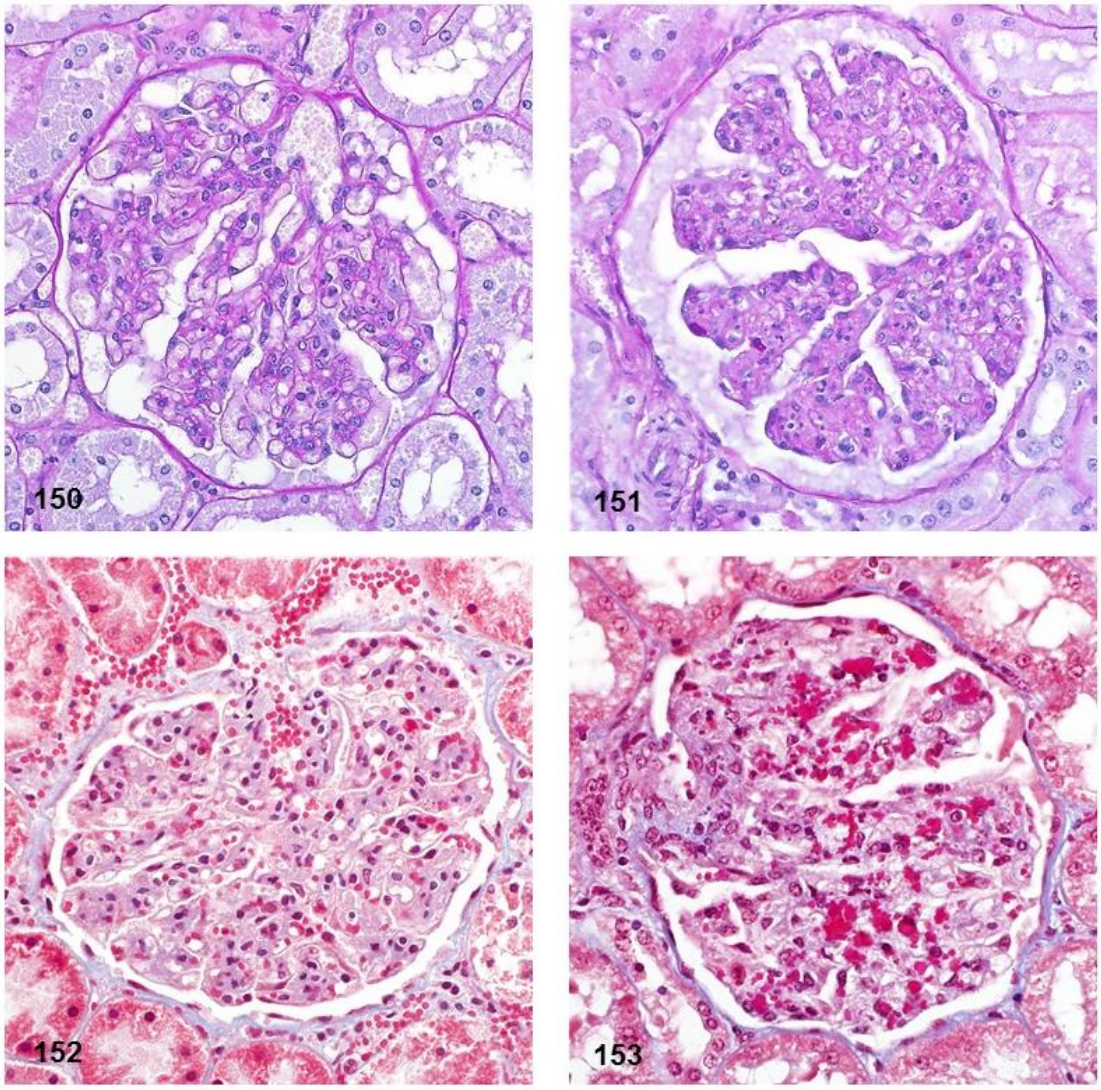

Figure 150. Case 18. Normal glomerulus, renal tubules and tubulointerstitium in an adult sheep not infected with RVFV, sectioned at 3 µm thickness. PAS. **Figures 151-153.** Kidney of RVFV-infected adult sheep, sectioned at 3 µm thickness. **Figure 151.** Case 48. The capillary loops are collapsed and there is a decrease in mesangial cellularity. PAS. **Figure 152.** Case 51. There is a mild decrease in the cellularity of the mesangium. MT. **Figure 153.** Case 55. Congestion in the glomerulus with nuclear fragments in the capillaries and a marked decrease in mesangial cellularity. MT.

Panel 28: Figures 154-157. Lymph node and spleen. Martius scarlet blue trichrome stain (MSB) for fibrin.

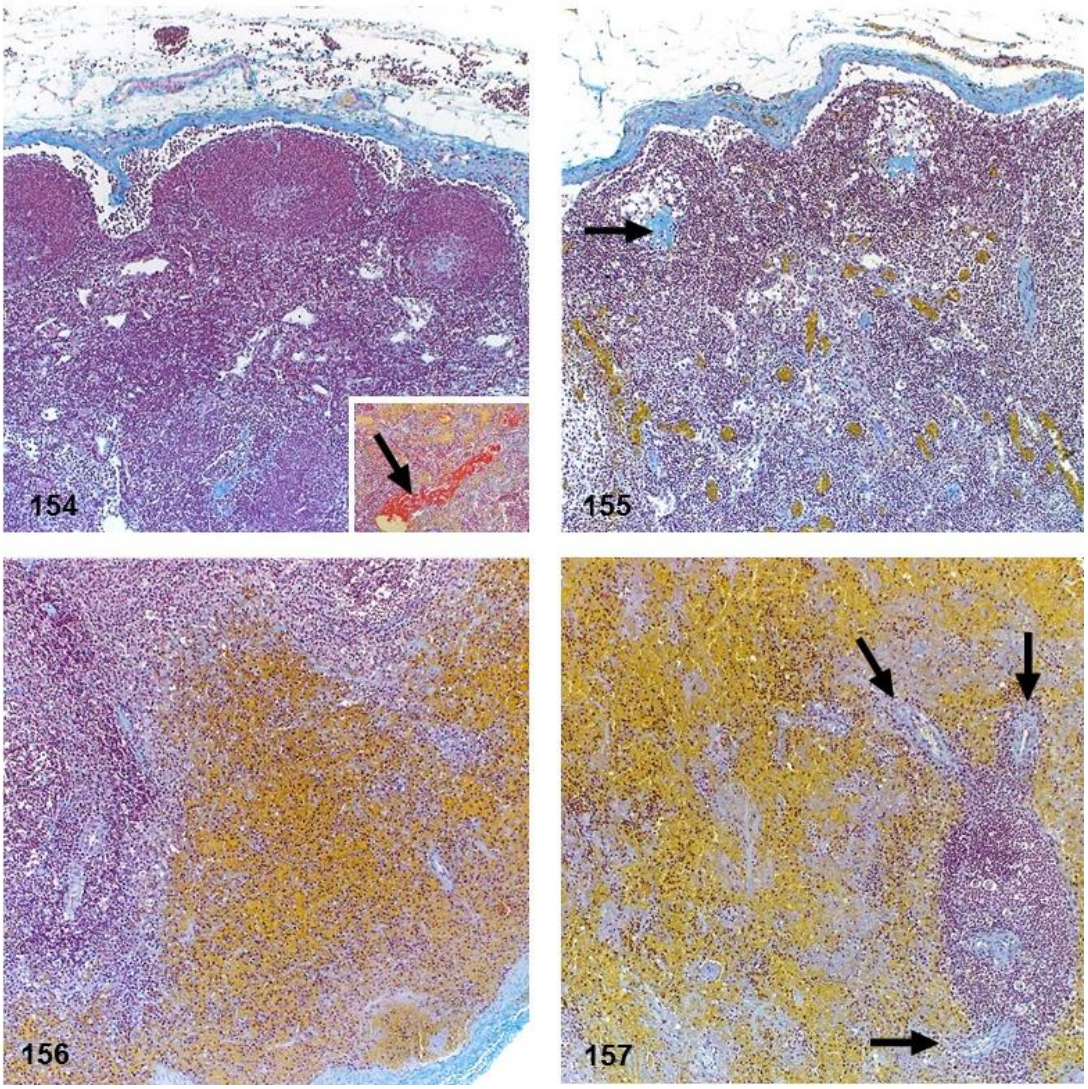

Figure 154. Lymph node. Negative tissue control from an adult sheep not infected with RVFV. MSB. **Insert:** Lymph node. Positive control (a dog with babesiosis) with a platelet-fibrin thrombus (arrow) in a blood vessel. MSB. **Figures 155-157.** Tissues of RVFV-infected adult sheep. MSB. **Figure 155.** Case 46. Lymph node. Depletion of the germinal centres and collapse of the connective tissue stroma (arrow). **Figure 156.** Case 48. Spleen. Depletion of the germinal centres. **Figure 157.** Case 70. Spleen. Severe depletion of the white pulp with only a narrow rim of lymphocytes remaining around the central arteries in the PALS (arrows).

Panel 29: Figures 158-161. Kidney. Martius scarlet blue trichrome stain (MSB) for fibrin.

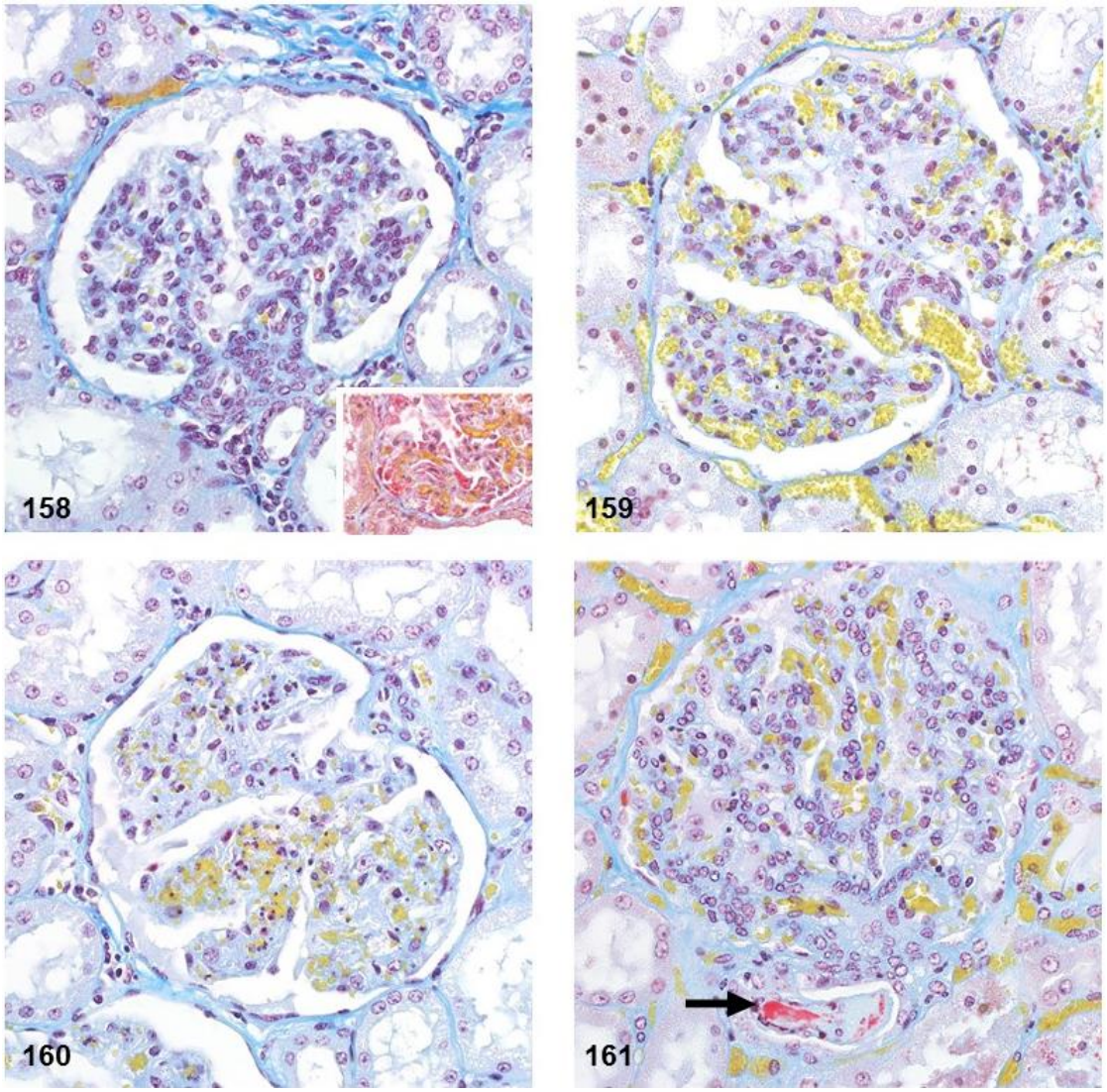

Figure 158. Negative tissue control from an adult sheep not infected with RVFV. MSB. **Insert:** Positive control (a dog with babesiosis) with platelet-fibrin thrombi (red) in the glomerular capillaries. MSB. **Figures 158-161.** Kidney. RVFV-infected adult sheep. MSB. **Figure 159.** Case 60. Scattered pyknosis and karyorrhexis in a renal glomerulus. **Figure 160.** Case 55. Widespread pyknosis and karyorrhexis in a renal glomerulus with a marked decrease in the cellularity of the mesangium. **Figure 161.** Case 5. Deposits of red staining fibrin-related materials (arrow) in the lumen of an arteriole.

5.5 Discussion

The first aim of the additional experiments described in this chapter was to inform future study design into the role of lymphocytes as well as fibrinolysis and the formation of fibrin thrombi in the pathogenesis of RVF. Additionally, the kidney lesion was examined further using standard histochemical stains to determine if an immune complex–mediated pathogenesis is likely.

Destruction of both B and T lymphocytes might be central to a fatal outcome in RVFV since both B and T lymphocyte numbers were reduced and the morphology of the white pulp was markedly disrupted. There are a few experiments that partially elucidated the role of lymphocytes in RVFV. Wild-type mice depleted of CD4+ lymphocytes and infected with NSs deleted RVFV were more likely to develop neurological disease (Dodd et al., 2013). The hypothesis is that activation of CD4+ T lymphocytes is required to augment RVFV antibody affinity maturation and class switching in B lymphocytes so that virus can be cleared from the peripheral tissues (Harmon et al., 2018). However, adult sheep and very young lambs (five weeks old) inoculated with an NSs deleted RVFV do not develop any clinical signs even though the virus can cross the placental barrier in early pregnancy (50 days after mating) causing foetal infections, malformations and stillbirths (Makoschey et al., 2016). Curiously, fetal malformations have not been documented in infections with wild-type virus infection but foetuses and young lambs are more susceptible to fatal RVFV infection (Pepin et al., 2010). Therefore, the study in mice indicates that functional CD4+ T lymphocytes are important but it is uncertain how this applies to sheep.

Lymphocytes also have a role in Ebola subtype Zaire and Marburg haemorrhagic fever virus infection, which causes depletion of B lymphocytes in the germinal follicles of lymph nodes similar to finding in the present study (Geisbert et al., 2000). Additionally, fatal outcomes in humans infected with Ebola subtype Zaire is characterized by very low levels of circulating cytokines produced by T lymphocytes and by massive loss of peripheral CD4 and CD8 lymphocytes causing a profound suppression of the adaptive immune responses (Wauquier et al., 2010). This might also be the case in RVFV infection and it should be investigated whether

the lymphocytes subsets decrease simultaneously or if some subsets are affected more severely initially with a drop in the other subsets later in the course of fatal disease. However, this would require a specifically designed experimental animal study in which exact disease time course is known and the addition of other laboratory methods (e.g. digital microscopy and image analysis, flow cytometry). However, the application of lymphocyte subset markers to extant RVF natural disease case material presented here is a useful starting point.

The kidney lesion caused by RVFV infection might be more important than previously surmised. The lesion in the kidney appeared to be pyknosis and karyorrhexis of vascular endothelial cells in the glomeruli and interstitial capillaries followed by necrosis of mesangial cells and a concomitant decrease in the mesangial cellularity. An immune complex–mediated pathogenesis appears to be unlikely. Instead, the kidney lesion may be caused by hypoxia related to hypotension. Renal dysfunction is occasionally a serious complication of fulminant liver failure secondary to the development of portal hypertension, which leads to vasodilatation and a relative hypovolemia with hypotension (Betrosian et al., 2007). However vascular damage with plasma leakage may exacerbate hypovolaemia and contribute to the development of renal failure. In DHF, the most severely affected children develop Dengue shock syndrome due to excessive depletion of intravascular volume as a result of plasma leakage (Wills et al., 2002). Hypovolaemia may be further exacerbated by reduced synthesis of albumin by hepatocytes and impaired secretion of steroid synthesizing enzymes by virus infected adrenal cortical cells (Geisbert and Jahrling, 2004). Reduced albumin would cause reduced plasma oncotic pressure and contribute to plasma leakage, whereas reduced levels of steroid synthesizing enzymes from the adrenal glands may contribute to hypotension and sodium loss (Geisbert and Jahrling, 2004). However, renal impairment may also occur as a result of direct virus-related injury to kidneys which has been demonstrated in RVFV infection in humans and sheep (Daubney et al., 1931, Coetzer, 1977, Van Der Lugt et al., 1996, Al-Hazmi et al., 2003, Shieh et al., 2010, Faburay et al., 2016a, Faburay et al., 2016b). A more detailed study with wild-type RVF in adult sheep that includes electron microscopy and other

renal function tests at specific time intervals would be beneficial to the elucidation of the exact series of events in the kidney as well as the exact cause of the lesion.

Lastly, none of the spleen, lymph node or kidney specimens had convincing platelet-fibrin thrombi with the MSB stain. Additional histochemical stains such as a phosphotungstic acid-haematoxylin or Movat's pentachrome may provide further insights based on the extant natural disease case material. However, a RVFV infection study in sheep wherein blood samples are analysed using various tests of the coagulation cascade (e.g. prothrombin and thromboplastin time, D-dimers and FDPs) would provide a better indication as to whether fibrinolysis and the formation of fibrin thrombi occur concomitantly so that thrombosis does not occur, as has been suggested by observations made in prior studies (Olaleye et al., 1996, Cosgriff et al., 1989, Marchi et al., 2009, Asakura, 2014)

An unfortunate limitation in this study was that samples were not suitable for electron microscopy. Even minimal autolysis as observed on HE sections translated into severe disruption of tissue morphology on the electron microscopy level and attempts to study tissues from natural cases using this method was abandoned early in the study. Consequently, we used histochemical stains and immunohistochemistry. Also, the exact age of the sheep was not known since these were natural cases and it was not known at what time-point the sheep died following RVFV infection. An attempt to investigate B cell proliferation in the spleen with anti-Ki67 mouse monoclonal antibody was also unsuccessful (data not shown).

CHAPTER 6

CONCLUSION

The broad aim of the present study was to summarize the pathology of RVF and describe the cellular tropism of the virus in multiple age groups of sheep including: adults, young lambs and foetuses. This project markedly expanded the current knowledge about the pathology of RVFV in sheep and the host response in different age groups, by analysing viral antigen distribution in a variety of organs in naturally occurring cases and determining the extent to which virus could be present in the various organs. The results raised new questions concerning RVFV pathogenesis that warrant further research. Additionally, the detailed information about the lesions and cellular tropism of RVFV provided here should improve future interpretation of histopathology in RVF cases and the recognition of RVFV antigen in tissues using IHC.

To successfully diagnose RVF in sheep, ideally tissues from multiple age groups should be examined. There is a clear distinction between the severity of disease in young lambs and adult sheep. Specifically, RVF is typically more acute in young lambs than in older sheep, and there are important differences in the lesions and tropism particularly in the liver, kidneys and lymphoid organs of young lambs. Additionally, diagnosing RVF in foetuses is challenging if samples from the ewe or the placenta are not available or when a limited number of deaths and abortions occurs during an interepidemic period, when the disease is not expected to be present. Consequently, continued virus surveillance in endemic areas, where RVFV infection is a plausible differential diagnosis in the interepidemic periods, is warranted. Appropriate samples, as recommended in this work, should be taken and suitable additional tests requested.

A new finding is that acute renal tubular and glomerular injury is the most frequent RVF lesion in some sheep adult cases suggesting that an atypical renal form of RVF might occur in sheep. Therefore, we recommend that in endemic areas, cases of acute renal tubular injury be investigated further using RVFV IHC if other more common differential diagnoses have already

been excluded. Furthermore, the unique finding of RVFV antigen in the testis of sheep, although the antigen was only present in the connective tissue surrounding seminiferous tubules, efferent ductules, or the duct of the epididymis, indicates there is a risk that RVFV might be transmitted through semen.

This research also confirmed that the lesions in young animals are different from those observed in adult sheep. In young lambs, the liver lesion is much more severe than in adults with widespread labelling of virtually every hepatocyte. In contrast, the kidney lesion is much less severe in young lambs than in adults, but viral antigen is easier to find and generally widespread. Histological lesions in the lungs of young lambs, mirrors that of adults. However, as in the kidneys viral antigen is easier to find in the lungs of lambs than those of adults. As in adult sheep, splenic lymphocytolysis is a prominent feature. However due to a developmentally normal lack of germinal centres in lambs, the lymphocytolysis is more prominent at the edge of the periarteriolar lymphoid sheaths and the red pulp. Viral antigen is again much easier to detect in young lambs whereas it often requires a detailed examination using higher power magnification to find the scattered labelled cells in an adult's spleen.

Lesions and tropism in foetuses are again different from the adult sheep and young lambs. Most foetuses have non-specific macroscopic lesions and liver lesions and viral antigen is absent in about 1 of 5 foetus cases. The cotyledon and caruncle are in fact more useful than the liver for diagnostic testing, with viral antigen present in almost all the specimens examined. Therefore, absence of liver lesions in foetuses does not necessarily exclude a diagnosis of RVF and a sample from the placentome is critical for a diagnosis. The heart is also more frequently positive by IHC than brain specimens. In the heart, viral antigen is often present in myocardial Purkinje fibres, cardiomyocytes and vascular smooth muscle cells. Labelling is only occasionally present in these cells in young lambs whereas in adult sheep viral antigen was only sporadically found in vascular smooth muscle cells and never in cardiomyocytes or myocardial Purkinje fibres. Bleeding manifestation in foetuses is also minimal but plasma leakage with effusions in body cavities, accompanied by brain and lung oedema, is very

common. Very young or unborn animals might have insufficient numbers of T lymphocytes to keep the proinflammatory innate responses under control and suffer severe microcirculatory dysfunction and shock as a result.

This research reinforces the likelihood that macrophages have an important role in RVF pathogenesis. Viral antigen positive macrophages included: Kupffer cells and infiltrating macrophages in the liver; marginal zone, metallophilic, tingible-body and red pulp macrophages in the spleen; sinus macrophages in the lymph nodes; pulmonary intravascular macrophages; lamina proprial macrophages in the intestinal tract; intravascular macrophages in the renal interstitium and glomerular tuft; testicular interstitial macrophages; and macrophages in the skin. Despite having a high viral load and necrotic lesions in fatal cases, only minimal inflammation is observed in infected tissues and organs, indicating a dysregulated immune response. Immunohistochemical studies have also shown a strong association between parenchymal necrosis in organs and the presence of abundant antigens with minimal inflammation. An imbalance in the immune response has been demonstrated in human cases with RVFV replicating to significantly higher levels in patients with fatal outcomes (Njenga et al., 2009, Jansen van Vuren et al., 2015). However, the details of such a model remain to be worked out and a sheep model might be useful to study the levels of pro-inflammatory and immunosuppressive cytokines and chemokines further.

Future RVF research could include studies of:

- RVFV-infected rams and bulls for presence of viable virus in semen and if virus is present, determination of the concentrations and duration of shedding.
- The role of genetic resistance in viral virulence and the outcome of RVFV infection in sheep.
- Whether the cellular tropism demonstrated for RVFV in sheep (tissue/infiltrating macrophages, smooth muscle cells and endothelial cells in particular) coincides with the distribution of SCARA1 in tissues.

- The susceptibility of ewes in the later stages of pregnancy to lethal disease compared to ewes in the earlier stages of pregnancy who might abort or resorb their foetuses and survive the infection.
- Whether the cell death morphology in the liver of RVFV-infected lambs is more heterogeneous than previously suspected, and the possibility that multiple cell death pathways are involved.
- The role of pro-inflammatory and immunosuppressive cytokines and chemokines in RVFV-infected sheep and how these might contribute to a fatal outcome.
- Various components in the clotting cascade in an animal model to investigate whether fibrinolysis and the formation of fibrin thrombi occur concomitantly in RVFV infection so that thrombosis does not occur.
- RVFV induced changes in the levels of various lymphocyte subsets, and the circulating cytokines produced by them to determine which subset is worst affected, at what time-point post-infection, and how this affects the adaptive immune responses.

Results of adult sheep and young lambs have been published in Veterinary Pathology and various aspects were presented at invited lectures and a conference.

REFERENCES

Abudurexiti A, Adkins S, Alioto D, Alkhovsky SV, Avsic-Zupanc T, Ballinger MJ, et al. Taxonomy of the order Bunyavirales: update 2019. *Archives of Virology* 2019:164(7):1949-1965.

Adam I, Karsany MS. Case report: Rift Valley Fever with vertical transmission in a pregnant Sudanese woman. *Journal of Medical Virology.* 2008:80(5):929.

Aguzzi A, Kranich J, Krautler NJ. Follicular dendritic cells: origin, phenotype, and function in health and disease. *Trends in Immunology.* 2014:35(3):105-113.

Al-Hazmi M, Ayoola EA, Abdurahman M, Banzal S, Ashraf J, El-Bushra A, et al. Epidemic Rift Valley fever in Saudi Arabia: A clinical study of severe illness in humans. *Clinical Infectious Diseases.* 2003:36(3):245-252.

Albornoz A, Hoffmann AB, Lozach P, Tischler ND. Early Bunyavirus-Host Cell Interactions. *Viruses*. 2016:(8)143. doi:10.3390/v8050143.

Antonis AF, Kortekaas J, Kant J, Vloet RP, Vogel-Brink A, Stockhofe N, et al. Vertical transmission of Rift Valley fever virus without detectable maternal viremia. *Vector Borne Zoonotic Diseases.* 2013:13(8):601-606.

Anyangu AS, Gould LH, Sharif SK, Nguku PM, Omolo JO, Mutonga D, et al. Risk factors for severe Rift Valley fever infection in Kenya, 2007. *American Journal of Tropical Medicine and Hygiene.* 2010:83(2 Suppl):14-21.

Aradaib IE, Erickson BR, Elageb RM, Khristova ML, Carroll SA, Elkhidir IM, et al. Rift valley fever, Sudan, 2007 and 2010. *Emerging Infectious Diseases.* 2013:19(2):246-253.

Archer BN, Thomas J, Weyer J, Cengimbo A, Landoh DE, Jacobs C, et al. Epidemiologic Investigations into Outbreaks of Rift Valley Fever in Humans, South Africa, 2008–2011. *Emerging Infectious Diseases.* 2013:19(12):1918-1925.

Arishi HM, Aqeel AY, Al Hazmi MM. Vertical transmission of fatal Rift Valley fever in a newborn. *Annals of Tropical Paediatrics International Child Health.* 2006:26(3):251-253.

Asakura H. Classifying types of disseminated intravascular coagulation: clinical and animal models. *Journal of Intensive Care.* 2014:6;2(1):20. doi: 10.1186/2052-0492-2-20.

Baer A, Austin D, Narayanan A, Popova T, Kainulainen M, Bailey C. Induction of DNA damage signaling upon Rift Valley fever virus infection results in cell cycle arrest and increased viral replication. *Journal of Biological Chemistry.* 2012:287(10):7399-410.

Bales JM, Powell DS, Bethel LM, Reed DS, Hartman AL. Choice of inbred rat strain impacts lethality and disease course after respiratory infection with Rift Valley Fever Virus. *Frontiers in Cellular and Infection Microbiology.* 2012:2:105. doi: 10.3389/fcimb.2012.00105.

Baskerville A, Hubbard KA, Stephenson JR. Comparison of the pathogenicity for pregnant sheep of Rift Valley fever virus and a live attenuated vaccine. *Research in Veterinary Science* 1992:52(3):307-311.

Basler CF. Molecular pathogenesis of viral hemorrhagic fever. *Seminars in immunopathology* 2017:39(5):551-561.

Baudin M, Jumaa AM, Jomma HJE, Karsany MS, Bucht G, Naslund J, et al. Association of Rift Valley fever virus infection with miscarriage in Sudanese women: a cross-sectional study. *Lancet Global Health.* 2016:4(11):e864-e871.

Belizário J, Vieira-Cordeiro L, Enns S. Necroptotic cell death signaling and execution pathway: Lessons from knockout mice. *Mediators of Inflammation.* 2015: Article ID 128076. doi: 10.1155/2015/128076.

Betrosian A-P, Agarwal B, Douzinas EE. Acute renal dysfunction in liver diseases. *World Journal of Gastroenterology.* 2007:13(42):5552-5559.

Bird BH, Githinji JWK, Macharia JM, Kasiiti JL, Muriithi RM, Gacheru SG, et al. Multiple virus lineages sharing recent common ancestry were associated with a large rift valley fever outbreak among livestock in Kenya during 2006-2007. *Journal of Virology.* 2008:82(22):11152-11166.

Bird BH, Khristova ML, Rollin PE, Ksiazek TG, Nichol ST. Complete genome analysis of 33 ecologically and biologically diverse Rift Valley fever virus strains reveals widespread virus movement and low genetic diversity due to recent common ancestry. *Journal of Virology.* 2007:81(6):2805-2816.

Bird BH, Ksiazek TG, Nichol ST, MacLachlan NJ. Rift Valley fever virus. *Journal of the American Veterinary Medical Association.* 2009:234(7):883-893.

Busch CM, Callicott RJ, Peters CJ, Morrill JC, Womack JE. Mapping a Major Gene for Resistance to Rift Valley Fever Virus in Laboratory Rats. *Journal of Heredity.* 2015:106(6):728-733.

Callis RT, Jahrling PB, DePaoli A. Pathology of Lassa virus infection in the rhesus monkey. *American Journal of Tropical Medicine and Hygiene.* 1982:31(5):1038-1045.

Caminade C, Ndione JA, Diallo M, MacLeod DA, Faye O, Ba Y, et al. Rift Valley Fever outbreaks in Mauritania and related environmental conditions. *International Journal of Environmental Research and Public Health.* 2014:11(1):903-918.

Cardier JE, Rivas B, Romano E, Rothman AL, Perez-Perez C, Ochoa M, et al. Evidence of vascular damage in dengue disease: demonstration of high levels of soluble cell adhesion molecules and circulating endothelial cells. *Endothelium.* 2006:13(5):335-340.

Caroline AL, Kujawa MR, Oury TD, Reed DS, Hartman AL. Inflammatory Biomarkers Associated with Lethal Rift Valley Fever Encephalitis in the Lewis Rat Model. *Frontiers in Microbiology.* 2015:6:1509. doi: 10.3389/fmicb.2015.01509.

Cêtre-Sossah C, Pédarrieu A, Guis H, Defernez C, Bouloy M, Favre J, et al. Prevalence of rift valley fever among ruminants, Mayotte. *Emerging Infectious Diseases.* 2012:18(6):972-975.

Chevalier V, Pépin M, Plée L, Lancelot R. Rift Valley fever - a threat for Europe? *Eurosurveillance.* 2010:15(10):Article ID 19506. doi.org/10.2807/ese.15.10.19506-en

Cianciolo RE, Mohr FC, Aresu L, Brown CA, James C, Jansen JH, et al. World Small Animal Veterinary Association Renal Pathology Initiative: Classification of Glomerular Diseases in Dogs. *Veteriary Pathology.* 2016:53(1):113-135.

Clements ACA, Pfeiffer DU, Martin V, Otte MJ. A Rift Valley fever atlas for Africa. *Preventive Veterinary Medicine.* 2007:82(1):72-82.

Coackley W. Alteration in virulence of rift valley fever virus during serial passage in lamb testis cells. *The Journal of Pathology and Bacteriology.* 1965:89(1):123-131.

Coetzer JAW. The pathology of Rift Valley fever. I. Lesions occurring in natural cases in new-born lambs. *Onderstepoort Journal of Veterinary Research.* 1977:44(4):205-211.

Coetzer JA, Barnard BJ. Hydrops amnii in sheep associated with hydranencephaly and arthrogryposis with Wesselsbron disease and Rift Valley fever viruses as aetiological agents. *Onderstepoort Journal of Veterinary Research*. 1977:44(2):119–126.

Coetzer JAW, Ishak KG. Sequential development of the liver lesions in new-born lambs infected with Rift Valley fever virus. I. Macroscopic and microscopic pathology. *Onderstepoort Journal of Veterinary Research.* 1982:49(2):103-108.

Coetzer JAW, Theodoridis A, Heerden A. Wesselsbron disease, pathological, haematological and clinical studies in natural cases and experimentally infected new-born lambs. *Onderstepoort Journal of Veterinary Research.* 1978:45(2):93-106.

Connolly-Andersen AM, Douagi I, Kraus AA, Mirazimi A. Crimean Congo hemorrhagic fever virus infects human monocyte-derived dendritic cells. *Virology.* 2009:390(2):157-162.

Cosgriff TM, Morrill JC, Jennings GB, Hodgson LA, Slayter MV, Gibbs PH, et al. Hemostatic derangement produced by Rift Valley fever virus in rhesus monkeys. *Reviews of Infectious Diseases.* 1989:11(Suppl 4):S807-14.

Daubney R, Hudson JR, Garnham PC. Enzootic hepatitis or Rift Valley fever: An undescribed virus disease of sheep, cattle and man from East Africa. *The Journal of Pathology and Bacteriology.* 1931:34:545-579.

Dodd KA, McElroy AK, Jones ME, Nichol ST, Spiropoulou CF. Rift Valley fever virus clearance and protection from neurologic disease are dependent on CD4+ T cell and virus-specific antibody responses. *Journal of Virology.* 2013:87(11):6161-6171.

Dodd KA, McElroy AK, Jones TL, Zaki SR, Nichol ST, Spiropoulou CF. Rift valley Fever virus encephalitis is associated with an ineffective systemic immune response and activated T cell infiltration into the CNS in an immunocompetent mouse model. *PLoS Neglected Tropical Diseases.* 2014:8(6). doi: 10.1371/journal.pntd.0002874

Easterday BC, McGavran MH, Rooney JR, Murphy LC. The pathogenesis of Rift Valley fever in lambs. *American Journal of Veterinary Research.* 1962:23:470-479.

Easterday BC, Murphy LC, Bennett DG. Experimental Rift Valley Fever in Lambs and Sheep. *American Journal of Veterinary Research.* 1962:23:1231-1239.

El Imam M, El Sabiq M, Omran M, Abdalkareem A, El Gaili Mohamed MA, Elbashir A, et al. Acute renal failure associated with the Rift Valley fever: a single center study. *Saudi Journal of Kidney Diseases and Transplantation.* 2009:20(6):1047-1052.

Ellis DS, Simpson DI, Stamford S, Abdel Wahab KS. Rift Valley fever virus: some ultrastructural observations on material from the outbreak in Egypt 1977. *Journal of General Virology.* 1979:42(2):329-337.

Erasmus BJ, Coetzer JAW. The symptomatology and pathology of Rift Valley fever in domestic animals. In: Goldblum N, Swartz TA, Klingberg MA, eds. *Contributions to Epidemiology and Biostatistics.* Basel: Karger 1981:77-82.

Ermler ME, Yerukhim E, Schriewer J, Schattgen S, Traylor Z, Wespiser AR. RNA helicase signaling is critical for type i interferon production and protection against Rift Valley fever virus during mucosal challenge. *Journal of Virology.* 2013:87(9):4846-4860.

Esmon CT. Crosstalk between inflammation and thrombosis. *Maturitas.* 2004:47(4):305-314.

European Centre for Disease Prevention and Control. Rift Valley fever outbreak in Mayotte, France. *Eurosurveillance.* 2019:24(13):Article ID 1903282.

Faburay B, Gaudreault NN, Liu Q, Davis AS, Shivanna V, Sunwoo SY, et al. Development of a sheep challenge model for Rift Valley fever. *Virology.* 2016:489:128-140.

Faburay B, Wilson WC, Gaudreault NN, Davis AS, Shivanna V, Bawa B, et al. A Recombinant Rift Valley Fever Virus Glycoprotein Subunit Vaccine Confers Full Protection against Rift Valley Fever Challenge in Sheep. *Scientific Reports.* 2016:6:27719. doi: 10.1038/srep27719.

Ferron F, Li Z, Danek EI, Luo D, Wong Y, Coutard B, et al. The Hexamer Structure of the Rift Valley Fever Virus Nucleoprotein Suggests a Mechanism for its Assembly into Ribonucleoprotein Complexes. *PLoS Pathogens.* 2011:7(5). doi: 10.1371/journal.ppat.1002030.

Findlay GM. Rift valley fever or enzootic hepatitis. *Transactions of the Royal Society of Tropical Medicine and Hygiene.* 1932:25(4):229-248.

Findlay GM, Daubney R. The virus of Rift Valley fever or enzoötic hepatitis. *The Lancet.* 1931:218(5651):1350-1351.

Frank D, Vince JE. Pyroptosis versus necroptosis: similarities, differences, and crosstalk. *Cell Death and Differentiation.* 2019:26(1):99-114.

Gear J, De Meillon B, Le Roux AF, Kofsky R, Innes RR, Steyn JJ, et al. Rift valley fever in South Africa; a study of the 1953 outbreak in the Orange Free State, with special reference to the vectors and possible reservoir hosts. *South African Medical Journal.* 1955:29(22):514-518.

Geisbert TW, Hensley LE, Gibb TR, Steele KE, Jaax NK, Jahrling PB. Apoptosis Induced In Vitro and In Vivo During Infection by Ebola and Marburg Viruses. *Laboratory Investigation.* 2000:80(2):171-186.

Geisbert TW, Hensley LE, Larsen T, Young HA, Reed DS, Geisbert JB, et al. Pathogenesis of Ebola Hemorrhagic Fever in Cynomolgus Macaques: Evidence that Dendritic Cells are Early and Sustained Targets of Infection. *American Journal of Pathology* 2003:163(6):2347-2370.

Geisbert TW, Jahrling PB: Exotic emerging viral diseases. Progress and challenges. *Nature medicine.* 2004:10(Suppl 12):S110-S121.

Geisbert TW, Young HA, Jahrling PB, Davis KJ, Larsen T, Kagan E, et al. Pathogenesis of Ebola Hemorrhagic Fever in Primate Models: Evidence that Hemorrhage Is Not a Direct Effect of Virus-Induced Cytolysis of Endothelial Cells. *American Journal of Pathology.* 2003:163(6):2371-2382.

Georges TM, Justin M, Victor M, Marie KJ, Mark R, Leopold MMK. Seroprevalence and Virus Activity of Rift Valley Fever in Cattle in Eastern Region of Democratic Republic of the Congo. *Journal of Veterinary Medecine.* 2018:2018:Article ID 4956378. doi: 10.1155/2018/4956378.

Gould EA, Solomon T. Pathogenic flaviviruses. *Lancet.* 2008:371(9611):500-509.

Grobbelaar AA, Weyer J, Leman PA, Kemp A, Paweska JT, Swanepoel R. Molecular epidemiology of Rift Valley fever virus. *Emerging infectious diseases.* 2011:17(12):2270-2276.

Haisma HJ, Boesjes M, Beerens AM, van der Strate BW, Curiel DT, Pluddemann A, et al. Scavenger receptor A: a new route for adenovirus 5. *Molecular Pharmaceutics.* 2009:6(2):366-374.

Haneche F, Leparc-Goffart I, Simon F, Hentzien M, Martinez-Pourcher V, Caumes E, et al. Rift Valley fever in kidney transplant recipient returning from Mali with viral RNA detected in semen up to four months from symptom onset, France, autumn 2015. *Eurosurveillance.* 2016:21(18). doi: 10.2807/1560-7917.

Harmon JR, Spengler JR, Coleman-McCray JD, Nichol ST, Spiropoulou CF, McElroy AK. CD4 T Cells, CD8 T Cells, and Monocytes Coordinate To Prevent Rift Valley Fever Virus Encephalitis. *Journal of Virology.* 2018:92(24):e01270-18. doi: 10.1128/JVI.01270-18.

Hartman A, Caroline A, Bethel L, Powell D, Oury T, Reed D. Dysregulated host inflammatory response in rats with fatal encephalitic Rift Valley Fever (VIR5P.1021). *The Journal of Immunology.* 2014:192(Suppl 1):144.4.

Hassan OA, Ahlm C, Sang R, Evander M. The 2007 Rift valley fever outbreak in Sudan. *PLoS Neglected Tropical Diseases.* 2011:5(9). doi.org/10.1371/journal.pntd.0001229

Heinrich N, Saathoff E, Weller N, Clowes P, Kroidl I, Ntinginya E, et al. High Seroprevalence of Rift Valley Fever and Evidence for Endemic Circulation in Mbeya Region, Tanzania, in a Cross-Sectional Study. *PLoS Neglected Tropical Diseases.* 2012:6(3). doi: 10.1371/journal.pntd.0001557.

Himeidan YE, Kweka EJ, Mahgoub MM, El Rayah EA, Ouma JO. Recent outbreaks of rift valley Fever in East Africa and the middle East. *Frontiers in Public Health.* 2014:6;2:169. doi: 10.3389/fpubh.2014.00169.

Hughes DA, Fraser IP, Gordon S. Murine macrophage scavenger receptor: in vivo expression and function as receptor for macrophage adhesion in lymphoid and non-lymphoid organs. *European Journal of Immunology.* 1995:25(2):466-473.

Hunter P, Erasmus BJ, Vorster JH. Teratogenicity of a mutagenised Rift Valley fever virus (MVP 12) in sheep. *Onderstepoort Journal of Veterinary Research*. 2002;69(1):95–98.

Ikegami T, Narayanan K, Won S, Kamitani W, Peters CJ, Makino S. Rift Valley fever virus NSs protein promotes post-transcriptional downregulation of protein kinase PKR and inhibits eIF2alpha phosphorylation. *PLoS Pathogens.* 2009:5(2). doi: 10.1371/journal.ppat.1000287.

Ikegami T, Narayanan K, Won SY, Kamitani W, Peters CJ, Makino S. Dual functions of Rift Valley fever virus NSs protein: inhibition of host mRNA transcription and post-transcriptional downregulation of protein kinase PKR. *Annals of the New York Academy of Sciences*. 2009:1171:E75-E85.

Jansen van Vuren P, Kgaladi J, Patharoo V, Ohaebosim P, Msimang V, Nyokong B, et al. Human Cases of Rift Valley Fever in South Africa, 2018. *Vector Borne Zoonotic Diseases.* 2018. doi: 10.1089/vbz.2018.2357.

Jansen van Vuren P, Shalekoff S, Grobbelaar AA, Archer BN, Thomas J, Tiemessen CT, et al. Serum levels of inflammatory cytokines in Rift Valley fever patients are indicative of severe disease. *Virology Journal.* 2015:12:159-159.

Jost CC, Nzietchueng S, Kihu S, Bett B, Njogu G, Swai ES, et al. Epidemiological assessment of the Rift Valley fever outbreak in Kenya and Tanzania in 2006 and 2007. *American Journal of Tropical Medicine and Hygiene.* 2010:83(Suppl 2):66-72.

Kalveram B, Lihoradova O, Ikegami T. NSs Protein of Rift Valley Fever Virus Promotes Post-Translational Downregulation of the TFIIH Subunit p62. *Journal of Virology.* 2011: 85(13):6234-43.

Kenawy MA, Abdel-Hamid YM, Beier JC. Rift Valley Fever in Egypt and other African countries: Historical review, recent outbreaks and possibility of disease occurrence in Egypt. *Acta Tropica.* 2018:181:40-49.

Kumar V, Abbas A, Mitchell R, Fausto N. Diseases of the Immune System. In: Kumar V AAK, Mitchell R, Fausto N, ed. *Robbins Basic Pathology 8th revised edition*. Philadelphia, USA: Saunders Elsevier Inc.; 2007:107-172.

LaBeaud AD, Muchiri EM, Ndzovu M, Mwanje MT, Muiruri S, Peters CJ, et al. Interepidemic Rift Valley fever virus seropositivity, northeastern Kenya. *Emerging Infectious Diseases.* 2008:14(8):1240-1246.

Leger P, Tetard M, Youness B, Cordes N, Rouxel RN, Flamand M, Lozach PY. Differential use of the C-type lectins L-SIGN and DC-SIGN for phlebovirus endocytosis. *Traffic.* 2016:(17):639–656.

Le May N, Dubaele S, De Santis LP, Billecocq A, Bouloy M, Egly J-M. TFIIH Transcription Factor, a Target for the Rift Valley Hemorrhagic Fever Virus. *Cell.* 2004:116(4):541-550.

Le May N, Mansuroglu Z, Leger P, Josse T, Blot G, Billecocq A. A SAP30 complex inhibits IFN-beta expression in Rift Valley fever virus infected cells. *PLoS Pathogens.* 2008:4(1). doi: 10.1371/journal.ppat.0040013.

Limonta D, Capo V, Torres G, Perez AB, Guzman MG. Apoptosis in tissues from fatal dengue shock syndrome. *Journal of Clinical Virology.* 2007:40(1):50-54.

Lozach, PY, Kühbacher A, Meier R, Mancini R, Bitto D, Bouloy M, Helenius A. DC-SIGN as a Receptor for Phleboviruses. *Cell Host & Microbe,* 2011:10:75-88.

Ly HJ, Ikegami T. Rift Valley fever virus NSs protein functions and the similarity to other bunyavirus NSs proteins. *Virology Journal.* 2016:13:118. doi: 10.1186/s12985-016-0573-8.

MacLeod DT, Nakatsuji T, Wang Z, di Nardo A, Gallo RL. Vaccinia virus binds to the scavenger receptor MARCO on the surface of keratinocytes. *Journal of Investigative Dermatology*. 2015:135(1):142-150.

MacLeod DT, Nakatsuji T, Yamasaki K, Kobzik L, Gallo RL. HSV-1 exploits the innate immune scavenger receptor MARCO to enhance epithelial adsorption and infection. *Nature communications.* 2013:4:1963-1963.

Madani TA, Al-Mazrou YY, Al-Jeffri MH, Mishkhas AA, Al-Rabeah AM, Turkistani AM, et al. Rift Valley Fever Epidemic in Saudi Arabia: Epidemiological, Clinical, and Laboratory Characteristics. *Clinical Infectious Diseases*. 2003:37(8):1084-1092.

Madi D, Achappa B, Ramapuram JT, Chowta N, Laxman M, Mahalingam S. Dengue encephalitis-A rare manifestation of dengue fever. *Asian Pacific Journal of Tropical Biomedicine.* 2014:4(Suppl 1):S70-72.

Magona JW, Galiwango T, Walubengo J, Mukiibi G. Rift Valley fever in Uganda: Seroprevalence and risk factor surveillance vis-à-vis mosquito vectors, anti-RVF virus IgG and RVF virus neutralizing antibodies in goats. *Small Ruminant Research.* 2013:114(1):176-181.

Makoschey B, van Kilsdonk E, Hubers WR, Vrijenhoek MP, Smit M, Wichgers Schreur PJ, et al. Rift Valley Fever Vaccine Virus Clone 13 Is Able to Cross the Ovine Placental Barrier Associated with Foetal Infections, Malformations, and Stillbirths. *PLoS Neglected Tropical Diseases.* 2016:10(3). doi: 10.1371/journal.pntd.0004550.

Maluleke MR, Phosiwa M, van Schalkwyk A, Michuki G, Lubisi BA, Kegakilwe PS, et al. A comparative genome analysis of Rift Valley Fever virus isolates from foci of the disease outbreak in South Africa in 2008-2010. *PLoS Neglected Tropical Diseases.* 2019:13(3). doi: 10.1371/journal.pntd.0006576.

Marchi R, Nagaswami C, Weisel JW. Fibrin formation and lysis studies in dengue virus infection. *Blood Coagulation & Fibrinolysis : an international journal in haemostasis and thrombosis.* 2009:20(7):575-582.

McElroy AK, Nichol ST. Rift Valley fever virus inhibits a pro-inflammatory response in experimentally infected human monocyte derived macrophages and a pro-inflammatory cytokine response may be associated with patient survival during natural infection. *Virology.* 2012:422(1):6-12.

McGavern DB, Kang SS. Illuminating viral infections in the nervous system. *Nature Reviews Immunology.* 2011:11(5):318-329.

McMillen CM, Arora N, Boyles DA, Albe JR, Kujawa MR, Bonadio JF, et al. Rift Valley fever virus induces fetal demise in Sprague-Dawley rats through direct placental infection. *Science Advances.* 2018:4(12):eaau9812.

Mehedi M, Groseth A, Feldmann H, Ebihara H. Clinical aspects of Marburg hemorrhagic fever. *Future virology.* 2011:6(9):1091-1106.

Mohamed M, Mosha F, Mghamba J, Zaki SR, Shieh WJ, Paweska J, et al. Epidemiologic and clinical aspects of a Rift Valley fever outbreak in humans in Tanzania, 2007. *American Journal of Tropical Medicine and Hygiene.* 2010:83(Suppl 2):22-27.

Morvan J, Saluzzo JF, Fontenille D, Rollin PE, Coulanges P. Rift Valley fever on the east coast of Madagascar. *Research in Virology.* 1991:142(6):475-482.

Moutailler S, Krida G, Schaffner F, Vazeille M, Failloux AB. Potential vectors of Rift Valley fever virus in the Mediterranean Region. *Vector Borne and Zoonotic Diseases.* 2008:8(6):749-754.

Mundel B, Gear J. Rift valley fever; I. The occurrence of human cases in Johannesburg. *South African Medical Journal.* 1951:25(44):797-800.

Munyua P, Murithi RM, Wainwright S, Githinji J, Hightower A, Mutonga D, et al. Rift Valley fever outbreak in livestock in Kenya, 2006-2007. *American Journal of Tropical Medicine and Hygiene.* 2010:83(Suppl 2):58-64.

Mutua EN, Bukachi SA, Bett BK, Estambale BA, Nyamongo IK, "We do not bury dead livestock like human beings": Community behaviors and risk of Rift Valley Fever virus infection in Baringo County, Kenya. *PLoS Neglected Tropical Diseases.* 2017:11(5). doi: 10.1371/journal.pntd.0005582.

Nailwal H, Chan FKM. Necroptosis in anti-viral inflammation. *Cell Death and Differentiation.* 2019:26:4–13.

Nainu F, Shiratsuchi A, Nakanishi Y. Induction of Apoptosis and Subsequent Phagocytosis of Virus-Infected Cells As an Antiviral Mechanism. *Frontiers in Immunology.* 2017:8:1220-1220.

Ngoshe YB, Avenant L, Rostal M, William KB, Paweska JT, van Vuren J, et al. Seroprevalence and factors associated with seropositivity to Rift Valley fever virus in livestock. *Online Journal of Public Health Informatics*. 2019:11(1):e408.

Njenga MK, Paweska J, Wanjala R, Rao CY, Weiner M, Omballa V, et al. Using a field quantitative real-time PCR test to rapidly identify highly viremic Rift Valley fever cases. *Journal of Clinical Microbiology.* 2009:47(4):1166-1171.

Nogusa S, Thapa RJ, Dillon CP, Liedmann S, Oguin TH, 3rd, Ingram JP, et al. RIPK3 Activates Parallel Pathways of MLKL-Driven Necroptosis and FADD-Mediated Apoptosis to Protect against Influenza A Virus. *Cell Host Microbe.* 2016:20(1):13-24.

Nyakarahuka L, Balinandi S, Mulei S, Kyondo J, Tumusiime A, Klena J, et al. Ten outbreaks of rift valley fever in Uganda 2016-2018: epidemiological and laboratory findings. *International Journal of Infectious Diseases.* 2019:79(Suppl 1):4.

Odendaal L, Clift SJ, Fosgate GT, Davis AS. Lesions and Cellular Tropism of Natural Rift Valley Fever Virus Infection in Adult Sheep. *Veterianry Pathology.* 2019:56(1):61-77.

Odendaal L, Fosgate GT, Romito M, Coetzer JAW, Clift SJ. Sensitivity and specificity of real-time reverse transcription polymerase chain reaction, histopathology, and immunohistochemical labeling for the detection of Rift Valley fever virus in naturally infected cattle and sheep. *Journal of Veterinary Diagnostic Investigation.* 2014:26(1):49-60.

OIE World Organisation for Animal Health. Terrestrial Animal Health Code. Infection with Rift Valley fever virus: Recommendations for importation from countries or zones not free from RVF. *Terrestrial animal health code*. Paris, France: Office International des Epizooties; 2017. https://www.oie.int/index.php?id=169&L=0&htmfile=chapitre_rvf.htm.

Okokhere PO, Erameh CO, Alikah F, Akhideno PE, Iruolagbe CO, Osazuwa OO, et al. Acute Lassa Virus Encephalitis with Lassa Virus in the Cerebrospinal Fluid but Absent in the Blood: A Case Report with a Positive Outcome. *Case Reports in Neurology.* 2018:10(2):150-158.

Olaleye OD, Tomori O, Fajimi JL, Schmitz H. Experimental infection of three Nigerian breeds of sheep with the Zinga strain of the Rift Valley Fever virus. *Revue d'élevage et de Médecine Vétérinaire des Pays Tropicaux*. 1996:49(1):6-16.

Owen DM, Gale M, Jr. Fighting the flu with inflammasome signaling. *Immunity.* 2009:30(4):476-478.

Paessler S, Walker DH. Pathogenesis of the Viral Hemorrhagic Fevers. *Annual Review of Pathology: Mechanisms of Disease.* 2013:8(1):411-440.

Pepin M, Bouloy M, Bird BH, Kemp A, Paweska J. Rift Valley fever virus (Bunyaviridae: Phlebovirus): an update on pathogenesis, molecular epidemiology, vectors, diagnostics and prevention. *Special Issue: Emerging and Re-emerging Animal Viruses.* 2010:41(6):41:61.

Peters CJ, Anderson GW, Jr. Pathogenesis of Rift Valley fever. *Contributions to Epidemiology and Biostatistics.* 1981:3:21-41.

Phoenix I, Nishiyama S, Lokugamage N, Hill T E, Huante MB, Slack O A, Carpio V H, Freiberg A N, Ikegami T. N-Glycans on the Rift Valley Fever Virus Envelope Glycoproteins Gn and Gc Redundantly Support Viral Infection via DC-SIGN. *Viruses.* 2016: 8(149). doi:10.3390/v8050149.

Pienaar NJ, Thompson PN. Temporal and spatial history of Rift Valley fever in South Africa: 1950 to 2011. *Onderstepoort Journal of Veterinary Research.* 2013:80(1):384. doi: 10.4102/ojvr.v80i1.384.

Ragan IK, Schuck KN, Upreti D, Odendaal L, Richt JA, Trujillo JD, et al. Rift Valley Fever Viral RNA Detection by In Situ Hybridization in Formalin-Fixed, Paraffin-Embedded Tissues. *Vector Borne Zoonotic Diseases.* 2019:19(7):553-556.

Rao VP, Poutahidis T, Marini RP, Holcombe H, Rogers AB, Fox JG. Renal Infarction and Immune-mediated Glomerulonephritis in Sheep (Ovis aries) Chronically Implanted with Indwelling Catheters. *Journal of the American Association for Laboratory Animal Science.* 2006:45(4):14-19.

Reed C, Steele KE, Honko A, Shamblin J, Hensley LE, Smith DR. Ultrastructural study of Rift Valley fever virus in the mouse model. *Virology.* 2012:431(1-2):58-70.

Saad S, Abd El-Sameea MM, Shalakamy E. Effect of Attenuated Rift Valley Fever Vaccine on Bull's Semen. *4th Scientific Conference of the Egyptian Society for Cattle Diseases*. Assiut, Egypt; 1997:7-9.

Sartorelli AC, Fischer DS, Downs WG. Use of sarcoma 180/TG to prepare hyperimmune ascitic fluid in the mouse. *Journal of Immunology* 1966:96(4):676-682.

Scarselli E, Ansuini H, Cerino R, Roccasecca RM, Acali S, Filocamo G, et al. The human scavenger receptor class B type I is a novel candidate receptor for the hepatitis C virus. *The European Molecular Biology Organization Journal.* 2002:21(19):5017-5025.

Schieffelin JS, Shaffer JG, Goba A, Gbakie M, Gire SK, Colubri A, et al. Clinical illness and outcomes in patients with Ebola in Sierra Leone. *The New England Journal of Medicine.* 2014:371(22):2092-2100.

Schlondorff D. The glomerular mesangial cell: an expanding role for a specialized pericyte. *The Federation of American Societies for Experimental Biology Journal.* 1987:1(4):272-281.

Schmaljohn C, Elliott RM. Bunyaviridae. In: Knipe DM, Howley PM, eds. *Fields Virology*. 6th ed. Philadelphia: Wilkins; 2013:1245-1282.

Schulz KCA. The pathology of Rift valley fever of enzootic hepatitis in South Africa. *Journal of the South African Veterinary Association.* 1951:22(3):113-120.

Sherman MB, Freiberg AN, Holbrook MR, Watowich SJ. Single-particle cryo-electron microscopy of Rift Valley fever virus. *Virology* 2009:387(1):11-15.

Shieh WJ, Paddock CD, Lederman E, Rao CY, Gould LH, Mohamed M, et al. Pathologic studies on suspect animal and human cases of Rift Valley fever from an outbreak in Eastern Africa, 2006-2007. *American Journal of Tropical Medicine and Hygiene.* 2010:83(Suppl 2):38-42.

Shoemaker T, Boulianne C, Vincent MJ, Pezzanite L, Al-Qahtani MM, Al-Mazrou Y, et al. Genetic analysis of viruses associated with emergence of Rift Valley fever in Saudi Arabia and Yemen, 2000-01. *Emerging Infectious Diseases.* 2002:8(12):1415-1420.

Shone DK. Rift Valley fever in Southern Rhodesia. *The Central African Journal of Medicine.* 1958:4(7):284-286.

Shrivastava G, Leon-Juarez M, Garcia-Cordero J, Meza-Sanchez DE, Cedillo-Barron L. Inflammasomes and its importance in viral infections. *Immunololy Research.* 2016:64(5-6):1101-1117.

Sissoko D, Giry C, Gabrie P, Tarantola A, Pettinelli F, Collet L, et al. Rift valley fever, mayotte, 2007-2008. *Emerging Infectious Diseases.* 2009:15(4):568-570.

Smith DR, Steele KE, Shamblin J, Honko A, Johnson J, Reed C, et al. The pathogenesis of Rift Valley fever virus in the mouse model. *Virology.* 2010:407(2):256-267.

Struthers JK, Swanepoel R. Identification of a major non-structural protein in the nuclei of Rift Valley fever virus-infected cells. *Journal of Genereal Virology.* 1982:60(Pt 2):381-384.

Struthers JK, Swanepoel R, Shepherd SP. Protein synthesis in Rift Valley fever virus-infected cells. *Virology.* 1984:134(1):118-124.

Suzich JA, Collett MS. Rift Valley fever virus M segment: cell-free transcription and translation of virus-complementary RNA. *Virology.* 1988:164(2):478-486.

Swanepoel R, Coetzer JAW. Rift Valley fever. In: Coetzer JAW, Thompson GR, Tustin RD, et.al, eds. *Infectious Diseases of Livestock with special reference to Southern Africa*. Cape Town, South Africa: Oxford University Press; 2004:1037-1070.

Swanepoel R, Gill DE, Shepherd AJ, Leman PA, Mynhardt JH, Harvey S. The Clinical Pathology of Crimean-Congo Hemorrhagic Fever. *Clinical Infectious Diseases.* 1989:11(Suppl 4):S794-S800.

Swanepoel R, Struthers JK, Erasmus MJ, Shepherd SP, McGillivray GM, Shepherd AJ, et al. Comparative pathogenicity and antigenic cross-reactivity of Rift Valley fever and other African phleboviruses in sheep. *Journal of Hygiene.* 1986:97(2):331-346.

Tomokiyo R, Jinnouchi K, Honda M, Wada Y, Hanada N, Hiraoka T, et al. Production, characterization, and interspecies reactivities of monoclonal antibodies against human class A macrophage scavenger receptors. *Atherosclerosis.* 2002:161(1):123-132.

Turell MJ, Dohm DJ, Mores CN, Terracina L, Wallette DLJ, Hribar LJ, et al. Potential for North American mosquitoes to transmit Rift Valley fever virus. *Journal of the American Mosquito Control Association.* 2008:24(4):502-507.

Ulrich R. 2019. Rift Valley Fever: An Ancient Plague on Its Way Out of Africa? *Veterinary Pathology*, 2019:(56)2:178-179.

van den Bergh C, Venter EH, Swanepoel R, Thompson PN. High seroconversion rate to Rift Valley fever virus in cattle and goats in far northern KwaZulu-Natal, South Africa, in the absence of reported outbreaks. *PLoS Neglected Tropical Diseases.* 2019:13(5). doi: 10.1371/journal.pntd.0007296.

van der Lugt JJ, Coetzer JA, Smit MM, Cilliers C. The diagnosis of Wesselsbron disease in a new-born lamb by immunohistochemical staining of viral antigen. *The Onderstepoort Journal of Veterinary Research.* 1995:62(2):143-146.

Van Der Lugt JJ, Coetzer JAW, Smit MME. Distribution of viral antigen in tissues of new-born lambs infected with Rift Valley fever virus. *Onderstepoort Journal of Veterinary Research.* 1996:63(4):341-347.

Van Velden DJJ, Meyer JD, Olivier J. Rift Valley fever affecting humans in South Africa. A clinicopathological study. *South African Medical Journal.* 1977:51(24):867-871.

Vloet RPM, Vogels CBF, Koenraadt CJM, Pijlman GP, Eiden M, Gonzales JL, et al. Transmission of Rift Valley fever virus from European-breed lambs to Culex pipiens mosquitoes. *PLoS Neglected Tropical Diseases.* 2017:11(12). doi: 10.1371/journal.pntd.0006145

WAHID. Rift Valley fever 2018 edition. World Organisation for Animal Health (OIE). Summary of Immediate notifications and Follow-ups – 2019: Rift Valley fever. http://www.oie.int/wahis_2/public/wahid.php/Diseaseinformation/Immsummary; 2018.

Walters AW, Kujawa MR, Albe JR, Reed DS, Klimstra WB, Hartman AL. Vascular permeability in the brain is a late pathogenic event during Rift Valley fever virus encephalitis in rats. *Virology.* 2019:526:173-179.

Wauquier N, Becquart P, Padilla C, Baize S, Leroy EM. Human fatal zaire ebola virus infection is associated with an aberrant innate immunity and with massive lymphocyte apoptosis. *PLoS Neglected Tropical Diseases.* 2010:5;4(10). doi: 10.1371/journal.pntd.0000837.

Wichgers Schreur PJ, van Keulen L, Kant J, Oreshkova N, Moormann RJM, Kortekaas J. Co-housing of Rift Valley Fever Virus Infected Lambs with Immunocompetent or Immunosuppressed Lambs Does Not Result in Virus Transmission. *Frontiers in Microbiology.* 2016:7:287. doi: 10.3389/fmicb.2016.00287.

Wills BA, Oragui EE, Stephens AC, Daramola OA, Dung NM, Loan HT, et al. Coagulation Abnormalities in Dengue Hemorrhagic Fever: Serial Investigations in 167 Vietnamese Children with Dengue Shock Syndrome. *Clinical Infectious Diseases.* 2002:35(3):277-285.

Won SY, Ikegami T, Peters CJ, Makino S. NSm protein of Rift Valley fever virus suppresses virus-induced apoptosis. *Journal of Virology.* 2007:81(24):13335-13345.

Wu MF, Chen ST, Yang AH, Lin WW, Lin YL, Chen NJ, et al. CLEC5A is critical for dengue virus-induced inflammasome activation in human macrophages. *Blood.* 2013:121(1):95-106.

Xiao B, Zheng P, Yuan Z, Qiao C, Li J, Xiao X. AAV9 Exclusively Targets the Juxtaglomerular Apparatus in the Adult Mouse Kidney After Intravenous Injection. *Molecular Therapy.* 2015:23:S43. doi.org/10.1016/S1525-0016(16)33707-8

Yamayoshi S, Iizuka S, Yamashita T, Minagawa H, Mizuta K, Okamoto M, et al. Human SCARB2-dependent infection by coxsackievirus A7, A14, and A16 and enterovirus 71. *Journal of Virology.* 2012:86(10):5686-5696.

Yamayoshi S, Yamashita Y, Li J, Hanagata N, Minowa T, Takemura T, et al. Scavenger receptor B2 is a cellular receptor for enterovirus 71. *Nature Medicine.* 2009:15(7):798-801.

Yedloutschnig RJ, Dardiri AH, Mebus CA, Walker JS. Abortion in vaccinated sheep and cattle after challenge with Rift Valley fever virus. *Veterinary Record.* 1981:109(17):383-384.

Zani IA, Stephen SL, Mughal NA, Russell D, Homer-Vanniasinkam S, Wheatcroft SB, et al. Scavenger receptor structure and function in health and disease. *Cells.* 2015:4(2):178-201.

Zhao J, Kim KD, Yang X, Auh S, Fu YX, Tang H. Hyper innate responses in neonates lead to increased morbidity and mortality after infection. Proceedings of the National Academy of Sciences of the United States of America. 2008:105(21):7528-7533.

ANNEXURE A: HISTOMORPHOLOGICAL AND IMMUNOHISTOCHEMICALLY FEATURES THAT WERE EXAMINED FOR EACH SLIDE

Case#:					Acid hematin grade:		Autolysis grade:	
Liver:	Histo:	*	Necrosis/haemorrhage grade:	Mild	Moderate	Severe		
		*	Extent of hepatocyte necrosis:	Central	Midzonal	Periportal	Limiting plate	
				None	None	None	None	
				Focal	Focal	Focal	Single / Focal	
				Multifocal	Multifocal	Multifocal	Multifocal	
				Focal-extensive	Focal-extensive	Focal-extensive	Focal-extensive	
				Diffuse	Diffuse	Diffuse	Diffuse	
			Diffuse	Up to 75% of lobules	Up to 50% of lobule	Less than 25% of lobule	Groups of up to 10 cells	Single cells
			Predominantly centrilobular		Predominantly midzonal		Predominantly peri-portal	Random
		*	Hydrop change in surviving hepatocytes	Fatty change in surviving hepatocytes	Infiltrating polymorph in necrotic foci	Infiltrating histiocytes in necrotic foci	Karyorrhexis in necrotic foci	stagnant blood in necrotic foci
		*	Lymphocytes in portal tract	Oedema in portal tract	Karyorrhexis in portal tract	Limiting plate prolif activity	Blood pooling in sinusoids	Prolif Kupffer cells in sinusoids
		*	Mineralization of single cells	Primary lytic foci	Nuclear inclusions	Fibrin thrombi	Central veins occluded by a necrotic mass	
	IHC:	*	Individualised rounded necrotic cells		Necrotic cytoplasmic remnants		Primary foci	
		*	Sinusoids	Kuffer cells	Endothelial cells	Circulating leukocytes	Lymphocytes	Circulating mononuc cells
		*	Portal tracts	Limiting plate hepatocytes	Limiting plate prolif cells	Larger blood vessels	Vascular s.m. cells	
		*	No labelling	Sparse / scattered / multifocal / widespread / diffuse cell labelling		Sparse / scattered / widespread intravasc fragments		Non-cell associated virus
Kidney	Histo:	*	Acute tubular injury grade:	None	Mild	Moderate	Severe	
		*	PTE cell degeneration	Apoptotic PTE cells in lumen	Increased pyknosis of nuclei	Patchy / diffuse PTE necrosis	Preferential damage to medullary ray (straight tub)	Attenuated PTE cells (slouged apical portion)
			Dilated empty tubular lumens	Casts in distal tubules / collecting ducts	Accum of leucocytes in dilated vasa recta	Perivascular / Interstitial oedema	Flattened, basophilic, karyomegalic epithelium	Tubulorrhexis
		*	Nuclear debris / pyknotic nuclei / neutrophils in glomeruli	Nuclear debris in capillary lumen	Mononuc cells in glomeruli	Microthrombi /fibrin in glomeruli	Haemorrhage in glomeruli	Haemorrhage in interstitium
	IHC:	*	Glomerular	Tubular	Both glomerul and tubular	Interstitial	Vascular	Transitional
		*	Cortex	Medualla	Glomerular capillaries	Interstitial capillaries	Larger blood vessels	
		*	Endothelial cells	Lymphocytes	Circulating leukocytes	Macrophages	Circulating mononuc cells	Vascular s.m. cells
		*	No labelling	Sparse / scattered / multifocal / widespread / diffuse cell labelling		Sparse / scattered / widespread intravasc fragments		Non-cell associated virus

Spleen	**Histo:**	*	Necrocis/depletion grade:	None	Mild	Moderate	Severe
		*	White pulp expansc/coalescence:	None	Mild	Moderate	Severe
		*	Lymphocytolysis white pulp:	None	Sparse	Scattered	Widespread
		*	Lymphocytolysis red pulp:	None	Sparse	Scattered	Widespread
		*	Tingible body macrophages in white pulp / red pulp	Foci of necrosis in follicles / germinal cent	Lymphocytes in PALS spared and / or Corona spared	Fibrin in red pulp	Polymorph leucostasis in red pulp	Mononuclear leucostasis in red pulp
	IHC:	*	White pulp:	PALS	Follicles	Germinal centers	Marginal sinus	Marginal zone
				Central artery	Lymphocytes	Macrophages	Dendritic cells	Plasma cells
		*	Red pulp:	Splenic cords:	Reticular cells			
				Venous sinuses:	Endothelial cells	Macrophages	Circulating mononuc cells	Circulating leukocytes
		*	Trabeculae	Trabecular artery/vein		Vascular s.m. cells		
		*	No labelling	Sparse / scattered / multifocal / widespread / diffuse cell labelling		Sparse / scattered / widespread intravasc fragments		Non-cell associated virus
Lung	**Histo:**	*	Pulmonary oedema:	None	Mild	Moderate	Severe
		*	Pulmonary haemorrhage:	None	Focal	Multifocal	Diffuse
		*	BALT necrosis:	None	Focal	Multifocal	Diffuse
		*	Alveolar oedema	Interstitial oedema		Atelectasis	
		*	Emphysema	Mononuclear leucostasis		Polymorph leucostasis	
	IHC:	*	Pleura	Bronchi(oles)	Interstitium	Bronchiolar epithelium	Alveolar epithelium	Glandular epithelium
		*	Vascular endothelium	PIMS	Circulating leukocytes	Macrophages	Circulating mononuc cells	Vascular s.m. cells
		*	No labelling	Sparse / scattered / multifocal / widespread / diffuse cell labelling		Sparse / scattered / widespread intravasc fragments		Non-cell associated virus
Heart	**Histo:**	*	_____ Haemorrhages:	None	Focal	Multifocal	Diffuse
		*	Oedema	Mononuclear leucostasis		Polymorph leucostasis	
	IHC:	*	Epicardium	Sub-epicard	Myocardium	Sub-endocard	Endocardium	Valves
		*	Myocardial fibres	Purkinje fibres	Interstitium	Capillaries	Larger blood vessels	
		*	Endothelial cells	Lymphocytes	Circulating leukocytes	Macrophages	Circulating mononuc cells	Vascular s.m. cells
		*	No labelling	Sparse / scattered / multifocal / widespread / diffuse cell labelling		Sparse / scattered / widespread intravasc fragments		Non-cell associated virus

GIT	Histo:	*	Haemorrhage in mucosa / l.p. / submuc / l . muscu / submuc:	None	Focal	Multifocal	Diffuse	
			Necrosis in mucosa / l.p. / submuc / l . muscu / submuc:	None	Focal	Multifocal	Diffuse	
		*	GALT necrosis:	None	Focal	Multifocal	Diffuse	
		*	Fibrin thrombi	Mononuclear leucostasis		Polymorph leucostasis		
	ICH:	*	Forestomach	Abomasum	Small int	Large int		
		*	Mucosa	Lamina prop	Submucosa	Muscularis	Serosa	
		*	Capillaries	Larger blood vessels				
		*	Endothelial cells	Lymphocytes	Circulating leukocytes	Macrophages	Circulating mononuc cells	Vascular s.m. cells
		*	No labelling	Sparse / scattered / multifocal / widespread / diffuse cell labelling		Sparse / scattered / widespread intravasc fragments		Non-cell associated virus
Adrenal	Histo:	*	Necrosis and haemorrhage in glomerul / fascicul / reticul:	None	Focal	Multifocal	Diffuse	
	IHC:	*	Cortex	Zona glomerulosa	Zona fasciculata	Zona reticularis	capillaries	Larger blood vessels
		*	Medulla	Central vein	Cells	Stroma	Capillaries	Larger blood vessels
		*	Endothelial cells	Lymphocytes	Circulating leukocytes	Macrophages	Circulating mononuc cells	Vascular s.m. cells
		*	No labelling	Sparse / scattered / multifocal / widespread / diffuse cell labelling		Sparse / scattered / widespread intravasc fragments		Non-cell associated virus
Lymph node	Histo:	*	Lymphoid depletion grade:	None	Mild	Moderate	Severe	
		*	Cortex lymphocytolysis:	None	Sparse	Scattered	Multifocal	Widespread
				Follicles	Germ centers	Interfoll cortex		
		*	Paracortex lymphocytolysis:	None	Sparse	Scattered	Widespread	
		*	Medullary cords /sinusses lymphocytolysis:	None	Sparse	Scattered	Widespread	
		*	Tingible body macrophages in cortex / paracortex / medulla	Sparing of follicle corona / paracortical DCU		Haemorrhages in cortex / paracortex / medulla		Polymorph leucostasis
	IHC:	*	Trabeculae	Sub capsular sinus	Trabecular sinus	Cortical sinus	Medullary sinus	Sinus histiocytes
		*	Superficial cortex:	Primary follicles	Secondary follicles	Germinal centers	Interfollicular cortex	
			Lymphocytes	Follicular dendritic cells	tingible body macrophages		Capillaries	
		*	Paracortex:	Central DCU	Peripheral DCU	T lymphocytes	Interdigitating dendritic cells	High endothel venules
		*	Medullary cords:	lymphocytes	Plasma cells	Macrophages	Capillaries	Larger blood vessels
		*	Medullary sinus	Fibroblastic reticular cells	Lymphocytes	Sinus histiocytes		
		*	Endothelial cells	Lymphocytes	Circulating leukocytes	Macrophages	Circulating mononuc cells	Vascular s.m. Cells
		*	No labelling	Sparse / scattered / multifocal / widespread / diffuse cell labelling		Sparse / scattered / widespread intravasc fragments		Non-cell associated virus

Thymus	**Histo:**	*	Necrosis in cortex /medulla:	None	Focal	Multifocal	Diffuse
		*	Hemorrhage / oedema in cortex / medulla:	None	Focal	Multifocal	Diffuse
	IHC:	*	Capsule	Septa	blood vessels in septa		
		*	Cortex	T cells	Thymocytes	Small lymphocytes	Large lymphocytes
		*	Medulla	Epithelial cells	Hassall's corpuscles	Lymphocytes	
		*	Capillaries	Larger blood vessels			
		*	Endothelial cells	Lymphocytes	Circulating leukocytes	Macrophages	Circulating mononuc cells	Vascular s.m. cells
		*	No labelling	Sparse / scattered / multifocal / widespread / diffuse cell labelling		Sparse / scattered / widespread intravasc fragments	Non-cell associated virus
Skin	**Histo:**	*	Necrosis in epidermis / dermis / subcutis	None	Single cell	Focal	Multifocal
	IHC:	*	Epidermis	Stratum basale	Stratum spinosum	Stratum granulosum	Stratum corneum
		*	Dermis	Papillary dermis	Reticular dermis	Hair follicles	Glands
		*	Subcutis	Fibroblasts	Collagen		
		*	Capillaries	Larger blood vessels			
		*	Endothelial cells	Lymphocytes	Circulating leukocytes	Macrophages	Circulating mononuc cells	Vascular s.m. cells
		*	No labelling	Sparse / scattered / multifocal / widespread / diffuse cell labelling		Sparse / scattered / widespread intravasc fragments	Non-cell associated virus
Brain	**Histo:**	*	Encephalitis:	None	Mild	Moderate	Severe
	IHC:	*	Cerebrum	Brain stem	Cerebellum		
		*	Grey matter	white matter	meninges		
		*	Neurons	Astrocytes	Microglia	Oligodendro-cytes	Ependymal cells	Purkinje cells
		*	Capillaries	Larger blood vessels			
		*	Endothelial cells	Lymphocytes	Circulating leukocytes	Macrophages	Circulating mononuc cells	Vascular s.m. cells
		*	No labelling	Sparse / scattered / multifocal / widespread / diffuse cell labelling		Sparse / scattered / widespread intravasc fragments	Non-cell associated virus
Other organ		*					
Other organ		*					
Other organ		*					

ANNEXURE B: ANIMAL ETHICS APPROVAL

UNIVERSITEIT VAN PRETORIA
UNIVERSITY OF PRETORIA
YUNIBESITHI YA PRETORIA

Animal Ethics Committee

PROJECT TITLE	**Diagnosis and pathology of Rift Valley Fever virus in sheep**
PROJECT NUMBER	**V096-16**
RESEARCHER/PRINCIPAL INVESTIGATOR	**Dr. L Odendaal**

STUDENT NUMBER (where applicable)	**UP_247 355 0**
DISSERTATION/THESIS SUBMITTED FOR	**PhD**

ANIMAL SPECIES	**n/a**	
NUMBER OF ANIMALS	**n/a**	
Approval period to use animals for research/testing purposes		**August 2016 –August 2017**
SUPERVISOR	**Prof. EH Venter**	

KINDLY NOTE:

Should there be a change in the species or number of animal/s required, or the experimental procedure/s - please submit an amendment form to the UP Animal Ethics Committee for approval before commencing with the experiment

APPROVED	Date 29 August 2016
CHAIRMAN: UP Animal Ethics Committee	Signature

S4285-15